Applied Optics

December
1963

A1N
A2N
ANN
j ≠ k

LENS DESIGN AND COMPUTERS

Effective Jan. 1, 1965. All back issues and single copies are sold at $3.00 per copy.

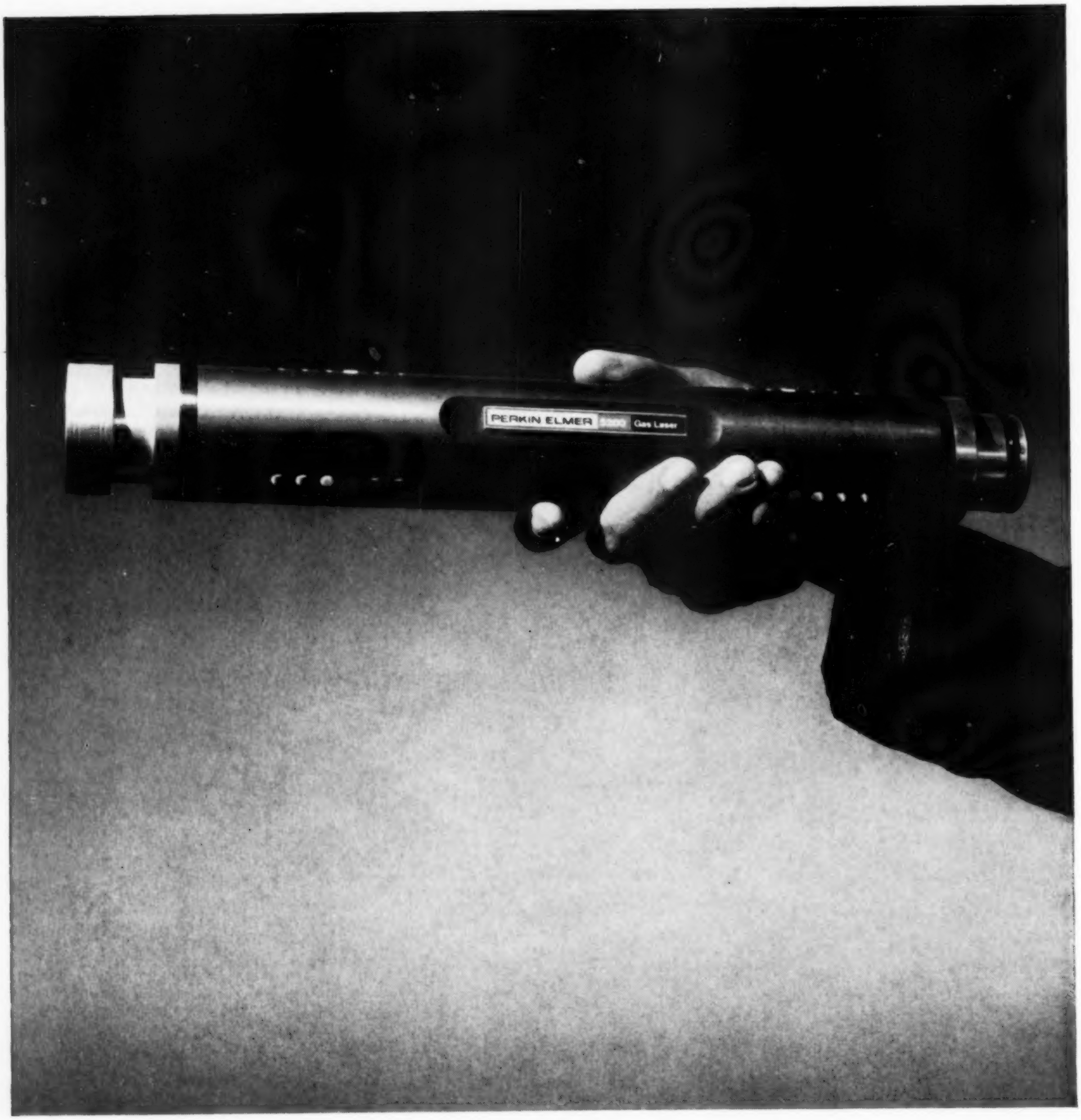

PERKIN-ELMER ANNOUNCES
THE LIBERATION OF THE LASER

Until now the gas laser has been tied to the laboratory — too big, too complicated, too fragile for practical uses. The new Perkin-Elmer Model 5200 Laser removes these limitations and sets new standards of technical performance.

The Model 5200 helium-neon laser features a newly-developed, double-walled, compact, gas discharge tube only 10" long. The plasma is generated inside a capillary by a small, direct-current discharge between an internal anode and heated cathode. The discharge tube is mounted inside a rugged, coaxial, cylindrical resonator with adjustable mirror holders and camera-type optical accessory mounts at each end. The result is a highly stable and useful configuration.

The superb quality of the Perkin-Elmer optics permits operation in the pure fundamental mode for diffraction-limited optical performance.

The separate electronically regulated Model 5201 power supply provides the necessary power to achieve a highly stable, noise-free light output from the discharge tube. Connection to an external jack on the 5201 permits direct modulation of the laser beam up to frequencies of 500 KC.

For detailed information on the new Model 5200 Laser and complete Perkin-Elmer Optical Maser Product Services contact Optical Maser Marketing, Perkin-Elmer Corporation, 960 Danbury Road, Norwalk, Connecticut. Telephone (203) 847-0411.

PERKIN-ELMER

Applied Optics

VOLUME 2
NUMBER 12
DECEMBER
1963

A monthly publication of the
Optical Society of America

John N. Howard, Editor

D. P. Feder, Feature Editor

Patricia R. Wakeling, Managing Editor

1209 **Automatic Optical Design**—Donald P. Feder
1227 **The Symposium Lens—An Epilogue**—Robert E. Hopkins and Donald P. Feder
1233 **Lens Design by Computer**—C. G. Wynne and P. M. J. H. Wormell
1239 **The Role of Eikonal and Matrix Methods in Contrast Transfer Calculations**—W. Brouwer, E. L. O'Neill, and A. Walther
1247 **Image Evaluation by Spot Diagram Using A Computer**—Kenro Miyamoto
1251 **First-Order Design and the $y, \bar{y}$ Diagram**—Erwin Delano
1257 **A Flexible Automatic Lens Correction Procedure**—Gordon H. Spencer
1265 **Coaxial, Dual-Field Optics for a Space Sextant**—H. E. Brunelle, Jr., and R. R. Willey, Jr.
1271 **Analysis and Design of Plane Mirror Systems**—R. J. Pegis and M. M. Rao
1275 **A Method for Localized Variation of the Paths of Two Paraxial Rays**—Loyd E. Sutton
1281 **Automatic Lens Design for Nonexperts**—Berlyn Brixner
1287 **A New Method for High-Speed Motion-Picture Photography of Transparent Drops**—Albert Pfeiffer
1295 **A Universal Spectrophotometer**—Wilbur Kaye
1303 **Photometric Accuracy of Infrared Spectrophotometers**—James E. Stewart
1309 **An Optical Null Double-Beam Double-Pass Infrared Spectrophotometer**—Shigeo Minami
1317 **A Large-Stage Photoelectric Planimeter for Leaves**—P. D. Carman
1323 **Optical Excitation of Mercury Vapor for the Production of Isolated Fluorescence**—R. Zito, Jr., and A. E. Schraeder

DEPARTMENTS

1329 **Letters to the Editor**
Effect of Pre-excitation on Flash Lamp Optical Quality—H. G. Heard
Precise Automatic Readout on Comparator with Photoelectric Detection—Jean M. Bennett
Note on the Paper "Tilted-Plate Interferometry with Large Plate Separations"—H. W. Moos, G. F. Imbusch, L. F. Mollenauer, and A. L. Schawlow
The Symposium Lens Improved—Berlyn Brixner
Correction of Phase Errors in Interferograms—Lawrence Mertz
Author's Reply—E. V. Loewenstein
A Precision Chopper Disk—Hans R. Rottmann
A Simple Method for Preparing Layers of Sodium Salicylate—R. A. Knapp
Index of Refraction of KDP—Jane H. Dennis and R. H. Kingston
A Low-Pressure Arc Source for the Emission Spectrum of the FeO Molecule—R. K. Dhumwad and Arnold M. Bass
Artificial Green Flashes—D. Deirmendjian
Immersion Null Test for Aspherics—Robert T. Holleran
A Note on the Testing of Homogeneity of Large-Aperture Parallel Plates of Glass—M. V. R. K. Murty
Nondestructive Laser Pumping by High Explosives—John K. Crosby and R. C. Honey
A Carbon Furnace as a Source of Continuous Infrared Radiation—Robert Spanbauer, Phillip E. Fraley, and K. Narahari Rao
1231 **Books**
1232 **Meeting Reports**
1256 **From the Editor**
1269 **Patents**
1294 **Optical Activities in Industry**
1328 **Of Optics and Opticists**
1343 **Index to Volume 2**

COVER: Mathematical programs for high-speed computers are becoming increasingly important in the field of optical design. Photograph by Raymond C. Holden, Eastman Kodak Company, Rochester, N.Y.

Published monthly by the Optical Society of America, Inc., in cooperation with the American Institute of Physics, at 20th and Northampton Streets, Easton, Pa. Editorial and advertising offices: 1155 16th St. N.W., Washington, D.C. 20036. 202-Di7-4131. Supported in part by a grant from the National Science Foundation. Subscription rates: $6.00 to OSA members, $8.00 other AIP Societies' members, nonmembers and libraries: $10.00 per year. Single copies $3.00. Second class postage paid at Easton, Pa. © Copyright 1963 by the Optical Society of America.

Optics at Xerox...and You

In the past eleven years, Xerox has been extremely successful with its commercial products for the copying equipment markets.
Revenues last year rose to over $104 million; profitability has increased every year and actually doubled in each of the past two years.
All this is the result of a long range planned growth program which extends far into the future. Exciting new products are now being readied for market; while our four major research and engineering laboratories are being strengthened to permit greater concentration on long-range planning.
Therefore, we seek talented personnel in many disciplines to work in modern facilities located in suburban Rochester, New York.

If you have a solid background in geometrical optics or physical optics, this may be your opportunity to take a major part in advancing Imaging Technology.

Projects include:

Research in Imaging Systems, Coherent Light Techniques, Modulation Techniques, Image Enhancement, Material Development, Image Storage Material, Image Translation Devices.

Design of Components, Systems and Equipment for UV applications, . Visual Displays, and IR recording.

Evaluation studies (Theoretical and Experimental) for Photographic Systems, Electrostatic Systems, and Visual Systems.

Please send resume and salary history in confidence to Mr. Robert Conboy, Xerox Corporation, Dept AP-121, P.O. Box 1540, Rochester 3, New York.

XEROX
CORPORATION
an equal opportunity employer

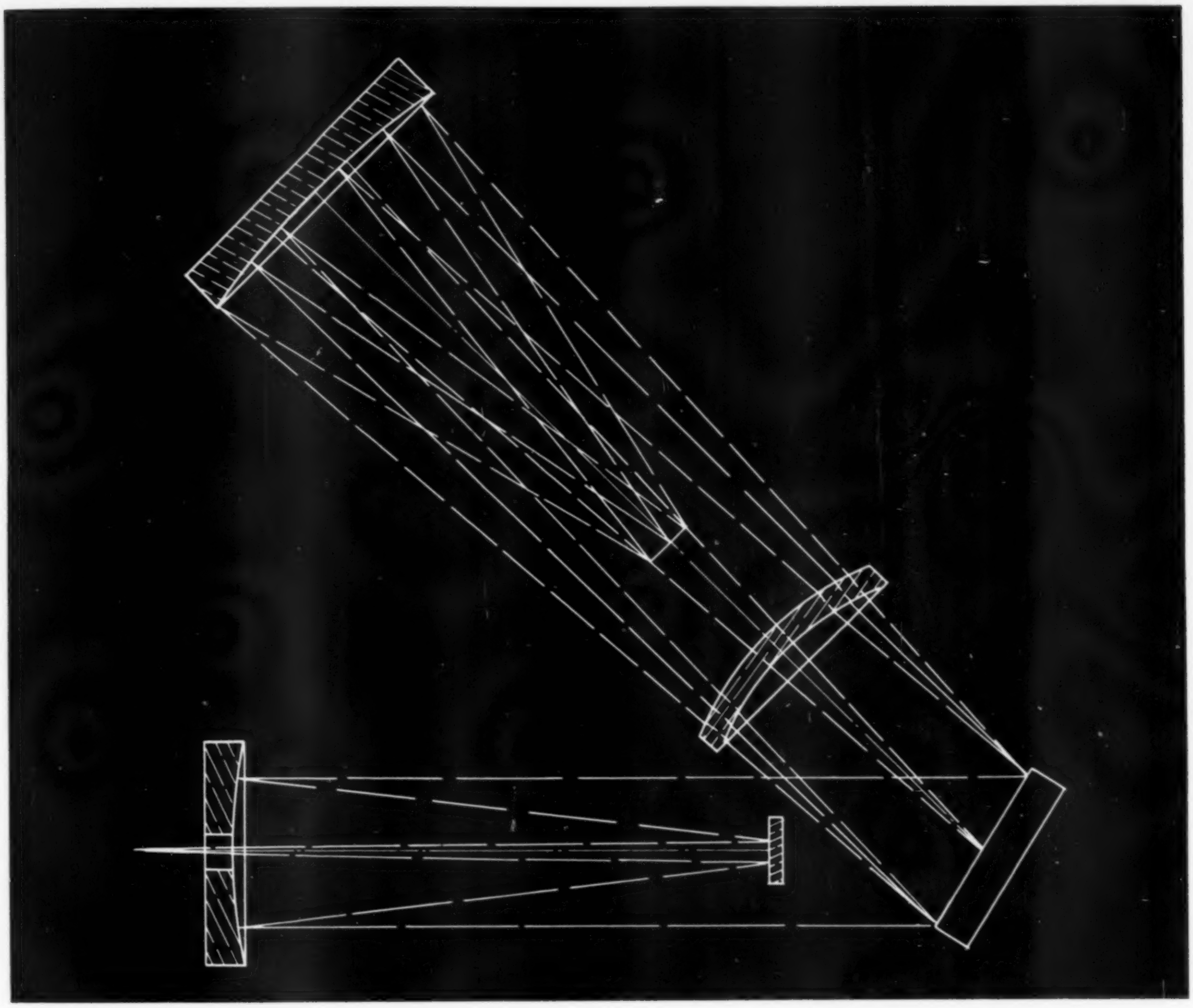

BE ASSURED OF AN EFFECTIVE IMAGE

To be diffraction limited, an optical system must produce an image smaller than the so-called "Airy disc".

Theory tells us that certain combinations of aspheric surfaces can be made to give "diffraction limited" performance over a specific field. Two or more such systems, in turn, are often combined to advantage in instrument designs. In certain instances spherical surfaces may be substituted for aspherics in such combinations, thereby reducing both time and cost in production.

On the other hand, if the design will not allow a given level of performance, no amount of workmanship can produce it. If a complete computer analysis shows the image structure to be within the Airy limit, we may proceed with confidence.

This will explain why we make it a practice to do such an analysis on every complex design submitted to us for production. The customer is not always right. But then, neither are we. We only like to think we are.

This analytical approach to design specifications has saved some of our customers a lot of time and money. Perhaps you can make use of our design and engineering experience before the final specifications are drawn. If so, write, wire or telephone Director of Research.

FERSON OPTICS, INC.

P. O. BOX 398/OCEAN SPRINGS, MISS./TEL. 875-5422 (Area Code 601)

EXPERIENCED OPTICAL PERSONNEL—send your resume for consideration in a fast growing company—equal opportunity for all.

Telescopes, Periscopes, Interferometers, Camera Optics, Radiometers for ultra-violet or infra red, Plane Surfaces, Spherical Surfaces, Aspheric Surfaces, Mirrors, Prisms, Optical Coatings, Machine Shop Facilities, Engineering and Computer Design.

SHED SOME COHERENT LIGHT ON YOUR RESEARCH PROBLEMS

... use the laser that has set the performance standards.

Whether your laser investigations are directed to basic research or industrial applications, the LSI Laser Systems Center can supply you with complete laser systems, components, and accessories with proven performance and reliability. A skilled Laser Systems Center research and development staff is prepared to give you complete assistance in designing special systems suited to your particular requirements.

The LSI H-130 Laser Head and C-100 Control Console with liquid nitrogen storage Dewar are shown below. This standard system has a maximum output of 3 to 4 joules; is equipped for manual, remote, or automatic firing; has a maximum pump input of 4000 joules; and has a repetition rate of three firings per minute at maximum output.

Write or call for complete information about this system and others with outputs in excess of 20 joules, laser Q-switch attachments, laser calorimeters, and an experimental micro-welding stand.

LEAR SIEGLER, INC.

LASER SYSTEMS CENTER
FORMERLY TRION INSTRUMENTS, INC.

2320 WASHTENAW AVENUE
ANN ARBOR, MICHIGAN
TELEPHONE 313-665-8844

This free book
is a
"MUST"
for
every
engineer
and
designer
working
with . . .

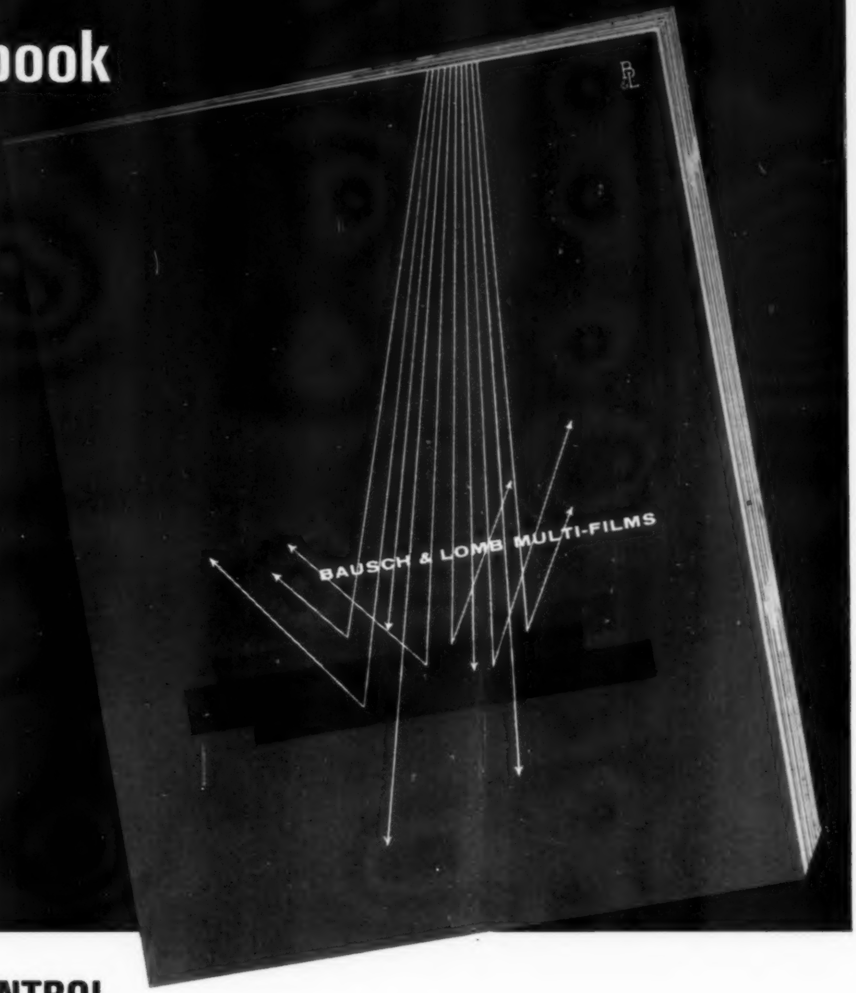

HEAT CONTROL
HIGH-EFFICIENCY REFLECTANCE • BEAM SPLITTING
WAVELENGTH SEPARATION • ARCHITECTURAL LIGHTING
COLOR CORRECTION • DECORATIVE COATING

Equipment, personnel, and experienced know-how in the engineering and production of vacuum deposited multi-layer films . . . available to you at Bausch & Lomb . . . *cannot be equalled anywhere.* Whether your problem requires a new multi-layer film engineered, and a single prototype produced . . . or multi-layer films on a million or two million products . . . we're ready to serve you. And the exclusive, complete manual tells the whole story with indispensable engineering data and curves on color filters, dichroic or color separating filters, heat control filters, neutral beam dividers and first surface mirrors. Just mail the coupon.

BAUSCH & LOMB

BAUSCH & LOMB INCORPORATED
77148 Bausch Street, Rochester 2, N. Y.

☐ Please send me your new 32-page handbook on B&L Multi-Films, E-306.

My special problem involves: ☐ High-efficiency reflectance ☐ Heat control ☐ Color separation ☐ Color correction ☐ Beam splitting ☐ Wavelength separation ☐ Architectural lighting ☐ Decorative coating

Name .... *Title* ....
(PLEASE PRINT)
Professional Address ....
....

In Canada, write Bausch & Lomb Optical Co., Ltd., Dept. 771, Scientific Instrument Division, 16 Grosvenor St., Toronto 5, Canada

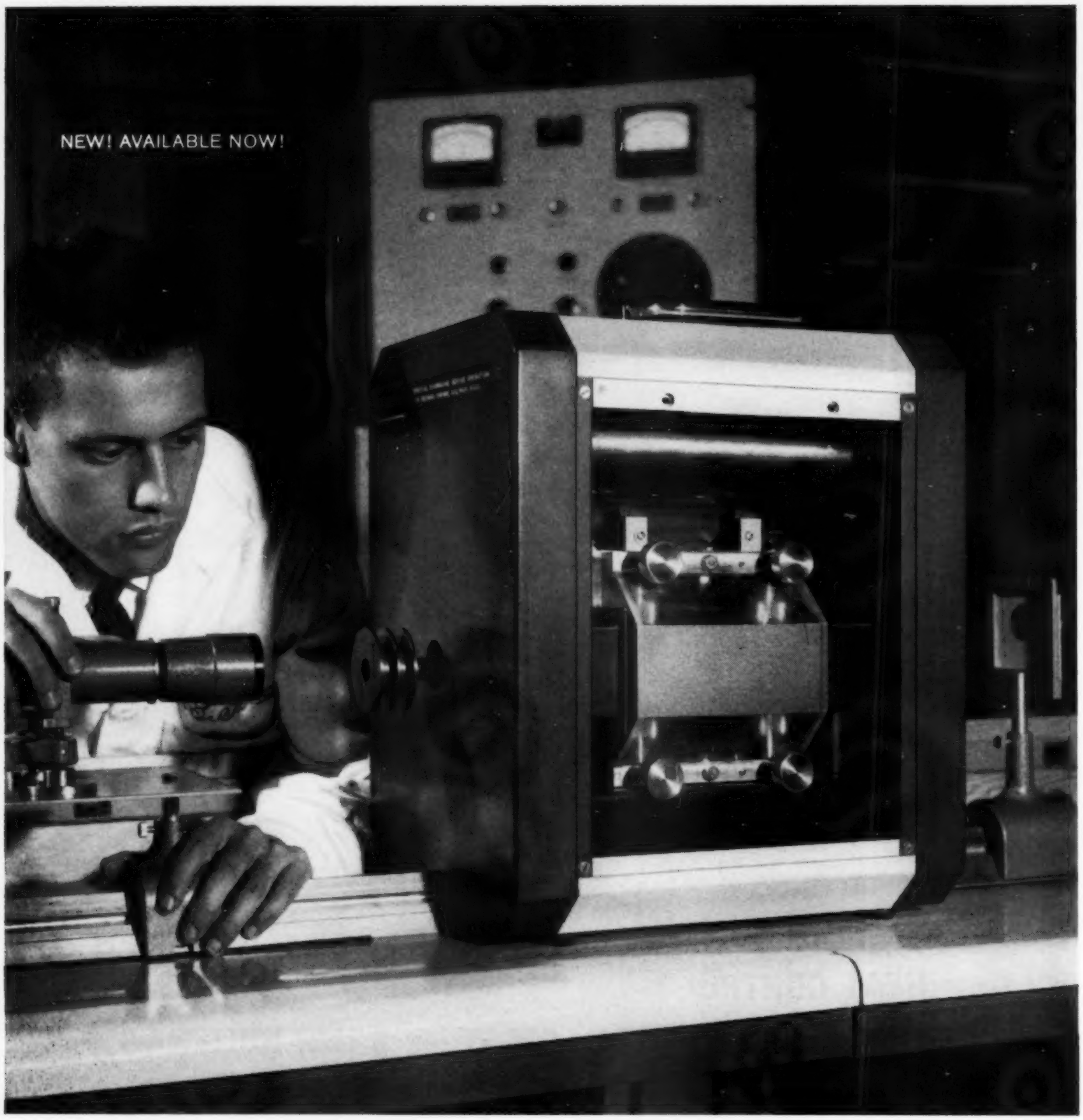

RAYTHEON LASER HEAD

WITH

250* JOULES OUTPUT!

Raytheon LHM6 Laser Head—one of a comprehensive line of laser devices—features high energy output to enhance your research capabilities and unique construction to preclude obsolescence. LHM6, as with all Raytheon Laser Heads, is supplied with a Ruby rod. All perform efficiently, too, with Neodymium-in-glass and other laser rods that can be pumped with Xenon lamps. In LHM6, both ends of the crystal are accessible to facilitate the use of Q-spoiling devices and external optics. LHM6 is designed for long-term use: when higher energy lamps and larger laser rods are available, they may be incorporated without modification. Your Raytheon Sales Engineer has a portfolio of Laser Data Sheets for you. Ask him for your set. Or, write Raytheon Company, Laser Advanced Development Center, Waltham 54, Mass.

RAYTHEON

*Ruby at liquid nitrogen temperature. With neodymium-doped glass, 175 joules have been obtained at room temperature.

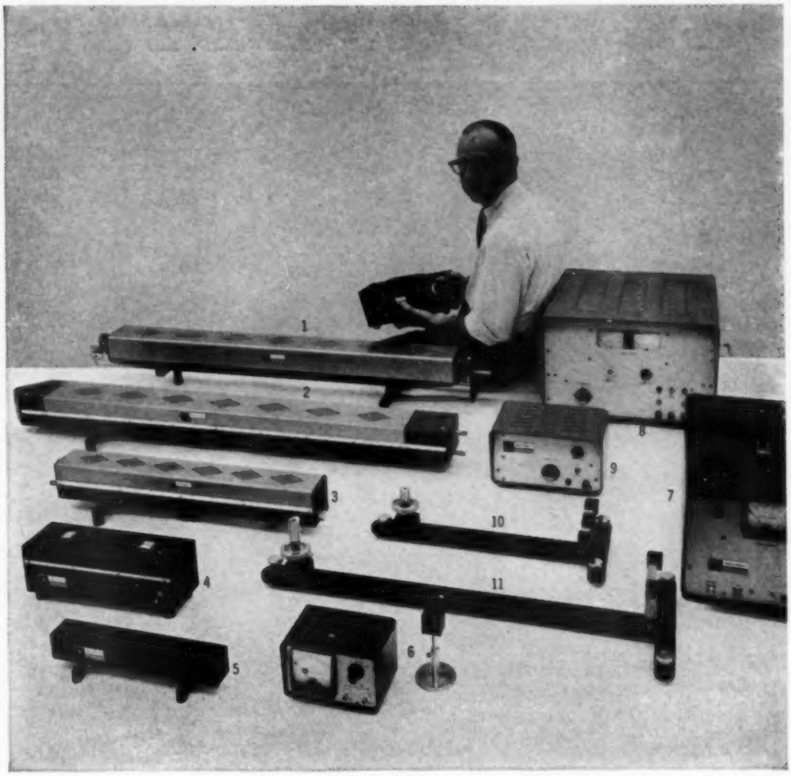

Gas Laser product spectrum

The label you see on the lasers above is the one that's best known among all commercial CW gas lasers in use today. What keeps the Spectra-Physics label in the forefront is the integrity and experience in back of it, and the quality which has gained acceptance for Spectra-Physics lasers throughout the scientific disciplines.

One of the five current production models of helium-neon lasers will likely fit your needs, whether for systems and instrument use, classroom demonstration, or advanced laboratory research. The newest, a Spectra-Physics invention,* is the Model 116, the first instrument capable of providing reliable high-gain operation over a wide range of wavelengths.

Full one-year warranty—When you purchase any Spectra-Physics laser, you can look forward to a high order of reliability in its operation, backed by a strong 1-year warranty which even includes the plasma tube.

1	Model 112 laser	$8200
2	Model 116 laser	$13,250
3	Model 115 laser	$4650
4	Model 130 laser	$1525
5	Model 131 laser	$1950
6	Model 401 Power Meter	$355
7	Model 200 Exciter (for Models 112, 115)	
8	Model 250 Exciter (for Model 116)	
9	Model 251 Exciter (for Model 131)	
10	Model 302 Precision Adjusting Base	
11	Model 301 Precision Adjusting Base	

May we send you data sheets and add your name to the mailing list for Spectra-Physics Laser Technical Bulletins? Address us at 1255 Terra Bella Avenue, Mountain View 5, California (or call collect—(415) 961-2550).

*PATENT PENDING

Spectra-Physics

TINSLEY CAPABILITIES

50-Inch Precision Optical Window

BUBBLE CHAMBER OPTICS

Proven experience in the fabrication of ultra high precision bubble chamber optical systems, including aspherics, for leading research laboratories.

LENS MANUFACTURE

All types of refraction systems-fabricators of the world's largest astronomical apochromatic telescope.

MASSIVE OPTICS

Schlieren systems—telescopes. Special equipment for generating and polishing high precision optical flats and mirrors up to 10 feet diameters.

DESIGN CAPABILITIES

Optical engineering staff experienced in all fields of optics with IBM 1620 computer design capability.

TEST FACILITIES

Air conditioned and constant temperature area. Approved quality control department with specially designed test equipment.

For optical engineering consultation or quotations: telephone (415) 843-6836 or TWX (415) 891-9316

TINSLEY LABORATORIES, INC.

2448 Sixth Street, Berkeley, California 94710

Optics at Itek

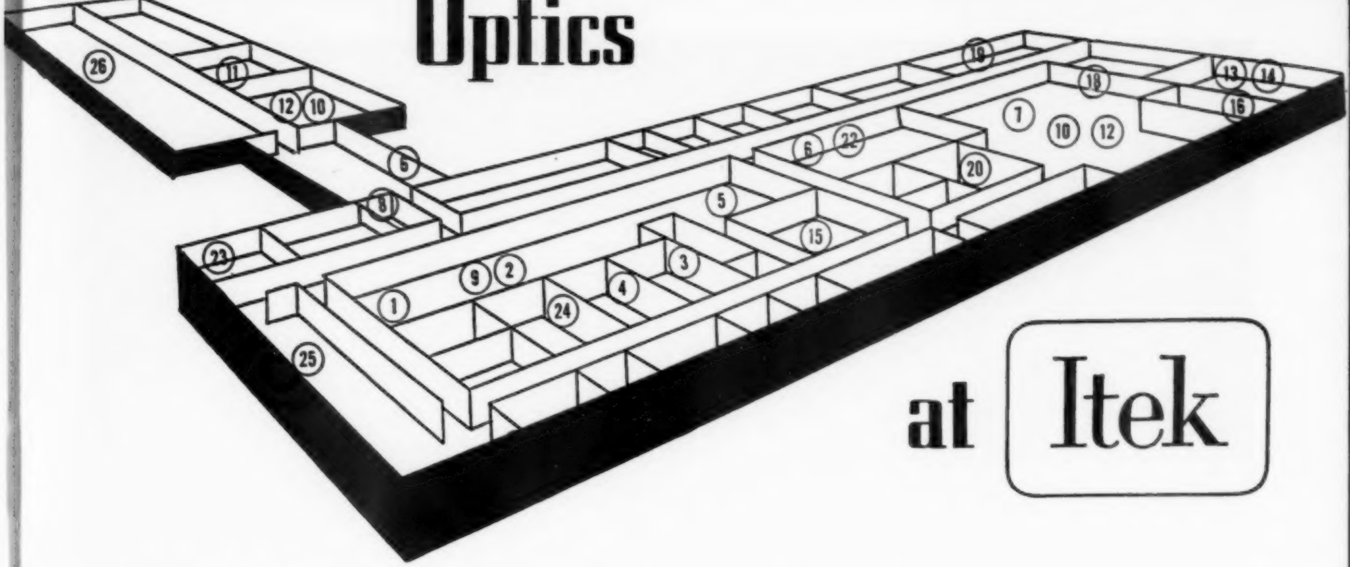

Itek has recently completed the expansion of its Applied Optics capability. The major emphasis in this department has been on the design and fabrication of systems applicable to aerial photography. Many of the current research and development programs involve unique systems, sub-systems and components demanding extremely close tolerances that will be applicable to a broader range of Government and commercial requirements.

This is but one facet of the work being done at Itek. Individuals interested in the career opportunities at our Lexington facility should forward their resumes to the address below. Immediate opportunities exist for the following:

Research Optics

Ph.D. or equivalent in optics with interest and record of publication in theory of diffraction, lens design, image evaluation and camera systems. To initiate fundamental programs in optics in support of advanced photo-recording, photoscanning and photo storage projects.

Optical Engineer

Assist in the optical engineering, fabricating and testing of optical subsystems and carry out experiments to prove engineering principles.

Senior Optical Instrumentation Engineer

Requires experience in projects directly related to optical instrumentation. Direct experience with high precision custom optics or astronomical systems is desirable. As cognizant task leader, superior engineering skill and judgement is essential.

Senior Optical Processing Engineer

Requires experience in optical processing methods and techniques. To be responsible for production planning and assist in the development of new fabrication and equipment techniques for optical components.

Photo-Optical Systems Engineer

Requires five to ten years' in the optical engineering of photographic equipment. Design and direct calibration controls, recommend lens systems-liaison with manufacturers, develop design and engineering input of photographic equipment and be responsible for total quality.

Staff Engineer Electro-Mechanical-Optical Systems

Requires an M.S. degree with mathematics through advanced calculus. Responsibilities include solution of special engineering problems associated with the design of electro-mechanical-optical systems and the determination of their basic parameters.

Optical Quality Assurance Engineer

Advanced engineering degree is required with experience in aerial photographic systems. Must have designed optical systems, prepared and evaluated their performance specifications and performed optical systems calibration.

Experimental Electro-Optics Engineers

B.S. in E.E. or Physics, with proven interest in the field of optical spatial filtering or experience with systems using coherent light to produce transformations of pictures via their diffraction patterns.

Experimental Photo-Optics Engineers

To investigate new optical concepts via experimental and theoretical analysis. Must have a minimum of two years' experience in optical systems design. Experience in a wide variety of unusual optical systems is sought.

Professional opportunities of equal significance exist for Research Electronic Engineers, Photographic Engineers, Photochemists, Opto-Mechanical Engineers and Photogrammatists. To gain more complete information concerning the rewarding personal and professional potential of these positions, address your resume to:

Mr. Richard D. Finnegan, Professional Staffing

PARTIAL EQUIPMENT LISTING

SUPER MANN LENS BENCH	1
CDC 924 COMPUTER WITH VISUAL DISPLAY	2
40-INCH BLANCHARD SPHERE GENERATOR	3
40-INCH PARABOLA COLLIMATOR	4
6 DRAPER POLISHING MACHINES 30 TO 50-INCH DIAMETERS	5
10 LOH POLISHING MACHINES, 18-INCH DIAMETER	6
24-INCH EDGING MACHINE	7
24-INCH DIAMETER ASPHERIC GRINDER	8
1 COATING TANK, 72 INCHES	9
NO. 586 MANN LENS BENCH	10
14 HAND-FIGURING SPINDLES 14 TO 18-INCH DIAMETERS	11
1 WILD T-4 THEODOLITE	12
10-INCH-BLANCHARD SPHERE GENERATOR	13
4 MULTISPINDLE POLISHING MACHINES, 6 TO 16-INCH DIAMETERS	14
16-INCH EDGING MACHINE	15
2 VACUUM COATING TANKS, 20 INCHES	16
SINE WAVE TEST BENCH	17
NO. 900 MANN LENS TEST BENCH	18
45-INCH ASPHERIC GRINDING AND POLISHING MACHINE	19
TWO-COORDINATE COMPARATOR	20
16-INCH SCATTEROMETER	21
24-INCH PRECISION ROTARY TABLE	22
1 CHANCE HILGER REFRACTOMETER	23
SPATIAL FILTER TEST BENCH	24
2 WILD T-2 ALIGNMENT THEODOLITES	25
SPECTROMETER	26

Itek

Itek Corporation
10 MAGUIRE ROAD, LEXINGTON 73, MASSACHUSETTS

An equal opportunity employer

B/A
.... ALL-DIELECTRIC
INTERFERENCE
FILTERS
you can
.... SEE ....
the
difference

Baird-Atomic's exclusive sidewing blocking techniques produce all-dielectric, multilayer interference filters with the highest total transmission and a transmission-rejection ratio of less than 0.1%. Only B/A Interference Filters have a block shape ⎍ band pass assuring the greatest degree of spectral purity.

B/A Interference Filters covering two ultraviolet ranges and the visible spectrum are stocked in 1″ x 1″ and 2″ x 2″ sizes. Half-band widths, additional blocking and special shapes and sizes are also available. Only 21 days maximum is required to fill special orders. Special quantity prices prevail.

B/A **BAIRD-ATOMIC, INC.**
33 University Road · Cambridge 38, Mass.

Filter Classifications

Visible Spectrum	4000-8000 Å
Standard Ultraviolet	2100-3400 Å
Special Ultraviolet	3900-3999 Å
Half-band Widths	4.8-1600 Å
Maximum Transmission (Complete Curves Available $15 Extra)	25-70%
Rejection	0.1%
Blocking	Maximum blocking with reduced thickness for improved signal-to-noise ratio.

For full information, write Adv. Dept. for brochure X-44

Engineers and Scientists: *Investigate challenging opportunities with B/A. Write Industrial Relations Director. An equal opportunity employer.*

ADVANCED OPTICS AND ELECTRONICS...SERVING SCIENCE

TWO FINE PRECISION LINES FOR LASER RESEARCH and APPLICATIONS

FROM THE

WORLD'S LARGEST SINGLE CRYSTAL SOURCE

1. Semi-Elements' NEW MKIB GAS LASER Precision Made . . . COMPLETE $750!

Wavelength—Visible and Infrared—6328Å 11,523Å 33,912Å

Power—1 to 2 Milliwatt Output

Adjustability—Resonator over 2 cm in length
Reflector Angle to 0.1 arc second resolution

Exciter—New simplified controls
Plasma Tube warranted for 300 continuous hours
(will usually run 500 continuous hours)
High precision End Windows and Reflecting Mirrors

2. Optical Crystals for DOUBLE HARMONIC Wave Generation

Ammonium Dihydrogen Phosphate (ADP)
Potassium Dihydrogen Phosphate (KDP)
Quartz • Sodium Chlorate
Triglycine Sulphate (TGS)
Rochelle Salt (Potassium Sodium Tartrate)

- Prepared from High Purity Materials
- Grown to High Optical Quality Specifications

- Available in Bulk, Coarse Cut, Finely Polished Cubes, Prisms, Cylinders, etc.

Other Second Harmonic Crystals with suitable Non-Linear Dielectric Coefficients are becoming available.

Inquire NOW about your particular requirements for Crystals.

Write or Call for
Complete Literature

Semi-elements, inc.
Saxonburg Boulevard, Saxonburg, Pa.
Phone: 412-352-1548

The Optical Society of America

Officers of the Society

President	Stanley S. Ballard, Department of Physics, University of Florida, Gainesville, Fla.
President-Elect	Richard C. Lord, Spectroscopy Laboratory, MIT, Cambridge 39, Mass.
Past President	David L. MacAdam, Research Laboratories, Eastman Kodak Company, Rochester 4, N.Y.
Executive Secretary	Mary E. Warga, OSA, 1155 16th Street N.W., Washington, D.C. 20036
Treasurer	Archie I. Mahan, Applied Physics Laboratory, 8621 Georgia Avenue, Silver Spring, Md.
Editor of the Journal of the Optical Society of America	Deane B. Judd, National Bureau of Standards, Washington 25, D.C.
Editor of Applied Optics	John N. Howard, AFCRL, Bedford, Mass.

Directors-at-Large

** Term expires December 31 of the indicated year.*

Rudolf Kingslake (63)* Eastman Kodak Company, Rochester 4, N.Y.
Earle K. Plyler (63)* Department of Physics, Florida State University, Tallahassee, Fla.
David Richardson (63)* Bausch & Lomb, Inc., Rochester 2, N.Y.
Georg H. Hass (64)* ERDL, Fort Belvoir, Va.
R. Clark Jones (64)* Polaroid Corp., Cambridge, Mass.
E. D. McAlister (64)* Scripps Institution of Oceanography, La Jolla, Calif.
W. Lewis Hyde (65)* University of Rochester, Rochester 20, N.Y.
John A. Sanderson (65)* Naval Research Laboratory, Washington 25, D.C.
George Wald (65)* Biological Laboratories, Harvard University, Cambridge 38, Mass.

Local Sections

Rochester	Joseph L. Rood *President* Robert M. Blakney *President-Elect* Joseph H. Altman *Secretary* Research Laboratories Eastman Kodak Co. Rochester 4, N.Y. Vernon L. Parks *Treasurer*
Niagara Frontier	E. Schustik *President* Thomas Frost *President-Elect* Calvin W. Young *Secretary* Carborundum Metals Co. Box 32, Akron, N.Y. Ray Annino *Treasurer*
New England	David S. Grey *President* Charles Koester *Vice-President* Geoffrey Harvey *Secretary* Itek Corporation 10 Maguire Rd. Lexington, Mass. William J. Davis *Treasurer*
Texas	P. O'B. Montgomery *President* Harry J. Auvermann *President-Elect* Norman C. Allen *Secretary-Treasurer* Texas Instruments, Inc. Box 6015 Dallas 22, Tex.
Delaware Valley	Morton L. E. Chwalow *President* George J. Rayl *President-Elect* Marvin E. Harper, Jr. *Vice-President, Programs* Marvin E. Gonshery *Vice-President, Membership* Harry M. Fitzgerald *Secretary* Frankford Arsenal Philadelphia, Pa. 19137 Edward R. Sanders *Treasurer*
Pittsburgh	Thomas P. Vogl *President* Jerome J. Wolken *President-Elect* George L. Buc *Secretary* Fisher Scientific Company 717 Forbes Street Pittsburgh 19, Pennsylvania Irving S. Stapsy *Treasurer*
Chicago	Harold Bennett *President* Howard Padgitt *Vice-President* Carl R. Lambrecht *Secretary* 7729 N. Ashland Avenue Chicago 31, Ill. Edward L. Somerville *Treasurer*
Southwestern Connecticut	Frank Wong *President* Abe Offner *Vice-President* Bennett Sherman *Secretary* Barnes Engineering Company 30 Commerce Road Stamford, Connecticut Irving Abel *Treasurer*
Southern California	Ernest Davidson *President* Wm. S. Gallaway *Vice-President* Milton Laikin *Secretary* 1913 Preuss Road Los Angeles 34, Calif. Jerome J. Rosenblatt *Treasurer*
Northern California	Clyde C. Shaw *President* John D. Armitage *Vice-President* Harvey Morton *Secretary-Treasurer* Tinsley Laboratories 2448 Sixth Street Berkeley, Calif.
National Capital	Matthew P. Thekaekara *President* Frederick W. Paul *First Vice-President* Harry K. Hammond, III, *Secretary* National Bureau of Standards Washington 25, D.C. Richard S. Hunter *Treasurer*
San Diego	E. D. McAlister *President* John M. Hood *Vice-President* Herschel R. Snodgrass *Secretary-Treasurer* General Atomic P. O. Box 608 San Diego 12, Calif.
Detroit	Carl J. Leistner *Chairman* W. K. Lesnick *Chairman-Elect* D. L. Harmon *Secretary* University of Detroit Detroit, Mich. Samuel Cohen *Treasurer*

The Optical Society of America was organized in 1916 **"to increase and diffuse the knowledge of optics in all its branches, pure and applied, to promote the mutual interests of investigators of optical problems, of designers, manufacturers and users of optical instruments and apparatus of all kinds and to encourage cooperation among them."** The Society invites to membership all who are interested in any branch of optics, either in research, in instruction, in optical or illuminating engineering, in the manufacture and distribution of optical goods of all kinds, or in physiological and medical optics. Further information may be obtained from the Executive Secretary of the Society. **Annual Dues:** Regular members and Fellows, $17.00; Associate members, $13.00; Corporate members, $125.00. These dues include subscription to the Society's official journal, the **Journal of the Optical Society of America**, but not to its other publications.

Automatic Optical Design

Donald P. Feder

Automatic computing methods are being increasingly applied to optical design, and the development of programs for this purpose forms an interesting chapter in optical history. Mathematically, the problem consists of solving sets of simultaneous nonlinear equations in a space of thirty or more variables limited by prescribed boundaries. Although these boundary conditions do not basically alter the mathematics, they greatly complicate the resulting program, and a specific example reveals how intricate such programs can become. The full impact of automatic methods has not yet been felt, but one result should be to shift the attention of the lens designer from the detailed correction of aberrations to the problem of securing a proper compromise between the system requirements and the conditions for sharp imagery so that better balanced optical instruments may result.

The art of optical design has been profoundly affected by the revolution in computing that has occurred during the past fifteen years. Several automatic design programs have now been in operation long enough to give considerable experience in their use. The time required to design a complicated lens has been cut from months to days, in some cases to hours. Designs have been produced whose quality exceeds those computed by conventional methods. Design times of a few days will soon become the rule rather than the exception, and further improvements in quality may be anticipated.

This paper will discuss the history of automatic design, give a mathematical formulation of two suitable methods, and finish by describing the particular program most familiar to the author. At the very outset, however, we must consider the word "automatic" used in the title. The author has a very distinct mental image of what he means by this word but recent discussions with other lens designers have shown that no common basis exists for its use in this connection. Therefore, in order to avoid misunderstanding, the author will attempt to spell out in detail his concept of "automatic optical design".

I. Meaning of the Title

Imagine a scale of automation going from 0 to 1. At the zero end sits a man with a table of logarithms. Every change in the system is under his control. He alone decides when a curvature is to be increased or a glass changed. Working with a combination of computing skill, experience, and art, he is the traditional optical designer. At the unit end of the scale is the hypothetical program accepting as input the following specifications:

> To design an aerial camera lens capable of transmitting N bits of information per second from objects 12 km below. The program is to select the focal length, field angle, aperture, number of elements, glasses, curvatures, thicknesses, and all other necessary data so as to optimize a merit function consisting of an appropriate combination of cost and weight.

Between these two extremes many degrees of automation are possible. Almost everyone now traces rays automatically. Many have analysis programs to compute spot diagrams, energy distributions, and the like. A variety of semiautomatic programs could be placed near 0.5 on our scale. They range from simple ones to correct third-order imagery in systems of thin lenses to those dealing with higher order aberrations of thick lenses. Finally, near 0.75, could be placed those programs containing several thousand instructions directed to large fast computers and able to carry an initial design to practical completion with little intervention by the designer.

Let us examine these requirements in some detail.

A. The "Automatic" Program

An automatic program, in my opinion, should fulfill the conditions outlined below.

The input is to be of three kinds:

The author is with the Eastman Kodak Company, Rochester, New York.

Received 16 August 1963.

(*1*). *Specifications for focal length, field coverage, aperture, minimum corner illumination, number of elements, minimum glass thicknesses, maximum diameter of each element, minimum back focal length, and spectral range.*

(*2*). *A set of weighting factors assigning the relative importance of various image defects, such as distortion, chromatic aberration, lack of sharpness, lack of contrast, etc.*

(*3*). *An initial starting point consisting of data from a partially completed design.*

The output is to be a design meeting the original specifications and ready for fabrication. Its performance is to be optimum for its type. With the possible exception of changing weighting factors, the lens designer should not have to interfere with the program after it has been started.

Certain aspects of these requirements need elaboration. The initial starting point, for example, may be as crude or as finished a design as desired. At one time the idea of starting from a system of thin glass plates received considerable attention. The advantage of handicapping oneself in this way was not made clear, and it is our personal opinion that any yielding of control to the automatic program ought to be accompanied by a tangible gain in speed or convenience. On the other hand, it is perfectly feasible to start with a rough design based on a sketch made on a drafting board (see, for example, "The Symposium Lens--An Epilogue", this issue, p. 1227).

The requirement that the design be an optimum should be understood to mean that any small change in it would cause it to deteriorate. In other words, an optimum design is better than all other designs in the immediate neighborhood. More than this is at present impracticable, and indeed, even if one succeeded in designing the best possible lens, no method exists for verifying the fact. Fortunately, practical experience indicates that lenses satisfying the optimum criterion are very good indeed. It appears likely that a given type of lens possesses only a very few optima, and that these can all be reached by starting from different initial designs.

It has been suggested that such a program should be called an automatic "improvement" program rather than an automatic "design" program. While this viewpoint is technically correct, we think it fails to emphasize sufficiently the impact of automatic methods on optical design. In the case of the Symposium lens, the starting point was nothing but a combination of casual guesses furnished by a group of lens designers. To dignify by the word "design" such a set of radii, thicknesses, and glasses seems a bit far-fetched. The improvement brought about by the program was several orders of magnitude, and the final design bore only a remote resemblance to the initial one. If the use of the word "design" is denied to such a program, it is difficult to see where it can be applied at all. Just picture the indignation of a human who, upon achieving the same success, finds that he is not entitled to be called "designer"!

II. History

The history of automatic optical design might be said to date from 1950. Even before this, however, farseeing individuals were predicting the possibility and occasionally suggesting methods which might be suitable. In 1945 Arthur C. Hardy indicated to James G. Baker that he visualized an era not far away when machines could run rapidly through all possible optical designs and arrive at the one best for a given application. Even earlier, in 1941 R. Minkowski had suggested to the National Defense Research Council that the method of least-squares might be applicable and should be investigated. Undoubtedly, there were other suggestions of this kind, but they fell mostly on incredulous ears. Furthermore, it must be admitted that the facts as they were then known supported the view of the professional lens designer that no machine would be able to design a lens.

Consider, for example, a simple triplet. Supposing that the glasses and their thicknesses have been preselected, there are six radii and two air spaces available to the designer. If we assume that each of these numbers has only ten distinguishable values, we find the enormous number of 10^8 possible different triplets. Even today the problem of analyzing all possible triplets is beyond the capacity of any computer. But even supposing such a computer to exist, one has only to ask what happens when two more elements are added. At least seven new variables are introduced, and the number of designs is multiplied by $10.^7$ A hypothetical machine capable of handling the triplet problem in one hour would need a thousand years for the five-element lens! It is clear that we are dealing with a combinatorial problem, and that no possibility exists for solving it by simply listing all the possible combinations.

The possibility remained to program the computer to design a lens in a manner similar to that used by a human being. However, a human seems to possess the ability to visualize a complex situation in a way essentially different from a digital computer. For example, one can represent a black-and-white picture by a table of binary numbers. (This is easily done in a halftone reproduction where a dot corresponds to a 1 and no dot to a 0.) If a computer were presented with such a table and asked to recognize a familiar object, it could probably do it, but the necessary program would be cumbersome, to put it mildly. By contrast, a lens designer could readily recognize a picture of a Biotar, a Tessar, or a Cooke triplet. Furthermore, his recognition would take place almost instantaneously in the time scale of human reflexes.

Nor would it matter much whether it was a carefully drawn picture or a rough sketch, whether the axis was horizontal or tipped, whether it was drawn by black lines on white paper, or the reverse. Such variations in form, however, would immensely complicate the problem for the digital computer. Of course, we are not playing fair, because if the human were presented with the table instead of the picture, he would be no better off than the machine. But the fact remains that the human *can* make effective use of the picture whereas the digital computer cannot. Not only that, but the human can often dispense with an actual physical picture and utilize a mental image instead and in addition he can alter this mental image and use it as a basis for logical operations, which is to say he can "reason" about it. By combining these human abilities with some optical theory and using a minimum of computation, the lens designer has been able to thread his way through his N-dimensional maze and emerge with a design. The problem of programming a digital computer to design a lens in this manner seemed a formidable task in 1945 and, to the author at least, still seems a formidable task in 1963.

Although lens designers were dubious of automatic design, it must not be imagined that they rejected automatic computers. In the early fifties there was such a rush to get aboard the bandwagon that ray-tracing programs sprouted up all over, and many new computers cut their baby teeth on optical problems. As early as 1944, Baker used the Mark I Calculator at Harvard for tracing some skew rays.[6] This is believed to be the earliest use of automatic computing machines for ray tracing. It required 120 sec to trace one ray through one surface on the Mark I. In 1945, Grosch used IBM equipment for the tracing of meridional and skew rays,[7] and later, in 1949, he used the Selective Sequence Electronic Calculator for the same purpose.[8] By and large these attempts were handicapped because the early machines were too slow and cumbersome. By March of 1950, however, the Card Programed Calculator (CPC) was made available for optical work at the National Bureau of Standards.[9] The CPC soon became widely distributed, and was used for ray tracing by various groups for several years until it was gradually displaced by faster machines. At almost exactly the same time (March 1950) the National Bureau of Standards put its new computer into operation. The Standards Eastern Automatic Computer (SEAC) was the first machine in the U.S. with an internally stored program, and it was a thousand times faster than the Mark I. One of its first tasks was the tracing of optical rays,[10] but it was soon occupied by such high priority military work that it was not available for optics until 1953. During this period, a group at the Bureau used the CPC extensively for ray tracing. Our principal responsibility there was to analyze optical designs submitted by the Air Force. When SEAC again became available, the work was greatly facilitated.

It is noteworthy that personal experience with electronic computers, acquired in the early fifties, caused some of us to change our attitudes toward the possibility of automatic design. This was especially true for those fortunate lens designers who were able to do their own programming. For one who had traced rays on a desk calculator for several years, it was a stimulating experience to write a ray-tracing program. We recall feeling that for the first time, we now really understood the problem. Writing such a program gives unexpected insight into the nature of ray tracing and indirectly into lens design itself. The ability of an automatic computer to make decisions based upon the results of its calculations is one of the most striking facts observed by the neophyte programmer, and it became clear that this ability would be essential to any design program. Another property of a computer is its suitability for repetitive operations, and optical design is nothing if not repetitive. One starts with a trial design, analyzes it, makes a change, and arrives at a new trial. One repeats the process until either a satisfactory solution is found or until all hope is gone.

A. The Merit Function

During this early period, it became clear to many people that other possibilities existed for the automatic design of lenses different on the one hand from an impossible program to search blindly through an N-dimensional space for the best design, and different on the other from an unlikely program which would simulate a human optical designer. Coming back to the problem of searching an N-dimensional space, it became obvious that what was needed was some kind of guiding principle.

Remember the childhood game in which one child tries to guide another to a hidden object by crying "warmer" or "cooler"? In a similar way, we need to associate with each point in our space a kind of "temperature", which we call a merit function. This idea is so fundamental that it occurred to many people and no one individual can claim credit for it. However, there has been some misunderstanding of the idea, and some people have thought it represented a *special* approach to automatic optical design. Some have even attempted to differentiate between automatic design programs on the basis of whether they did or did not employ a merit function. In fact, however, the idea of a merit function is basic to any type of design, whether optical or not and whether conducted by automatic methods or not.

Suppose one has a collection of designs intended for a certain application and is faced with the problem of choosing one for manufacture. Frequently information about the intended application is lacking or incomplete, and, in this case, specific assumptions must be made to fill in the gaps; otherwise a choice could not be made. In the case of only two designs, one must be able to write one of the following statements:

$$\left.\begin{array}{ll}\text{Design } A \text{ is preferred to design } B. & (A \supset B)\\ \text{Neither design } A \text{ nor design } B \text{ is preferred.} & (A = B)\\ \text{Design } A \text{ is less preferred than design } B. & (A \subset B)\end{array}\right\} \tag{1}$$

These expressions define the operation of preference. It is perhaps unnecessary to state that this operation must satisfy the law of reflexivity. That is,

$$A \supset B \rightarrow B \subset A, \qquad A = B \rightarrow B = A. \tag{2}$$

If the set contains more than two elements, the operation of preference must satisfy the law of transitivity. That is,

$$\begin{aligned} A \supset B \text{ and } B \supset C &\rightarrow A \supset C,\\ A = B \text{ and } B = C &\rightarrow A = C. \end{aligned} \tag{3}$$

Transitivity is somewhat restrictive; for example, the operation "beat" does not satisfy it. (Consider the football scores.) Nevertheless, a designer who simultaneously prefers A over B, B over C, and C over A, is really in difficulty, for that way lies chaos.

Once the preference rule has been stated for two elements, it is possible to impose an ordering upon a collection of designs. That is, one can write $A \supseteq B \supseteq C \ldots \supseteq N$. (The symbol $\supseteq$ implies one or the other of two mutually exclusive events; either $A \supset B$ or $A = B$. A slight ambiguity arises in the ordering for the case of equal preferences, but this creates no difficulty in practice.) Actually, one can go a step further and number the designs in order of the preference. One has $A_1 \supseteq A_2 \supseteq A_3 \supseteq \ldots \supseteq A_N$. By this procedure each design in the collection is related to a positive integer, namely, the subscript. Such a relation can be considered a merit function. In other words, a merit function is any function which maps a collection of designs onto the positive integers according to a stated preference rule. The above definition applies only to a finite collection but can be generalized for the infinite case. The collection becomes infinite when one or more design parameters varies continuously over some interval. In this event one makes the obvious change of replacing the integers by the real numbers. The definition may be written formally as follows:

> *A merit function is any function which maps the design space upon the set of positive real numbers in a manner consistent with the preference rule. That is, if D is a design, and φ a real number, then $\varphi_1 < \varphi_2$ if and only if, $D_1 \supset D_2$.*

In this view, therefore, a merit function is simply a convenient way of expressing the preferences of the designer. The order here is important. It is the preferences which determine the merit function, not the merit function which determines the preferences. Uniqueness is not implied; any function consistent with the preference rule is allowed.

Having conceded the existence of such functions, one is left with the problem of selecting one suitable for optical design. From a mathematical standpoint it is desirable that the function be continuous and differentiable in the design parameters and also easy to compute. By far the most common choice for a merit function is the one employed by Legendre in the classical method of least-squares. If $(f_1, f_2, \ldots f_M)$ are a set of residual image errors, and $(\mu_1, \mu_2, \ldots, \mu_M)$ a set of positive weighting factors, then the merit function φ is defined by the equation

$$\varphi = \mu_1 f_1^2 + \mu_2 f_2^2 + \ldots + \mu_M f_M^2. \tag{4}$$

There are many ways to chose the (f_j). They could be elementary aberrations such as ray or wavefront deviations for selected rays. But equally well, they might be combinations of elementary aberrations. Such combinations could be used to represent the frequency response of a lens or the distribution of energy in the image of a point source. To be complete, they should include terms representing the color correction and distortion of the lens as well as the monochromatic image sharpness. However chosen, the (f_j) are ultimately functions of the lens parameters $(x_1, x_2, \ldots x_N)$.

This type of merit function has many advantages. The quantity φ is a positive number which is zero only if all the residuals are zero (a perfect lens!). With appropriate choices for the (f_j) and their associated weighting factors (μ_j), the function φ can be made to satisfy the basic definition for a merit function. It means that the values of φ correspond to the preferences of the lens designer. We recognize his preference by his action upon being confronted with two different designs. He must decide which to keep and which to discard. In the ordinary course of design such decisions must be made many times. Explicit use of a merit function supplies the automatic program with a decision rule which is in accordance with the previously expressed wishes of the lens designer. The novelty of the idea lies in the words "explicit" and "previously expressed". In manual work, the designer makes each decision as he comes to it. This is the happy-go-lucky approach, but it lacks both consistency and precision. The necessity of preparing his decisions in advance forces the designer to use much greater care and this in turn will, in the long run, lead to lenses having a better balance of aberrations.

B. The Harvard Study Group

The first serious attempt at automatic optical design was made by a study group at Harvard University under the direction of James G. Baker and financed by the Air Force through a contract with the Perkin-Elmer Corporation. It extended over a four-year period from 1951 to 1955, and the results are contained in a series of technical reports titled "The Utilization of Automatic

Calculating Machinery in the Field of Optical Design".[13] The fact that these reports were classified until 1959 not only prevented the work of the study group from becoming widely known but also lessened the impact that it otherwise would have had. Reading these reports in the light of present knowledge turned out to be a stimulating experience. Baker writes in a conversational style which allows the reader to share in the development of the ideas and to sense both the frustrations and the achievements incidental to the progress made by the group. This progress was made despite such difficulties as personnel turnover associated with short-term contracts and the quirks and general balkiness of the early electronic computers.

The actual accomplishments were impressive. At least one of the methods of automatic design in successful use today was anticipated by this group. If one turns to Report #6, written in May 1953, one finds a rather complete discussion of a series of mathematical methods applicable to automatic lens design. A merit function similar to that already described, consisting of a weighted sum of squares of the residual aberrations, was employed as the basic tool. Various methods of minimizing this function were then discussed. Among them was one they called the *squared weighting scheme*. This has been variously termed by other workers the *optimum-gradient method* or the *steepest-descent method*, and is basically the same as described by Cauchy[1] in 1847. One takes an arbitrary starting point in the parameter space (i.e., an arbitrary initial design), and computes the merit function φ and its derivatives with respect to the system parameters. Starting at this initial point, one moves in a direction along the gradient, but in the opposite sense so as to reduce φ. One continues in a straight line to a point at which φ begins to increase and then repeats the entire calculation with this new starting point. Baker also called this the zig-zag method, and observes that after the first few iterations, it converges very slowly. In another place he remarks*

> What actually takes time with the fully automatic approach is the very slow convergence of the design to final form. In months ahead the most difficult task confronting us will be to explore the best means for overcoming the convergence problem.

This comment touches the heart of the problem. The gradient method is the most general approach, the simplest to program, and easiest to understand of the possible methods for minimizing a function of several variables. Nevertheless, it suffers from very slow convergence. This fact was soon discovered by each worker in the field although the source of the difficulty was not always understood. Sometimes it was blamed upon the nonlinearity of the functions or upon the existence of a large number of local minima in the merit function. It turns out, however, that the gradient method will converge very slowly even if the basic functions are exactly linear. This was known to people working in numerical analysis at least as early as 1952, when a paper was published by Stein discussing the convergence for a set of six simultaneous linear equations.[11] It was again[21] pointed out by the author in 1957, and perhaps it still needs more emphasis. Clearly any method suitable for nonlinear equations ought to be capable of handling linear ones very rapidly, since a linear set can be regarded as a special case of a nonlinear set with vanishingly small higher order terms. The ordinary gradient method, however, converges so slowly that it would be impracticable, for example, to apply it to a set of twenty linear equations of a type solved by the usual elimination procedure in a few seconds. This difficulty naturally is accentuated if the equations are ill-conditioned, as they are in optics.

Various ways of improving the convergence of this method were tried by the Harvard group. From the author's own attempts in this direction, however, we would doubt whether any of the various accelerating techniques which they tried could have been really satisfactory. Because of this difficulty, another approach was made, which was basically the method of least-squares invented by Legendre[2] about 1805. Originally, it was intended to solve overconstrained sets of linear equations by minimizing a function consisting of the sum of the squared residuals. Later it was extended to the nonlinear case by the use of a linearization technique,[3] and in this form it was later discussed by Rosen and Eldert in a paper[15] on optical design published in 1954.

The linearization technique consists in expanding the functions into Taylor's series and neglecting higher order terms. In the optical case one obtains a set of simultaneous linear equations for the aberration functions expressed in terms of the parameters of the system. The number of parameters can be less than, equal to, or greater than the number of equations. In most practical lens-design problems the number of parameters is less than the number of equations. Such a set is said to be overconstrained, and one can apply the least-squares procedure to obtain a solution which minimizes the sum of the squares of the aberrations. Although the solution is in error owing to the neglect of the higher order terms, the aberrations may have been reduced from their original values, and if this is the case, the entire process can be repeated using the first solution as a new starting point. One may continue in this fashion until a stable solution is reached and successive iterations produce no further changes in the parameters. If this happens, a minimum has been found and the process is called convergent. It is a matter of practical experience that, when the process converges, the speed of convergence is much greater than in the gradient method. On the other hand, if the equations are sufficiently nonlinear, the process will diverge, and if this occurs, the characteristic behavior of the solution vector is to oscillate wildly about the minimum without ever getting close to it. This, in fact, seems to be the normal behavior of the method when used in optical design.

---

* See Technical Rept. #7 in ref. 13.

It is quite apparent from reading Technical Report #6 that Baker was familiar with the oscillatory behavior of the least-squares method. In order to force convergence, a method is discussed for damping the oscillations of the solution vector. This method will be described in detail in Sec. III D. It was first published by Levenberg[4] of Frankford Arsenal in 1944 but did not come to the author's attention until 1956. Apparently, it was developed independently by the Harvard group and first applied to optical design in 1953. One gathers that they acquired considerable practical experience in using the method and became well satisfied with it. (See page 16 of Technical Report #12, ref. 13.)

One might ask whether an automatic design method had been developed by the Harvard group at the time of its final report in 1955. If one means by the question, whether they had a running program, turning out designs in a routine manner, then the answer is probably no. In the first place Mark IV was a slow machine even by 1955 standards. It required about 1 sec per surface for tracing a ray. With the programs available today, a minimum speed of ten surfaces per sec is required to make automatic optical design feasible. In the second place the study group was not allowed the use of Mark IV on a routine basis and, when it became clear that no funds were available for using the faster machines just coming on the market, the entire contract was terminated at Baker's request. On the other hand, the group had the know-how to assemble a workable program although it is probable that they were not yet sure which of their various methods were most suitable, and that this knowledge would have to wait for sufficiently fast computers to make any method practicable. They understood the importance of weighting and were concerned to develop appropriate methods for handling boundary conditions. The change in attitude toward the problem of automatic design is admirably expressed by Baker in the following quotation taken from a supplementary report dated 31 May 1954:

> The author must confess that at the beginning of the project he believed that the electronic calculator would indeed reduce the tedium of the extensive calculations always required in the design of complex optical systems, but felt that a designer would still be needed for making judgments hardly suited to the inflexibility of the machine.
>
> During these two years of application of computing machinery to optical design, the above described beliefs of the author have undergone transformation to the point where it now seems clear that the very fastest electronic machines can do the entire task of optical design and can produce superior designs. The question devolves largely into a matter of expense.

C. The University of Manchester

Partly overlapping the Harvard work was that of Black in England. It was sponsored by the British Scientific Instrument Association and conducted at the University of Manchester, where a Ferranti calculator was available. The author visited Black in 1954 to discuss the problem of optical design. We have always been grateful for that visit, because his example encouraged us to attempt our own programming, which up to that time had been done by others. This personal experience with an electronic computer was instrumental in convincing us of the feasibility of automatic methods.

Black reported on this work[16] in 1955. He used a merit function similar to that of Baker, but, instead of computing derivatives, he used a variable-by-variable method in which φ is successively minimized with respect to one variable at a time. This method behaves much like the gradient method. In its simplest form, it is too slow even for linear equations. It possesses the characteristic property of the gradient method of producing large improvements in φ for the first few steps and then tapering off until further improvement is negligible. In order to accelerate the procedure, Black employed what he called "block" and "group" operations. A "block" operation is similar to a bending in that two or more variables are changed simultaneously. A "group" operation is an extrapolation, which is carried out after a series of simpler changes have already produced a sensible improvement in the design.* Although the work was not continued long enough to be completely fruitful, Black was nevertheless able to employ these methods in the improvement of certain lenses.

There have been occasional isolated papers on the subject, and one such was written by Wachendorf in 1955.[19] This paper gave an excellent discussion of the conditions to be satisfied for a lens system to be optimum and also considered the problem of choosing a suitable merit function. Unfortunately, he was not able to try out his methods in practice because of the difficulty of getting sufficient machine time.

---

* In this method Black appears to have anticipated in part the procedure now known as "direct search" published by Hooke and Jeeves in 1961.[34]

D. The Institute of Optics

Although the fundamental problem of optical design may not be so difficult, it possesses a complicated structure not easy to enclose in a neat little package readily solved by a mathematician. The nature of the problem requires an extended siege rather than a single quick thrust. Such a sustained assault has been conducted by Hopkins and his associates at the University of Rochester from 1955 to the present. The approach taken by Hopkins has, in our opinion, been largely conditioned by the type of computer available at the University. Until recently this consisted of an IBM 650, which has neither the speed nor the memory capacity for automatic design. It has now been replaced by an IBM 7074, which considerably extends the computing capacity of this group.

The earliest work published by Hopkins describes the automatic correction of third-order aberrations with the aid of a Card Programed Calculator.[18] This program was suitable only for lenses whose individual elements are reasonably thin so that bending is an effective means of correction. Since the powers were held approximately constant, the only aberrations which could be controlled were spherical, coma, astigmatism, and (to a limited extent) distortion. The derivatives of these aberrations were computed with respect to the bendings of the separate elements, and a system of three or four linear equations solved to reduce the aberrations. Because the functions are nonlinear, the process had to be iterated until a stable solution was reached. The authors state that the method was used successfully on various types of lenses, including doublets, triplets, Tessars, Biotars, and inverted telephotos. Generally four or five iterations were sufficient for convergence.

Despite the fact they were using an undamped linearization method, they apparently had little difficulty with convergence. Several things may account for this: (a) By restricting the problem to third-order aberrations which could be corrected by bending alone, they had only three or four equations to solve instead of thirty or forty. (b) The use of bending is equivalent to a favorable choice of metric. (c) The initial design was picked to lie near what experienced designers hoped was a solution. (d) Finally, the progress of the solution was closely observed, and if oscillatory behavior developed, the program was stopped and steps taken to remedy the trouble. This usually occurred when one of the separate aberrations was near a minimum, and a power change was all that was needed to get convergence.

Since the program did not consider boundary conditions or higher-order aberrations, it occasionally took out after a solution not considered feasible. In this event, the solution was rejected and a new starting point selected. Also, in the case of lenses having more than three or four elements, a problem arose of how to choose the independent variables. This was solved by McCarthy in a note[20] published later in 1955. The solution is identical with the damping method used by Baker for the case where the number of equations is less than the number of variables.

From this beginning the methods were gradually expanded. In 1959 an IBM 650 program was written to obtain least-squares solutions for telescope doublets.[29] In 1960 two of Hopkins' students, Hennessy and Spencer, described a program[31] from which many of the earlier restrictions had been removed. Both power changes and bendings were allowed so that all the third-order aberrations could be controlled. The usual starting point was a third-order solution for a system of thin elements. Certain refinements were introduced into this program to deal with such things as reflecting surfaces, stop position, and aspheric surfaces.

The present methods used by Hopkins and his colleagues are similar to these early methods, but a good deal more elaborate. Automatic correction of the third-order and fifth-order aberrations is the keystone of the method. These can be corrected to target values, or else a merit function consisting of the sum of their squares can be minimized. A combination of these two procedures is also available. When this is used, certain errors are corrected to target values and others are minimized. A program incorporating these features is called ORDEALS, and the second paper in this issue (p. 1227) deals in part with an actual design produced by the aid of the ORDEALS program.

The work of this group has been characterized by a gradual transition to more and more automatic methods. This approach may be conservative, but it has the great advantage that they always have a working program available to solve current problems. A more radical approach might have left them in the position of being unable to complete any design until a sufficiently fast computer became available. Nevertheless, it must not be assumed that they are disinterested in fully automatic methods. One of Hopkins' students has been encouraged to write a generalized design program intended for the 7090, and this work is also reported in this issue (p. 1257). It is clear that the acquisition of the new computer will make more fully automatic methods available to this group. (See also refs. 37, 38, and 42.)

E. National Bureau of Standards and Eastman Kodak Company

The author's own work started in 1954 when SEAC again became available for optical design. The SEAC, designed and built at the National Bureau of Standards, had a total internal memory of 1024 words and some rather primitive magnetic tape units. Its operating speed was about 400 multiplications per second, so that it took an eighth of a second to trace a ray through a single surface. The output facilities were not extensive, and the printout had to be kept at a minimum. The first automatic program for this machine was written in 1955 and the results[21,22] reported in 1957. A gradient method was used to reduce a merit function consisting of a weighted sum of the squares of wavefront deviations, chromatic aberrations, distortion, and boundary violations. By varying curvatures, thicknesses, and glasses, the program was able to improve simple lenses such as triplets, but it was soon realized that the rate of convergence needed to be increased. Therefore, after joining Eastman Kodak in 1957, the author embarked on a series of numerical experiments with various methods of solving nonlinear equations and, as a result, a program was written using the conjugate-gradient method. This was developed by Hestenes and Stiefel[12] for solving linear equations, but it can readily be extended to the nonlinear case.

The new program also contained a much better technique for treating boundary conditions as well as a method for controlling the back focal distance. The program was in operation by 1960 and has been undergoing gradual improvement since that time. Some of the early experiments[39] with it were reported in 1962. At that time the author was still plagued with problems of convergence, some of which turned out to be connected with rounding errors that were alleviated by using ten-decimal accuracy in the ray-tracing routine. Even this is not sufficient, and it has just been increased to eleven places. This is particularly easy to do in a computer having a variable word-length such as the IBM 7080 which we are using. The 7080 is the business version of the 7090 and, while perhaps an order of magnitude slower than the latter, is nevertheless an acceptable machine for automatic lens design. It has 8000 ten-character words of internal memory backed up by ten tape units. The present program intended for this machine is described in more detail in Sec. IV.

F. Other Foreign Work

By 1959 automatic computers were becoming generally available and several new papers appeared about this time. Among the most readable of these were two by Wynne, at that time associated with Wray Optical Works but now at Imperial College in London.[25,26] The first paper gave a general discussion of the convergence problem and suggested a method for solving it. Wynne called this SLAMS, but it is identical with the "Damped Least-Squares" method invented by Levenberg and first used in optical design by Baker. The second paper showed the method in actual application. Before becoming interested in automatic computers, Wynne had already had considerable experience in optical design, and he has a very clear physical picture of the processes involved which, coupled to a facility for expressing himself clearly, has made his work very accessible and easy to read.[37] On a visit to Rochester last year he showed the author several results from his work which consisted of improved designs that seemed to be very meritorious. He hopes shortly to acquire an extremely fast machine, and we may expect that he will turn out noteworthy designs at an accelerated pace. The latest contribution by Wynne is to be found also in this issue (p. 1233).

Slightly before Wynne's paper appeared, Girard published a doctoral thesis on automatic design in *Revue d'Optique*.[24] The ideas expressed in this thesis fall within the main stream of development outlined so far. They include the definition of a standard type of merit function and appropriate methods for reducing it, one of which is the damped least-squares method mentioned above. It is clear that Girard did not have at his disposal at that time (1958) a computer of sufficient speed and capacity to carry out his ideas to their full extent but his approach seems perfectly practical and, given a computer, it should yield very tangible results.

The work of Meiron, formerly at the Weizmann Institute of Science at Rehovoth, is summarized in a series of three papers[23,27,30] published starting in 1957. All of these are based upon the reduction of an explicit merit function by various techniques. The first is a steepest-descent method; the second is the standard method of least-squares, and the third is a variation of the variable-by-variable minimization called by Meiron the "Parabolic Approximation Method". Meiron is now at the Perkin-Elmer Corporation, where he is continuing this work.

Before closing this historical account, it is necessary to mention the interesting program which Grey has written for the 7090. It is the author's opinion, based partly on personal conversations with Grey, that the concept of orthonormal aberrations developed in his paper[43] is closely related to the idea of a metric mentioned in Sec. III E. The idea is to find a linear transformation of the parameter space which improves the metric, and then to operate in this transformed space as long as consistent with the range of linearity of the functions. The program is now operating and, according to Grey, is yielding useful results.

III. Mathematical Treatment

The mathematical formulation of optical design can be discussed from many viewpoints. In this section, however, we want only to consider the problem of minimizing a given merit function defined in an N-dimensional space. The details of the function—how it is defined—how it is to be computed—are not to be considered. Such important things as ray-tracing formulas, evaluation of image errors of various orders, computation of energy distribution—are all to be ignored. We shall assume that you, the reader, know all about such matters or, if not, do not care.

A. Formulation

Suppose that the merit function is of the type already defined by Eq. (4), where $\varphi = \mu_1 f_1^2 + \mu_2 f_2^2 + \ldots + \mu_M f_M^2$. To simplify the notation, let us allow the weighting factor μ_j to be absorbed into the function f_j. Without any loss of generality, we can write

$$\varphi = f_1^2 + f_2^2 + \ldots + f_M^2. \tag{5}$$

In the previous discussion, accompanying Eq. (4), it was suggested that the individual f_j might be an elementary aberration such as a ray deviation or a complex combination of elementary aberrations. In any event, the (f_j) are functions of the lens parameters $(x_1, x_2, \ldots, x_N)$, and one may write formally

$$\left.\begin{array}{l} f_1 \ = f_1(x_1, x_2, \ldots, x_N) \\ f_2 \ = f_2(x_1, x_2, \ldots, x_N) \\ \cdot \\ \cdot \\ \cdot \\ f_M = f_M(x_1, x_2, \ldots, x_N) \end{array}\right\}. \tag{6}$$

The designer's problem is to choose a set of independent variables (x_k) which will cause φ to attain a minimum. In choosing the (x_k), however, the designer must stay within a region limited by certain boundaries. These can be expressed by the following set of inequalities:

$$\left.\begin{array}{ll} b_1(x_1, x_2, \ldots, x_N) & \geqslant 0 \\ b_2(x_1, x_2, \ldots, x_N) & \geqslant 0 \\ \cdot & \cdot\ \cdot \\ & \cdot\ \cdot \\ \cdot & \cdot\ \cdot \\ b_T(x_1, x_2, \ldots, x_N) & \geqslant 0 \end{array}\right\}. \tag{7}$$

Each of these inequalities expresses a condition of the type illustrated by the following statements:

(1) The center thickness of the negative element must be greater than 0.100.

(2) The edge thickness of the first lens must be $\geqslant 0.050$.

(3) The distance from the front vertex to the image plane must not exceed 1.100.

(4) The index of refraction of the last element must be $\leqslant 1.620$.

The care and feeding of boundary conditions is a vital part of the programmer's job and may represent as much as 50% of the instructions. Nevertheless their existence complicates the mathematics without altering the basic structure, so we shall defer their detailed treatment until Sec. III F.

Recognizing that certain basic quantities are useful in any method for minimizing φ, let us proceed to define these fundamental quantities.

B. Definitions

(1)

$$A_{jk} \equiv \partial f_j / \partial x_k \tag{8}$$

is the partial derivative of the jth function with respect to the kth variable. It may be computed by exact differentiation or approximated by the method of finite differences. We happen to use differentiation; it is immaterial as long as the accuracy is sufficient.

(2) The matrix*

$$\mathbf{A} \equiv \begin{pmatrix} A_{11} & A_{12} & \ldots & A_{1N} \\ A_{21} & A_{22} & \ldots & A_{2N} \\ \cdot & \cdot & & \cdot \\ \cdot & \cdot & & \cdot \\ \cdot & \cdot & & \cdot \\ A_{M1} & A_{M2} & \ldots & A_{MN} \end{pmatrix} \tag{9}$$

comprising all the above first partial derivatives is important in all the present methods for minimizing φ. It is an $M \times N$ matrix, where M is the number of residual image errors and N the number of independent variables. Ordinarily M is greater than N. In a typical example, $M = 60$ and $N = 35$.

(3) The quantity $\partial\varphi/\partial x_k$ is a component of the gradient of φ. By differentiating Eq. (5) with respect to x_k, one sees that

$$\frac{\partial\varphi}{\partial x_k} = 2\left(f_1 \frac{\partial f_1}{\partial x_k} + f_2 \frac{\partial f_2}{\partial x_k} + f_3 \frac{\partial f_3}{\partial x_k} + \ldots + f_M \frac{f\partial_M}{\partial x_k}\right). \tag{10}$$

It is convenient to get rid of the factor 2 by defining

$$G_k \equiv {}^1/_2(\partial\varphi/\partial x_k). \tag{11}$$

With this definition and the definition of A_{jk}, one can transform Eq. (10) to read

$$G_k = f_1 A_{1k} + f_2 A_{2k} + \ldots + f_M A_{Mk}. \tag{12}$$

(4) It is convenient to introduce at this point three matrices.* Since each of them consists of only a single column, they can be considered either matrices or column vectors. They are:

$$\mathbf{x} \equiv \begin{pmatrix} x_1 \\ x_2 \\ \cdot \\ \cdot \\ \cdot \\ x_N \end{pmatrix} \quad \mathbf{f} \equiv \begin{pmatrix} f_1 \\ f_2 \\ \cdot \\ \cdot \\ \cdot \\ f_M \end{pmatrix} \quad \mathbf{G} \equiv \begin{pmatrix} G_1 \\ G_2 \\ \cdot \\ \cdot \\ \cdot \\ G_N \end{pmatrix} \tag{13}$$

The column vector **x** defines a point in an N-dimensional space. Each of its components is a parameter of the lens so that each point corresponds to a particular design.

The components of **f** are the residual image errors so **f** itself may be thought of as being the residual vector. The vector **G**, of course, is equal to $^1/_2$ grad φ. By an extension of Eq. (12), one can write in matrix form the relation

---

* Throughout this paper boldface type will be used to represent vectors and matrices.

$$\mathbf{G} = \mathbf{A}^T\mathbf{f}, \tag{14}$$

where $\mathbf{A}^T$ is the transpose of the matrix $\mathbf{A}$. This is an important equation because at a point $\mathbf{x}$ where φ has a minimum, the vector $\mathbf{G}$ must be equal to zero.

(5) A linear approximation. Up to this point, no restrictions have been put on the form of the functions (f_j). If they should happen to be linear functions of (x_k), one could write

$$\mathbf{f} = \mathbf{A}(\mathbf{x} - \mathbf{x}_0) + \mathbf{f}_0. \tag{15}$$

In the case of interest to us, the functions are certainly not linear; nevertheless, Eq. (15) can be regarded as an approximation valid in a sufficiently small neighborhood around the point $\mathbf{x}_0$.

With the above definitions in mind, let us proceed to the consideration of two methods for reducing φ, both of which have been successfully employed in automatic optical design programs and both of which converge with reasonable speed.

C. The Conjugate Gradient Method

This method was developed by Hestenes and Stiefel to solve sets of linear equations.[12] In the linear case it is doubtful whether this method offers any advantage over the standard elimination method, but it turns out to be useful in the nonlinear case.

Let us first write down the equations for the optimum-gradient method and then indicate the changes necessary to convert it to the conjugate-gradient method. In the optimum-gradient method, one starts with an arbitrary initial point $\mathbf{x}_0$ and defines a sequence of points $\mathbf{x}_1, \mathbf{x}_2, \mathbf{x}_3 \ldots$ as follows:

$$\left.\begin{array}{lllllll}
\mathbf{D}_0 & = & -\mathbf{G}_0 & \qquad & \mathbf{x}_1 & = & \mathbf{x}_0 + h_0\mathbf{D}_0 \\
\mathbf{D}_1 & = & -\mathbf{G}_1 & & \mathbf{x}_2 & = & \mathbf{x}_1 + h_1\mathbf{D}_1 \\
\cdot & & \cdot & & \cdot & \cdot & \cdot\ \cdot \\
\cdot & & \cdot & & \cdot & \cdot & \cdot\ \cdot \\
\mathbf{D}_j & = & -\mathbf{G}_j & & \mathbf{x}_{j+1} & = & \mathbf{x}_j + h_j\mathbf{D}_j \\
\cdot & & \cdot & & \cdot & \cdot & \cdot\ \cdot \\
\cdot & & \cdot & & \cdot & \cdot & \cdot\ \cdot
\end{array}\right\} \cdot \tag{16}$$

The scalars $h_0, h_1, h_2, \ldots$ are chosen so that the equations

$$\mathbf{D}_0{}^T\mathbf{G}_1 = \mathbf{D}_1{}^T\mathbf{G}_2 = \mathbf{D}_2{}^T\mathbf{G}_3 = \ldots = \mathbf{D}_j{}^T\mathbf{G}_{j+1} = \ldots = 0 \tag{17}$$

are fulfilled. These products $(\mathbf{D}_j{}^T\,\mathbf{G}_{j+1})$ are simply dot products, and Eq. (17) states that the new gradient $\mathbf{G}_{j+1}$ is perpendicular to the previous direction vector $\mathbf{D}_j$.

From Eq. (16) it is seen that it is necessary to compute the gradient at each new point and then to take a step along the negative gradient. It may seem strange to define a direction vector $\mathbf{D}$ differing from the gradient $\mathbf{G}$ only by a minus sign, but in the conjugate-gradient method (as will be seen below) these two factors differ significantly.

To put the entire process in simple words: after arriving at the point $\mathbf{x}_j$, one computes the gradient $\mathbf{G}_j$ and follows it in the negative direction until φ stops getting smaller and starts to increase. At this new point the gradient $\mathbf{G}_{j+1}$ must be perpendicular to the direction of motion, and the procedure is repeated.

In the case of linear equations, the choice of h_j is facilitated by using the formula

$$h_j = G_j{}^2/H_j{}^2, \text{ where } \mathbf{H}_j = \mathbf{AD}_j. \tag{18}$$

This formula is a consequence of Eq. (17) and may be obtained as follows: the equation

$$\mathbf{x}_{j+1} = \mathbf{x}_j + h_j\mathbf{D}_j \tag{19}$$

is multiplied by the matrix $\mathbf{A}$, yielding

$$\mathbf{A}(\mathbf{x}_{j+1} - \mathbf{x}_j) = h_j\mathbf{AD}_j. \tag{20}$$

Since we are assuming for the moment that the functions are linear, we can use Eq. (15), which says that

$$\mathbf{A}(\mathbf{x}_{j+1} - \mathbf{x}_j) = \mathbf{f}_{j+1} - \mathbf{f}_j.$$

This gives

$$\mathbf{f}_{j+1} - \mathbf{f}_j = h_j\mathbf{AD}_j. \tag{21}$$

Multiplying by $\mathbf{A}^T$ and using Eq. (14), one gets

$$\mathbf{G}_{j+1} - \mathbf{G}_j = h_j\mathbf{A}^T\mathbf{AD}_j. \tag{22}$$

Finally, multiplying by $\mathbf{D}_j{}^T$ gives

$$\mathbf{D}_j{}^T\mathbf{G}_{j+1} - \mathbf{D}_j{}^T\mathbf{G}_j = h_j\mathbf{D}_j{}^T\mathbf{A}^T\mathbf{AD}_j = h_j(\mathbf{AD}_j)^T(\mathbf{AD}_j). \tag{23}$$

But

$$\left.\begin{array}{ll}
\mathbf{D}_j{}^T\mathbf{G}_{j+1} & = 0 \text{ from (17) and} \\
\mathbf{D}_j{}^T\mathbf{G}_j & = -G_j{}^2 \text{ from (16)}
\end{array}\right\}. \tag{24}$$

Hence

$$h_j(\mathbf{AD}_j)^T(\mathbf{AD}_j) = G_j{}^2 \tag{25}$$

which implies Eq. (18) immediately. For the nonlinear case, this equation gives a first approximation to the value of h_j. It can then be improved by interpolation to obtain a value of h_j for which $\mathbf{G}_{j+1}{}^T\mathbf{D}_j = 0$. This can always be done very readily in practice.

The necessary modifications to Eq. (16) to obtain the conjugate-gradient method are quite simple. By examining ref. 12, it can be seen that the modified equations become

$$\left.\begin{array}{lllllll}
\mathbf{D}_0 & = & -\mathbf{G}_0 & \qquad & \mathbf{x}_1 & = & \mathbf{x}_0 + h_0\mathbf{D}_0 \\
\mathbf{D}_1 & = & -\mathbf{G}_1 + (G_1{}^2/G_0{}^2)\mathbf{D}_0 & & \mathbf{x}_2 & = & \mathbf{x}_1 + h_1\mathbf{D}_1 \\
\cdot & \cdot & \cdot\quad\cdot & & \cdot & \cdot & \cdot\ \cdot \\
\cdot & \cdot & \cdot\quad\cdot & & \cdot & \cdot & \cdot\ \cdot \\
\mathbf{D}_j & = & -\mathbf{G}_j + (G_j{}^2/G_{j-1}{}^2)\mathbf{D}_{j-1} & & \mathbf{x}_{j+1} & = & \mathbf{x}_j + h_j\mathbf{D}_j \\
\cdot & \cdot & \cdot\quad\cdot & & \cdot & \cdot & \cdot\ \cdot \\
\cdot & \cdot & \cdot\quad\cdot & & \cdot & \cdot & \cdot\ \cdot
\end{array}\right\} \cdot \tag{26}$$

As before, the quantities h_0, h_1, h_2, ... are chosen to satisfy the conditions

$$\mathbf{D}_0^T\mathbf{G}_1 = \mathbf{D}_1^T\mathbf{G}_2 = \mathbf{D}_2^T\mathbf{G}_3 = \dots = \mathbf{D}_j^T\mathbf{G}_{j+1} = \dots = 0. \quad (27)$$

Again, as before, if the equations are linear, one has the same formula for $h_j = G_j^2/H_j^2$, where $\mathbf{H}_j = \mathbf{AD}_j$. If the equations are not linear, this value must be improved by interpolation to satisfy (27).

The important distinction between the conjugate-gradient method and the optimum-gradient method (or zig-zag method!) is that the former always converges to an exact solution in N steps or less when the equations are linear, whereas the latter converges too slowly to be of practical use. This means that a system of ten simultaneous linear equations is solved in ten steps of the conjugate-gradient method instead of perhaps 10^7 steps of the optimum-gradient method. The proof of this is very elegant,[12] but for our purposes, the important thing is that this gain in convergence speed carries over to the nonlinear case.

D. The Method of Damped Least-Squares

This method[4] was originally described and named by Levenberg in 1944. It has been independently discovered by several others since that time.

First let us review the ordinary method of least-squares. Starting at an arbitrary point, we may write

$$\mathbf{f} = \mathbf{Ax} + \mathbf{f}_0 \quad (28)$$

valid for sufficiently small $\mathbf{x}$. This is identical to Eq. (15) with the origin shifted to the point $\mathbf{x}_0$. To minimize the function φ requires that $\mathbf{x}$ be chosen so as to make the gradient $\mathbf{G}$ equal to zero. Multiplying Eq. (28) by the transpose of $\mathbf{A}$, one obtains, after applying Eq. (14), the equation

$$\mathbf{G} = \mathbf{A}^T\mathbf{Ax} + \mathbf{G}_0. \quad (29)$$

Upon setting $\mathbf{G} = 0$, this represents a set of simultaneous linear equations known as the normal equations of least-squares. Providing the matrix $\mathbf{A}^T\mathbf{A}$ is not singular, these equations can always be solved, and the formal solution may be written

$$\mathbf{x} = -(\mathbf{A}^T\mathbf{A})^{-1}\mathbf{G}_0. \quad (30)$$

Although this is a solution of Eq. (29), the corresponding gradient, computed at the new point $\mathbf{x}$, will nevertheless not be zero. This is because Eq. (29) is only an approximation when the functions are nonlinear.

In this case one takes the point $\mathbf{x}$ as a new origin, recomputes the functions and their derivatives, and repeats the process. Continuing in this way, one generates a sequence of points which converges rapidly to a solution if the amount of nonlinearity is small. However, as mentioned earlier, if the functions are sufficiently nonlinear, the sequence will diverge with successive points oscillating wildly about the minimum. In order to prevent these oscillations, Levenberg suggested restricting the magnitude of the vector $\mathbf{x}$. Instead of trying to minimize φ at each step, he proposed minimizing ψ, where

$$\psi \equiv \varphi + p\mathbf{x}^T\mathbf{x} \equiv \varphi + p(x_1^2 + x_2^2 + \dots + x_N^2). \quad (31)$$

The quantity $\mathbf{x}^T\mathbf{x}$ is the square of the distance between successive trial solutions. The scalar p is a damping factor chosen to expedite convergence. If p is large, each step is correspondingly small, and the oscillations are highly damped. This would be necessary if the degree of nonlinearity were high. If p is small, the step would be larger and the damping less. This would be a good choice in a region where the functions are more nearly linear.

To minimize ψ, we proceed exactly as before, by computing its gradient and setting it equal to zero. Differentiation yields

$$\text{grad } \psi = \text{grad } \varphi + p \text{ grad } (\mathbf{x}^T\mathbf{x}). \quad (32)$$

One sees directly from Eq. (31) that

$$\text{grad } (\mathbf{x}^T\mathbf{x}) = 2\mathbf{x}. \quad (33)$$

Remembering from Eq. (14) that grad $\varphi = 2\mathbf{A}^T\mathbf{f}$, one has

$${}^1/_2 \text{ grad } \psi = \mathbf{A}^T\mathbf{f} + p\mathbf{x}. \quad (34)$$

Since this is a linear approximation, we may employ Eq. (28) to obtain

$$^1/_2 \text{ grad } \psi = \mathbf{A}^T(\mathbf{Ax} + \mathbf{f}_0) + p\mathbf{x} = \mathbf{A}^T\mathbf{Ax} + \mathbf{G}_0 + p\mathbf{x}. \quad (35)$$

Setting grad $\psi = 0$, one gets a set of linear equations

$$\mathbf{A}^T\mathbf{Ax} + p\mathbf{x} = -\mathbf{G}_0, \quad (36)$$

which are quite similar to those obtained from Eq. (29). In fact, Eq. (36) is obtained from Eq. (29) by adding the scalar p to each diagonal element of $\mathbf{A}^T\mathbf{A}$. One can write $\mathbf{x} = \mathbf{Ix}$, where $\mathbf{I}$ is the identity matrix, and then factor the left side of (36) to obtain

$$(\mathbf{A}^T\mathbf{A} + p\mathbf{I})\mathbf{x} = -\mathbf{G}_0. \quad (37)$$

The formal solution of these equations is written

$$\mathbf{x} = -(\mathbf{A}^T\mathbf{A} + p\mathbf{I})^{-1}\mathbf{G}_0, \quad (38)$$

which is quite analogous to Eq. (30). This solution always exists for any positive p, whereas the solution of Eq. (30) does not exist when $\mathbf{A}^T\mathbf{A}$ is singular.

This may be seen as follows: first of all the matrix $\mathbf{A}^T\mathbf{A}$ has no negative eigenvalues for, if it did, the associated quadratic form $\mathbf{y}^T\mathbf{A}^T\mathbf{Ay}$ would have to possess negative values. However, this form can be written $(\mathbf{Ay})^T(\mathbf{Ay})$, which is the square of a vector and therefore always positive. Secondly one gets the matrix $(\mathbf{A}^T\mathbf{A} + p\mathbf{I})$ by adding p to every element in the main diagonal of the original matrix. As is well known, this increases every eigenvalue by p. This makes every one of them positive and nonzero, so that the new matrix cannot be singular.

It is interesting to notice that this method includes the ordinary gradient method and the least-squares method as special cases and may be thought of as a sort of combination of the two. Obviously $p = 0$ gives the ordinary least-squares solution. On the other hand, as $p \rightarrow \infty$, the $p\mathbf{I}$ term in (38) dominates, so that one gets

$$\mathbf{x} = -(p\mathbf{I})^{-1}\,\mathbf{G}_0 = -p^{-1}\mathbf{I}\mathbf{G}_0 = -p^{-1}\mathbf{G}_0. \tag{39}$$

This equation shows that the solution vector becomes parallel to the gradient as p becomes large. Of course, for excessively large p, the step size would approach zero, but this doesn't happen until long after the two vectors have become substantially parallel.

One might anticipate trouble in selecting the best possible value of p, but an adequate value can be chosen easily. One way is to start with a large p and gradually reduce it until excessive oscillation is experienced. Another, suggested by Wynne, is to reduce p until the step exceeds the region of approximate linearity of the functions. The linear change in the functions can be predicted from Eq. (28) and compared with the actual computed change. If the two are in agreement, p is reduced slightly; if they disagree, it can be increased. Either method can be readily programmed for an automatic computer.

E. The Metric

This section is of no practical value. It contains a discussion of the previous methods from an integrated viewpoint that arose because of a flaw in the logic of the steepest-descent method as usually stated. This flaw is implicit in the statement, "The direction of steepest descent is along the gradient of φ." It is not so much that the statement is wrong, as that it is meaningless. One thinks of the direction of steepest descent as that direction along which φ decreases most rapidly, i.e., the direction for which $-\Delta\varphi/\Delta d$ is a maximum. The trouble lies in the definition of Δd, the change in distance. Without giving the matter much thought, one could take the ordinary measure of distance defined by the equation

$$d^2 = \mathbf{x}^T\mathbf{x} \equiv x_1^2 + x_2^2 + \ldots + x_N^2. \tag{40}$$

In this equation $(x_1, x_2, \ldots, x_N)$ are the components of a vector joining any two separated points and d is defined to be the distance between the points. This is all very well, except that we are dealing with a parameter space in which each point represents a lens design. The distance d is the distance from one design to another (whatever that means). Furthermore, the components of a point in parameter space have various dimensions such as curvature, thickness, index of refraction, etc. It is not at all obvious that one should use the same yardstick in measuring these differing quantities. One might use a different yardstick along each coordinate axis and write

$$d^2 = m_{11}x_1^2 + m_{22}x_2^2 + \ldots + m_{NN}x_N^2, \tag{41}$$

where $(m_{11}, m_{22}, \ldots, m_{NN})$ are a set of positive scale factors. This allows the axes to be stretched in varying degrees. It may be, however, that it is desired to stretch the space in a direction *not* parallel to the coordinate axes. In this case one could define

$$\begin{aligned} d^2 = m_{11}x_1^2 &+ 2m_{12}x_1x_2 + \ldots + 2m_{1N}x_1x_N \\ &+ m_{22}x_2^2 \quad + \ldots + 2m_{2N}x_2x_N \\ &\qquad\qquad\quad + \ldots + \\ &\qquad\qquad\qquad\quad \cdot \\ &\qquad\qquad\qquad\quad \cdot \\ &\qquad\qquad\qquad\quad \cdot \\ &\qquad\qquad\qquad\quad + m_{NN}x_N^2. \end{aligned} \tag{42}$$

Stated in matrix form

$$d^2 = \mathbf{x}^T\mathbf{M}\mathbf{x}, \tag{43}$$

where $\mathbf{M}$ is a positive definite symmetric matrix whose elements are (m_{ij}). We insist that $\mathbf{M}$ be positive definite to avoid the embarrassing possibility of getting imaginary distances between some of the points in the parameter space. Equations (43) and (42) are identical and include (40) and (41) as special cases.

Once the matrix $\mathbf{M}$ has been specified, it makes sense to talk about the distance between points, and sense to talk about the direction of steepest descent. In fact it is shown in ref. 17 that the direction of steepest descent is given by the vector

$$\mathbf{x} = -\mathbf{M}^{-1}\mathbf{G}, \tag{44}$$

where as usual the gradient $\mathbf{G}$ has the components $(-^1/_2\ \partial\varphi/\partial x_k)$. The metric $\mathbf{M}$ can be chosen in any convenient manner. If one makes the simple choice $\mathbf{M} = \mathbf{I}$ (where $\mathbf{I}$ is the identity matrix), one gets the Euclidean metric defined by Eq. (40) and finds that $\mathbf{x} = -\mathbf{G}$. This leads to the optimum-gradient method discussed previously.

Another choice for $\mathbf{M}$ would be

$$\mathbf{M} = \mathbf{A}^T\mathbf{A} \tag{45}$$

which gives $\mathbf{x} = -(\mathbf{A}^T\mathbf{A})^{-1}\,\mathbf{G}$. This direction is identical with that given by the least-squares method in Eq. (30).

Finally, by taking a linear combination of these two metrics, one can write

$$\mathbf{M} = \mathbf{A}^T\mathbf{A} + p\mathbf{I} \tag{46}$$

which leads to the damped least-squares method with $\mathbf{x}$ given by Eq. (38). It is well to note that, although the choice of $\mathbf{M}$ may affect the rapidity of convergence, all choices of a metric lead to the same ultimate minimum. This is a direct consequence of Eq. (44) and the fact that $\mathbf{M}$ is positive definite, so that $(\mathbf{x} = 0)$ implies $(\mathbf{G} = 0)$ and conversely.

The above argument shows that, with an appropriate choice of metric, the steepest-descent method can be considered to embrace both the gradient method and the least-squares method. For a more familiar example of the influence of the metric consider the traditional method of optical design in which powers and bendings are independently varied. In the case of a singlet with curvatures c_1 and c_2, this method is equivalent to making a transformation of variables of the form

$$\left.\begin{aligned} x_1 &= (c_1 - c_2)(N - 1) \\ x_2 &= (c_1 + c_2) \end{aligned}\right\}. \tag{47}$$

The new variable x_1 is called the "power" while x_2 might be called the "bending". The advantage of the procedure is that changing x_2 does not appreciably change the Gaussian optics, the color correction, or the Petzval sum but does change the spherical aberration, coma, and astigmatism. This separability makes it much easier to correct the aberrations. The change in variables indicated by Eq. (47) can be interpreted as a choice of a non-Euclidean metric in the c-space. In matrix form this equation is written

$$\mathbf{x} = \begin{pmatrix} N-1 & 1-N \\ 1 & 1 \end{pmatrix} \mathbf{c}, \text{ where } \mathbf{x} \equiv \begin{pmatrix} x_1 \\ x_2 \end{pmatrix} \text{ and } \mathbf{c} \equiv \begin{pmatrix} c_1 \\ c_2 \end{pmatrix}. \tag{48}$$

Defining the metric in the x-space by the equation

$$d^2 = \mathbf{x}^T\mathbf{x} \tag{49}$$

one gets by direct substitution

$$d^2 = \mathbf{c}^T \begin{pmatrix} N-1 & 1-N \\ 1 & 1 \end{pmatrix}^T \begin{pmatrix} N-1 & 1-N \\ 1 & 1 \end{pmatrix} \mathbf{c}. \tag{50}$$

Performing the indicated multiplication, one finds the metric in the c-space to be

$$\mathbf{M} = \begin{pmatrix} 1 + (N-1)^2 & 1 - (N-1)^2 \\ 1 - (N-1)^2 & 1 + (N-1)^2 \end{pmatrix}. \tag{51}$$

This argument means that choosing $\mathbf{M}$ to be the metric in the c space is equivalent to rotating and stretching the coordinate system according to Eq. (47). It is clear that such transformations can be applied on a more general basis than the classical method of varying powers and bendings independently. In fact one method for solving nonlinear equations depends upon continuously changing the metric during the computation.[28]

F. The Boundary Conditions

Treatment of the boundary conditions is a very important part of any automatic program. The author has called the method, which is described below, the elimination method. Consider the set of inequalities given by (7). One might have about fifteen such inequalities in a typical problem. Each time the design is evaluated, one must compute every b_j as well as all of its derivatives with respect to the independent variables. This yields two matrices which are quite analogous to those already obtained for the image errors. They are the column vector

$$\mathbf{b} \equiv \begin{pmatrix} b_1 \\ b_2 \\ \cdot \\ \cdot \\ \cdot \\ b_T \end{pmatrix} \text{ and the matrix } \mathbf{B} \equiv \begin{pmatrix} B_{11}B_{12} & \ldots & B_{1N} \\ B_{21}B_{22} & \ldots & B_{2N} \\ \cdot \quad \cdot & & \cdot \\ \cdot \quad \cdot & & \cdot \\ \cdot \quad \cdot & & \cdot \\ B_{T1}B_{T2} & \ldots & B_{TN} \end{pmatrix}, \tag{52}$$

where $B_{jk} \equiv \partial b_j/\partial x_k$. The number of boundary conditions is T, and the number of variables is N.

By examining the components of $\mathbf{b}$, one can divide the boundary conditions into three classes. These are

Quiescent those for which $b_j > \epsilon$,
Effective those for which $|b_j| \leqslant \epsilon$,
Forbidden those for which $b_j < -\epsilon$.

The positive number ϵ is a tolerance which permits occasional small violations of the boundary conditions. For example, an edge thickness slightly less than the stated minimum may be permitted during the course of the design. (The tolerance ϵ can be the same for all the boundaries because each b_j has its own scale factor absorbed in it.)

Quiescent boundary conditions are kept under surveillance during the course of design, and the magnitude of the change vector is limited in order to prevent the corresponding b_j from becoming negative. *Forbidden* boundary conditions are subject to a special correction loop which restores them to zero. *Effective* boundary conditions form the most interesting group, and it is these whose treatment we shall first discuss.

Suppose that, by one of the methods already described, a tentative solution vector $\mathbf{x}$ has been obtained. It is called a tentative solution, because the boundary conditions have not yet been considered. The effect of this tentative solution must now be examined. On the assumption that the functions are linear, one has

$$\mathbf{Bx} = \mathbf{b} - \mathbf{b}_0 = \Delta\mathbf{b}. \tag{53}$$

This equation, which shows the change in each boundary condition as a function of the step $\mathbf{x}$, is strictly analogous to Eq. (28). The algebraic sign of each component of $\Delta\mathbf{b}$ shows the direction in which the corresponding boundary condition will move. Every effective boundary condition is now examined and classified *active* or *inactive* depending upon whether its respective Δb_j is negative or positive. At the end of this classification, a small number of active boundary conditions have been isolated and need to be constrained. These active conditions are those which are on the boundary ($|b_j| \leqslant \epsilon$) and which are tending to become negative. The process of constraining them consists of choosing a new tentative solution vector which keeps them zero (or at least smaller than ϵ). This is accomplished by selecting an equal number of independent variables with which to constrain the active boundary conditions. These constraining variables are chosen by examining the **B** matrix to find a set particularly suitable for the purpose. This yields a set of linear equations for the constraining variables in terms of the remaining free variables. The space of the free variables is called the *reduced variable space*. One recomputes a new tentative solution in this reduced variable space using one's favorite minimization procedure. It may now happen that an effective condition, formerly inactive, has become active because the new tentative solution is in a different direction from the previous one.

In order to guard against this possibility $\mathbf{Bx}$ is recomputed and $\Delta\mathbf{b}$ reexamined. Any new active boundary conditions are eliminated by repeating the above procedure. Eventually a tentative solution is obtained which constrains all the active boundary conditions. Usually the procedure ends after one or two passes; in any event it *must* end when all effective boundaries are constrained. It might be imagined that the process consumes a great deal of time, but actually it takes about 1% of the time required to read this paragraph. Those skilled in linear algebra will recognize that the above process consists in a sequence of elementary transformations of the matrices. The constraining variables are selected by a process of pivotal condensation in which the pivotal elements are chosen to be the largest elements in any row. The formal mathematics outlined below may easily be skipped by those who are not planning to write such a program.

First, adjoin Eqs. (28) and (53) and write the entire set in matrix form.

$$\begin{pmatrix} \mathbf{A} \\ \mathbf{B} \end{pmatrix} \mathbf{x} = \begin{pmatrix} \Delta\mathbf{f} \\ \Delta\mathbf{b} \end{pmatrix}. \tag{54}$$

Suppose that there are r active boundaries and that $r + s = T$. Partition the matrix as follows:

$$\begin{pmatrix} \mathbf{A} \\ \mathbf{B}_r \\ \mathbf{B}_s \end{pmatrix} \mathbf{x} = \begin{pmatrix} \Delta\mathbf{f} \\ \Delta\mathbf{b}_r \\ \Delta\mathbf{b}_s \end{pmatrix}. \tag{55}$$

Constraining the r active boundary conditions is equivalent to solving the linear set

$$\mathbf{B}_r\mathbf{x} = \Delta\mathbf{b}_r = 0. \tag{56}$$

This can be done by pivotal condensation. Select the largest element in the first row of $\mathbf{B}_r$ as the pivot. By means of elementary transformations, put a one in this position and zeros in all the other elements in the pivotal column. Treat each row of $\mathbf{B}_r$ in a similar manner. For convenience suppose that the first r columns of the matrix are the pivotal columns. If not originally so, this can be brought about by suitably permuting the columns. Then partition the entire matrix again as follows, obtaining the matrix equation

$$\begin{pmatrix} \mathbf{A}_r & \mathbf{A}_q \\ \mathbf{B}_{rr} & \mathbf{B}_{rq} \\ \mathbf{B}_{sr} & \mathbf{B}_{sq} \end{pmatrix} \begin{pmatrix} \mathbf{x}_r \\ \mathbf{x}_q \end{pmatrix} = \begin{pmatrix} \Delta\mathbf{f} \\ 0_r \\ \Delta\mathbf{b}_s \end{pmatrix}. \tag{57}$$

Here $r + q = N$ is the total number of variables. The pivotal condensation described above is equivalent to multiplying Eq. (57) by the matrix

$$\begin{pmatrix} \mathbf{I} & -\mathbf{A}_r\mathbf{B}_{rr}^{-1} & 0 \\ 0 & \mathbf{B}_{rr}^{-1} & 0 \\ 0 & -\mathbf{B}_{sr}\mathbf{B}_{rr}^{-1} & \mathbf{I} \end{pmatrix}$$

This yields the new equation

$$\begin{pmatrix} 0 & \mathbf{A}^* \\ \mathbf{I} & \mathbf{B}_{rr}^{-1}\mathbf{B}_{rq} \\ 0 & \mathbf{B}^* \end{pmatrix} \begin{pmatrix} \mathbf{x}_r \\ \mathbf{x}_q \end{pmatrix} = \begin{pmatrix} \Delta\mathbf{f} \\ 0_r \\ \Delta\mathbf{b}_s \end{pmatrix}, \tag{58}$$

whose right side is identical with that of Eq. (57), and the matrices $\mathbf{A}^*$ and $\mathbf{B}^*$ are defined by the equations

$$\mathbf{A}^* \equiv \mathbf{A}_q - \mathbf{A}_r\mathbf{B}_{rr}^{-1}\mathbf{B}_{rq} \text{ and } \mathbf{B}^* \equiv \mathbf{B}_{sq} - \mathbf{B}_{sr}\mathbf{B}_{rr}^{-1}\mathbf{B}_{rq}. \tag{59}$$

Then Eq. (58) may be written as three matrix equations

$$\left.\begin{aligned} \mathbf{A}^*\mathbf{x}_q &= \Delta\mathbf{f}, \\ \mathbf{B}_{rr}^{-1}\mathbf{B}_{rq}\mathbf{x}_q &= -\mathbf{x}_r, \\ \mathbf{B}^*\mathbf{x}_q &= \Delta\mathbf{b}_s. \end{aligned}\right\}. \tag{60}$$

The significance of Eq. (60) is that the original **A** matrix has been replaced by $\mathbf{A}^*$ in the reduced variable space defined by $\mathbf{x}_q$. The constrained variables $\mathbf{x}_r$ are determined from the free variables $\mathbf{x}_q$ by the second equation of the set. The third equation gives the leftover boundary conditions as functions of the reduced variables. The minimization procedure may now be carried out in the reduced space just as though no boundary conditions were present.

Having disposed of the active conditions, the remaining ones are easy. Any effective ones which are inactive will become more positive as a result of the step. This follows from the definition. The quiescent conditions, however, can move in either direction. The only ones which concern us are those moving toward the boundary, i.e., those for which Δb_j is negative. For those, one calculates the ratio $-b_j/(\Delta b_j)$ for each such condition. The smallest ratio is obtained for that condition which will first cross the boundary. This is used to limit the step size. Most of the time, of course, this is not a real limitation, because the minimization process itself imposes limitations on the step, but occasionally a new boundary is encountered and the size of the step has to be limited. Once the boundary has actually been reached so that $|b_j| < \epsilon$, it is picked up by the constraining loop and controlled in the manner described above.

Occasionally a forbidden boundary condition is encountered. This may occur at the start of the design or after a step during which the constraining loop failed. This can happen if the boundary function is extremely nonlinear. It is not very frequent, because each effective boundary has a buffer zone of width 2ϵ surrounding it. It is only after an escape from the buffer zone that it needs to be restored. The restored loop is really quite simple. All of the effective and forbidden boundaries are brought back to zero together by solving the equations

$$\mathbf{Bx} = -\mathbf{b}. \tag{61}$$

Since one has many more variables than equations, one writes

$$\mathbf{x} = \mathbf{B}^T\lambda, \tag{62}$$

which gives

$$\mathbf{B}\mathbf{B}^T\lambda = -\mathbf{b}. \tag{63}$$

After solving for λ and substituting back, one gets a solution for which $\mathbf{x}$ is a minimum. Ordinarily this does not hurt the merit function very much although no effort is made during the restored loop to keep the latter small.

IV. Description of an Actual Program

A real design program is richer and more complex than the foregoing mathematical discussion might imply. In this section the author has chosen to describe the only program with which he is thoroughly familiar. As all proper programs, it is endowed with a catchy set of initials. The first version of LEAD, which stands for Lens Electronic Automatic Design, was completed in 1960, and many modifications have been made since then. At any given time there are usually three versions of LEAD: the operating version, the one being coded, and the one being planned. We shall describe the second version because it will become the operating one long before this is published.

A. Input

A most significant feature of any program is the input, because it implies a great deal about the purpose and internal workings of the program. The input is of several kinds:

(1) First there is an initial design consisting of a set of curvatures, indices, dispersions, thicknesses, the location of the stop and the entrance pupil, and the focal shift from the paraxial focus to the position of best focus. Associated with each parameter is a code which tells the program whether or not the parameter may be varied.

(2) A set of control data to specify the required focal length, minimum back focal distance, the semiaperture, the position of the object, and certain weighting factors. There are weights on distortion, chromatic aberration, wavefront deviations, and lateral ray errors. The introduction of lateral ray errors is new; in the older versions only wavefront deviations were used to describe the monochromatic image quality. In addition, there are scale factors on the independent variables which help in defining an appropriate metric for the parameter space. Also entered as input is the tolerance ϵ and the scale factors on the boundary conditions.

(3) The boundary conditions are actually divided into two classes, explicit and implicit. The explicit boundary conditions are restrictions on the range of the independent variables. They can be evaluated immediately without ray-tracing and include minimum vertex distances and limitations on the region of variation of the glass data. The implicit boundary conditions, on the other hand, limit the dependent variables and require considerable ray-tracing for their evaluation. These include minimum edge thicknesses, a minimum back focal distance, and others described below. In principle, the treatment described in Sec. III F applies to both classes of boundary conditions but is only applied in fact to the implicit ones, since the others can be treated directly in a much simpler manner. There is also an implicit boundary condition on the height of the chief ray* where it intersects the stop. This is necessary because the entrance-pupil position and the stop position are treated as independent variables. The condition that the height of the chief ray be at zero at the stop serves to correlate these two independent positions without the awkward necessity of tracing a ray backward from the stop. In addition there is an implicit boundary condition on the focal length. Incidentally, the boundary conditions on the stop and on the focal length are two-sided rather than one-sided, which requires a minor modification of the treatment described in Sec. III F.

(4) Finally, it is necessary to tell the program which rays are to be traced and which image errors are to be computed for each ray. The chief ray is specified by the angle it makes with the optical axis and the distance from the entrance-pupil position to the first surface of the lens. The chief ray serves to define an object point which is used as a source for a bundle of meridian and skew rays. The size and general shape of the bundle are determined by two numbers, the semiaperture a and the meridian vignetting V. (See Fig. 1.) Each ray in the bundle is specified by its coordinates in the entrance-pupil plane normalized, however, to an aperture of 1.0 and a V of 1.0. This normalization makes it easy to use the same ray deck for widely differing lenses. Usually for each meridian ray the program will compute three residuals, the chromatic aberration according to Conrady, the wavefront deviation, and the lateral ray-error. The skew rays get wave aberrations only. Furthermore, residuals from different rays can be weighted differently. Such weights are in addition to the over-all weights mentioned earlier.

It is perhaps well to mention that the upper and lower meridian rays in each ray bundle can be distinguished by a special code. The program will then guarantee that these rays are transmitted by the system. This is insured if the length along the ray in each medium is greater than an assigned mini-

---

* In an effort to standardize with the notation of Hopkins and others, we define the chief ray as the central ray of the vignetted beam, and the entrance-pupil position as the point where the chief ray appears to cross the axis in the object space.

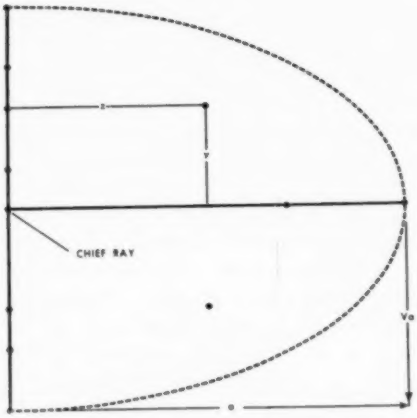

Fig. 1. The entrance pupil plane showing a typical ray pattern. The coordinates of each ray are $y = Va\eta$ and $z = a\zeta$ where a is the semiaperture and V is the ratio by which the aperture is reduced in the meridian direction. The normalized ray coordinates are η and ζ.

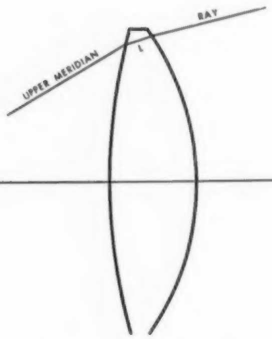

Fig. 2. The program guarantees that the upper and lower meridian rays are transmitted. It calculates the length L along the ray intercepted in each medium and establishes the implicit boundary conditions ($b = L - t \geqslant 0$) where t is the minimum permitted for a particular medium.

mum. (See Fig. 2.) For air this minimum is often zero, for glass it is a positive quantity. The manner in which such an implicit boundary condition is controlled has been described in Sec. III F.

(5) In addition, it is possible to specify certain elastic constraints which are midway between image errors and boundary conditions. Basically any linear combination of the independent variables (and some of the dependent ones as well) can be constrained. Here is how it works.

Suppose one has a requirement that the over-all distance from the front vertex to the image plane be maintained at 2.563. The requirement is entered as input together with a weighting factor which defines its importance. A deviation from this requirement is treated as an image error and added into the merit function. By suitably choosing the weight, the over-all distance can be held as tightly or as loosely as desired. This type of constraint is linear (or nearly so) and should cause no convergence problem.

There are other uses for elastic constraints. One is to guarantee symmetry in a lens operating at unit magnification. Another is to handle certain problems in reflecting systems. Still another possibility is to examine a limited region of the parameter space. By tying all variables elastically to a point in this region, the program can be forced to find a solution near the point. This may or may not prove useful.

(6) In rare cases we have had the unpleasant experience of having the program alter the original design so that one or more rays became complex. This means that either the ray became totally internally reflected or else flew right over the top of a spherical surface. To avoid this, it is possible to specify to the program that a particular angle of incidence or refraction must not exceed a specified amount. The restriction is handled internally exactly like any other one-sided boundary condition.

B. Internal Organization

The details are too complicated to be of general interest. Suffice it to say that the program is divided into two parts which have been made as independent as possible. The evaluation routine traces the rays, computes the image errors, the boundary conditions, and the merit function. It also calculates the derivatives of all these quantities with respect to the parameters of the lens. These derivatives constitute the **A** and **B** matrices. Based on this evaluation the design routine computes a change in the parameters calculated to reduce the merit function. At the same time it controls the boundary conditions to prevent or possibly correct any violations. Available to the design routine are subroutines containing the conjugate-gradient and the damped least-squares methods. Both are included because they are still undergoing improvement and it is not clear which is better.

C. Output

After each design step, the lens parameters are printed together with an evaluation. This consists of a list of residual image errors (the vector **f**), the merit function φ, and the boundary conditions (the vector **b**). Auxiliary variable quantities such as the clear aperture of each surface and the location of the entrance pupil are also printed. More information is available, including the values of the **A** and **B** matrices and a great mass of data showing the detailed operation of the program. Some of this was printed in the early stages, particularly while the program was being debugged. However, one must exercise considerable discretion lest the printout become not merely too long to read but also too heavy to lift.

D. Operation

The strategy of lens design with an automatic program is very different from working with a desk calculator. In the first place the time scale is enormously compressed. Suppose, for example, the LEAD program is asked to design a twelve-surface lens. A drawing-board sketch is made showing the approximate shape and placement of the elements. This initial design becomes input data for the program, which is now required to take twenty improvement steps. At each iteration the program evaluates the new design and computes the next step. The entire process will take about 20 min on the 7080 (or about 3 min on a 7090). If it were done by a human computer on a Marchant, it would take 2 years! Even so, twenty iterations are probably not enough to complete such a complex design. The actual number of iterations would be closer to sixty, which requires an hour of 7080 time (or about 10 min of 7090 time). Such a long computer run would be very inadvisable, because it places too great a premium on the accuracy of the input data. It is far safer to run the design for only ten or fifteen iterations and keep track of the intermediate results. In this way any initial numerical mistakes can be corrected. Furthermore, it may become obvious that some of the weights need to be changed. The weighting factors (μ_j) are only constants in first approximation, and in reality ought to be slowly varying functions of the image errors. By interrupting the run, the designer has a chance to inspect the progress of the design and change the weights if he desires. It could be objected that such discretionary operations might better be handled under program control, and it is true that such a program would not be difficult to write, but reserving these functions to the human lens designer is unlikely to cause a serious increase in elapsed time and has the additional advantage of being good for his ego. Makes him feel needed.

The desirability of short runs gives rise to the idea of carrying on multiple designs. If several designs are each given a few iterations during a single computer run, the cost of setup and tape-mounting time is reduced and efficiency improved. This, in fact, is the way in which the LEAD program is used. Ordinarily three or four lenses are sent to the computer each evening and the results analyzed the following morning. This is something like simultaneous chess and is a lot more fun than doing one design at a time. It also prevents one from becoming engrossed in details and completely overlooking broader aspects of the design problem.

V. Impact of Automatic Methods

The influence of the computer on lens design is already large but it will soon become much larger as a result of rather routine modifications of present programs. What principally remains is to bring the unusual applications under the aegis of the automatic program. Zoom systems, aspherics, some types of reflecting systems, and decentered optics require modifications of the evaluation routine. The problem of secondary spectrum is especially difficult because the easy assumption that the glass catalog represents a continuous manifold is no longer tenable, and it may be necessary to carry on such designs with a combination of manual and automatic methods. A considerable amount of programming needs to be done in the near future, and as far as possible this programming should be done so that extensions to new applications can be made without excessive difficulty.

The assignment of target values is becoming an increasingly unrealistic procedure in automatic design because ordinarily one does not know in advance the values of the individual aberrations required to produce the best compromise in the final lens. A much more flexible procedure is to incorporate all the pertinent requirements into a merit function which can then yield somewhat on this or that requirement to produce an over-all balance more consistent with the possibilities inherent in the particular system being designed. As this method of using the merit function becomes better understood its importance is bound to increase. In a recent discussion, for example, Hopkins pointed out that a fixed assignment of the amount of vignetting (determined by the quantity V) is somewhat unrealistic because it is conceivable that, by reducing the illumination requirement, a considerable gain in image quality might be possible. If this is so, the remedy is to make φ a function of V by including the latter among the independent variables. Then, to prevent the automatic program from reducing V to zero, it should be included in the merit function by the method of elastic constraints described earlier. Assignment of a suitable weighting factor to V would enable the program to produce a balance between illumination and image quality entirely consistent with the preferences of the designer. Although this example is very simple, the same principle *can* be extended to more important cases. There seems to be no reason, for example, why the cost of manufacture should not be included in the merit function. This would enable the program to come up with a more realistic balance between cost and quality.

Finally we come to the difficult question of the role of the lens designer—a role which is rapidly changing wherever computers are available. Broadly, the process of producing a design can be divided into three parts:

I. Specifying the problem
II. Choosing the lens type
III. Correcting the lens

These parts interact with one another in very complicated ways. Parts II and III have been traditionally the province of the designer, with the overwhelming preponderance of his time devoted to correcting the lens. It is obvious that he will now be able to spend somewhat more time on part II, where present automatic methods are not particularly applicable. Part I, however, is the weakest link in the whole process.

Often a set of specifications are given to the designer as though fixed for all time whereas, in reality, many compromises ought to be considered. It is not always realistic to specify such things as field angle, focal length, *f* number, zoom range, or size of the lens, as though they were immutable requirements. Many possibilities need exploring in producing an optical instrument. The balance between the optical design requirements and the system requirements is the subject at issue. Who is to make these balances? Certainly not the person who gives the assignment. He usually does not have the knowledge of the effect of such compromises upon the design. Certainly not the lens designer, because he may not be sufficiently familiar with the over-all system. It is only by pooling the knowledge of the lens designer with that of the instrument designer that proper compromises can be made. In the past, however, the lens designer has not had sufficient time to contribute to this initial phase as much as desirable. Furthermore, he was often only too glad to escape this aspect of the problem and retreat to his table of logarithms or his desk calculator. In the future, however, he will be without an excuse for evading his responsibility since most of part III will be performed automatically. The additional time and thought given to the initial phase of the procedure should pay off by yielding optical instruments with a better balance between all the conflicting requirements.

References (in chronological order)

1. A. Cauchy, Compt. rend. **25,** 536 (1847).
2. D. E. Smith, *Source Book in Mathematics* (Macmillan, New York, 1929), pp. 576–579.
3. E. T. Whittaker and G. Robinson, *The Calculus of Observations* (Blackie and Sons London, 1932), p. 214.
4. K. Levenberg, Quart. Appl. Math. **2,** 164 (1944).
5. H. B. Curry, Quart. Appl. Math. **2,** 258 (1944).
6. J. G. Baker, *Design and Development of an Automatically Focusing 40-inch f/5.0 Distortionless Telephoto and Related Lenses for High-altitude Aerial Reconnaissance,* N.D.R.C., Section 16.1, Optical Instruments (1944).
7. H. R. J. Grosch, J. Opt. Soc. Am. **35,** 803 (1945).
8. H. R. J. Grosch, J. Opt. Soc. Am. **39,** 1059 (1949).
9. D. P. Feder and B. F. Handy, Jr., *Optical Ray Tracing Problems and The Card Programed Calculator,* Paper presented to the Association for Computing Machinery, Rutgers Univ. (March 1950).
10. D. P. Feder, J. Opt. Soc. Am. **41,** 630 (1951).
11. M. L. Stein, J. Research Natl. Bur. Standards **48,** 407 (1952).
12. M. R. Hestenes and E. Stiefel, J. Research Natl. Bur. Standards **49,** 409 (1952).
13. J. G. Baker, Technical Reports 1–12, and a Supplement, prepared by the Perkin-Elmer Corp., under Air Force Contract AF 33(038)-10836 Declassified 1959 (issued at intervals from 1951–1955).
14. O. N. Stavroudis and D. P. Feder, J. Opt. Soc. Am. **44,** 163 (1954).
15. S. Rosen and C. Eldert, J. Opt. Soc. Am. **44,** 250 (1954).
16. G. Black, Nature **175,** 164 (1955); also, an expansion of this theme in Proc. Phys. Soc. (London) **B68,** 729 (1955).
17. J. B. Crockett and H. Chernoff, Pacific J. Math. **5,** 33 (1955).
18. R. E. Hopkins, C. A. McCarthy, and R. Walters, J. Opt. Soc. Am. **45,** 363 (1955).
19. F. Wachendorf, Optik **12,** 329 (1955).
20. C. A. McCarthy, J. Opt. Soc. Am. **45,** 1087 (1955).
21. D. P. Feder, J. Opt. Soc. Am. **47,** 902 (1957).
22. D. P. Feder, J. Opt. Soc. Am. **47,** 913 (1957).
23. J. Meiron and H. M. Loebenstein, J. Opt. Soc. Am. **47,** 1104 (1957).
24. A. Girard, Rev. opt. **37,** 225, 397 (1958).
25. C. G. Wynne, Proc. Phys. Soc. (London) **73,** 777 (1959).
26. M. Nunn and C. G. Wynne, Proc. Phys. Soc. (London) **74,** 316 (1959).
27. J. Meiron, J. Opt. Soc. Am. **49,** 293 (1959).
28. W. C. Davidon, *Variable Metric Method for Minimization,* Argonne National Laboratory, Rept. ANL-5990 (May 1959).
29. H. D. Korones and R. E. Hopkins, J. Opt. Soc. Am. **49,** 869 (1959).
30. J. Meiron and G. Volinez, J. Opt. Soc. Am. **50,** 207 (1960).
31. W. P. Hennessy and G. H. Spencer, J. Opt. Soc. Am. **50,** 494 (1960).
32. J. C. Holladay, *Computer Design of Optical Lens Systems (IBM 704),* Proc. of the 1960 Comp. Applications Symp. sponsored by Armour Research Foundation (Macmillan Co., New York, 1961).
33. S. Kato, Science of Light (Tokyo) **10,** 1 (1961).
34. R. Hooke and T. A. Jeeves, J. Assoc. Computing Mach. **8,** 212 (1961).
35. H. Slevogt, Optik **18,** 571 (1961).
36. E. Glatzel, Optik **18,** 577 (1961).
37. *Proceedings of the Conference on Optical Instruments and Techniques, London 1961* (Chapman and Hall, London, 1962). (This contains a section on optical design techniques by various authors.)
38. R. E. Hopkins and G. H. Spencer, J. Opt. Soc. Am. **52,** 172 (1962).
39. D. P. Feder, J. Opt. Soc. Am. **52,** 177 (1962).
40. R. R. Willey, Jr., Appl. Opt., **1,** 368 (1962).
41. H. A. Spang, III, SIAM Rev. **4,** (1962).
42. R. E. Hopkins, J. Opt. Soc. Am. **52,** 1218 (1962).
43. D. S. Grey, J. Opt. Soc. Am. **53,** 672 (1963).

YOUR 1964 SUBSCRIPTION

To avoid interruption of service on your subscription to *Applied Optics,* subscription renewal monies must be paid **by 10 December at the latest.** Such renewals should be sent to *Applied Optics* Subscription Handling, American Institute of Physics, 335 East 45th Street, New York 17, N.Y.

The Symposium Lens—An Epilogue

Robert E. Hopkins and Donald P. Feder

A lens design problem was proposed by a group of lens designers. Several alternative designs have been corrected on two different automatic correcting programs. The final designs are similar and exhibit a high degree of correction.

The authors have engaged in a friendly design contest with our machine design programs. The experiences we have had show the strength and weaknesses of present automatic design programs.

Feder's program is called LEAD and is described in the first paper of this issue (p. 1209). Hopkins uses a program called ORDEALS.[1] In its latest form ORDEALS, as written for the IBM 7070, includes ray tracing and automatic correction of all third- and fifth-order aberrations. It also provides for ray tracing through conic sections, aspherics, tilted surfaces, and decentered elements. Thicknesses and curvatures can be varied automatically; refractive indices for two wavelengths may be varied automatically but this feature was not used in this contest. The program can find target values for one set of aberrations and simultaneously minimize a merit function. The merit function is defined as the sum of the squares of weighted aberration residuals plus the sum of the squares of the parameter changes.

The basic differences between the ORDEALS program and the LEAD program are the following:

(1) The ORDEALS program uses third- and fifth-order aberration theory instead of ray tracing in the automatic correction phase. This is done for two reasons—for speed and understanding of the lens system. ORDEALS uses the Buchdahl third- and fifth-order aberrations surface by surface. By correcting these aberrations, one can rapidly find the many regions of solution. The final evaluation of the system, however, uses full ray tracing. It is necessary for the designer, therefore, to make some minor readjustments to allow for the high-order aberrations.

(2) The ORDEALS program essentially uses no boundary conditions. There are features in ORDEALS which will constantly adjust spaces and thicknesses to provide adequate edge thicknesses and central spaces, but if a particular thickness is to be varied as a free parameter the control of the thickness is lost. This means that the air spaces and thicknesses if they are varied may go negative. Boundary conditions add to the length of the program, the time to run it, and they are difficult to fit into a program for a machine the size of the IBM 7070. Without this feature the program is not entirely automatic-correcting.

Not having these boundary conditions has not been a serious limitation. Actually, one can derive considerable insight into the problem by not having them.

The design contest started when Feder, at a small symposium for lens designers, offered to design a lens completely automatically. The group requested a four-element, $f/1.5$ lens to cover a field of 6°. Some of the designers present then guessed at a preliminary design, which we have since designated SYM-0, and which is shown in Fig. 1. (See also Table I.) Needless to say, the image quality for such a guess is not high. The first of the fully automatic designs, called SYM-1, was presented to the group on the following day, and later the specifications were published in a report in *Applied Optics*.[2] A drawing of this lens accompanied by an analysis of its performance is shown in Fig. 2(a). The design parameters for this lens are given in Table II. This design, although certainly not the last word, represents the major portion of the improvement possible over the preliminary guess. The remaining three designs in Figs. 2(b)–(d) represent further progress in the attempt to improve this lens.

Several months after the symposium, Hopkins entered the lists by designing ORD-1 with the aid of the ORDEALS program. This design is shown in Fig. 2(b) and the design parameters given in Table III. In designing ORD-1, Hopkins used the same

---

R. E. Hopkins is with the Institute of Optics, College of Engineering, University of Rochester, Rochester, New York. D. P. Feder is with Eastman Kodak Company, Rochester, New York.

Received 30 July 1963.

Table I. The SYM-0 Design[a]

N	V	t	c
			1.1500
1.6200	59.2 (DBC 7)	0.1200	
			0.0000
		0.0010	
			1.8000
1.6200	59.2 (DBC 7)	0.1200	
			0.5000
		0.2100	
			−1.5000
1.6490	33.8 (EDF 2)	0.0500	
			1.5000
		0.2500	
			−0.5000
1.620	59.2 (DBC 7)	0.1200	
			−1.8000

[a] The entrance pupil is 0.450 to right of first surface. The focal length is 1.253. The back focal length is 0.3573. The energy distribution curves shown in Fig. 1 were computed on a plane shifted 0.0560 from the paraxial focus.

Table II. The SYM-1 Design[a]

N	V	t	c
			0.8025
1.6208	59.1	0.1670	
			−0.3864
		0.0010	
			1.3209
1.6253	58.8	0.1840	
			0.1526
		0.0440	
			−1.1067
1.6519	32.0	0.2500	
			2.1663
		0.0540	
			0.3234
1.6488	57.1	0.1440	
			−2.1399

[a] The entrance pupil is 0.359 to right of first surface. The focal length is 1.011. The back focal length is 0.5550. The energy distribution curves shown in Fig. 2 were computed on a plane shifted −0.0025 from the paraxial focus. The glass data are approximations in this design.

Table III. The ORD-1 Design[a]

N_D	V	t	c
			1.1296
1.6200	59.2 (SK 16)	0.2209	
			−0.1180
		0.0010	
			1.2527
1.6200	59.2 (SK 16)	0.1607	
			0.0592
		0.0234	
			−0.5800
1.6887	31.1 (SF 8)	0.3105	
			2.6933
		0.0565	
			1.2101
1.6200	59.2 (SK 16)	0.2757	
			−1.6938

[a] The entrance pupil is 0.810 to the right of the front surface. The focal length is 1.000. The back focal length is 0.4033. The energy distribution curves shown in Fig. 2 were computed on a plane shifted −0.0010 from the paraxial focus.

Table IV. The SYM-2 Design[a]

N	V	t	c
			1.2402
1.4980	67.0 (BSC 1)	0.1970	
			−0.4856
		0.0010	
			1.6807
1.6968	56.1 (EK 110)	0.2114	
			0.6311
		0.0318	
			−0.5602
1.7200	29.3 (EDF 3)	0.2000	
			3.4657
		0.2190	
			0.9257
1.6968	56.1 (EK 110)	0.0941	
			−1.9046

[a] The entrance pupil is 1.352 to the right of the first surface. The focal length is 1.000. The back focal length is 0.4017. The energy distribution curves shown in Fig. 2 were computed on a plane shifted −0.0020 from the paraxial focus.

starting point used to produce SYM-1. In this way the game was kept fair, and the only advantage he possessed was that of having a goal at which to shoot. Actually, in lens design, as practiced in the past, this advantage is not entirely negligible, and indeed, it is probable that he might have stopped the procedure at an earlier stage had it not been for the existence of SYM-1.

It took approximately 4 h of computing time to find the solution ORD-1. This is not a fair estimate of the time required to design a lens like SYM-1. The problem Hopkins faced was to improve on SYM-1. Many solutions were found before one was obtained which appeared to offer some advantages.

In this phase of the design the positive elements were assumed to be made of SK16. This glass is readily available and has become more or less a favorite among designers. It became apparent that in order to improve significantly on SYM-1 it would be necessary to increase substantially the difference in dispersions between the positive and negative elements. The Symposium group put an upper limit on the index of the elements so this prevented using a higher index flint with increased dispersion. The only solution then was to use lower index positive elements in order to reduce their dispersion. Upon insertion of these glasses a new solution was found in 8 min. The image quality of this modification was superior to that of ORD-1, but the distortion had increased from 0.6 to 1.4% and the lateral color was twice what it was in ORD-1. The modification is not shown in this paper, because later on a still better design was found in which the distortion remained well corrected. Experience with the design showed that the distortion and lateral color could not be corrected with the low-dispersion glass in the rear component. Hopkins felt that the best way to improve on ORD-1 would be to use a high-index flint or use an achromatic rear element. However, believing that he was slightly ahead, he returned the design to Feder with the suggestion that LEAD should be able to do better. Examination showed, as in the case of SYM-1, that the new design was a tremendous improvement over the original guess. Compared with SYM-1, it appeared that the energy distribution at 0 and 4° was slightly better, while that at 6° was slightly worse. The chromatic aberration was slightly better, and the distortion was substantially the same.

The LEAD program was rerun for about 20 min using SYM-1 as a starting point. The program had been modified since the first running in order to increase the decimal accuracy. The increased sensitivity of the program caused the glasses to move into a more favorable region and produced a better design, as shown in Fig. 2(c). The reader should compare SYM-1 and SYM-2 to see how the glasses changed. See Tables II and IV, respectively. It is well known to lens designers that the choice of glasses is not usually a highly sensitive way of improving a lens. It has been Feder's experience with the LEAD program that with all parameters varying, the glasses are the last to move. The improvement of SYM-2 over SYM-1, brought about by better glass choice, is not spectacular, but it may be significant when the ultimate in design quality is sought.

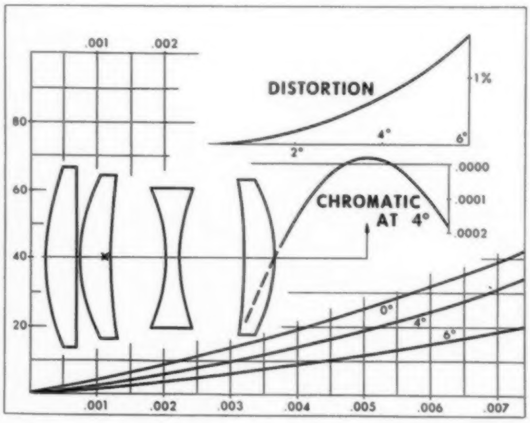

Fig. 1. Shown here is SYM-0, the initial rough design suggested by the symposium group. Its corresponding energy distribution curves are labeled 0°, 4°, and 6° and appear directly below the lens drawing. Because of the enormous size of the point image, only a small portion of the curves are plotted here. However, the scale used is identical with that used for the improved designs in Fig. 2.

Up to this point the LEAD program had treated the glass parameters as continuous variables. SYM-1, in fact, has fictitious glasses, and it was originally intended to publish SYM-2 in the same manner. As long as the glass parameters lie within the region enclosed by the boundaries imposed by available glasses, it is always possible to find actual glasses which can be substituted for the fictitious ones. (A possible exception exists if secondary spectrum is considered.) It has become routine to make a final computer run with fixed glasses which have been chosen manually to lie close to those selected by the program as the best. Ordinarily, this final run requires about 5 min of 7080 time. In the case of the symposium design, it was perfectly obvious that changing to real glasses was a trivial problem. However, so much criticism was directed to this point by people unfamiliar with the power of automatic methods, that it was finally decided to publish SYM-2 with actual glass data. No significant loss in quality was observed as a result of this operation. It is interesting to notice that LEAD was smart enough to use a low index in the front element. It then chose a sneaky way* to solve the distortion and lateral color problem by using the rare-earth type of glasses in the rear and second elements.

Upon receiving the data on SYM-2, Hopkins was put on the spot. From his experience with trying to improve on SYM-1, he knew it was futile to use the glasses in SYM-2 and try to improve on the image quality. He was convinced that the machine could optimize. The only hope was to criticize the design in other areas. On the basis that a new type of four-element lens must be found, he designed 22 complete solutions, taking 82 min of machine time. It was possible to maintain the low index in the front two elements provided the negative lens was allowed to thicken. Finally, it was decided to violate one of the conditions and use a high-index flint element. The best performance was obtained with the solution shown in Fig. 2(d). The lens specifications are given in Table V.

Now is the problem solved? Within the framework of the original formulation the answer is yes. Any of the four finished designs would make good lenses. If the best quality is desired, it is necessary to use high-index glasses, such as those in SYM-2 or ORD-2. On the other hand, SYM-1 or ORD-1 would be cheaper.

In a broader sense, however, the problem cannot be solved until more information is available. Questions such as the following need answers.

(1) What is the purpose? Is it a camera lens? A projector lens? A device for collecting energy?

---

* According to Hopkins.

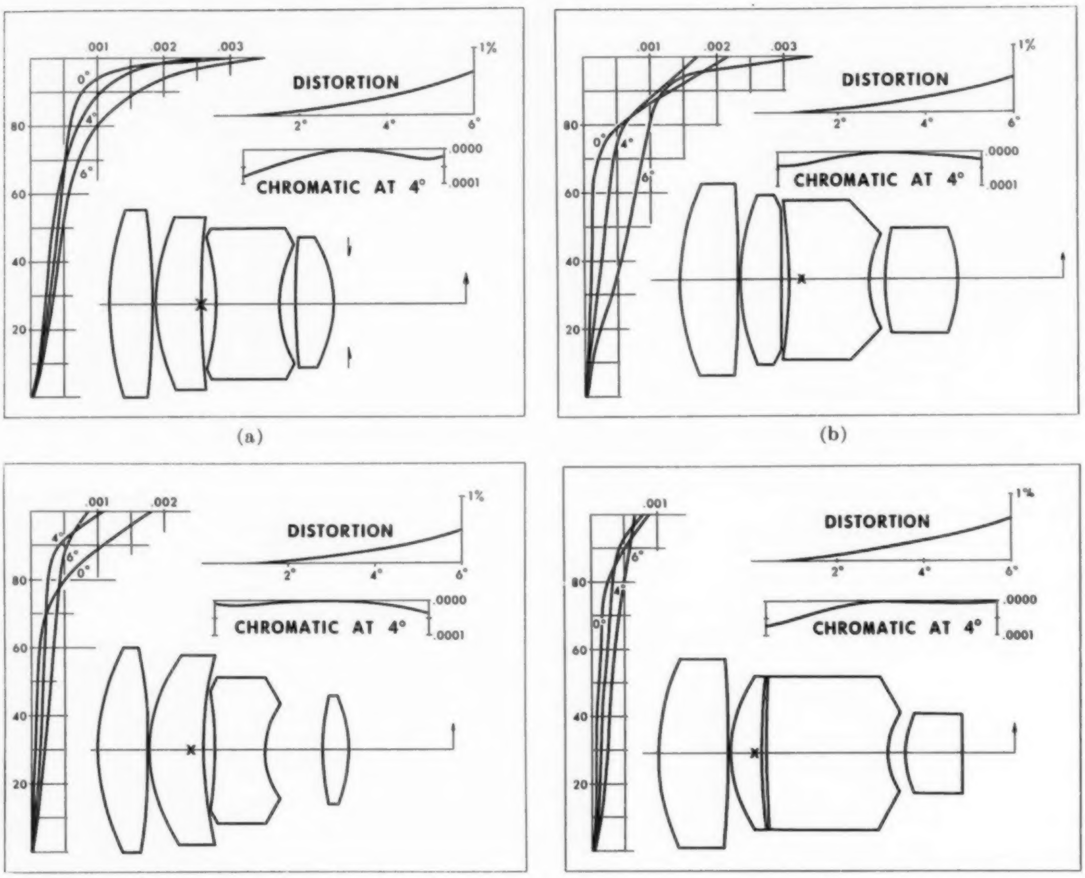

(a)

(b)

(c)

(d)

Fig. 2. These lenses and their accompanying image errors are plotted on the same scale as Fig. 1. The left-hand curves (labeled 0°, 4°, 6°) represent the distribution of energy in the images of three point sources at corresponding angular distances from the axis for light of wavelength 5893 Å. The abscissa gives the diameter of the smallest circle in the image plane containing that percentage of the total energy given by the corresponding ordinate. The chromatic aberration curve is based upon Conrady's D-d method and represents the wavefront deviation between F and C for a meridian section of the 4° field. The vertical scale gives the deviation in terms of unit focal length whereas the horizontal scale (not marked on the graph) represents the aperture of a meridian section for an $f/1.5$ beam at 4°. The cross appearing in the drawing of the lens marks the location of the second principal plane. The baffle in (a) restricts the illumination at 6° to 70% of that on axis. (a) SYM-1, the first LEAD design. (b) ORD-1, the first ORDEALS design. (c) SYM-2, the second LEAD design. (d) ORD-2, the second ORDEALS design.

(2) For the intended application, how is cost balanced against image quality or image quality against weight?

(3) How many lenses will be made? By what process?

Only after such questions have been asked, and answered, can the lens designer make an intelligent appraisal of the fine differences between the four designs presented here. Certain details strike one immediately, for example, the extremely thick flint in ORD-2. Is this going to cut transmission too much? Will it increase the weight too much? On the other hand, SYM-2 has a little haze around the image at 0°. Should one prefer the haze in SYM-2 over the extra weight in ORD-2? What about the relative cost?

Beyond these detailed questions, a host of others are lurking. Basically they all arise when the lens designer asks himself one question. "Were the original requirements sensible?" Is 70% illumination necessary? Would 60% be still satisfactory? How about the back focal length? Perhaps a big improvement can be made by relaxing this restriction a bit. What about the field angle and focal length? Would it be better to increase the focal length and reduce the field angle? Or vice versa? Does the image quality have to be this good? In a 1-in. (2.5-cm) focal length, this lens should resolve over 150 lines/mm at the edge of the field. How about increasing the aperture and accepting a smaller resolution?

Some of this may sound like changing the rules in

Table V. The ORD-2 Design[a]

N_D	V	t	c
			1.2390
1.5004	66.0 (BK 4)	0.2735	
			−0.0688
		0.0010	
			2.0050
1.5004	66.0 (BK 4)	0.1242	
			0.3665
		0.0147	
			0.0176
1.7213	29.3 (SF 18)	0.4688	
			4.0320
		0.0701	
			2.7460
1.6967	55.6 (LAK 14)	0.2181	
			0.0468

[a] The entrance pupil is 0.707 to the right of the first surface. The focal length is 1.000. The back focal length is 0.1982. The energy distribution curves shown in Fig. 2 were computed on a plane shifted −0.0012 from the paraxial focus.

the middle of the game. Unfortunately, the lens designer must recognize that this is part of his job. Usually he who submits the original specifications is not equipped to say that they are reasonable. Sometimes you can guarantee that they are definitely unreasonable! In any event, the reorganization of the specifications to make them sensible is part of the design problem. Furthermore, this cannot always be done in advance, but has to await knowledge accumulated during the course of the design. It has become apparent that less of the energy of the designer needs to be directed toward "design" in the traditional sense of varying radii, thicknesses, and indices, whereas more attention must be given to the over-all problem. The computers are rapidly taking over the correction process and doing the job better and far faster than human designers. It is likely that they can also be used in the broader aspects of design. One of the first needs is a program to compute construction costs and to balance their reduction against improvement in quality. Conventional machines and conventional programming should be able to handle this task, but it will take a great deal of programming and will require judgment to use it.

References

1. R. E. Hopkins and G. H. Spencer, J. Opt. Soc. Am. **52,** 172 (1962).
2. D. P. Feder, Appl. Opt. **2,** 272 (1963).

Applied Optics BOOKS

Books for review should be submitted to the Managing Editor, APPLIED OPTICS, 1155 16th St., N.W., Washington 6, D.C.

Fundamentals of Theory Design and Application of Electronic Computers. V. A. Zimin, Gos. Nauchn.-Tekhn. Izd. Mashinosh Str. Lit., Moscow, 1962. 738 2r. 64k ($2.93).

This seems to be the first full-scale Russian treatment on the engineering aspects of the construction and organization of large high-speed computing machines. It is systematically arranged in a fashion that would make it useful as a text (for readers of Russian!). On the other hand, it contains enough detail so that, while not a handbook, it can also play the role of a reference treatise. The book is organized in the same fashion as a computer itself would be; there are groups of chapters on logic and arithmetic, control, storage, and input and output. The amount of material on each of these topics decreases in the order in which they have been listed. As usual, the subject of input and output receives least attention.

In two introductory chapters there are discussions of the mathematical and the physical foundations of automatic calculation. This includes a brief perusal of the use of algorithms, the influence of different number systems, and the process of coding. The physical principles of switching, the transmission of information signals, the employment of various power supplies, and other such basic topics are also taken up in this introductory section. A large amount of space is given to a detailed explanation of the use of passive components and switching elements in the formation of logic and arithmetic circuitry. Specific examples are given of the circuits required for the various digital operations. The use of vacuum tubes, transistors, diodes, cores, and other particular components is described. Larger functional blocks—shift registers, counters, summing circuits—which employ these basic digital circuits, are discussed in a separate chapter. In the chapter on input and output devices the standard equipment is described and compared. This includes punch cards, paper and magnetic tape systems, and various information transformers such as digital to binary converters. Block diagrams and schematics of particular systems are exhibited. Some of the problems involved with magnetic reading and writing are presented. The discussion of information storage takes up the use of magnetic drums but emphasizes the application of ferrite cores in memory systems. The use of cores with tube and transistor circuitry is evolved in some detail. Auxiliary storage equipment, such as magnetic tape and magnetic disks which are used for reference data, are briefly taken up. There are several chapters on the actual realization of calculational operations and the control facilities required for this realization. Sequential and parallel operations are discussed as are the implications of fixed and floating point arithmetic for the control function. The book does not deal extensively with programming, but programming is mentioned in the chapter on control, especially the program requirements for automatic direction of the flow of computation. Block diagrams, flow charts, and timing charts are used to relate the requirements in direction and control to the physical systems that have been earlier described. Finally, the entire computer is evaluated as a system, and comparisons are made between various specific machines. Here (and elsewhere in the book) the IBM-704, the British machine Mercury, and the Russian BESM are compared. The special requirements in the way of programming, storage, speed, flexibility, etc., needed for engineering calculations on the one hand and other more general scientific computations on the other are pointed out. In the last chapter some future developments and expectations are considered. Multiprogramming is mentioned, as are new external memory systems and new digital elements. The need for continuing development of machine organization is stressed. The book is an engineering treatment and should be of use both to the person learning the field of computer engineering and design and to the person in the field who has already become specialized and wishes to broaden himself. It is not oriented toward the computer user nor does it intend to provide much information on the programming and coding of problems.

As with any such attempt to set down the technical details of so many topics in this young and fast moving field, this book will, in its turn, fall out of date. At present, it appears to be an adequate summary of the engineering aspects of high-speed computers. It is to be compared with *Digital Computer Components and Circuits* by R. K. Richards Van Nostrand, Princeton, N.J. 1957), although it probably has a more extensively technical treatment than the Richards' book. Another comparable American text is that of R. S. Ledley, *Digital Computers and Control Engineering* (McGraw-Hill, N.Y., 1960), but the book under review has far greater emphasis on circuitry and other technical detail.

H. G. Cohen

Donald P. Feder *Eastman Kodak* the editor for the feature on Lens Design and Computers in this issue.

Meeting Reports

8th Annual AFOSR Summer Scientific Seminar on "Topics in Optics", Cloudcroft, N.M., 17–28 June 1963

Reported by W. L. Hyde, University of Rochester

Every year for the last eight, the Air Force Office of Scientific Research has sponsored a seminar on a topic of current interest designed to inform Air Force officers, reserve officers on temporary duty, and civilian scientific workers of recent scientific progress in a particular field of knowledge. This year's topic was optics. During the period 17–28 June, about 175 participants listened to nearly 40 hours of lectures presented by 15 lecturers, listed here with their respective topics: E. C. Watson (history of optics); Claus Müller (electromagnetic wave theory); J. R. Oppenheimer (waves and particles); George W. Stroke (velocity of electromagnetic radiation); John Strong (diffraction gratings, balloon infrared astronomy); J. Dyson (interferometry); Arthur Cox (lens design); W. Lewis Hyde (fiber optics); Ira S. Bowen (spectroscopy); Robert Danielson (balloon astronomy—visible); Emil Wolf (coherence); William Baum (light amplification); C. H. Townes (lasers); and J. F. Hamilton (photochemical processes in the silver halides—formation of the photographic latent image). The talks generated lively discussions, and the isolated location of Cloudcroft, 25 km from Alamagordo, New Mexico, and 1200 m higher, gave lots of opportunity to speak privately with the lecturers.

Although the series will be continued next year (15–26 June 1964), the topic will change to "Communications and Cybernetics", with emphasis on man–machine relationships, information storage and retrieval, and data presentation. A limited number of participants not attached to the Air Force can be accepted, and interested persons should write to J. R. Foote, P.O. Box 1053, Holloman AFB, New Mexico.

THE SCIENCE OF COLOR

is reprinted

CHANGES OF ADDRESS

Changes of address should be sent to Applied Optics SUBSCRIPTION HANDLING, American Institute of Physics, 335 East 45th Street, New York, New York *as far in advance as possible.* Eight weeks should be allowed to effect such changes.

HAVE YOU RENEWED

YOUR SUBSCRIPTION?

Lens Design by Computer

C. G. Wynne and P. M. J. H. Wormell

A method of semiautomatic optical designing previously described has been developed further on a faster electronic digital computer. The new programs embody comprehensive controls of boundary conditions and are more fully automatic in operation. With these refinements and increased machine speed, it has become possible to explore the nature of the process of convergence to an optimum design.

I. Introduction

A method of semiautomatic optical designing suitable for use on an electronic digital computer has been described by Wynne,[1] and the application of this method on a computing machine (a Ferranti Mark I*) has been described by Nunn and Wynne.[2] This paper describes further developments of this work, using a faster computer (Ferranti Mercury). The mathematical method is the same as that previously described, but several limitations that existed in the programs on the earlier machine have been eliminated; in particular, more comprehensive and sophisticated procedures are now used for the control of various boundary conditions, and the program has been made more fully automatic. Moreover, the increased speed of the Mercury machine has made it possible to pursue the process of automatic aberration correction much further, so that a clearer picture is emerging of the nature of the aberration function with which the machine deals and the nature of the process of convergence to an optimum design.

II. Method

The method used is an iterative one, using a linear approximation to the change of aberrations with design parameters. Since, in fact, the dependence of the aberrations of an optical system on the design parameters is highly nonlinear if large changes are made, the linear approximation can only be used for steps of the iteration of limited size. The essence of the method we are using is that it enables this permissible step length to be as large as the limited range of approximate linearity allows, making the best use of all the available design parameters within this range, the range in each case being determined by the machine. It proves, in practice, to be the case that, under these conditions, the rate of improvement of aberration correction is quite rapid.

The machine is given an initial design of an optical system, together with a representative set of rays to be traced through it. The aberrations along these rays are calculated and multiplied by weighting factors also supplied to the machine. These weighted aberrations will be denoted by A_i. Our current programs will accommodate up to 50 such aberrations, which is adequate for many purposes. A "figure of merit"

$$\psi = \sum_{i=1}^{i=m} (A_i)^2,$$

where m is the total number of aberrations controlled, is then calculated, and it is this number ψ that the machine reduces in successive iterations. The form of the aberrations used is not significant as far as the method is concerned: we use the transverse-ray aberrations, although to economize machine time chromatic aberrations are calculated by Conrady's approximate formula[3] for the wavefront aberration, and a factor converting these to effective transverse aberrations is included in the weighting factors.

The machine then calculates the first differential of each weighted aberration A_i with respect to each of the design parameters x_j, giving a matrix of differentials $\partial A_i/\partial x_j = a_{ij}$. Again, up to 50 variable design parameters can be accommodated in our current programs. For reasons connected with the characteristics of the computer we are using, the differentials are, in fact, calculated by using small finite differences, and we use composite variables, similar to those described by Nunn and Wynne,[2] which conserve the equivalent focal length and aperture of the optical system. In addition, these composite variables also have the effect of reducing the magnitude of most of

---

The authors are with the Optical Design Group, Imperial College, London, England.

Received 15 August 1963.

the cross terms among the second differentials, which are neglected (see below). Our current programs are restricted to systems of spherical surfaces; the earlier versions only changed curvatures and separations, not the refractive indices and dispersions of the optical materials. A program changing optical materials has recently been completed, but it has not been used extensively, so this paper will mainly deal with the earlier versions.

If changes x_j be made to the design parameters, where j goes from 1 to n (n being the number of parameters), and if A_i' be the new value of the aberration A_i after the changes have been made, then the matrix equation

$$[a_{ij}]x_j + A_i = A_i' = 0 \tag{1}$$

gives the changes x_j which would be required to reduce all the aberrations to zero, assuming linearity. If the number of parameters were equal to the number of aberrations that are controlled, these equations could be solved, or if, as is more often the case, the number of aberrations that need to be controlled be in excess of the number of design parameters, then the normalized least-squares equations

$$[a_{ji}][a_{ij}]x_j + [a_{ji}]A_i = 0 \tag{2}$$

give the changes x_j required to make ψ a minimum, assuming linearity. But the linear approximation is only valid for small values of x, while, as Wynne[1] showed, it is inherent in the nature of the physical problem that these equations are highly ill-conditioned, having, in general, some roots that are enormously beyond the range of approximate linearity.

This dilemma we overcome by adding to Eqs. (1) a second set

$$Px_j = 0, \tag{3}$$

where P is a weighting factor discussed below, and by performing a least-squares solution on the combined set of Eqs. (1) and (3). The mathematical effect of this addition of Eqs. (3) is simply to add a constant term P^2 to each diagonal element of the product matrix $[a_{ji}][a_{ij}]$ in Eqs. (2), which is a trivial operation for the computer. The effect of Eqs. (3) on the solutions x_j is to reduce the excursion of the variables by an amount depending on the size of the weighting factor P. For any finite value of P, the least-squares solutions x_j will be such that $\Sigma x_j^2 = R^2$ will be less than the corresponding solution of Eqs. (2) alone, R will be increased or decreased as P is decreased or increased, and this step length R in parameter space can be made equal to the approximate range of validity of the linear Eqs. (1) by a suitable choice of P. The method of controlling the step length is discussed below. If Eqs. (1) are valid, it can be shown[1] that the solution leads to the smallest value of ψ within a distance R from the origin. In fact, Eqs. (1) are only valid for limitingly small values of x_j, higher terms in the Taylor expansion always being present, but it proves possible, in practice, to take quite large steps R in parameter space with good linearity. Some aspects of the effect of the higher terms are discussed below (Sec. III). The method we use, then, is to take the least-squares solution of Eqs. (1) and (3) combined, P being chosen to make the step as large as linearity will allow, set up the new system corresponding to the x_j values found, calculate its actual ψ, recompute the matrix $[a_{ij}]$ for the new improved system, and iterate the procedure. This method, which Wynne called by the acronym SLAMS (successive linear approximation at minimum step) is equivalent to the method of "damped least squares" described by Levenberg.[4]

III. The Missing Quadratic Terms

To the approximation we are using, when changes x_j are made to the system, the figure of merit $\psi = \Sigma A_i^2$ is given by

$$\psi' = \sum_{i=1}^{i=m} \left\{ A_i + \sum_{j=1}^{j=n} x_j \frac{\partial A_i}{\partial x_j} \right\}^2 \tag{4}$$

which includes second-order terms of the form

$$x_j x_k \frac{\partial A_i}{\partial x_j} \frac{\partial A_i}{\partial x_k}. \tag{5}$$

In fact, higher terms than the first in the Taylor series for A_i' in terms of x_j are certainly significant. Inserting these second-order terms, in place of (4) we have

$$\psi' = \sum_{i=1}^{i=m} \left\{ A_i + \sum_{j=1}^{j=n} x_j \frac{\partial A_i}{\partial x_j} + \frac{1}{2} \sum_{k=1}^{n} \sum_{j=1}^{n} x_j x_k \frac{\partial^2 A_i}{\partial x_j \partial x_k} \right\}^2. \tag{6}$$

Comparing this equation with Eq. (4), it appears that second-order terms of the form

$$A_i x_j x_k \frac{\partial^2 A_i}{\partial x_j \partial x_k} \tag{7}$$

have been neglected in the latter. These are mathematically of the same order as the quadratic terms (5) which are included in (4), and hence the neglect of these terms might appear to invalidate the method. The fact that the method works well, in practice, shows that the effect of the neglected quadratic terms must, in fact, be numerically smaller than that of the included terms. Grey[5] has discussed some reasons why the individual neglected terms may be expected to be numerically smaller than the included terms.

In addition to the factors affecting the magnitude of the individual terms discussed by Grey, a consideration of the signs of the different sets of terms shows that their combined effect will be relatively small. The quadratic terms which are included may be subdivided into two sets,

$$mn \text{ terms of the form } x_j^2\left(\frac{\partial A_i}{\partial x_j}\right)^2,$$

$$mn(n-1) \text{ terms of the form } x_jx_k\,\frac{\partial A_i}{\partial x_j}\,\frac{\partial A_i}{\partial x_k},\quad j \neq k.$$

In the former set, the terms are all essentially positive; in the second set they are, in general, as likely to be positive as negative, so that their combined effect may be expected statistically to be equivalent to $\{mn(n-1)\}^{1/2}$ of the first set of terms, or to be of the order of $(m)^{-1/2}$ as large as the first set.

Similarly, the neglected terms consist of mn^2 terms of the form

$$A_ix_jx_k\,\frac{\partial^2 A_i}{\partial x_j\partial x_k}.$$

These, again, generally have an equal probability of being positive or negative, so that, even if they were individually of the same magnitude as the terms included, their combined effect would be expected statistically to be of the order of $(m)^{-1/2}$ as large as the first set. In applying the method, we are concerned with problems where the number of aberrations m that are controlled is fairly large, ranging from 30 to 50: so that, even if the neglected terms were not individually smaller, their combined effect on the value of ψ would be expected to be only from one-sixth to one-eighth as large as that of the included terms.

IV. Control of Step Length

Originally, the value of P, which controls the step length, was made by manual intervention on the machine console, after inspection of the printed results at each iteration. With a faster machine this becomes no longer practicable, but quite simple criteria prove efficient for enabling the machine to choose its own P value at each stage.

The machine, at each iteration, computes the value of ψ for the initial system, the value of ψ' for the new system corresponding to the solution x_j it has found (in each case by tracing the specified rays), and, in addition, it calculates the value ψ_{LIN}' to be expected, assuming linearity, by substituting the x_j values into Eqs. (1). If too large a step length R has been taken, well beyond the range of approximate linearity, ψ' will be larger than ψ, and the step length must be reduced (P increased). If there is very close agreement between the values of ψ' and ψ_{LIN}' compared with the improvement $(\psi - \psi')$ that has been achieved, the step length will have been smaller than it need have been, and a greater improvement of the system is to be expected if the step length R is increased (P reduced).

The step length R that results from a given value of P is different at different points in parameter space. The least-squares solution of the combined set of Eqs. (1) and (3) is the solution which minimizes $(\psi' + P^2R^2)$. In a region of parameter space where $d\psi'/dR$ is large (where rapid improvement of the aberrations is possible), a given value of P will result in a larger step size than when $d\psi'/dR$ is small; and hence, in the former case, a larger value of P is required to maintain linearity than in the latter case. The slope $d\psi'/dR$ proves, in practice, to vary considerably from region to region, so considerable variations of P may be necessary over the course of a number of iterations.

However, the choice of P is not critical, since a plot of ψ against R in a region where improvement is possible, will show ψ initially falling to a minimum and subsequently increasing for larger values of R, where the range of approximate linearity is greatly exceeded. The machine is given a value of P for the first iteration, and thereafter it chooses the value of P on the following criterion: if at any iteration ψ' is greater than ψ, that solution is rejected and the matrix operations are repeated with P doubled, giving a new solution. If ψ' is less than ψ, the solution is accepted as the start of a new iteration; if, in this case, $(\psi - \psi')/(\psi - \psi_{\text{LIN}}')$ lies between 0.5 and 0.9, P remains unchanged at the next iteration; if this ratio is less than 0.5, P is doubled at the next iteration, and if this ratio is greater than 0.9, P is halved at the next iteration. These simple criteria have proved adequate to give efficient convergence.

In the course of a typical series of iterations, a plot of the figure of merit ψ against the step length R in parameter space generally shows initially a rapid fall of ψ for a few (four to six) steps, after which it improves more slowly and P is reduced to maintain a reasonable step length. The initial rapid improvement simply results from the fact that it is inherent in the method we are using that the machine reduces first those aberrations that are most readily reduced. The initial region of rapid improvement is followed by a larger region of slower but significant improvement, and P may be maintained constant for a longer series of iterations, but with a variety of different types of optical system, we have found fairly sudden subsequent increases in the slope of ψ (the design has reached a situation where more rapid correction again becomes possible) and in these regions P will be temporarily increased, until the slope of the curve falls again. In addition, local regions of increased nonlinearity occur without an increase of slope of ψ, which also require a temporary increase of P. With every optical system we have run for long enough to show the effect, the slope of the curve gradually becomes extremely small, and a very long series of designs are produced having, over a long run, very considerable differences in the design parameters but extremely small differences in ψ. In this region of very slow improvement, P is again increased, since errors of linear prediction, of a size which were negligible before in relation to the improvement achieved at each step, become significant, so that only small steps R can be taken. In a few systems, we have reached what appears to be a real minimum, judged by the test that P can be put equal to zero and the solutions x_j are still very small. But in most cases this does not occur, the curves finally becoming so flat that the maximum permissible step length gives a reduction of ψ less than the rounding errors inherent in the machine word length (equivalent to nine decimal digits) and further iterations become pointless.

This extreme flatness of the minimum region was not expected, but it seems to be typical. From the point of view of lens designing for practical purposes, this region is, of course, of only academic interest. Starting from a reasonably well corrected system, a series of from 10 to 20 iterations commonly gives almost all the improvement that is of practical significance.

V. Control of Boundary Conditions

It is necessary that the thicknesses of lenses and air spaces in an optical system, over the apertures traversed by rays, be maintained at positive values adequate for manufacture to be possible. In addition, other physical limitations may be required, such as a maximum over-all length from front vertex to focal plane, for example, in a telephoto lens, or a minimum back focal distance, for example, in a lens for a reflex camera, and the refractive indices and dispersions of the optical materials must lie within the ranges that are available. An automatic design program must be constrained to comply with these boundary conditions, which are specified to the machine as part of the initial data.

These conditions fall logically into two groups: Considering thicknesses only at first, the first group consists of axial thicknesses, which can be checked for violations as soon as a new system has been set up, corresponding to a set of solutions x_j, and which are changed only by a single design parameter. The second group consists of edge thicknesses along the ray farthest from the axis, which cannot be checked until the ray trace through the new system is carried out and which are functions of all the design parameters in the part of the system preceding the space in question. The procedures to be used for the two groups are different.

For axial-thickness control, the machine tests at each iteration, when it has set up a new system, whether any of the axial boundary conditions have been violated. If they have, this solution is rejected, and the machine returns to the matrix operations, removing the lines from the $[a_{ij}]$ matrix corresponding to the axial-thickness changes that have produced violations, and resolves the reduced matrix; this may occur several times in succession. The effect of this procedure is that the axial thicknesses in question are removed from the list of variables, these thicknesses being frozen at their previous values. Since it is found from experience that when any given direction of parameter change is desirable for aberration correction at one iteration, the probability is about six or seven to one that this will be the case for the next iteration; the machine is given a memory, and an axial thickness which has violated and been frozen remains invariant for subsequent iterations. Over a series of iterations, these trends often change, so that it is expedient to remove the memory at about every sixth iteration (this is, at present, done by switching at the console) so as to enable the machine to increase an axial thickness that has been frozen, if this has become desirable for aberration correction.

Edge-thickness violations, being dependent on many variables, require different treatment. An edge violation is detected when rays are traced through a new optical system, and when it is detected the machine discards the solution, and the largest edge violation in the space in question is then treated as an aberration; it is multiplied by a fairly large weighting factor, added to the aberrations A_i of the previous system, its differentials with respect to the design parameters are added as an additional column to the matrix $[a_{ij},]$ and a new solution is obtained, in which the violation is substantially eliminated. As before, the machine is given a memory of edge violations and maintains them in the aberration list for subsequent iterations until the memory is removed.

Programs embodying this system of control of boundary conditions have been used on a wide variety of different types of optical system and have proved satisfactory. The method is essentially simple, in principle, but the machine programing to carry it out is fairly complicated; about 40% of the whole design program is concerned with the control of boundary conditions.

Turning now to boundary conditions other than thicknesses, such limitations as maximum over-all length are treated exactly as edge thicknesses.

For glass changes, the treatment used at present is similar to that for axial thicknesses. The machine is given the limits of refractive index and dispersion for which optical glasses exist and is left free to choose any values within these boundaries. At each iteration, the machine determines whether the values of index and dispersion chosen for each component lie within the boundaries, and if any do not, the machine returns to the matrix operations, removing the lines of the matrix corresponding to changes of this glass, and solves the reduced matrix; that is to say, the glass that has moved outside the boundaries is frozen at its previous value. An extension of this control is in hand, but not yet completed, which will enable the machine to move a glass along the boundary, i.e., to make a change of index, provided this is associated with the change of dispersion necessary to keep the glass within the range available.

These glass-changing procedures are clearly subject to various limitations. The fact that optical glasses are not available as a continuum within specified limits is met by treating the problem as if they were a continuum until the machine approaches an optimum. The nearest glass values actually available to those which the machine has chosen are then inserted, and a new optimum is found by using curvature and separation changes only. This glass-changing method essentially allows of correction for a single pair of wavelengths; a program that included the automatic correction of secondary spectrum would necessarily be much more complicated.

VI. Use of the Programs

We have a series of different programs, adapted to different requirements, for example, systems with flat or curved image fields, and systems of unit magnification with symmetry about a central stop have separate programs. As stated above, extensive work has so far been undertaken with programs that alter only curvatures and separations but not optical materials.

Clearly, the main practical use of automatic design programs of this kind is for systems of some considerable complexity; for simple systems having only two and three glass elements it is to be expected that the potentialities have been fairly fully explored by traditional methods. The applications of our programs have therefore been restricted to fairly complicated systems, and for these they have become a standard working tool. We have generally taken as starting data an existing optical design of reasonable performance, often a design that had previously been brought to as high a state of correction as proved practicable by traditional designing methods. Our experience so far is that, for any system of five or more glasses, the machine has always been able to achieve at least a somewhat higher degree of correction than the human designer, and often much higher. The machine often effects very considerable improvements to higher order aberrations that the human designer finds great difficulty in correcting because no adequate theory is available, such as skew-plane aberrations and chromatic differences of aberrations.

The probability that the machine will do better than the human designer naturally increases as the complexity of the system—the number of design parameters—increases, as is to be expected since the human mind finds it difficult to manipulate effectively a large number of parameters simultaneously, and, when a large number of aberration terms have to be controlled, this will normally only be possible by the simultaneous variation of a large number of parameters. We have found it unequivocally desirable to allow the machine to use all the available design parameters simultaneously, rather than in smaller groups; when the number of parameters available to the machine is increased, the permissible step length R to maintain adequate linearity is reduced, but this effect is more than offset by the increased potentialities of correction.

Although most of the work we have done has been on systems that were fairly well corrected initially, this is by no means necessary; an initially very poorly corrected system is rapidly brought by the machine to a reasonable state of correction, provided it is of a form that has this potentiality. Such tasks as the rebalancing of a given system for a different aperture, field angle, wavelength range, or magnification are rapidly effected, and in the last case, for example, correcting for an object at infinity a system originally designed for unit magnification, systems that were poorly corrected initially have been treated successfully.

The possibility offered by these programs of rapidly bringing any optical system to a near-optimum form makes it possible to undertake systematic investigations of a type that were not previously practicable. For example, we have recently investigated the effect of the use of lanthanum oxide glasses in a double-Gauss lens of aperture $f/2$ covering a 40° field. Starting from a design involving older type glasses that had previously been optimized, we reoptimized using a high index glass, first for the front single lens, then for the rear single lens, and then for both together. It emerges that, with the criterion we were using, the improvement effected by raising the index of the rear element is more than double that from raising the index of the front element, while the improvement gained by raising both simultaneously is almost double the sum of the improvements gained by raising either separately. In the last case, the secondary-plane oblique aberration was reduced to about two-thirds of its value for the three other versions, in all of which the size of this aberration was about the same.

Optimization, in the sense in which we are using the word, implies a particular definition of ψ, which, in turn, implies a choice of rays and aberrations to be calculated and of weights to be attached to them. The choice of rays to be traced is not at present made by the machine, but by the designer. It is determined from an inspection of fairly full ray-tracing results on the initial system to find the most significant sampling points of the aperture and field; this was discussed more fully by Nunn and Wynne.[2] The shapes of the aberration curves may change basically in the course of a run, especially when the machine effects very considerable improvement to a system, and it may become desirable to use different or additional rays. No attempt has been made so far to program the machine to carry out this process.

The extremely complicated nature of the relation between the aberrations of an optical system and the design parameters emerges very strikingly from all the work we have done with our programs. Some aspects of this have been discussed above. The problem is conveniently considered in terms of a multidimensional relief map of ψ in parameter space. The ill-condition of Eq. (1) then means that the map consists of very narrow valleys. The nature of the SLAMS process is such that successive iterations give points on the map, near the floor of a valley, located successively farther down its course, and, as discussed in Sec. IV, it emerges that the slope along the valley floor is markedly variable along its length. As mentioned in Sec. V, the direction of change of any given parameter commonly remains the same for a few iterations, but thereafter it may reverse its direction of change, and this may happen a number of times; in the course of 20 or 30 iterations, several parameters may change their direction of change five or six times. The valleys in the multidimensional ψ-map, therefore, take a very meandering course; it seems likely that the local increases of nonlinearity referred to in Sec. IV may be associated with bends in the course of a valley.

From this extreme complexity of the aberration function—the highly convoluted form of the ψ-map—some general conclusions can be drawn about the likely efficacy of other methods of optical design. It is immediately clear that the use of simple change tables will not be adequate for optimization. It has sometimes been suggested that, as larger and faster machines become available, it might be profitable to calculate the second-order terms in the Taylor expansion of the aberrations with respect to the design parameters. The aberration function is obviously of such complexity that the first- and second-order terms alone would be quite inadequate for a process leading directly to a minimum, without the need for iteration; to achieve this, very many higher order terms would be necessary, and, for the multiparameter systems that are of practical interest in optical designing, this would be beyond the range of any computing machine at present envisaged.

Acknowledgment is due to R. N. Wilson, who did much of the program writing.

References

1. C. G. Wynne, Proc. Phys. Soc. (London) **73,** 777 (1959).
2. M. Nunn and C. G. Wynne, Proc. Phys. Soc. (London) **74,** 316 (1959).
3. A. E. Conrady, *Applied Optics and Optical Design*, Part II (Dover, New York, 1960), p. 640.
4. K. Levenberg, Quart. Appl. Math. **2,** 164 (1944).
5. D. S. Grey, J. Opt. Soc. Am. **53,** 672 (1963).

Information for Contributors

Scope: Papers are welcomed in the broad areas of applied optics, in disciplines related to optics and employing optical techniques. Papers should be sent to *The Editor, APPLIED OPTICS,* AFCRL, Bedford, Mass. Manuscripts may be submitted in English, French, German, or Russian, and the presentation should be as succinct as comprehension will permit. In general, the metric system of units is preferred. One original and one carbon copy of the manuscript, with two sets of all illustrations, must be sent in. Manuscripts should be typed double or triple spaced on one side of 22 × 28 cm ($8^{1}/_{2}$ × 11 in.) paper, leaving a 3.8 cm ($1^{1}/_{2}$ in.) margin all around. Equations must be typed not hand written wherever possible. Papers on the more fundamental aspects of experimental and theoretical optics should be sent to *The Editor, JOURNAL OF THE OPTICAL SOCIETY OF AMERICA,* 68 Hammond Street, Rochester, N.Y. 14615.

An **abstract,** adequate as an index and a summary, of not more than 100 words should appear at the beginning of the paper after the *title, author's name, affiliation, and address.* In the case of papers in a non-English language, they must be accompanied by an abstract in English as well as an abstract in the language of the paper. It should be borne in mind that this abstract may be used in toto by the abstracting journals, therefore it should be self-contained.

Figures suitable for printer's use should be sent. Bear in mind that illustrations will normally be reduced to column width (8.4 cm—$3^{5}/_{16}$ in.—20 picas). *Halftones:* two sets of glossy prints are needed, which should be mailed flat, with any proportion or framing indicated on a working copy. *Line drawings* should be suitable for reproduction and be not larger than 22 × 28 cm ($8^{1}/_{2}$ × 11 in.). *Captions* should be listed on a separate sheet in addition to each caption appearing on each illustration.

Tables should be typed on separate sheets and the data therein be intelligible, by title, without reference to the text. Tables should include a minimum of vertical ruling.

References must be typed on a separate sheet, be numbered consecutively in the order of their appearance in the text, and follow this form:

1. F. C. Brown, Phys. Rev. **12,**345 (1821).
2. J. Culpeper, *Space Optics* (Georgetown Institute of Technology Press, Washington, D.C., 1861), pp. 12, 345.

A list of abbreviations for the names of journals is published in *Chem. Abstr. List of Periodicals 1961.* To make for uniformity of presentation generally, the American Institute of Physics *Style Manual*, second edition, should be used. In general, *APPLIED OPTICS* differs from the *Style Manual* only inasmuch as footnotes appear at the bottom of the page of text, while references are listed numerically at the end of the paper.

There will be no **page charge** for publishing in *APPLIED OPTICS* for the time being.

Letters to the Editor should follow the above suggestions, but no abstract is required.

The Role of Eikonal and Matrix Methods in Contrast Transfer Calculations

W. Brouwer, E. L. O'Neill, and A. Walther

The notion that the optical contrast transfer function is a useful tool for assessing the performance of image-forming instruments has been accepted generally for some time and is now well established. This paper discusses one method of making the transition from ray-trace data to the evaluation of this important function. First, the light distribution in the point image is rigorously derived in terms of an integral over angular coordinates involving the eikonal function about a reference surface at infinity. Then, the ray-trace procedure is developed in the language of refraction and translation matrices culminating in matrix elements which are simply related to the eikonal coefficients of wave optics. Finally, the numerical evaluation of the contrast transfer function in amplitude and phase from these eikonal coefficients is presented, and the paper ends with an example showing the off-axis transfer function for line structures oriented at various azimuths. All calculations are carried out to fifth order in the eikonal coefficients, and emphasis is placed on the usefulness of this approach on relatively slow, low-capacity computing machines.

I. Introduction

The application of Fourier techniques to the theory of image formation has been studied extensively in the preceding decade.

The theory that was developed has been accepted generally as a useful tool in the analysis of optical systems. It centers on two concepts: point-spread function and frequency-transfer function, one being the Fourier transform of the other. Each of these functions can, in principle, be determined when the geometrical aberrations of the lens are known.[1-3]

In practical problems of lens design the ability to evaluate the transfer function numerically would be a great asset to the lens designer. The authors have the impression that one step in the procedure of computing this function is not well known to many workers in the field: the conversion of ray-trace data into wavefront deviations. Following Luneberg[4] and Wolf,[5] we shall treat this problem in a way which is at once simpler and more rigorous, by using eikonal functions instead of wavefront shapes. This approach has the additional advantage that it shows in a unique way the transition from wave optics to geometrical optics.

In the ray-tracing calculations a system of two by two matrices as introduced by Smith[6] and Brouwer[7] will be used to great advantage: the relation between the matrix elements and the eikonal functions will be shown to be very simple, and easier to apply than the usual ray intercepts. This leads to a way of calculating the transfer function that is well suited to relatively slow computers with a rather small memory capacity.

In Sec. II we derive an expression for the point-image amplitude distribution using the eikonal function to describe the aberrations and perform a Fourier transformation over the angular coordinates of a reference surface at infinity. In Sec. III we relate the matrix elements determined from geometrical lens design calculations to the eikonal function. Finally, in Sec. IV, starting with the coefficients in the eikonal expansion, we show several examples of off-axis transfer functions using the numerical integration scheme of Hopkins.[8]

II. Transition from Geometrical Wave Optics

A. Notation

We shall have occasion to use four planes associated with a rotationally symmetrical lens [Fig. 1(a)]. These planes are perpendicular to the axis of the lens and are, respectively, the object plane (coordinates x and y), the entrance pupil plane (coordinates x_1 and y_1), the exit pupil plane (coordinates x_1' and y_1'), and

---

W. Brouwer and A. Walther are with Diffraction Limited, Inc., Bedford, Massachusetts. E. L. O'Neill is with the Physics Department, Boston University, Boston, Massachusetts.

Received 5 August 1963.

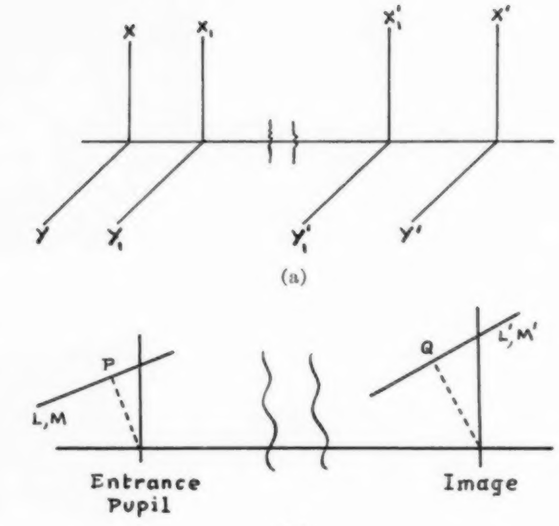

(a)

(b)

Fig. 1. (a) Coordinate systems. (b) Definition of angle–angle eikonal.

the image plane (coordinates x' and y'). The four axes marked with x lie in one plane, and so do the axes marked with y. The x and y axes are mutually perpendicular and intersect in the axis of the lens, marked by z, z_1, z_1', or z' depending on which of the four planes is used as a reference. The refractive index in the object space is denoted by n; in the image space it is n'. Since we consider only axially symmetric lenses and, unless indicated otherwise, an object point will be understood to lie on the x axis, we are allowed to refer to the x–z plane as the meridional plane.

B. Summary of Fourier Optics

In order to establish our notation and for reference purposes we shall give a brief summary of the basic concepts in Fourier optics. In what follows, $F(x_1',y_1')$ describes the complex scalar disturbance over the exit pupil plane, $a(x',y')$ the complex amplitude distribution in the image of a point source, $s(x',y')$ the intensity-spread function, and finally $D(\nu_x,\nu_y)$ the frequency response or transfer function for the system. By a direct application of Huygen's principle together with approximations that are quite valid for most optical systems it is not difficult to show that $a(x',y')$ and $F(x_1',y_1')$ are Fourier transform pairs in the form

$$a(x', y') = \iint_{-\infty}^{+\infty} F(\nu_x, \nu_y) \exp\,[2\pi i(\nu_x x' + \nu_y y')]\; d\nu_x d\nu_y, \qquad (1)$$

where ν_x and ν_y are reduced coordinates in the exit pupil about which we shall say more later, and where all constants and the finite area of integration have been absorbed into $F(\nu_x,\nu_y)$. Now by virtue of the fact that we are treating the optical system as a filter of spatial frequencies there exists a further Fourier transformation between $s(x',y')$ and $D(\nu_x,\nu_y)$ in the form

$$D(\nu_x, \nu_y) = \frac{\iint_{-\infty}^{+\infty} s(x', y') \exp\,[-2\pi i(\nu_x x' + \nu_y y')] dx'dy'}{\iint_{-\infty}^{+\infty} s(x', y')\, dx'dy'}, \qquad (2)$$

where the denominator has been introduced for normalization purposes ($|D(0)| = 1$). Capitalizing both on the fact that $s(x',y') = |a(x',y')|^2$ and the convolution theorem for the transform of a product, we end up with a direct relation between the disturbance over the exit pupil and the frequency response in terms of the well-known integral

$$D(\nu_x, \nu_y) = \frac{\iint_{-\infty}^{+\infty} F(\mu_x, \mu_y) F^*(\mu_x - \nu_x, \mu_y - \nu_y) d\mu_x d\mu_y}{\iint_{-\infty}^{+\infty} |F(\mu_x, \mu_y)|^2 d\mu_x d\mu_y}. \qquad (3)$$

These relations together with their physical interpretations have been fully described in the literature, and the uninitiated reader is invited to consult the references for further details of the Fourier approach (e.g., refs. 2 and 3). As it stands, the phase portion of $F(\mu_x, \mu_y)$ describes a surface of constant phase about a reference sphere passing through the center of the exit pupil whose center is an appropriate point in the image plane. Unfortunately, we have not found this a convenient reference surface in our attempts to bridge the gap between wave optics and geometrical optics. This transition is an important point. We wish to emphasize that the shape of the wavefront can be determined to *any accuracy desired* by means of the laws of geometrical optics. Consequently, any approximation in the translation of these geometrical data to data used in the work on diffraction involves an unnecessary waste of available information. Methods have been suggested to remove the wavefront deformation function from the exponent of the diffraction integral in an artificial manner so as to use quasi-geometrical methods in passing from the exit pupil to the image plane. These techniques (e.g., spot diagrams) must be treated with utmost care; in this paper we shall not take recourse to these approximations.

C. Wavefront Deviations

Our first aim shall be to establish a reasonably exact derivation for Eq. (1), which will automatically lead to the proper definition of ν_x and ν_y. We shall, as is usual in this field, restrict ourselves to the Huygens–Fresnel diffraction theory. There are several undesirable features in the usual derivation of Eq. (1). We mention:

(1) The shape of the wavefront depends on where one choses its location.

(2) Some authors measure the deviation of the wavefront along the rays. Others measure along the radii of the reference sphere.

(3) The relations between the coordinates that define a ray geometrically and the coordinates suited to diffraction calculations are very complicated.

(4) The diffraction integral takes only approximately the form of a Fourier integral.

The approach taken to this problem in the present paper, found to be due to Luneberg,[4] and also treated by Wolf[5] avoids these problems.

In Fig. 2, let $P(x,y)$ be an object point of which an optical system creates a diffraction image in the (not necessarily Gaussian) image plane (x',y'). Let $P'(x_0' + \xi', y_0' + \eta')$ be a point in which we wish to evaluate the amplitude of the diffracted light; ξ' and η' are coordinates in the diffraction pattern, measured in the image plane with respect to a reference point (x_0', y_0') which conventionally is chosen as the intersection point of the principal ray with the image plane.

When the light has traversed the optical system, the pencil of light is completely determined by a wavefront Σ. The line AQ represents a ray in the image space.

The wavefront being a surface of equal phase, the amplitude in the point P' is proportional to:

$$a(P') = \int_\Sigma F(A) \exp\left(\frac{2\pi i}{\lambda} W\right) d\sigma, \qquad (4)$$

in which $W = \overline{AP'}$ and $F(A)$ is the amplitude distribution over the wavefront Σ. A discussion of this amplitude distribution in the wavefront is outside the scope of this paper.

Let the direction of rays in the image space be given in terms of their optical direction cosines (L', M', N') which are defined as the geometrical direction cosines multiplied with the refractive index of the image space. Let OS be the normal drawn from the origin in the (x',y') plane onto the ray AQ. Then the optical path length $\overline{PAS}$ considered as a function $E(x,y,L',M')$ of x, y, L', and M' is known as the (point-angle) mixed eikonal of the system.[9,10]

When this function is known, the coordinates (x',y') of the intersection point of a ray with the image plane are given by:

$$\frac{\partial E}{\partial L'} = -x', \quad \frac{\partial E}{\partial M'} = -y', \qquad (5)$$

and the direction cosines of the rays in the object space:

$$\frac{\partial E}{\partial x} = -L, \quad \frac{\partial E}{\partial y} = -M.$$

Let RP' be the normal from P' drawn onto the ray AQ. Then we can write for the path length $\overline{AP'}$ in Eq. (4):

$$\overline{AP'} = E(L', M') - \overline{PA} + \overline{SR} + (\overline{AP'} - \overline{AR}), \qquad (6)$$

in which the dependence of E on x and y is omitted because we assume the object point to be fixed. The path $\overline{PA}$ is constant and may accordingly be dropped. The location of the wavefront is irrelevant, as long as we do not choose it "too close to the image plane." A great simplification is obtained if we make full use of this freedom and move the wavefront out to infinity. In that case the term $(\overline{AP'} - \overline{AR})$ in (6) reduces to zero and the line AP' becomes parallel to the ray AQ. For the projection $\overline{SR}$ of the line OP' onto the ray AQ we can write:

$$\overline{SR} = L'(x_0' + \xi') + M'(y_0' + \eta');$$

consequently, we have:

$$W = E(L,' M') + L'x_0' + M'y_0' + \xi'L' + \eta'M'.$$

A point on the wavefront is now no longer specified by linear coordinates; it must be specified as a direction. So the diffraction integral (1) reduces to:

$$a(P') = \iint_\Sigma F(L'M') \exp \frac{2\pi i}{\lambda} [W_0(L',M') + \xi'L' + \eta'M'] dL'dM' \qquad (7)$$

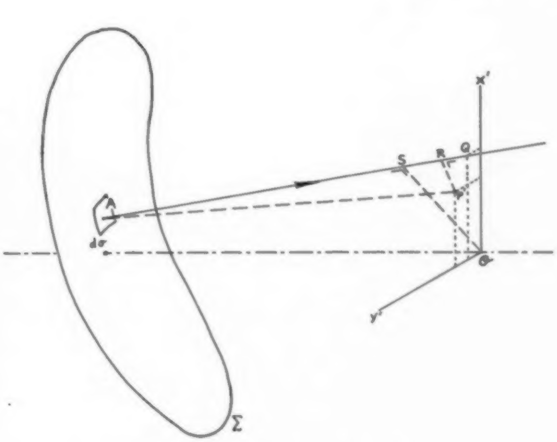

Fig. 2. Wavefront configuration.

in which

$$W_0(L,'M') = E(L,'M') + L'x_0 + M'y_0, \quad (8)$$

a function which is open to easy numerical evaluation, as will be shown subsequently.

Comparing Eqs. (7) and (8) with Eq. (1) we observe first of all that the rather vague concept of wavefront deformation has been replaced by a well-defined eikonal function. We also notice that (7) represents a Fourier transformation, provided that we use as variables in the frequency domain:

$$\begin{aligned} \nu_x &= L'/\lambda, \\ \nu_y &= M'/\lambda. \end{aligned} \quad (9)$$

Every pair of values for ν_x and ν_y defines uniquely a point in the exit pupil. The integration over the exit pupil coordinates is now replaced by an integration over direction cosines in the image space. These direction cosines are a natural product of the ray trace, and, consequently, one does not need the linear exit pupil coordinates at all. Luneberg[4] has shown that the limiting procedure of moving the wavefront to infinity is an essential step in the electromagnetic theory of image formation (see also Wolf[5]).

The amplitude function $\bar{F}(L',M')$ is still unknown and must be determined by external means. It may often be assumed to be constant. (See, however, refs. 11 and 12, in which an object point is assumed that radiates uniformly in all directions.)

Equations (7) and (8) form an ideal bridge between geometrical optics and wave optics. Equation (7) shows that the diffraction integral may be considered as a Fourier transform, even for wide apertures and large field angles. Neither an artificially tipped image plane nor a troublesome reference sphere need be introduced. Equation (7) shows a close relationship between the eikonal functions and diffraction theory. This relationship becomes even more apparent when we apply the method of stationary phase to Eq. (7). For large aberrations, the direction (L',M') contributing most to the amplitude in the point $(x_0' + \xi', y_0' + \eta')$ is found by requiring that the exponent be stationary with respect to L' and M'. This yields:

$$\frac{\partial E}{\partial L'} + x_0' + \xi' = 0,$$

$$\frac{\partial E}{\partial M'} + y_0' + \eta' = 0,$$

which are the exact geometrical relations to be expected. We see that in the diffraction theory of image formation all of geometrical optics remains valid; it is however, elevated into the exponent of the diffraction integral.

III. Numerical Evaluation of the Eikonal

The wave-optics description completed, we turn now to the calculation of the eikonal function. In the conventional ray-tracing procedure it is not feasible to determine the relation between the heights of intersection in the image plane and the pupil coordinates in a closed form. We must sample this function numerically, and, if we wish, then determine intermediate values by interpolation. For the eikonal function we have to apply the same technique, for the same reason. This could be done by path-length computations along the rays traced; however, to attain the desired accuracy a double word-length computation has to be used. With moderately small computers this becomes time-consuming. One can, however, simplify these computations considerably by applying the interpolation not to the eikonal function itself but to its first derivatives with respect to the rotationally invariant variables. In a power series development of the eikonal function a term of a degree n in the linear variables leads to terms of a degree $n - 2$ in the power series of the above-defined first derivative, whence the greater accuracy obtainable. Furthermore, these first derivatives are directly related to matrix elements (obtained from a ray trace), that we shall define presently.

A ray-trace procedure consists in following a ray through an optical system. There are fundamentally two steps involved. At each refracting surface the ray changes direction, and in going from one surface to the next the intersection point of the ray with this next surface has to be found. Let us first describe the refraction of a ray at the ith surface of the system. The coordinates of the point of intersection of the ray with the surface in the space before refraction are denoted by x_i, y_i and by x_i' and y_i' when considered in the space after refraction. The optical direction cosines in these two spaces are denoted by L_i, M_i and L_i' and M_i'. It has been shown that the refraction can be written in the form (see ref. 7):

$$\begin{bmatrix} L_i \\ x_i' \end{bmatrix} = \begin{bmatrix} 1 & -A_i \\ 0 & 1 \end{bmatrix} \begin{bmatrix} L_i \\ x_i \end{bmatrix} = R_i \begin{bmatrix} L_i \\ x_i \end{bmatrix}$$

and (10)

$$\begin{bmatrix} M_i \\ y_i' \end{bmatrix} = \begin{bmatrix} 1 & -A_i \\ 0 & 1 \end{bmatrix} \begin{bmatrix} M_i \\ y_i \end{bmatrix} = R_i \begin{bmatrix} M_i \\ y_i \end{bmatrix},$$

where

$$A_i = \frac{n_i' \cos\varphi_i' - n_i \cos\varphi_i}{r_i}.$$

n and n' are the refractive indices of the media in front and behind the surface, φ_i and φ_i' are the angles of incidence and refraction, and r_i is the subnormal of the refracting surface for the ray considered. For a spherical surface this is the radius itself.

Now, with a similar notation, we can write for the translation to the next surface:

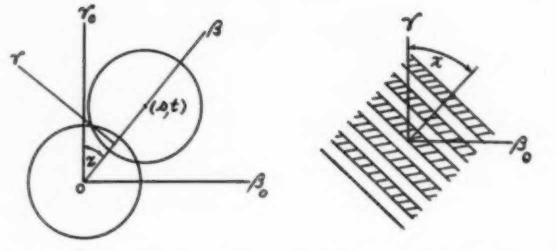

Fig. 3. Rotation of coordinate axes for the computation of the contrast transfer function.

$$\begin{bmatrix} L_{i+1} \\ x_{i+1} \end{bmatrix} = \begin{bmatrix} 1 & 0 \\ T_i' & 1 \end{bmatrix} \begin{bmatrix} L_i' \\ x_i' \end{bmatrix} = T \begin{bmatrix} L_i' \\ x_i' \end{bmatrix}$$

and (11)

$$\begin{bmatrix} M_{i+1} \\ y_{i+1} \end{bmatrix} = \begin{bmatrix} L & 0 \\ T_i' & 1 \end{bmatrix} \begin{bmatrix} M_i' \\ y_i' \end{bmatrix} = T_i \begin{bmatrix} M_i' \\ y_i' \end{bmatrix},$$

where

$$T_i' = t_i'/n_i.$$

t_i' is the distance measured along the ray between the points x_i', y_i' and x_{i+1}, y_{i+1}. It should be noted that the ray between object point and point of incidence on the first surface can be described by a matrix of the form T and will be denoted by T_0. In the same way in the image space we have a matrix T_n giving the coordinates of the ray in the image plane in terms of the coordinates of the ray at the last surface k. When all matrices R_i and T_i are computed the ray coordinates in the image plane in terms of the coordinates of the ray in the object plane can be found by

$$\begin{bmatrix} L' \\ x' \end{bmatrix} = T_k R_k T_{k-1} R_{k-1} \ldots T_2 R_2 T_1 R_1 T_0 \begin{bmatrix} L \\ x \end{bmatrix},$$

and similarly for M' and y' as a function of M and y. Since both T and R are 2×2 matrices, the result of the matrix multiplications will be a 2×2 matrix of the form:

$$\begin{bmatrix} L' \\ x' \end{bmatrix} = \begin{bmatrix} B & -A \\ -D & C \end{bmatrix} \begin{bmatrix} L \\ x \end{bmatrix} \text{ and } \begin{bmatrix} M' \\ y' \end{bmatrix} = \begin{bmatrix} B & -A \\ -D & C \end{bmatrix} \begin{bmatrix} M \\ y \end{bmatrix}. \tag{12}$$

Note that the final "x" and "y" matrices are the same; this is due to the rotational symmetry.

Since the optical systems considered here have an axis of symmetry, we can achieve a simplification by introducing the following rotationally invariant quantities:

$$\begin{aligned} u_1 &= {}^1/_2(x^2 + y^2), \\ u_2 &= L'x + M'y, \\ u_3 &= {}^1/_2(L'^2 + M'^2). \end{aligned} \tag{13}$$

Introducing (13) and (5) into Eq. (12) yields

$$\left(-B\frac{\partial E}{\partial u_1} - A\right)x - \left(B\frac{\partial E}{\partial u_2} + 1\right)L' = 0,$$

$$\left(D\frac{\partial E}{\partial u_1} + C + \frac{\partial E}{\partial u_2}\right)x + \left(D\frac{\partial E}{\partial u_2} + \frac{\partial E}{\partial u_3}\right)L' = 0.$$

Since these relations are valid for all values of x and L' each coefficient should be zero; yielding:

$$\begin{aligned} \frac{\partial E}{\partial u_1} &= -\frac{A}{B}, \\ \frac{\partial E}{\partial u_2} &= -\frac{1}{B}, \\ \frac{\partial E}{\partial u_3} &= \frac{D}{B}, \\ BC - AD &= +1. \end{aligned} \tag{14}$$

Numerical values for these partial derivatives of the eikonal function are thus easily obtained from ray traces. A simple integration will then give the function E.

There are many ways in which this calculation can be performed. In the following a procedure is worked out using truncated power series up to and including the sixth order in the aperture variables to find E as a function of u_2 and u_3, and thus as a function of the coordinates L' and M' that we wish to use in the work on diffraction.

Since we are interested only in the function E for one object point, u_1 is a constant and E is a function of u_2 and u_3 only. Let us assume the form

$$\begin{aligned} E(u_2, u_3) &= \Sigma_i \Sigma_j E_{ij} u_2^i u_3^j \\ &\approx E_{00} + E_{10}u_2 + E_{01}u_3 \\ &\quad + E_{20}u_2^2 + E_{11}u_2u_3 + E_{02}u_3^2 \\ &\quad + E_{30}u_2^3 + E_{21}u_2^2u_3 + E_{12}u_2u_3^2 + E_{03}u_3^3 \\ &\quad + \ldots . \end{aligned} \tag{15}$$

From this it follows that

$$\begin{aligned} \frac{\partial E}{\partial u_2} &= -\frac{1}{B} = E_{10} + 2E_{20}u_2 + E_{11}u_3 + 3E_{30}u_2^2 + 2E_{21}u_2u_3 \\ &\qquad + E_{12}u_3^2 + \ldots, \\ \frac{\partial E}{\partial u_3} &= \frac{D}{B} = E_{01} + E_{11}u_2 + 2E_{02}u_3 + E_{21}u_2^2 + 2E_{12}u_2u_3 \\ &\qquad + 3E_{03}u_3^2 + \ldots . \end{aligned} \tag{16}$$

All coefficients appearing in the desired function E appear in the functions (16) except E_{00}. However, E_{00} is a constant and therefore not needed in the computations on diffraction. The coefficients E_{ij} in (16) can now be found from the values of the matrix elements B and D for five or more rays. We use a least-square method where the number of rays used is determined by the desired fit.

It is interesting to note that in this approximation only five meridional rays are needed. The object is situated on the x axis, and so we have for meridional rays:

$$u_2 = L'x,$$

$$u_3 = {}^1/_2\, L'^2,$$

and thus:

$$-\frac{1}{B} = E_{10} + (2E_{20}x)L' + ({}^1/_2E_{11} + 3E_{30}x^2)\, L'^2 + (E_{21}x)L'^3 + {}^1/_4E_{12}L'^4,$$

$$\frac{D}{B} = E_{01} + (E_{11}x)L' + (E_{02} + E_{21}x^2)L'^2 + (E_{12}x)L'^3 + {}^3/_4E_{03}L'^4.$$

Five meridional rays, using the first equation gives: E_{10}, E_{20}, $({}^1/_2E_{11} + 3E_{30}\, x^2)$, E_{21}, and E_{12}. Four of the same rays, and the second equation gives: E_{01}, E_1, $(E_{02} + E_{21}\, x^2)$, E_{03}. Simple inspection shows that all coefficients can then be computed. When the object is at infinity the same procedures can be used with the help of the angle–angle eikonal as shown in the appendix.

IV. Calculation of the Transfer Function

Having shown the relation between the information supplied by the ray trace (the matrix elements) and the coefficients E_{ij} of the eikonal function we now proceed to calculate the transfer function. In doing so it proves convenient to define normalized variables over which we carry out the numerical integration. Letting L_m' and M_m' represent the maximum* direction cosines as seen from the image field point we now define

$$\beta_0 = L'/L'_m \text{ and } \gamma_0 = M'/M_m'.$$

Further, we define normalized polar coordinates $\beta_0 = \rho\cos\phi$; $\gamma_0 = \rho\sin\phi$ such that $0 \leq \rho \leq 1$ and we see that aside from scale factors which can be absorbed into the coefficients, u_2 can be replaced by β_0 and u_3 by ρ^2. We now can write the basic integral for the evaluation of the transfer function in terms of these normalized variables as:

$$D(s, t) = \frac{\int\int_{-\infty}^{\infty} F(\beta_0, \gamma_0)F^*(\beta_0 - s, \gamma_0 - t)\, d\beta_0 d\gamma_0}{\int\int_{-\infty}^{\infty} |F_0(\beta_0, \gamma_0)|^2\, d\beta_0 d\gamma_0}, \quad (17)$$

where s and t are line frequencies normalized such that they run from 0 to 1, and where for our purposes we take

$$F(\beta_0, \gamma_0) = \exp\left[\frac{2\pi i}{\lambda}E(\beta_0, \gamma_0\right], \quad \beta_0^2 + \gamma_0^2 \leq 1$$

$$= 0, \qquad \beta_0^2 + \gamma_0^2 > 1.$$

Finally, for ease in computation it turns out to be convenient to perform a translation and rotation of axes to β, γ centered at the common area of the displaced circles* such that β points along the direction of the normal (ψ) of the line structure in the object plane (see Fig. 3). With these changes of variables our basic integral can be cast into the form:

$$D(s, \psi) = \frac{\int\int_{-\infty}^{\infty} F\left(\beta + \frac{s}{2}, \gamma\right)F^*\left(\beta - \frac{s}{2}, \gamma\right) d\beta d\gamma}{\int\int_{-\infty}^{\infty} |F(\beta, \gamma)|^2 d\beta d\gamma}. \quad (18)$$

At this point we adopt the numerical integration scheme of Hopkins[8] and write first

$$D(s, \psi) = \frac{1}{a}\int\int_{\infty} \exp\, [iksV(\beta, \gamma;\ \psi)]\ d\beta d\gamma, \quad (19)$$

where $a = \int\int\ d\beta d\gamma$ is the normalization constant and $V(\beta, \gamma; \psi)$ is given by:

$$V(\beta, \alpha;\ \psi) = \frac{1}{s}\left[E\left(\beta + \frac{s}{2}, \gamma;\ \psi\right) - E\left(\beta - \frac{s}{2}, \gamma;\ \psi\right)\right] \quad (20)$$

$$= \frac{\partial E}{\partial \beta} + \frac{1}{3!}\left(\frac{s}{2}\right)^2\frac{\partial^3 E}{\partial \beta^3} + \frac{1}{5!}\left(\frac{s}{2}\right)^4\frac{\partial^5 E}{\partial \beta^5}.$$

Now as Hopkins[8] has demonstrated (see also Marchand and Phillips[13]) this integral can be approximated by a double summation taken over all the elementary cells (ϵ_x, ϵ_y) that fall within the common area in the form

$$D(s, \psi) = \frac{1}{N}\ \Sigma_m\Sigma_n e^{iZ}\ \frac{\sin X}{X}\ \frac{\sin Y}{Y}, \quad (21)$$

where $N = a/(4\epsilon_x\epsilon_y)$ is the number of rectangles of area $4\epsilon_x\epsilon_y$ that fall within the full area a and where

$$X = \epsilon_x ks\frac{\partial V}{\partial \beta},$$

$$Y = \epsilon_y ks\frac{\partial V}{\partial \alpha}, \quad (22)$$

$$Z = ksV(\beta, \gamma;\ \psi),$$

each of which is evaluated at the center of the elementary cells. Finally, to complete this description we note that we can also write $D(s, \psi)$ in the form

$$D(s, \psi) = |D(s, \psi)|e^{i\theta(s,\psi)}, \quad (23)$$

---

* Actually L_m' and M_m' are symmetrized forms of the direction cosines that limiting rays make with the x', y' axes as seen from an off-axis field point.

* In actual practice as one gets off-axis the region of integration is the common area of two displaced ellipses. Further, the effect of vignetting must be taken into consideration.

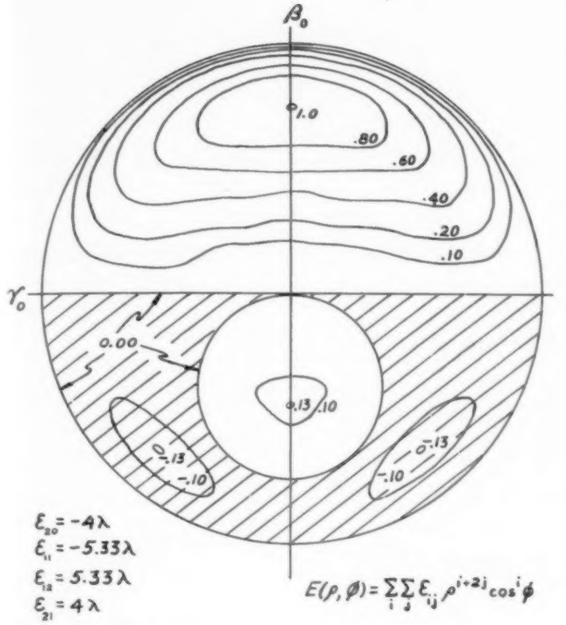
β_0
1.0
.80
.60
.40
.20
.10
γ_0
0.00
.13
.10
-.13
-.10
-.13
-.10
$\varepsilon_{20} = -4\lambda$
$\varepsilon_{11} = -5.33\lambda$
$\varepsilon_{12} = 5.33\lambda$
$\varepsilon_{21} = 4\lambda$
$E(\rho,\phi) = \sum_i \sum_j \varepsilon_{ij} \rho^{i+2j} \cos^i \phi$

Fig. 4. Rough sketch of normalized wave deformation.

where

$$|D(s, \psi)|^2 = D_R^2(s, \psi) + D_I^2(s, \psi),$$

$$\theta(s, \psi) = \tan^{-1} D_I/D_R,$$

and where

$$D_R(s, \psi) = \frac{1}{N}\Sigma_m\Sigma_n \cos Z \, \frac{\sin X}{X} \, \frac{\sin Y}{Y},$$

$$D_I(s, \psi) = \frac{1}{N}\Sigma_m\Sigma_n \sin Z \, \frac{\sin X}{X} \, \frac{\sin Y}{Y}.$$

It is to be noted in this approach that X, Y, and Z depend upon $V(\beta,\gamma;\ \psi)$ which in turn depends upon $E(\beta,\ \alpha;\ \psi)$. We have found it convenient to express $E(\beta,\ \alpha;\ \psi)$ in the form

$$E(\beta,\ \alpha;\ \psi) = \sum_{k,l}^{k+l\le 6} \sum_{=0} A_{kl}(\psi)\beta^k \gamma^l, \qquad (24)$$

where the original eikonal coefficients and the orientation of the line structure have been absorbed into the 49 matrix elements A_{kl} (of which 25 are zero in fifth-order theory). As Marchand and Phillips have pointed out, the extension of Hopkins' method to fifth order is a straightforward problem in numerical integration. It is our experience also that a cell size of 0.05 units is sufficiently accurate for all purposes encountered in practice. Moreover, this approach does not necessarily require a high-speed, large-capacity computer. For our purposes we find the RPC 4000, a relatively modest computer, perfectly adequate. A complete curve, yielding 20 equally spaced points for the amplitude and 20 points for the phase takes $4^1/_2$ hr. Often the amplitude falls off and remains below a physically meaningful value before the run is completed, and the computer is instructed to proceed directly to the next case of physical interest. These remarks are not meant to minimize the advantages of high-speed computers in optical design. The point we wish to make here is simply that the transfer function is not an end in itself but merely the most useful tool we have to date to assess the relative merits of one design over another. As such this function becomes useful only during the final stages of design after earlier attempts have been rejected for practical and other reasons. Having reached the point where one wishes now to concentrate on a few critical cases, the assessment using the contrast transfer function comes into play, and we here merely wish to emphasize that such evaluations are well within the scope of the more modest computers.

We should like to close this section by giving a numerical illustration for a wave deformation often encountered in practice. Figure 4 shows a wave deformation exhibiting a typical "bubble" along the meridional section as seen from an off-axis field point. On axis all coefficients are zero, and the now familiar transfer function for this case is shown in Fig. 5. Off axis the situation is different, and we show in Fig. 5 the amplitude and phase of the contrast transfer function for line structures whose normals point along the sagittal and meridional section and at 45° to these. Needless to say we find such curves quite useful in evaluating the performance of optical systems.

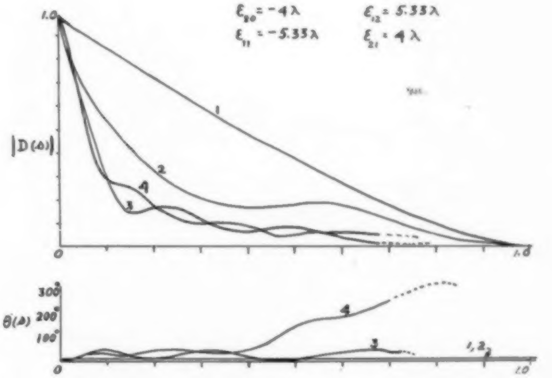

Fig. 5. Contrast transfer functions for wave deformation shown in Fig. 4 at several azimuth angles. Curve 1—on-axis; curve 2—off-axis $\psi = 0$; curve 3—off-axis $\psi = \pi/4$; curve 4—off-axis $\psi = \pi/2$.

We wish to express our gratitude to S. Daniels and H. Sijgers for their roles in bringing this paper to completion.

Appendix

In the case that the object is at infinity it is convenient to use a slightly different eikonal function, the so called angle–angle eikonal.

From the center of the entrance pupil we construct a perpendicular to the ray considered. (See Fig. 1.) The same is done in the object plane. The eikonal is now the optical path length P between the footpoints of these perpendiculars and is a function of L, L', M, and M'.

For a given point at infinity L and M are constants and all points P for rays from this object point are on one wavefront. For this eikonal the following relations hold (see ref. 9)

$$x = \frac{\partial E,}{\partial L} \quad -x' = \frac{\partial E}{\partial L'},$$

$$y = \frac{\partial E,}{\partial M} \quad -y' = \frac{\partial E}{\partial M'}.$$

For rotational symmetric systems the following rotationally invariant quantities are introduced

$$\bar{u}_1 = {}^1/_2(L^2 + M^2),$$

$$\bar{u}_2 = LL' + MM',$$

$$\bar{u}_3 = {}^1/_2(L'^2 + M'^2).$$

From this it is easily derived that

$$\frac{\partial E}{\partial \bar{u}_1} = \frac{B}{A},$$

$$\frac{\partial E}{\partial \bar{u}_2} = -\frac{1}{A},$$

$$\frac{\partial E}{\partial \bar{u}_3} = \frac{C}{A},$$

$$BC - AD = +1.$$

All other computations are the same as in the case with a finite object distance.

References

1. B. R. A. Nijboer, thesis, Groningen (1942).
2. M. Born and E. Wolf, *Principles of Optics* (Pergamon Press, London, 1959).
3. E. L. O'Neill, *Introduction to Statistical Optics* (Addison-Wesley, Reading, Mass., 1963).
4. R. K. Luneberg, Lecture Notes, Brown University, Providence (1944).
5. E. Wolf, Proc. Roy Soc., A, *253*, 349 (1959).
6. T. Smith, *A Dictionary of Applied Physics*, R. T. Glazebrook, ed. (Macmillan, London, 1923), Vol. IV, p. 287.
7. W. Brouwer, *Matrix Methods in Optical Instrument Design* (Benjamin, to be published).
8. H. H. Hopkins, Proc. Phys. Soc., London **B70** 1002, 1162 (1957).
9. J. L. Synge, *Geometrical Optics, An Introduction to Hamilton's Method* (Cambridge Univ. Press, New York, 1937).
10. M. Herzberger, *Strahlen Optik* (Springer, Berlin, 1932).
11. H. Osterberg and R. A. McDonald, "Symposium on Optical Image Evaluation," NBS Circ. **526** (1954).
12. R. Barakat and D. Lev, J. Opt. Soc. Am. **53,** 324 (1963).
13. E. Marchand and R. Phillips, Appl. Opt. **2,** 359 (1963).

Bruce H. Billings, vice-president and technical director of Baird-Atomic, has been elected a vice-president of Aerospace Corporation and will be general manager of the Corporation's laboratories at El Segundo.

Image Evaluation by Spot Diagram Using A Computer

Kenro Miyamoto

The development of electronic computers has brought greater possibilities in evaluation methods for lens systems, and the theory of transfer functions is now being applied to practical lens design. In this paper, the evaluation by spot diagrams is discussed. A method of plotting spot diagrams is proposed, utilizing the line printer of a computer as the X-Y plotter. The geometrical optical intensity distribution $I_g(x,y)$ given by the spot diagram is expressed in the form

$$I_g(x,y) = N^{-1}\sum_{i=1}^{N}\delta(x - x_i, y - y_i).$$

The convolution $t(x,y)$ with the turbidity $r(x,y)$ of the image receiver, the total impulse response, is given by

$$t(x,y) = N^{-1}\sum_{i=1}^{N} r(x - x_i, y - y_i).$$

Intensity distributions calculated by the computer are compared with the measured ones for an actual lens, and the agreement is satisfactory. This procedure can also be applied to the case of the transfer function. The Strehl definition $t(0,0)$ is calculated for several cases of primary and secondary spherical aberrations, and it is confirmed that there are two extremum positions of the spot diagram in some cases.

Introduction

The recent development of electronic computers has made possible the introduction of new lens design techniques, utilizing the large memory of computers and their ability to perform the logical and calculating operations very quickly. Many papers have been already published on automatic correction or automatic design of lens systems: variable by variable method,[1] steepest descent method,[2] linearizing and least square method,[3] and so on.

However, choosing a proper merit function for evaluating a lens is one of the important problems in lens design, as the quality of lens finally designed depends mainly on which merit function is used. In this paper, the method of image evaluation by spot diagram is discussed using a computer, and the results obtained by the theory of transfer functions are introduced.

Plotting Method of Spot Diagram

As is well known, the various curves representing the generalized Seidel aberrations are used as merit functions of image qualities in ordinary lens design. These curves give much information to an expert designer with a small amount of calculation, and this is one reason why this method is still widely used. However, as the lens with large aperture has become of particular interest in recent years, more appropriate image evaluation is desirable. Now, the use of computers has removed the labor of calculation, and it becomes unnecessary to try to avoid hard calculations.

The method of spot diagrams which Herzberger[4] proposed should be one of several good starting points. This shows the intensity distribution fairly accurately, if the diffraction effect can be neglected (as in the case of a photographic lens), and also gives a good visual representation of the image. Although the method of skew ray tracing is well established, the plotting of spot diagrams still takes more time than that of ray tracing. In the methods in which a mechanical X-Y plotter[5] or an oscilloscope[6] are used, the coordinates of spots (x,y) must be taken on tape or on cards through the output device and then the spots are plotted by a digital-analog converter.

Here, the line printer is used as an X-Y plotter to make spot diagrams. As is shown in the flow diagram (Fig. 1), (x_i, y_i) are quantized by a proper scale to (m_i, n_i) and then sorted in order of the magnitude of n_i. The number of line feeds is controlled by n_i, and the positions of dots on the line are controlled by m_i.

The author is with the Department of Research, Nippon Kogaku K. K. (Japan Optical Industry Co.).

Received 9 May 1963.

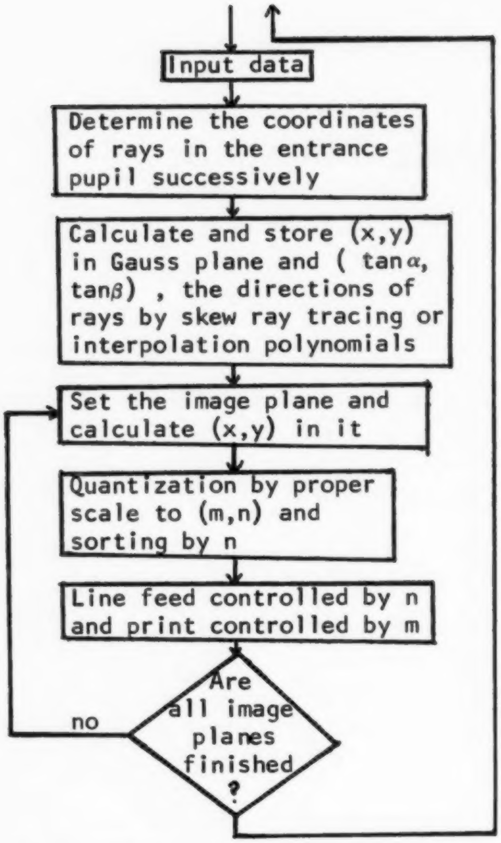
Input data
Determine the coordinates of rays in the entrance pupil successively
Calculate and store (x,y) in Gauss plane and (tanα, tanβ) , the directions of rays by skew ray tracing or interpolation polynomials
Set the image plane and calculate (x,y) in it
Quantization by proper scale to (m,n) and sorting by n
Line feed controlled by n and print controlled by m
Are all image planes finished ?
no

Fig. 1. The flow diagram for plotting the spot diagram.

The time of plotting by this method is less than that of ray tracing and can be used for image evaluation as routine work. If the subroutine of n_i sorting is added, this method can be used for the computers equipped with a typewriter only.

Calculation of Intensity Distribution and Transfer Function

There would probably be some differences in the evaluation of the same spot diagram by different people. In order to evaluate the image objectively, it is necessary to treat it analytically. One method is the calculation of its intensity distribution, that is, the density of spots per unit area. Let us formulate the expression for the geometrical optical intensity distribution $I_g(x,y)$ using a δ function,

$$I_g(x,y) = N^{-1} \sum_{i=1}^{N} \delta(x - x_i, y - y_i), \qquad (1)$$

where (x_i, y_i) are the coordinates of the spots. The lens system always has its receiver. When the turbidity (impulse response) is $r(x,y)$, then the impulse response of the total system $t(x,y)$ is

$$t(x,y) = \int\int I_g(x',y')\, r(x - x', y - y')\, dx'\, dy' = N^{-1} \sum_{i=1}^{N} r(x - x_i, y - y_i). \qquad (2)$$

This formula is very convenient for computers because of the iterative calculation process. The transfer function $R_g(x,y)$ is given by the Fourier transform of $I_g(x,y)$ and we have

$$R_g(s,t) = \int\int I_g(x',y') \exp\left[-2\pi i(sx' + ty')\right] dx'dy' = N^{-1} \sum_{k=1}^{N} \exp\left[-2\pi i(sx_k + ty_k)\right]. \qquad (3)$$

This formula can also be obtained by the equation derived by Miyamoto[7] and Hopkins,[8]

$$R_g(s,t) = \int\int \exp\left\{-2\pi i[s\cdot x(u,v) + t\cdot y(u,v)]\right\} du dv, \qquad (4)$$

where u,v are the coordinates in the entrance pupil, $x(u,v)$ and $y(u,v)$ are geometrical optical aberrations given by

$$x = f(\partial/\partial u)\phi(u,v), \qquad y = f\,(\partial/\partial v)\,\phi(u,v), \qquad (5)$$

$\phi(u,v)$ being the wave aberration function and f being the radius of its reference sphere. The accuracy of the geometrical optical transfer function as compared to the wave optical one was examined by Miyamoto.[9] If the wave aberration function is larger than twice the wavelength λ, its approximation is good within the range of spatial frequency $|s|$, $|t| \leqslant 0.2/(\lambda F) \sim 400/F$ line/mm, where F is the F number of the lens. Therefore, when details smaller than $400/F$ line/mm of the intensity distribution can be neglected, the geometrical optical intensity distribution—the inverse Fourier transform of $R_g(x,y)$—is nearly equal to the wave optical one. This is the case when the transfer function of the receiver reduces to zero quickly beyond this limit. Comparison of calculated and measured transfer functions and the intensity distribution of an actual lens shows the good accuracy of this method (Fig. 3* and Fig. 4).[10]

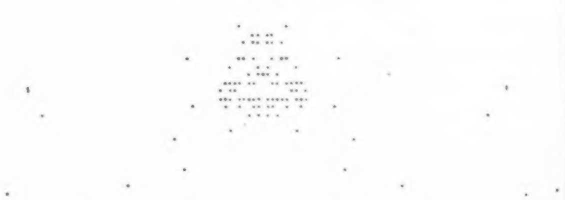

Fig. 2. Spot diagram plotted by line printer.

---

* The author is indebted to Prof. Ose and Mr. Takashima of the Institute of Industrial Science, the University of Tokyo, who kindly measured the intensity distribution of the line image for this purpose.

Single Merit Function of Spot Diagram

Some trials to evaluate spot diagrams by a single merit function have been carried out. One example is the radius of gyration (R.G.)

$$\mathrm{R.G.} = N^{-1} \sum_{i=1}^{N} (x_i^2 + y_i^2). \tag{6}$$

This merit function was applied to the error balancing of Schmidt cameras by Linfoot.[11] This merit function expresses the degree of dropping of the transfer function in the very low-frequency region[12] but cannot figure out its state in the high-frequency region. When the spot diagram consists of a core and halo broadly spreading around the core, this merit function is too unfair. Lucy[13] proposed the intensity criterion (I.C.), taking account of this point,

$$\mathrm{I.C.} = N^{-1} \sum_{i} [(x_i^2 + y_i^2)^{1/2} + \Delta r]^{1/2}, \tag{7}$$

where Δr is the radius of Airy's disk and prevents the right-hand side from becoming infinite. Hopkins[14] gives as a merit function the radius of the circle in which 30% of the total energy is contained. These foregoing criteria are practical but still rather arbitrary.

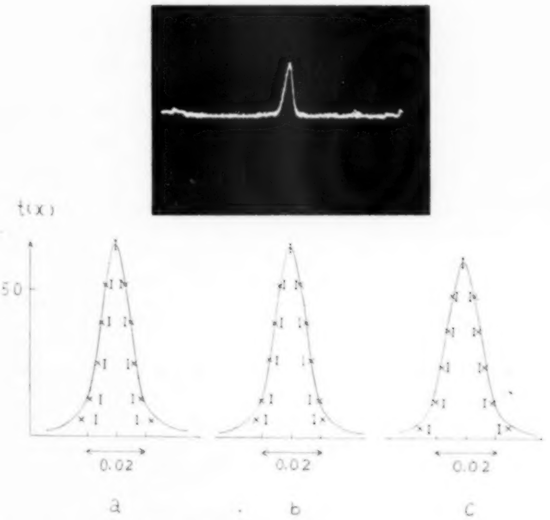

a b c

Fig. 3. Intensity distribution of line image on axis of an actual lens (Gauss type). Full lines are values calculated by the formula (2) with $r(x,y) = (2\pi)^{-1/2}\sigma^{-1} \exp(-x^2/2\sigma^2)$, σ being 0.0035. I notations are measured values. x notations are the convolutions of measured intensity and $r(x,y)$. Figs. 3 (a), (b), and (c) are for the defocused image planes shifting -0.14 mm and 0.12 mm and -0.1 mm from the Gauss plane, respectively. Minus sign corresponds to the direction toward the lens.

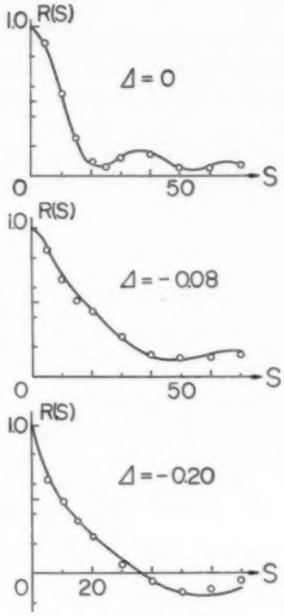

Fig. 4. Transfer function of an actual lens (Sonnar type) vs the spatial frequency variable s (line/mm). Full lines are values calculated by the formula (3) and the circles are measured values. Δ in the figures is the distance from Gauss image plane (Kubota, Miyamoto, and Murata).[10]

On the other hand, the introduction of Fourier techniques into optics has provided fruitful results in the image evaluation. Fellget and Linfoot[15] combined the treatment based on Fourier analysis with information theory and deduced the statistical mean information content per unit area of image by making a few practical assumptions. Three criteria are proposed by Linfoot,[16]

relative structural content: $T \propto \int\int |\tau\tau_1|^2 \overline{|\epsilon_0|^2}\, du\, dv;$
fidelity: $\phi \propto \int\int [1 - |1 - \tau\tau_1|^2] \overline{|\epsilon_0|^2}\, du\, dv;$
correlation quality: $Q \propto \int\int \tau\tau_1 \overline{|\epsilon_0|^2}\, du\, dv;$

where $\overline{|\epsilon_0|^2}$ is the statistical mean of spectral powers of object intensity distribution and τ, τ_1 are the transfer function of the lens and its receiver, respectively, with spatial frequency variables u, v. T may be considered to express a statistical mean information content in the case when the image details are almost completely smothered in the noise of the image plane. ϕ represents the degree of similarity of object and image. Q shows the correlation of object and image and is the mean of T and ϕ. Furthermore, if $\overline{|\epsilon_0|^2}$ is constant, Q becomes equal to the intensity at the center (the Strehl definition) except for a constant coefficient. Fortunately, the Strehl definition can be calculated very easily within the geometrical optical approximation by

$$t(0,0) = N^{-1} \sum_{i=1}^{N} r(-x_i, -y_i). \tag{8}$$

It is interesting to note that this formula includes the R.G. [Eq. (6)] and the I.C. [Eq. (7)] in its form.

Combination of the primary and secondary spherical aberration is taken as an example in order to calculate the spot diagram of point and line image with the receivers of $r(x,y) = (2\pi\sigma^2)^{-1}\exp[-(x^2+y^2)/2\sigma^2]$ and $r(x,y) = (2\pi)^{-1/2}\sigma^{-1}\exp(-x^2/2\sigma^2)$, respectively, by Eq. (8). Expression of the lateral spherical aberration l is

$$l = (S_1/2F)\,[4\rho^2(\rho^2 - \rho_0^2) - a]\rho, \qquad \rho \leqslant 1 \tag{9}$$

where ρ is the normalized radial coordinate in the entrance pupil ($\rho \leqslant 1$) and ρ_0 is the position at which the spherical aberration is corrected; a is a parameter of defocus, F is the f number of the lens, and S_1 is the extremum value of the longitudinal spherical aberration when $\rho_0 = 1$ (Fig. 5). The cases of $\sigma = 0.0035$ and $(S/2F) = 0.05$ are calculated for the cases of $\rho_0 = 0.9$, 0.95, 1.0, 1.05, and 1.1 in different image planes, using the computer Okitac 5090. Figure 6 shows that two extremum positions of the spot diagram appear in the cases of $\rho_0 = 0.95$ to 1.1. These results agree with those derived by Kuwabara.[17]

It is a pleasure to acknowledge the assistance of H. Ikeda in programming for the plotting of the spot diagram.

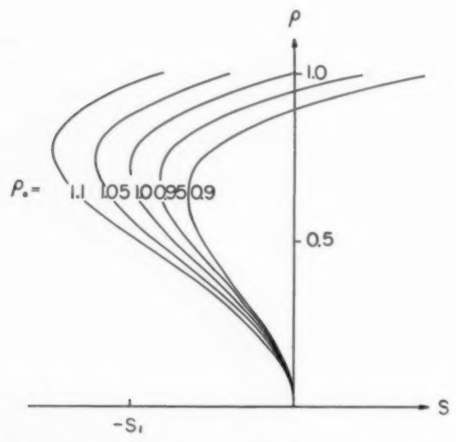

Fig. 5. The primary and secondary longitudinal spherical aberration $S = 4S_1\,\rho^2(\rho^2 - \rho_0^2)$, which corresponds to Eq. (9) for the lateral spherical aberration.

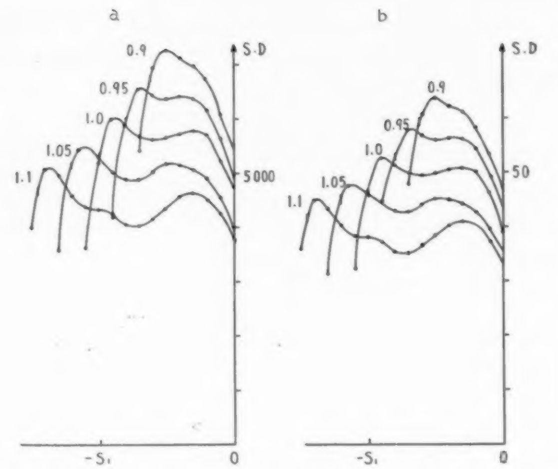

Fig. 6. Strehl definition of lens with the spherical aberration given by Fig. 5 vs position of image plane on axis. a and b are the Strehl definition of the point image and the line image, respectively.

References

1. G. Black, Proc. Phys. Soc. **B68,** 729 (1955).
2. D. P. Feder, J. Opt. Soc. Am. **47,** 902 (1957); J. Meiron and H. M. Loebenstein, J. Opt. Soc. Am. **47,** 1104 (1957).
3. S. Rosen and C. Eldert, J. Opt. Soc. Am. **44,** 250 (1954); C. G. Wynne, Proc. Phys. Soc. **73,** 777 (1959).
4. M. Herzberger, J. Opt. Soc. Am. **37,** 485 (1947).
5. R. E. Hopkins, Report Inst. Optics, Univ. Rochester (1955).
6. T. Suzuki *et al.*, Program of 1963 Spring Meeting of Society of Applied Physics, Japan, p. 65.
7. K. Miyamoto, J. Appl. Phys. Japan **26,** 421 (1957); K. Miyamoto, J. Opt. Soc. Am. **48,** 57 (1958).
8. H. H. Hopkins, Proc. Phys. Soc. **B70,** 1162 (1957).
9. K. Miyamoto, J. Opt. Soc. Am. **48,** 567 (1957).
10. H. Kubota, K. Miyamoto, and K. Murata, Optik **17,** 143 (1960).
11. E. H. Linfoot, *Recent Advances in Optics* (Oxford Univ. Press, New York, 1955).
12. K. Sayanagi, *Proceedings of the Conference on Optical Instruments and Techniques* (Chapman and Hall Ltd., London, 1962), p. 95.
13. F. A. Lucy, J. Opt. Soc. Am. **46,** 699 (1956).
14. R. E. Hopkins, *Proceedings of the Conference on Optical Instruments and Techniques* (Chapman and Hall Ltd., London, 1962), p. 65.
15. P. B. Fellget and E. H. Linfoot, Trans. Roy. Soc. **A247,** 367 (1955).
16. E. H. Linfoot, J. Opt. Soc. Am. **46,** 740 (1956); E. H. Linfoot, Opt. Acta **5,** 1 (1958).
17. G. Kuwabara, J. Opt. Soc. Am. **45,** 309, 625 (1955).

Erratum

Robert L. Christensen and Robert J. Potter, "Double Monochromator Systems", Appl. Opt. **2,** 1049 (October 1963). *Last line of page 1049* should read:

$$D = dx/d\lambda = nf/(d\cos\theta) \tag{1}$$

First-Order Design and the $y, \bar{y}$ Diagram

Erwin Delano

A new method is described for graphically representing the first-order layout of any optical system of axially symmetric refracting or reflecting surfaces. Such a system can be uniquely defined by the actual path of an arbitrary paraxial skew ray traversing it, provided the value of the Lagrange invariant is also known. This paper describes some interesting properties of the diagram obtained by projecting the ray onto the object plane. The diagram has proved to be a very useful aid in first-order design, particularly in systems where lens diameters and locations are severely constrained.

Introduction

The idea of choosing a different set of independent parameters from the radii, thicknesses, and indices in order to simplify the first-order theory of axially symmetric optical systems is not new. Luneberg[1] has shown how the path of an arbitrary paraxial ray together with the indices completely defines any such system, assuming all surfaces to be spheres. However, the path of a second paraxial ray cannot be independent of the first, since the Lagrange relation must be satisfied. It proves desirable in some respects to be able to define the optical system in terms of arbitrary data from both the paraxial marginal and paraxial principal rays and any additional independent parameters required to impose uniqueness.

In his two articles on the theory of periscopes, Smith[2,3] describes a graphical construction which allows one to define a certain class of periscopic systems. This special class of systems may be represented by polygons circumscribed about a circle, and this representation has some interesting properties which will not be discussed here. The present paper describes a more general representation than the one given by Smith and includes his method as a special case. It is quite possible that the method to be described was known to him, but no reference to it can be found in his works. This method has been found to be very useful in the first-order design of axially symmetric systems of thick lenses and mirrors, particularly where certain mechanical constraints must be satisfied.

Basic Relationships

Given an arbitrary system of axially symmetric refracting or reflecting surfaces, consider the path of any two paraxial rays such that the Lagrange invariant Q for them does not vanish, for example, the paraxial marginal ray and the paraxial principal ray. Since we will only be concerned with first-order properties, the subsequent discussion will be understood to be limited to paraxial rays. Among the numerous ways in which the system can be uniquely defined there is one representation which is of unusual interest in first-order theory. In the discussion below, the data for the marginal ray will be distinguished from the data for the principal ray by using plain letters for the marginal ray quantities and placing a bar (-) over each letter for the principal ray quantities.

As defining parameters, choose the heights y_i of the marginal ray, the heights $\bar{y}_i$ of the principal ray, the coordinates x_i of the vertices relative to some arbitrary origin, and the Lagrange invariant Q for the two rays. In addition to the optical surfaces of the system, the object and image planes must be included—or any other two reference planes not coincident with the external vertices of the system—one in the object space and the other in the image space.

It is easy to show that these are independent parameters and are just enough in number uniquely to determine not only all the radii, indices, and separations but also to define completely the paths of the two rays through the system. Let r_i be the radius of curvature of the ith surface, and let N_i, d_i, u_i, and $\bar{u}_i$ be the index, axial thickness, and slope angles of the marginal and principal rays, respectively, for the preceding space. Then, all of these may be calculated by

---

The author was with Bausch & Lomb, Inc., Rochester, New York. His present address is St. John Fisher College, Rochester, New York.

Received 10 April 1963.

means of the following equations, which are derived in the Appendix. Given the value of Q and the parameters y_i, $\bar{y}_i$, x_i at every surface, then:

$$\begin{aligned}
d_i &= x_i - x_{i-1}, & D_i &= (y_{i-1}\bar{y}_i - y_i\bar{y}_{i-1})/Q,\\
N_i &= d_i/D_i, & &\\
\alpha_i &= (y_i - y_{i-1})/D_i = N_i u_i, & K_i &= (\alpha_i\bar{\alpha}_{i+1} - \alpha_{i+1}\bar{\alpha}_i)/Q,\\
\bar{\alpha}_i &= (\bar{y}_i - \bar{y}_{i-1})/D_i = N_i\bar{u}_i, & & \qquad (1)\\
r_i &= (N_{i+1} - N_i)/K_i, & Q &= y_i\bar{\alpha}_i - \bar{y}_i\alpha_i\\
& & &= y_i\bar{\alpha}_{i+1} - \bar{y}_i\alpha_{i+1}.
\end{aligned}$$

The quantity D_i is the equivalent air path for the thickness d_i, and K_i is the surface power of the ith surface.

General Properties

In general, any axially symmetric optical system may be represented by the actual path of a single paraxial skew ray traversing the system. To demonstrate this, choose a set of right-handed Cartesian coordinates (x, y, z) such that the x axis is coincident with the optic axis, placing the origin at the axial point of either the object or pupil planes. Because of the linear nature of first-order optics, it is possible to choose a skew ray such that its projection on the x, y plane is the marginal ray and its projection on the x, z plane is the principal ray. Therefore, this single skew ray uniquely determines the optical system according to Eqs. (1) if one substitutes z for $\bar{y}$. To simplify the notation, the z axis will hereafter be referred to as the $\bar{y}$ axis.

Since the marginal and principal rays could have been chosen arbitrarily except for meeting the condition $Q \neq 0$, it follows that the path of an arbitrary skew ray uniquely determines the system it traverses. The projection of this skew ray onto the y, $\bar{y}$ plane has the following interesting property: as the ray travels from surface to surface, its projection winds about the origin in a clockwise direction if $Q > 0$, and in a counterclockwise direction if $Q < 0$. The viewer is assumed to be looking in the direction of increasing x.

To prove this, consider the projections onto the y, $\bar{y}$ plane of any two successive points 1 and 2 along the ray path. If a triangle is formed with the origin as one vertex and the two projections as the other two vertices, then from elementary analytic geometry the area of this triangle is

$$A = {}^1/_2(y_1\bar{y}_2 - y_2\bar{y}_1) = {}^1/_2 QD_2,$$

where D_2 is the equivalent air distance from point 1 to point 2. Since D is positive for any physically realizable case (including reflection, when both d and N change sign), A must have the same sign as Q, which proves that the radius vector to the projected point always sweeps in a constant direction about the origin. For convenience, it will hereafter be assumed that $Q = 2$ so as to make area A equal to D directly. This implies no loss of generality, since it can always be accomplished by simply changing the unit of length, and has the advantage of simplifying the exposition.

It is clear that the projection onto the y, $\bar{y}$ plane defines the system of thin lenses in air which is equivalent to the actual system in a first-order sense. Therefore, for a system of thin lenses in air the parameters x are redundant and the system is completely defined by only the y, $\bar{y}$ projection. In general, however, the value of x_i for the ith surface is needed and may be recorded next to the corresponding point $(y_i, \bar{y}_i)$ on the y, $\bar{y}$ projection. In this way, all the necessary information is contained on a two-dimensional plot which will hereafter be referred to as the y, $\bar{y}$ diagram.

By means of an example, some properties of the y, $\bar{y}$ diagram which are very useful in practice will now be described. Figure 1 shows the y, $\bar{y}$ diagram for an objective of the telephoto type, consisting of two thin separated components and working at finite conjugates. It is easy to show (see Appendix) that the polygon is always concave toward the origin at surfaces of positive power and convex toward the origin at surfaces of negative power.

Since the points J and A represent the positions of the object plane and first component, respectively, the area OJA is equal to the axial distance between these; similarly, area OAB is equal to the separation between the two components, and area OBM is equal to the distance from the second component to the image plane.

If line OC is constructed parallel to JA and line AB is extended till it intersects it at point D, say, the area OAD is equal to the focal length of the A lens, as will be evident later. Similarly, constructing line OE parallel to AB and extending line BM, the negative area OBE is equal to the focal length of the B lens. To find the magnifications and positions of the stop S and lens B as imaged into the object space by lens A, one connects the origin O with points S and B, respectively, and extends lines OS and OB till they intersect line JA extended in points S′ and B′ as shown. This construction uses the fact that planes conjugate to each other have the same value of $\bar{y}/y$. The areas OAS' and OAB' are equal to the distances from lens A to the images of S and B. The magnifications of S and B as imaged by lens A are OS'/OS and OB'/OB, respectively. In a similar manner one may determine the image positions and magnifications for the lens A and stop S as imaged by lens B into the image space. These images are represented by the points of intersection S″ and A″, respectively.

The point P represents the two principal planes of the objective. It is located at the intersection of lines JA and BM extended, since, by definition, the principal planes are imaged onto each other with a magnification of plus unity. The negative areas OAP and OBP are, respectively, equal to the distances from lens A to the first principal plane and from lens B to the second principal plane. The area OPF equals the focal length of the combination.

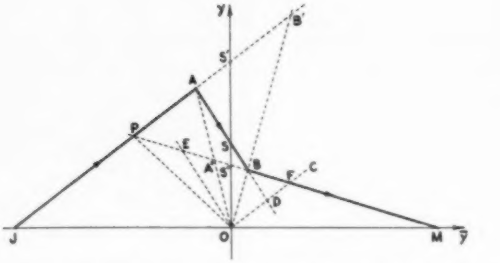

Fig. 1. y, $\bar{y}$ diagram for telephoto objective. Both components thin.

The y, $\bar{y}$ diagram has the additional important property that any conjugate shift may be rigorously represented by a pure shear parallel to the y axis. Similarly, any stop shift is represented by a shear parallel to the $\bar{y}$ axis. This is easily demonstrated for the case of a conjugate shift by noting that, since the principal ray and the value of Q are unaltered during conjugate shift,

$$Q = y\bar{\alpha} - \bar{y}\alpha = y^*\bar{\alpha} - \bar{y}\alpha^*,$$

where y^* and α^* are the modified values of y and α. Hence,

$$(y^* - y)\bar{\alpha} = (\alpha^* - \alpha)\bar{y},$$

so that

$$(y^* - y)/\bar{y} = (\alpha^* - \alpha)/\bar{\alpha}.$$

It is clear that the left-hand side of the last equation is not changed by refraction and the right-hand side is not changed by transfer to the next surface; hence,

$$a = (y^* - y)/\bar{y}$$

has the same value at every surface, so that the entire y, $\bar{y}$ diagram is transformed by the shear:

$$\bar{y}^* = \bar{y}, \qquad y^* = y + a\bar{y}.$$

Alternatively, the diagram may be left intact and the y, $\bar{y}$ coordinate system may be transformed by an identical shear in the opposite direction to convert it into the appropriate system of oblique coordinates. Figure 2 illustrates this property for the case of conjugate shift. The diagram $JABCM$ represents an objective consisting of three thin separated elements. The quantity "a" measures the amount of conjugate shift; the diagram $J^*A^*B^*C^*M^*$ results from transforming the diagram $JABCM$ by the shear

$$\bar{y}^* = \bar{y}; \; y^* = y + a\bar{y}.$$

To perform this shear, a $\bar{y}^*$ axis is drawn at an angle of $\theta = -\tan^{-1} a$ to the $\bar{y}$ axis, and any point P on the diagram is transformed by drawing a line through P parallel to the y axis till it meets the $\bar{y}$ axis in R and the $\bar{y}^*$ axis in S. Then, the transformed point P^* must also lie on this line at a position such that $P^*R = PS$. Since straight lines are preserved, transforming the points J, A, B, C, and M is sufficient to determine the new diagram. Note that the new object and image planes correspond to the points K and L at the intersection of the lines JA and CM extended to meet the $\bar{y}^*$ axis.

The basis for the previously given graphical construction for focal length is now clear. In Fig. 1, the line OC is the $\bar{y}^*$ axis corresponding to a conjugate shift of the object plane to infinity. Since a shear preserves areas, the area OAD equals the rear conjugate distance corresponding to object at infinity, which is just the focal length of lens A.

Figure 3 gives six examples of the y, $\bar{y}$ diagram for six optical systems made up of thin components in air. Case (a) represents a Petzval lens with stop at the front component and object at infinity. Careful inspection of the diagram in view of the properties already described shows that the distance from front component

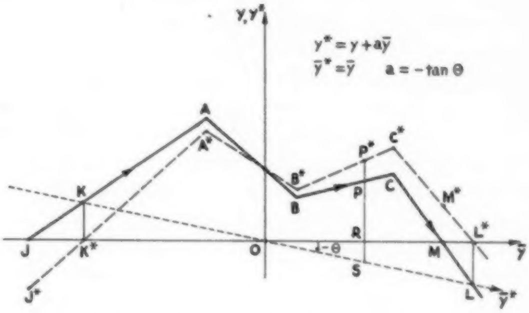

Fig. 2. Shear of y, $\bar{y}$ diagram due to conjugate shift.

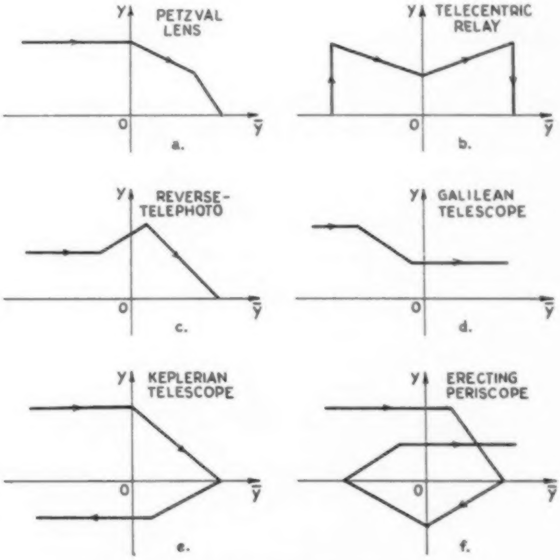

Fig. 3. Examples of different lens types.

to image plane exceeds the focal length and also that the nodal points are crossed, the first one being to the right of the first component, the second being to the left of the second component. Case (b) illustrates a three-component 1:1 relay with stop at the central negative component and having both entrance and exit pupils at infinity. Case (c) illustrates a reverse telephoto lens working at infinity with stop about two-thirds of the way from the first component to the second. The diagram shows the characteristic long back focal length and demonstrates that the nodal points cannot be crossed. Cases (d) and (e) show a Galilean and a Keplerian telescope, respectively, both having 2× magnification and positive eye relief. The entrance pupils are located behind the objective for the Galilean and at the objective for the Keplerian telescope. The latter employs a field lens. Finally, case (f) illustrates a 2× erecting periscope employing a field lens at each of the two intermediate images and having positive eye relief. Since over-all length of the system is determined by the total area swept over by the radius vector on the diagram, additional circuits about the origin would be required to obtain a substantially longer periscope having similar diameter constraints.

The y, $\bar{y}$ diagram reduces to the construction given by Smith[2,3] for the special case of systems for which the sides of the polygon, when extended, are tangent to a circle with center at the origin. In this case it is seen that all separations and focal lengths can be measured as distances along the sides of the polygon itself. Now a central ellipse can always be transformed into a circle by combining a shear with a change of scale, both along either axis. Therefore, any system for which the sides of the polygon are tangent to a central ellipse can be more easily treated using the method of Smith.

Applications

As a first application, consider Fig. 4, which illustrates the general condition which must be satisfied by an optical system, in air, having the requirement that the front nodal point be to the left of the first vertex and the rear nodal point be to the right of the last vertex. In addition, suppose that a real object and a real inverted image are required. Since the y, $\bar{y}$ polygon must always wind clockwise about the origin for $Q > 0$, the point B corresponding to the front vertex must lie clockwise from the node N, and the point C corresponding to the last vertex must lie counterclockwise from N. Therefore, the only way to connect B to C is to wind clockwise about O, meanwhile crossing the $\bar{y}$ axis an even number of times, with a minimum of two times. This demonstrates that the system must form an even number of intermediate real images. Similarly, it may be shown that for the case where the image is required to be real and erect, an odd number of intermediate real images is necessary.

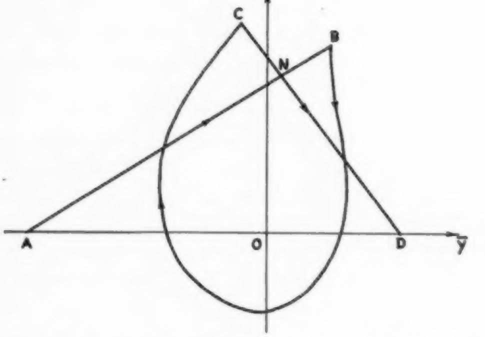

Fig. 4. y, $\bar{y}$ diagram for system with externally situated nodal points.

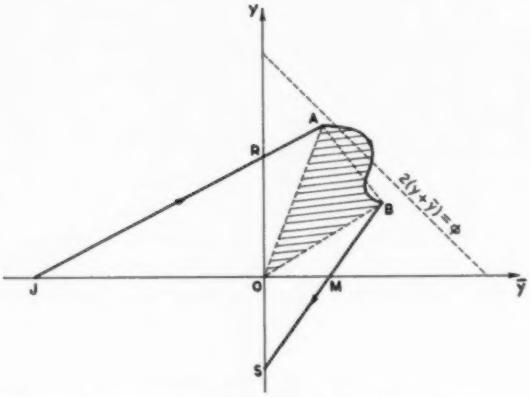

Fig. 5. y, $\bar{y}$ diagram for system subject to constraints on diameter and over-all length.

A second example of a typical practical problem that arises in the design of optical instruments is illustrated in Fig. 5. For the given system, the over-all object-to-image distance and the magnification are both specified. In addition, the position of the entrance and exit pupils are given as well as the size of the entrance pupil. The lens elements are constrained to lie within a cylinder of specified diameter, length, and location along the optic axis. The problem is to determine the minimum required number of thin lenses as well as their focal lengths and positions.

The lengths OJ and OM are equal to the object and image heights, respectively. The height on the entrance pupil is OR; the length OS is determined by the fact that the area OMS equals the distance from image plane to exit pupil. Points A and B correspond to the front and rear faces of the constraining cylinder and must lie along the straight lines JR and SM extended, their locations along their respective lines being determined from the known position of the cylinder faces along the optical axis. The required optical system may be represented by some undetermined curve traveling clockwise from A to B in such a fashion that it includes an area (shown shaded) equal to the length of the cylinder. It must, moreover, be consistent with the diameter constraint of the cylinder. Assuming no vignetting, the diameter constraint may be represented by the condition

$$2(|y| + |\bar{y}|) \leqslant \phi,$$

where ϕ is the maximum permissible free aperture. In the present example, the shaded area must therefore lie to the left of the line $2(y + \bar{y}) = \phi$. If some vignetting were permissible, this condition would be modified. For instance, if vignetting were permissible only to the degree that both marginal and principal rays would at least barely get through, then the condition becomes

$$2|y| \leqslant \phi,\ |y| \geqslant |\bar{y}|; \qquad 2|\bar{y}| \leqslant \phi,\ |y| \leqslant |\bar{y}|.$$

Let the area of the triangle OAB be denoted by T. Then, if the shaded area is not less than T, the problem can always be solved with at most two thin lenses (possibly one), provided the diameter constraint is not violated. If the shaded area is less than T, the problem can always be solved with three thin lenses of which the outer two are positive and the inner one negative. Once the exact curve connecting A and B is determined, the focal lengths and locations of the required thin lenses can be calculated using Eq. (1).

Most of the discussion above has dealt with thin lenses to avoid complexity. However, application to thick lenses is essentially the same, except that the replacement of actual distances by air equivalent distances requires the introduction of refractive indices. In fact, it is sometimes more convenient to regard the N_i for every space as independent parameters instead of the x_i for every surface. Depending on what values of x_i or N_i are chosen, every y, $\bar{y}$ diagram may be interpreted as either a system of thin lenses or of thick ones. Thus, Fig. 1 may alternatively be regarded as the diagram for a thick meniscus singlet for which the thickness would be determined once the value of N is given, or vice versa.

Finally, it is of interest to note that many of the above results are valid even for the case of an axially symmetric medium with continuously varying index of refraction. The curved path of an arbitrary paraxial skew ray uniquely defines the first-order properties of such a system, in the same manner as before, except that Eqs. (1) must be written in differential form. Here again, it is possible to work only with the projection on the y, $\bar{y}$ plane and treat the monotone increasing variable x as a parameter along the curve.

Conclusion

The method of first-order design described above has been applied to numerous problems at Bausch & Lomb and has frequently been found to yield insights which cannot readily be obtained using better known methods. It has proved to be a direct and time-saving tool during the early stages of the optical design of any instrument in which the location and diameter of the lenses and images are of primary importance. Also because of the ease with which individual surfaces can be imaged into the object and image spaces via the intervening components, the method has proved useful for the determination of cosmetic specifications as well as for relative illumination calculations.

Appendix

It will first be proven that $Q = y\bar{\alpha} - \bar{y}\alpha$ is invariant. The well-known ray tracing equations for a paraxial ray are:

$$\alpha_{i+1} = \alpha_i - K_i y_i,\ y_{i+1} = y_i + D_{i+1}\alpha_{i+1}, \tag{2}$$

where $K_i = (N_{i+1} - N_i)/r_i$, $D_i = d_i/N_i$, $\alpha_i = N_i u_i$.

Using bars for a second ray,

$$\begin{aligned} y_i\bar{\alpha}_i - \bar{y}_i\alpha_i &= y_i(\bar{\alpha}_{i+1} + K_i\bar{y}_i) - \bar{y}_i(\alpha_{i+1} + K_i y_i) \\ &= y_i\bar{\alpha}_{i+1} - \bar{y}_i\alpha_{i+1} = (y_{i+1} - D_{i+1}\alpha_{i+1})\bar{\alpha}_{i+1} \\ &\quad -(\bar{y}_{i+1} - D_{i+1}\bar{\alpha}_{i+1})\alpha_{i+1} = y_{i+1}\bar{\alpha}_{i+1} \\ &\quad - \bar{y}_{i+1}\alpha_{i+1}, \end{aligned}$$

which shows, by mathematical induction, that Q is invariant. Now

$$\begin{aligned} Q = y_i\bar{\alpha}_i - \bar{y}_i\alpha_i &= [y_i(\bar{y}_i - \bar{y}_{i-1}) - \bar{y}_i(y_i - y_{i-1})]/D_i \\ &= (y_{i-1}\bar{y}_i - y_i\bar{y}_{i-1})/D_i \\ &= [\bar{\alpha}_i(\alpha_i - \alpha_{i+1}) - \alpha_i(\bar{\alpha}_i - \bar{\alpha}_{i+1})]/K_i \\ &= (\alpha_i\bar{\alpha}_{i+1} - \alpha_{i+1}\bar{\alpha}_i)/K_i \end{aligned}$$

therefore,

$$D_i = (y_{i-1}\bar{y}_i - y_i\bar{y}_{i-1})/Q, \qquad K_i = (\alpha_i\bar{\alpha}_{i+1} - \alpha_{i+1}\bar{\alpha}_i)/Q. \tag{3}$$

The other relations of Eqs. (1) follow immediately from the definitions of x_i, D_i, and K_i and simple rearrangement of Eqs. (2).

It will now be shown that any vertex V of the y, $\bar{y}$ polygon is concave or convex toward the origin according to whether the corresponding power is positive or negative respectively. Let I be the side preceding V and R the side following, and let K be the surface power associated with V. If the angles after refraction are indicated by primes, the equations of I and R are:

$$Q = y\bar{\alpha} - \bar{y}\alpha$$

and

$$Q = y\bar{\alpha}' - \bar{y}\alpha',$$

where we regard the angles as constant. Letting θ' be the slope angle of R, then $\tan\theta' = \alpha'/\bar{\alpha}'$ and differentiating,

$$\sec^2\theta'\,\frac{d\theta'}{dK} = \left(\bar{\alpha}'\frac{d\alpha'}{dK} - \alpha'\frac{d\bar{\alpha}'}{dK}\right)\Big/\bar{\alpha}'^2.$$

But $\alpha' - \alpha = -Ky$, hence

$$d\alpha'/dK = -y, \qquad d\bar{\alpha}'/dK = -\bar{y};$$

moreover,

$$\sec^2\theta' = (\alpha'^2 + \bar{\alpha}'^2)/\bar{\alpha}'^2,$$

therefore, substituting into the equation for $d\theta'/dK$, one obtains:

$$\frac{d\theta'}{dK} = -\frac{Q}{\alpha'^2 + \bar{\alpha}'^2}. \tag{4}$$

Equation (4) states that $d\theta'/dK$ and Q differ in sign. Therefore, for a small increment $\Delta K > 0$, line R is deviated clockwise ($\Delta\theta' < 0$) for $Q > 0$ and counterclockwise ($\Delta\theta' > 0$) if $Q < 0$, with exactly the reverse situation if $\Delta K < 0$. Since R is parallel to I for $K = 0$, the truth of the proposition immediately follows.

References

1. R. K. Luneberg, *Mathematical Theory of Optics* (Brown University, Providence, Rhode Island, 1944), pp. 301–303.
2. T. Smith, Trans. Opt. Soc. (London) **23,** 217 (1921–22).
3. T. Smith, *Dictionary of Applied Physics, IV* (Peter Smith, New York, 1950), pp. 357–359.

From the Editor

At last some readers have been stirred to write us short notes concerning units. We are happy to point out that these letters are running two to one in favor of the metric system. (To be completely frank, we should say that two of the three have been in favor, and the other opposed.) One of them referred to the report of a formal inquiry relative to the possible introduction of the metric system into England—as reported in the *Philosophical Magazine*, Series IV, Vol. 25, p. 74 (1863)—a Professor Miller was being questioned. The interrogation went as follows:

Question: "Do you find in your learned pursuits that our present system of weights and measures interferes with scientific investigation in any way?"

Answer: "Not in the least; they are so complicated that it is quite impossible to use them. . . . Since 1830 no chemist ever made use of any weights which were not decimally divided." (Decimally divided balances were made by Robinson and by Oertling.)

Question: "So far as scientific investigations are concerned, our present system is useless?"

Answer: "Entirely. . . ."

That was one hundred years ago, but at last it appears that Christopher Robin's world of pounds, shillings, and ounces is beginning to crumble. *The New York Times* of 22 and 24 September 1963 presented the long-awaited recommendations of the Royal Commission under Lord Halsbury concerning the decimalization of the pound into 100 cents. Gone will be the guineas, half crowns, and florins, the sixpence and the threepenny bit. But there will still be a five-cent piece to be called a shilling, so that 20 shillings remains a pound. You may say that this monetary change has little to do with the metric system, but not so: this is the first British unit or conversion factor involving 10 since Henry Briggs proposed decimal logarithms in 1617, and few Britons use logarithms in their daily life. (It is also reported that those who do prefer Napierian logarithms.) There is some hope that they may find it almost as easy to think in terms of tens and tenths as in terms of twelfths, fourteenths, and sixteenths now used in divisions of feet, stones, and pounds. (It is interesting to observe that the *ounce*, one-sixteenth of a pound, derives from the Latin *uncia*, meaning twelfth part. Our word *inch* also derives from *uncia*.)

If the host at a present-day British supper party desires to figure quickly a ten percent tip on a bill of £25 18s 9$^1/_2$ d, he must work his way first through the £ : 2.5 or £2 10s, then the shillings: 1.8s or 1s 9.6d, finally the pence: 0.95; and then total to obtain £2 11s 10.55d, which, if he is from the southern parts of Great Britain, he will round off to £2 12s. (In decimal pounds the bill is £25.94, and a generous tip £2.60.)

Our nonmetric reader does not mind metric units being used for purely scientific purposes, but demurs when common objects (the kitchen sink, a sheet of paper, a $^1/_4$-in. pipe or a 6-ft man) are dimensioned this way. "If I spoke of a 183-cm man you would have no idea whether he was a giant or a runt." We have checked this particular point with several European friends, and they assure us that they *can* still mentally picture stature in cm, although one can no longer sing "157.5 cm, eyes of blue". (Perhaps "157, eyes like heaven".) In fact it gives one a new goal to shoot for: the Russians are very proud of the fact that Peter the Great was over 2 m tall. Our reader asks "Would you go into our machine shop and ask for a piece of 6-mm tubing?" Probably one would, if it were glass tubing; and in these days of small foreign cars practically every mechanic, if not every machinist, now has his collection of metric wrenches and metric nuts and bolts. He might even have some metric calipers. We agree with the reader, however, that even in our own machine shop the machinists might be dismayed by some of the dimensions expressed in our pages; but this journal is not really addressed to them, and few of them read it regularly. To those readers who desire to construct in their own laboratory an exact copy of something described in this journal, we would recommend that you write directly to the author and ask him for a set of his working drawings: the author would probably tell you many things that he would do differently if he were starting again.

Our goal in these pages is not to convert your machine shop, but to make the optics audience more metric minded. In 1940 the Director of Purchasing at Eli Lilly and Company, a leading pharmaceutical supplier, began a campaign to convert the company to metric operations. Many of their raw materials came from metric parts of the world, and suppliers in the U.S. variously used apothecary and avoirdupois systems, so that problems of materials control, inventory management, and accounts payable began to tax even electronic computers. During the war a series of so-called wonder drugs was developed, and it became commonplace to express dosage in metric units, usually in milligrams per dose. In early 1954 the Company began experimentally to include on the labeling the exact metric equivalent to the avoirdupois-apothecaries weights and measures. Over a period of four years all of the company's scales, balances, and other measuring equipments were converted to metric, as were the bookkeeping and supply records. Suppliers of such bulk commodities as sugar, starch, and salt were asked to quote and supply in packages of even kilograms, such as 30, 50, 70, or 100 kilos; and Lilly was pleasantly surprised to find that they did so readily and without complaint. Money talks. The only organization with which they had real difficulty was the U.S. Government, who insisted that taxes on grain alcohol must be computed in terms of gallons. This company is now completely metric in its internal operations and almost so externally. There is no reason why the optical industry and the optics community could not be similarly in advance of its times.

John N. Howard

A Flexible Automatic Lens Correction Procedure

Gordon H. Spencer

Since the advent of high-speed automatic computing machinery, workers in the field of optical design have been intrigued by the idea of automating the lens design process. Various methods have been proposed and tested. Most of these, in the author's view, do not allow sufficient control to be exercised over the nature of the design solution. Those which do allow such control appear to be inefficient because of slow convergence to a solution. This paper describes a correction procedure which permits a high degree of control over the nature of the design solution and which has shown a reasonably good rate of convergence in a limited number of tests. The operation of a computer program to carry out the procedure is described, and the results of a typical design problem are presented.

Introduction

Before attempting to develop an automatic lens correction procedure it is, of course, necessary to formulate a philosophy of approach. Two distinct philosophies are evident in the published work on automatic lens design. The first of these asserts that the lens design problem can be completely stated in explicit mathematical terms and, hence, that a computer can reasonably be expected to carry out the entire lens design procedure.[1] The second asserts that lens design inevitably requires qualitative judgments and compromises to be made and, hence, that the computer should be regarded as a tool capable of presenting the designer with provisional solutions only.[2] This philosophy suggests the development of a flexible procedure which allows the designer to exercise individual control over a number of image characteristics. The characteristics should be easily calculable since several sequences of correction iterations may be performed as the designer changes his estimates of the relative importance of various characteristics.

If one is sure that all of the systems to be dealt with are capable of a high state of correction, the first philosophy is reasonable. In many cases, however, the state of correction attainable may be marginal, and it is in anticipation of these cases that the second philosophy becomes more tenable. Suppose, for example, that cost considerations limit a system to four elements made from inexpensive glasses. It is required that the area weighted average resolution over the field be 50 lines/mm and that the distortion not exceed 1%. It is found that the minimization of a selected merit function yields a system having an AWAR of 30 lines/mm and a maximum distortion of 0.5%. An alteration of the merit function leads to a system having an AWAR of 45 lines/mm and a maximum distortion of 1.5%. Neither system meets the initial requirements. What is to be done? Perhaps by compromising the original cost requirements and allowing greater freedom of glass choice, a system can be obtained which meets the original resolution and distortion requirements. Perhaps, instead, the image requirements may be compromised. If so, a decision must be made regarding the importance of distortion relative to AWAR. One application may dictate that the maximum distortion be rigidly held to 1% while a different application may place heavy emphasis upon the AWAR.

It is the purpose of this paper to describe the development and testing of an automatic lens correction procedure consistent with the second philosophy of approach expressed in the preceding paragraphs. Two distinct problems are involved in the development of such a procedure. The first is that of formulating a correction method of sufficient flexibility to allow the designer a high degree of control over the nature of the design solution. The second is that of choosing a set of system performance functions which is small enough to avoid redundancy, large enough to define reasonably well the imagery over the whole field, and simple enough to be calculated rapidly. It is, of course, mandatory that all design solutions be physically

---

The author was with the Institute of Optics, University of Rochester, New York when this work was done. He is presently with Scientific Calculations, Inc., Rochester, New York.

Received 19 September 1963.

This work was supported by the U.S. Air Force and in part by the International Business Machines Corporation.

realizable, and this requires that the variation of system parameters be governed by certain boundary conditions.

The correction method to be described is a linearization method designed to accommodate both absolute and relative requirements. Absolute requirements are taken here to mean those requirements which must be met exactly (or almost exactly) by the design solution. Relative requirements are those which may be lumped together, with various weighting factors, into a single merit function whose value is to be minimized. It is felt by this author that the accommodation of both types of requirements is necessary in order to allow the designer sufficient control over the nature of the design solution.

A variety of methods have been described in the literature. Of these, however, only the Lagrangian gradient methods described by Feder[3] and by Meiron and Loebenstein[4] are capable of maintaining absolute requirements while simultaneously minimizing a merit function. Unfortunately, such gradient methods generally exhibit extremely slow convergence to a design solution. Limited experience with the method to be described indicates a much more satisfactory rate of convergence.

A General Linearization Method

Statement of the Problem

One is given an optical system of J variables, $p_1, \ldots, p_J$. These variables may be surface curvatures, axial separations of surfaces, refractive indices, or aspheric deformation coefficients. In terms of these variables a number of functions, $f_1(p_1, \ldots, p_J), \ldots, f_K(p_1, \ldots, p_J)$, may be defined which measure various characteristics of the system, both with regard to its physical structure and its performance. The correction problem is that of finding a simultaneous solution, or something approaching a simultaneous solution, to the set of equations

$$f_k(p_1, \ldots, p_J) = s_k, \; k = 1, \ldots, K, \tag{1}$$

where the s_k are constants representing the desired values for the performance functions.

Frequently, a simultaneous solution to the entire set of equations will not exist. In such cases, the minimization of a merit function,

$$\sum_{k=1}^{K} w_k^2 (f_k - s_k)^2,$$

where the w_k are weight factors, may be an acceptable alternative to an exact solution.

In general, there will be certain of the functions, f_k, for which it is required that specified values be attained while for the remaining functions the minimization of the merit function will suffice. One thus divides the performance functions into two groups,

$$g_m(p_1, \ldots, p_J), \; m = 1, \ldots, M$$

and

$$h_n(p_1, \ldots, p_J), \; n = 1, \ldots, N < J,$$

and seeks to minimize

$$\phi = \sum_{m=1}^{M} w_m^2 (g_m - s_m)^2, \tag{2}$$

while at the same time securing a simultaneous solution to the set of equations

$$h_n(p_1, \ldots, p_J) = t_n, \; n = 1, \ldots, N, \tag{3}$$

where the t_n are the required values of the functions, h_n.

The chief difficulty in solving the problem set forth above is that the functions which measure the system performance are nonlinear. A common approach to such problems is to approximate the nonlinear functions by linear ones and solve the linear problem. The repeated application of this procedure can be expected to lead ultimately to a solution of the nonlinear problem, assuming such a solution exists. This approach is adopted here.

The initial lens system configuration is defined by a set of values, $p_1', \ldots, p_J'$, of the system variables. Each of the performance functions may be expanded in a Taylor series about this initial configuration point and linear approximations obtained by neglecting all but the first-order terms in the expansions. Defining

$$\left.\begin{aligned} d_m &= s_m - g_m' \\ e_n &= t_n - h_n' \\ q_j &= p_j - p_j' \\ a_{mj} &= (\partial g_m/\partial p_j)' \\ b_{nj} &= (\partial h_n/\partial p_j)' \end{aligned}\right\}, \tag{4}$$

where the primes denote values at the initial configuration point, our problem becomes that of minimizing the quadratic

$$\phi = \sum_{m=1}^{M} w_m^2 \left(\sum_{j=1}^{J} a_{mj} q_j - d_m \right)^2, \tag{5}$$

while at the same time securing a simultaneous solution to the set of linear equations

$$\sum_{j=1}^{J} b_{nj} q_j = e_n, \; n = 1, \ldots, N. \tag{6}$$

Solution by Lagrange Multipliers

The problem of finding an extremum of a function subject to constraints on the variables can be solved by using the method of Lagrange multipliers.[5] In the present case the method selects from the continuum of solutions which will ordinarily exist for Eqs. (6) that solution for which ϕ is minimum. The solution is most easily expressed in matrix form and for that purpose we define the matrices

$$\left.\begin{aligned}
\mathbf{A} &= \begin{pmatrix} a_{11} \ldots\ldots a_{1J} \\ \cdot \qquad \cdot \\ \cdot \qquad \cdot \\ \cdot \qquad \cdot \\ \cdot \qquad \cdot \\ a_{M1} \ldots\ldots a_{MJ} \end{pmatrix} \\
\mathbf{B} &= \begin{pmatrix} b_{11} \ldots\ldots b_{1J} \\ \cdot \qquad \cdot \\ \cdot \qquad \cdot \\ \cdot \qquad \cdot \\ \cdot \qquad \cdot \\ b_{N1} \ldots\ldots b_{NJ} \end{pmatrix} \\
\mathbf{W} &= \begin{pmatrix} w_1 & & & \\ & \cdot & & \bigcirc \\ & & \cdot & \\ & \bigcirc & & \cdot \\ & & & w_M \end{pmatrix}
\end{aligned}\right\} \tag{7}$$

and the vectors

$$\mathbf{d} = \begin{pmatrix} d_1 \\ \cdot \\ \cdot \\ \cdot \\ d_M \end{pmatrix}, \quad \mathbf{e} = \begin{pmatrix} e_1 \\ \cdot \\ \cdot \\ \cdot \\ e_N \end{pmatrix}, \quad \mathbf{q} = \begin{pmatrix} q_1 \\ \cdot \\ \cdot \\ \cdot \\ q_J \end{pmatrix}. \tag{8}$$

The matrix **A** and vector **d** will always appear multiplied by the matrix of weight factors, **W**. For convenience, these products are defined to be

$$\mathbf{M} = \mathbf{WA} \tag{9}$$

and

$$\mathbf{r} = \mathbf{Wd}. \tag{10}$$

Now each of Eqs. (6) represents a J-dimensional plane having the normal vector

$$\mathbf{v}_n = \begin{pmatrix} b_{n1} \\ \cdot \\ \cdot \\ \cdot \\ b_{nJ} \end{pmatrix}. \tag{11}$$

The common intersection of these planes, which is the locus of all points $(q_1, \ldots, q_J)$ satisfying Eqs. (6), is a surface (or line) in the J-dimensional configuration space to which each of the vectors $\mathbf{v}_n$ is normal. The solution we seek is the point on this surface at which the merit function, ϕ, is stationary. By stationary, we mean that ϕ remains unchanged when differential departures from the solution point are made within the surface. At such a point grad ϕ must have no component lying in the surface. Consequently, it is possible to write grad ϕ as a linear combination of the vectors, $\mathbf{v}_n$. Thus we set

$${}^1/_2 \operatorname{grad} \phi = \sum_{n=1}^{N} \lambda_n \mathbf{v}_n, \tag{12}$$

where the λ_n are scalar multipliers.

From Eqs. (5),

$${}^1/_2 \operatorname{grad} \phi = \mathbf{M}^T(\mathbf{Mq} - \mathbf{r}), \tag{13}$$

where the superscript, T, denotes the transpose. Then, defining

$$\lambda = \begin{pmatrix} \lambda_1 \\ \cdot \\ \cdot \\ \cdot \\ \lambda_N \end{pmatrix}, \tag{14}$$

Eq. (12) becomes

$$\mathbf{M}^T\mathbf{Mq} - \mathbf{B}^T\lambda = \mathbf{M}^T\mathbf{r}. \tag{15}$$

This equation together with Eqs. (6), whose matrix form is

$$\mathbf{Bq} = \mathbf{e}, \tag{16}$$

yields our solution, for Eqs. (15) and (16) together form a set of $N + J$ linear equations in the $N + J$ unknowns which are the elements of **q** and λ.

Now it is quite possible for the above set of equations to be indeterminate. The possibility of indeterminacy may be removed, however, by employing a device suggested by Levenberg[6] and later used by Hopkins *et al.*[7] and Wynne.[8] This device consists of adding the sum

$$S = \sum_{j=1}^{J} c_j^2 q_j^2 \tag{17}$$

to the merit function, ϕ, where the c_j are weight factors. In addition to removing the indeterminacy, the addition of S affords a control over the influence of the different variables on the solution and provides a means of limiting the magnitude of the computed changes in the system parameters. With this modification of ϕ, Eq. (15) becomes

$$(\mathbf{M}^T\mathbf{M} + \mathbf{C})\mathbf{q} - \mathbf{B}^T\lambda = \mathbf{M}^T\mathbf{r}, \tag{18}$$

where

$$\mathbf{C} = \begin{pmatrix} c_1^2 & & \\ & \cdot & \bigcirc \\ & \cdot & \\ \bigcirc & & \cdot \\ & & c_J^2 \end{pmatrix}. \tag{19}$$

Once a solution to the linear problem has been obtained, the resulting configuration is taken as a starting point from which a new linear solution is generated. This procedure is continued iteratively to arrive at a solution to the nonlinear problem. It is important that the changes produced at each iteration be kept within reasonable limits so that the linear approximations retain some degree of validity. Otherwise, a system configuration may be generated which is so far removed from the final solution that the chance of convergence is reduced to the vanishing point. If the e_n have been reduced to near zero values, the weight factors, c_j, may be used to limit the changes produced at a given iteration. If the e_n are appreciable, however, it is impossible to confine the changes within arbitrary limits by use of the weights. In such cases one may apply only a fraction of the computed changes to the system.

The present method may be regarded as a wedding of the methods introduced by Hopkins *et al.*[7] and Wynne.[8] If there are no relative requirements, **M** and **r** disappear and the solution coincides with that obtained by Hopkins *et al.* for absolute correction to required target values. If absolute requirements are omitted, **B** and **e** disappear and we are left with Wynne's method.

Image Errors

We now turn to the problem of selecting a suitable set of image errors upon which to operate. The choice of these image errors is governed by two opposing factors. First, they must define the imagery over the whole field with reasonably good accuracy, and second, they must be rapidly calculable. In the region of small aperture and small field angle, the Seidel aberrations meet the requirements of accuracy and ease of calculation. Beyond this region, ray-trace data may be used to achieve as accurate a geometrical description of the imagery as desired.

In order to avoid redundancy and to reduce computing time to a minimum it is necessary to determine the minimum quantity of ray-trace data which will describe the imagery with acceptable accuracy. It has been suggested by the author that data obtained from tracing eleven rays is sufficient to define adequately the imagery for all but very wide aperture or very wide field systems.[9] A similar conclusion has been reached by Feder.[10] The ray set suggested by the author is defined in Table I. It consists of ten meridional and one skew rays. Along with the meridional rays, twelve differential rays are traced to obtain derivatives of the image-plane ray deviations with respect to object height and aperture coordinates. Altogether, twenty-three image errors are thereby obtained. These data together with the Seidel aberrations are sufficient to determine all of the coefficients through the seventh order in interpolation polynomials expressing the image-plane ray deviations as functions of the object and aperture coordinates. A comparison of spot diagrams computed from such polynomials with corresponding diagrams obtained solely by ray tracing is shown in Fig. 1. These diagrams represent the geometrical images on axis and at three field points for an $f/4$ unvignetted triplet objective. The agreement between the polynomial approximations and exact ray tracing is obviously excellent for this example.

Chromatic aberrations may be easily calculated for any of the ten meridional rays by the $D - d$ method introduced by Conrady[11] and elaborated upon by Feder.[12] The data generated by differential ray tracing may be used to calculate directly the change in the image-plane ray deviations associated with a change in wavelength.

The Computer Program

In order to test the utility of the correction procedure, a computer program was prepared. The program was coded in the FORTRAN language and used with an IBM 7090 computer. This section describes the organization of the program. An important consideration in the development of such a program is that tight control over the changes in system configuration be maintained. This means that successive changes in the system configuration should be kept small enough so that the linear approximations retain reasonable accuracy and that the changes be consistent with physical constraints. If the changes are unrestricted nonlinearity may severely impair convergence, and physically unrealizable configurations may be generated. The program contains adequate safeguards against such contingencies.

In its present form the program is capable of accepting lens configurations consisting of spherical refracting and/or reflecting surfaces only. It was felt that the additional program complexity required to handle aspheric surfaces would be unjustified in an experimental program designed to test the method. Surface curvatures and surface separations may be varied, but refractive indices are fixed.

The program operates upon the image errors discussed in the preceding section. The image errors upon which the program is to operate are divided by the user into two groups. The first group consists of those image errors which are to be corrected to specific values. We shall call these C-mode image errors.

Table I. Ray-Traced Image Error Set

Opening ray data			Image errors obtained				
$h/h_{\max}$	$X/X_{\max}$	$Y/Y_{\max}$	x	y	$h_{\max}\dfrac{\partial y}{\partial h}$	$X_{\max}\dfrac{\partial x}{\partial X}$	$Y_{\max}\dfrac{\partial y}{\partial Y}$
0	0	0.7		[b]	[b]		
0	0	1.0		[b]	[b]		
0.7	0	0		[b]		[b]	[b]
1.0	0	0		[b]		[b]	[b]
0.7	0	0.7		[b]		[b]	
0.7	0	−0.7		[b]		[b]	
0.7	0	1.0		[b]		[b]	
0.7	0	−1.0		[b]		[b]	
1.0	0	−0.7		[b]		[b]	
1.0	0	−0.7		[b]		[b]	
1.0	0.7	0	[a]				

[a] (X,Y) denote entrance pupil coordinates; (x,y) denote image plane coordinates referred to the Gaussian image point as origin, and h denotes object height.

[b] Aperture stop.

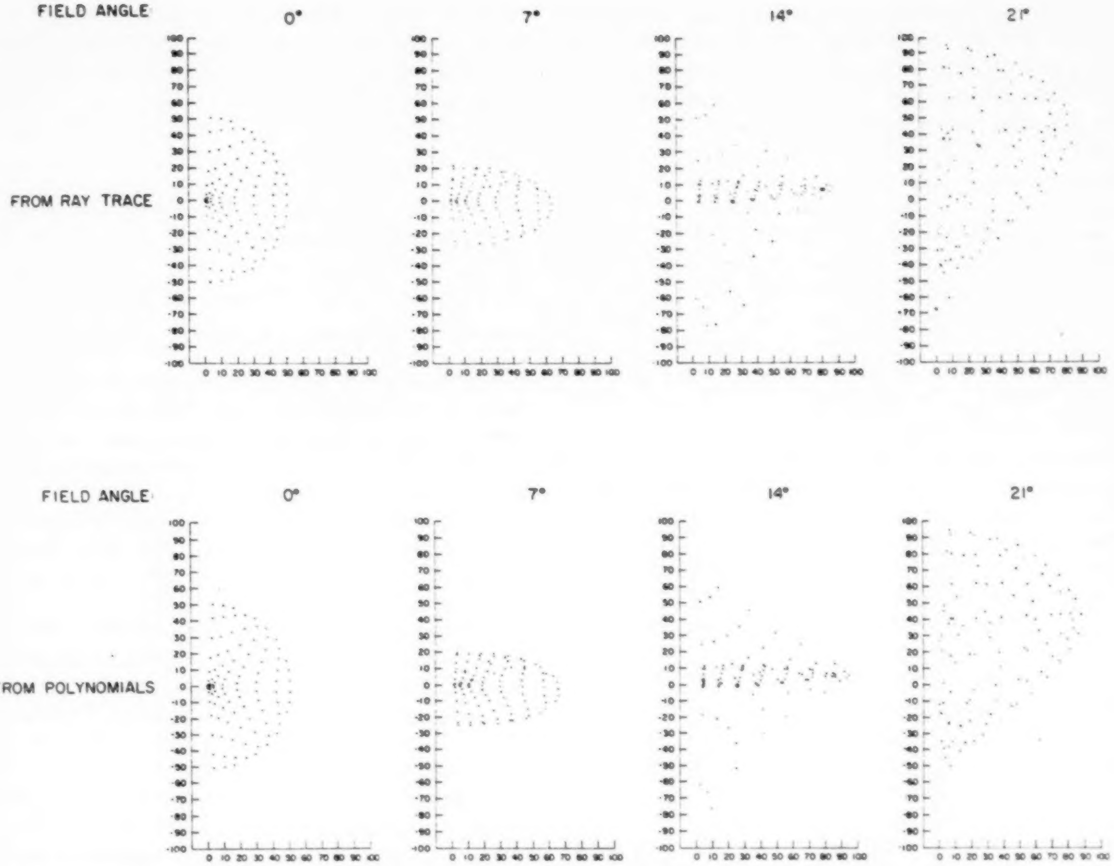

Fig. 1. A comparison of spot diagrams computed from seventh order ray aberration polynomials with diagrams computed by ray tracing for an $f/4.0$ triplet objective.

The second group consists of those errors which are required to approach desired values in the least-squares sense (i.e., to appear as terms in the merit function, ϕ). We shall call these M-mode image errors. Associated with the M-mode errors are the weight factors, w_m, which are specified as input to the program. Upon completion of a successful run, the program should yield a system configuration possessing the specified values for the C-mode errors and at least a relative minimum for the weighted sum of squares of the differences between the M-mode errors and their desired values. The system must also be capable of passing an axial meridional ray fan of specified half-width, R, a meridional fan of half-width f_1R from the 0.7 zone of the field, and a meridional fan of half-width f_2R from the edge of the field. f_1 and f_2 are specified vignetting factors. Symmetrical vignetting is assumed.

We now describe in some detail the sequence of operations performed by the program:

(1) The first step in the program is the calculation of initial values for all of the C- and M-mode image errors. This is followed by a calculation of the minimum requisite clear apertures at each surface. The clear aperture calculations are made using the paraxial ray approximations and, hence, are not precise. High accuracy is not necessary in this calculation, however, and the paraxial approximations should be acceptable for all systems but those of unusually large aperture or field.

Meridional distances from surface to surface at the clear aperture heights are next calculated. The following questions are then asked at each surface:

(a) If the medium following this surface is glass, is the axial separation from the next surface greater than one-tenth the clear aperture at this surface?

(b) If the medium following this surface is air, is the axial separation from the next surface greater than zero?

(c) If the answer to either of the above questions is "yes", is the meridional distance from this surface to the following surface at the clear aperture heights greater than zero?

A "no" answer to any of these questions indicates a physically unacceptable system configuration. If the answer to either question (a) or (b) is "no", the axial separation from the following surface is adjusted to a value slightly greater than one tenth the clear aperture or slightly greater than zero, depending upon whether the following medium is glass or air. If the answer to question (c) is "no", the surface separation at the clear aperture heights is treated as a C-mode image error in subsequent operations and is corrected to a value slightly greater than zero. It should be noted that the separation at the clear aperture heights is not only a function of the axial separation and curvatures of the surfaces in question, but is also a function of preceding surface parameters, inasmuch as these influence the clear aperture heights.

(2) Having obtained initial values for each of the C- and M-mode image errors, the program proceeds to calculate finite difference approximations to their derivatives with respect to each of the system variables. Each variable, with the exception of axial separations fixed in step (1), is, in turn, altered by a small increment, and the change in each image error is calculated. The **A** and **B** matrices are thus generated. One increment is used for all curvatures and another increment for all axial separations. Each time a parameter is changed, the curvature of the last surface of the system is adjusted to maintain a constant f/number.

(3) The program next proceeds to calculate a solution for the C-mode image errors. The M-mode image errors are omitted at this stage. The weight factors, c_j^2, are assigned one value for all curvatures and another value for all axial separations, the assignment of values being made by the user. If none of the predicted parameter changes exceeds ten times the increment used in the derivative calculations, the program branches to a calculation which takes the M-mode errors into account. This will be described subsequently. If one or more of the predicted changes exceeds ten times the increment used in the derivative calculations, the following procedure is adopted:

(4) The ratio of each parameter change to the increment used in the derivative calculations is examined and the largest ratio determined. If the magnitude of the ratio exceeds fifty, the value of a scale factor, s_1, is set equal to the reciprocal of this magnitude. Otherwise the value of the scale factor is set equal to unity. Each predicted change is then multiplied by the scale factor, s_1, and the resultant scaled changes are applied to the lens system. In this way, no system parameter is changed by an amount greater than fifty times the increment used in the derivative calculations. All of the C-mode image errors are now evaluated for the new system configuration. The sum of the squares of the differences between the current values and the required values is then formed. We shall call this sum ψ_1.

When the predicted changes are multiplied by a variable factor, s, and substituted in the expressions which give the C-mode image errors as functions of the system parameters, these image errors become functions of s only. If we define a function $\psi(s)$ to be the sum of squares of the differences between the values of these errors and their required values we may write

$$\psi(s) = (1 - s)^2\psi(0) + \text{higher order terms}, \tag{20}$$

where the higher order terms arise because of the nonlinearity of the image error functions. We may take partial account of the nonlinear effects by assuming a third-order term only and thus setting

$$\psi(s) = (1 - s)^2\psi(0) + \alpha s^3. \tag{21}$$

Since we have evaluated $\psi(s)$ at $s = s_1$ and obtained the value ψ_1, we may compute α. If α is positive, $\psi(s)$ has a minimum for some value of s less than unity. We shall call this value s_2. s_2 is computed by the program, and if it is less than s_1 the original system configuration is modified by the set of changes s_2q_j rather than s_1q_j. This sort of procedure has been suggested by Feder[13] in connection with gradient methods.

In summary, this phase of the correction procedure has consisted of finding a linear solution for the C-mode image errors, scaling the resultant parameter changes to avoid excessive alterations of the system, and taking partial account of nonlinear effects to find a more favorable scaling. The reason for omitting a consideration of the M-mode image errors is that nonlinear effects are likely to become significant for parameter changes in excess of ten times the increments used to compute the derivatives. Incorporation of the M-mode image errors would only result in the generation of larger parameter changes, and the likelihood of securing a significant reduction in the value of the merit function would be slight.

(5) If there are no C-mode image errors or if the changes required to secure a linear solution for these quantities do not exceed ten times the increments used for the derivative calculations, the following procedure is adopted:

Each weight factor, c_j^2, is set equal to the product of three factors. The first factor is specified as part of the input data and has one value for curvatures and another value for axial separations. This is the weight introduced in step (3). The second factor is the average value of the diagonal elements of the matrix $\mathbf{M}^T\mathbf{M}$. The third factor, which we shall denote by P, is assigned an initial value of unity. The second factor has the effect of producing a reasonable balance between the weighted sum of squares of the parameter changes and the merit function, ϕ, when the other factors are on the order of unity.

A solution to the complete problem is next obtained, i.e., a linear solution for both C- and M-mode image errors. The P factor is then reduced by a factor of ten and a second solution obtained. The actual value of the merit function for the second solution is compared with that for the first solution. If the second solution exhibits a smaller value for ϕ, the P factor is again reduced by a factor of ten and a third solution obtained. The process is repeated until one of two conditions is found to exist. The first condition is that the value of the merit function has increased over that for the previous solution. The second condition is that one or more of the C-mode image errors has departed from its required value by an amount greater than 0.001. For a system scaled in centimeters, this means a departure of 10μ. The value of 0.001 is somewhat arbitrary but seems to be a reasonable and not too restrictive tolerance. These conditions arise as a result of nonlinearity of the image errors. When one of these conditions is detected, the immediately preceding solution is selected as the terminal solution.

(6) Once a solution has been obtained as a result of completing steps (4) or (5), a check is made to determine whether or not any new violations of the conditions expressed by questions (a), (b), and (c) of step (1) exist. If such is the case, these violations are treated in the manner indicated in step (1), and control then reverts to step (4) or (5). The solution which is ultimately selected is that for which no new violations occur.

(7) The configuration generated as a result of carrying out steps (1)–(6) now serves as a starting point from which the entire correction procedure is repeated. Successive repetitions of the correction procedure are made until no further improvement in the system performance can be obtained.

A Design Example

As a test of the correction procedure a Tessar-type system was presented to the program. The system was required to operate at $f/3.5$ and to image a distant object field whose angular half-width at the lens was 21°. The focal length was maintained at a value of 10. The vignetting factors, f_1 and f_2, were assigned values of 0.7 and 0.5, respectively. Equal weights were placed on curvatures and axial separations in the C matrix, and all curvatures and axial separations were allowed to vary. An increment of 0.001 was used in computing derivatives with respect to curvatures, and an increment of 0.01 was used in computing derivatives with respect to axial separations.

It was required that spherical aberration at the margin, astigmatism at the edge of the field, axial color at the 0.7 zone of the aperture, and lateral color at the 0.7 zone of the field all be corrected to zero. These were designated C-mode errors. All of the remaining monochromatic errors were designated M-mode errors having weights of unity and desired values of zero with respect to the associated Gaussian image points.

Table II. Initial Configuration Data for $f/3.5$ Tessar

Surface No.	Curvature	Thickness	N_D	N_F	N_C
1	0				
		0.5	1.63842	1.64657	1.63506
2	−0.2				
		0.5	1.0	1.0	1.0
3	−0.2				
		0.2	1.64752	1.66122	1.64210
4	0				
		0.5	1.0	1.0	1.0
5[a]	0				
		0.5	1.0	1.0	1.0
6	−0.1				
		0.2	1.58908	1.59933	1.58495
7	0				
		0.5	1.65832	1.66749	1.65454
8	−0.2372				

[a] Aperture stop.

The initial configuation (see Table II) was purposely chosen to be a gross departure from the anticipated final form. The configuration is illustrated in Fig. 2. After sixty-six iterations, requiring approximately 5 min of IBM 7090 computer time, the final configuration (see Table III) illustrated in Fig. 2 was obtained. Figure 3 displays plots of the principal monochromatic aberrations for the initial system, while Fig. 4 displays similar plots for the final design. It should be noted that the scales of the final aberration plots have been expanded by a factor of ten in order to better show the nature of the correction. Circles on these plots indicate the points at which exact correction to zero values was demanded. The final configuration is well corrected for color and distortion and in the author's view represents an excellent Tessar design.

The author is deeply indebted to Robert E. Hopkins for his guidance and active interest in the work, to Donald P. Feder for several fruitful if somewhat argumentative discussions, and to William P. Hennessy for a number of useful suggestions in connection with programming techniques.

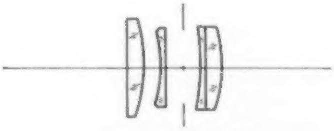

INITIAL CONFIGURATION

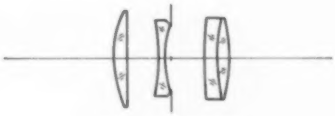

FINAL CONFIGURATION

Fig. 2. Initial and final configurations of $f/3.5$ Tessar.

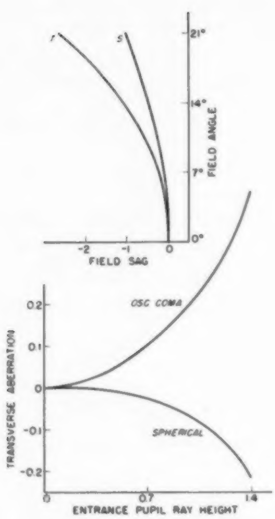

Fig. 3. Spherical aberration, OSC coma, and sagittal and tangential field plots for initial configuration of $f/3.5$ Tessar. Results are obtained from actual and differential ray tracing.

Table III. Final Configuration Data for $f/3.5$ Tessar

Surface No.	Curvature	Thickness	N_D	N_F	N_C
1	0.28573				
		0.41325	1.63842	1.64657	1.63506
2	0.00491				
		0.96497	1.0	1.0	1.0
3	−0.14563				
		0.21973	1.64752	1.66122	1.64210
4	0.29962				
		0.18000	1.0	1.0	1.0
5[a]	0				
		0.98388	1.0	1.0	1.0
6	0.04818				
		0.39238	1.58908	1.59933	1.58495
7	0.20231				
		0.38447	1.65832	1.66749	1.65454
8.	−0.19971				

[a] Aperture stop.

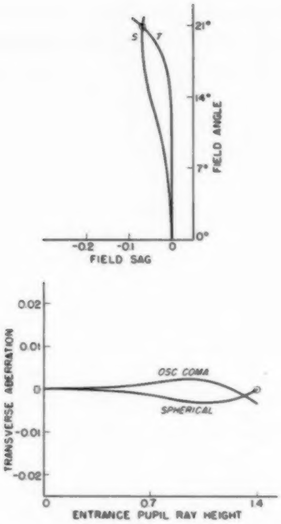

Fig. 4. Spherical aberration, OSC coma, and sagittal and tangential field plots for final configuration of $f/3.5$ Tessar. Results are obtained from actual and differential ray tracing.

References

1. D. P. Feder, J. Opt. Soc. Am. **52,** 177 (1962).
2. R. E. Hopkins and G. Spencer, J. Opt. Soc. Am. **52,** 172 (1962).
3. D. P. Feder, J. Opt. Soc. Am. **47,** 902 (1957).
4. J. Meiron and H. M. Loebenstein, J. Opt. Soc. Am. **47,** 1104 (1957).
5. See, for example, Harris Hancock, *Theory of Maxima and Minima* (Dover, New York, 1960), Chap. VI.
6. K. Levenberg, Quart. Appl. Math. **2,** 164 (1944).
7. R. E. Hopkins, C. A. McCarthy, and R. Walters, J. Opt. Soc. Am. **45,** 363 (1955).
8. C. G. Wynne, Proc. Phys. Soc. (London) **73,** 777 (1959).
9. G. H. Spencer, *A Computer Oriented Automatic Lens Correction Procedure* (Thesis, University of Rochester, Rochester, N. Y., 1963), Chap. III.
10. D. P. Feder (private communication).
11. A. E. Conrady, Monthly Notices Roy. Astron. Soc., 182 (January 1904); 458 (March 1904). These articles were cited by Feder in ref. 12.
12. D. P. Feder, J. Research Natl. Bur. Standards **52,** research paper 2471 (1954).
13. D. P. Feder, J. Opt. Soc. Am. **52,** 177 (1962).

photo F. S. Harris, Jr.

Participating in the Budapest Second Optical Conference during May 1963 are F. S. Harris, Jr. *Aerospace*, E. Hahn *Telecommunications Research Institute*, S. Tisza *Hungarian Optical Works*, A. Budincsevits *Telecommunications Research Institute*, L. Faragó *Hungarian Optical Works*, W. S. Rodney *NSF*, Z. Erdókurti *Control Research Institute for Physics* and K. Kantor *Hungarian Optical Works*. For a report of this meeting see the September 1963 issue.

Coaxial, Dual-Field Optics For a Space Sextant

H. E. Brunelle, Jr., and R. R. Willey, Jr.

A telescope having a 2° field of view and an optical system with a 165° inside-out, quasi-stigmatic field of view, which has been axially integrated to be mutually nonobscuring and confocal, is described. Navigation and guidance application requirements of space vehicles from which the optical specifications have been derived are discussed. The narrow-field system is a Schmidt-Cassegrain telescope of unusually short length as dictated by the requirements. A semiautomatic lens design program for the IBM 7090 computer developed by coauthor Willey was used in the optimization of the optical design. The final optical performance predictions are shown and have been essentially supported by the performance of the prototype unit which was constructed.

The Problem

Among the earliest developed, and still most fundamental, techniques in the art and science of navigation and guidance is the determination of present position and true bearing. The first mariner, who deliberately ventured far from the sight of land, must have relied on the constancy of the stars and planets and on his ability to determine from them his navigational needs.

The astronaut with his self-contained navigation system, venturing into the solar system beyond the domination of the earth's gravity, must rely on the same ultimate frame of reference to obtain the same navigational fix. He must have the means to perform a particular sequence of measurements related to a suitable coordinate system.[1] Each measurement, when reduced, constrains his position to a locus of points constituting a surface in three-dimensional space.

By measuring the angle between a planet (or moon) and a known star, a position locus in the form of a cone is established. Measurement of the angle between two planets (or one planet and the sun or moon) determines a locus in space called a navoid which has the form of an arc of a circle rotated about its chord. Observing and timing an occultation of a known star by the moon (or a planet) establishes a cylindrical locus. By measuring the angle subtended by a planet (or moon) disk, a positional locus in the form of a spherical shell provides range or altitude usable within a few diameters of the planet. A good approximation to the local vertical is also provided by aligning an optical axis on the center of the disk.

Proposed Solution

The present state of the art for obtaining positional fix measurements on a lunar mission might require an earth horizon tracker, a moon tracker, two or more star trackers, and a sun seeker. The extended source nature of the moon and earth (or planet), especially when viewed at a range of a few diameters, requires the use of a continuous mechanical scan technique for horizon tracking, which is, from reliability considerations, undesirable for long duration use in space. Two or more sets of gimbals, with drive mechanisms and angle readout transducers, are required to provide relative motion between earth tracker, moon tracker, and star trackers; and between star trackers, if other than preselected stars at fixed angles are to be tracked.

The problem of obtaining these measurements is greatly simplified and accuracy is increased through the use of the advanced optical-inertial space sextant.[2] A space sextant is any instrument capable of making measurements of the orientation of celestial bodies relative to some reference. This advanced instrumentation concept eliminates the multiple telescopes and duplicated gimbals and angle transducers for a single integrated optical system combined with an inertial reference system and mounted on a single gimbal system. This basic configuration is shown in Fig. 1. The two gyros, operated with their spin axes mutually orthogonal, are mounted with the tracker optics on a common gimbaled platform. Two precision two-

---

H. E. Brunelle, Jr., is with the Armament and Control Products Section, Light Military Electronics Department, General Electric Company, Johnson City, New York. R. R. Willey, Jr., is with Willey Optical Research Lab and Development Service, Farmington, Connecticut, now a division of the Instrument Corporation of Florida, Melbourne, Florida.

Received 1 May 1963.

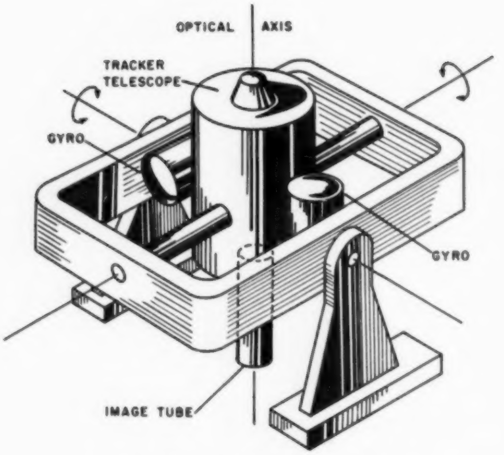

Fig. 1. Optical-inertial space sextant.

degree-of-freedom free rotor gyros, body-bound to the telescope, provide basic three-axis inertial reference during the sighting operation. The single telescope performs the desired sightings in sequence. For each sighting, alignment of the optical axis, relative to the inertial reference, is read directly by the precision gyro pickoff. The need for precision gimbaling and high-gain gimbal drives precisely to track and null targets is eliminated through the use of a high-resolution image tube. The tube electronically scans and resolves angular offsets between the optical boresight axis and the line of sight to a target at any point in the optical field of view imaged on its photoactive surface. An extremely wide field-of-view optical mode images extended disks for stadiametric ranging and local vertical determination, while a narrow field-of-view optical mode consistent with the image tube resolution capabilities is used for precise sightings on point sources.

Wide-Field Optics

The requirements of the wide-field system for planetary horizon tracking are appreciably different from those for which conventional extreme wide-angle lenses are developed. Typically, for these lenses, the center of the field of view is presented with little or no radial distortion in the central two-thirds of the image plane. Radial compression in the image is present at an ever-increasing degree for objects whose position in the field of view moves farther off-axis. It is obvious that, with these lenses, the region of interest to the horizon tracker is nonlinearly compressed into a narrow band at the periphery of the image while the bulk of the planetary disk dominates the center of the image.

Since the wide-field system will be used chiefly to look at planetary disks at close distances, it is optimized for large subtended angles up to 165° between horizons. It is desirable to provide a system which will exclude light from an area of no interest by obscuring a central 50° cone in the field of view, and, at the same time, to displace the image field radially inward toward the optical center so that a maximum of the central image area is used.

It is also desirable to reverse the image field boundaries so that the outer edge of the field $82^{1}/_{2}°$ off-axis will be near the center of the image, and the central boundary 25° off-axis will appear at the outer edge of the image. The "inside-out" field images the horizon of a planetary disk near the center of the image plane as the horizon subtends a larger angle. Since the central region of the photoactive surface of an image tube provides better resolution than the edges, the horizon can be more accurately determined in approach situations where resolution of stadiametric altitude and local vertical are critical.

Distortion is expected in the wide-field optical system. For accurate horizon location distortion must be axially symmetrical. The system is optimized at the tangential focus to minimize sagittal image smear so that a sharp horizon line can be obtained. Tangential smear is permissible if it is concentric about the axis, otherwise a sharp horizon line cannot be obtained.

The basic system chosen to satisfy the wide-field requirements consists primarily of a toroidal element which resembles the bell of a horn. Figure 2 shows the wide-field system schematically. The horn element serves almost exclusively as a device to produce the desired "inside-out" field distortion and appropriate angular expansion of the annular field. Modifications had to be made in the usual ray tracing equations in order to investigate this unusual horn surface.

The heavy inherent astigmatism of the horn element is rendered relatively harmless in the present application by making its scale large with respect to the aperture of the beam impinging upon it. The resolution of the wide-field system at $f/8$ closely matches the resolution of the image tube. The image is not only inside-out as in the device described by Killpatrick[3] for a similar application, but it is also stigmatic as Fig. 3 shows. There is point to point imaging of the object plane onto the image plane.

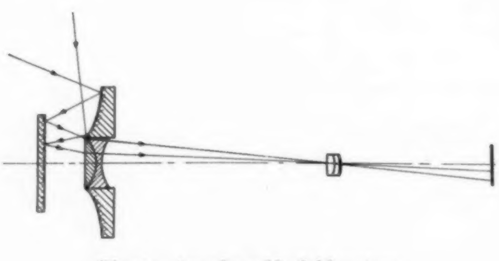

Fig. 2. Annular wide-field system.

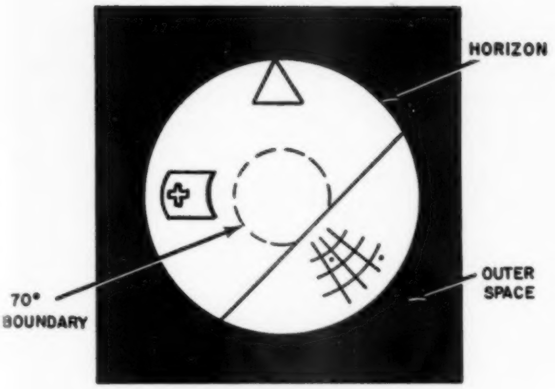

FIELD OF VIEW

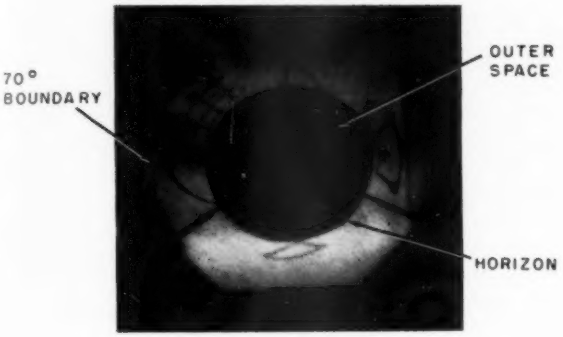

IMAGE

Fig. 3. Space sextant monitor display of field of view as seen by image tube through the wide-field system.

Narrow-Field Optics

Functionally the narrow-field system field of view is dictated by the usable diameter of the photoactive surface of the image tube and the number of elements or lines which can be resolved in this diameter. If, for example, an angular resolution of 1 sec of arc is desired, the field of view imaged on the photoactive surface of the image tube must not subtend more seconds of arc than the number of resolvable lines. The aperture real diameter must also be large enough so that the limit of angular resolution imposed by diffraction is less than that imposed by the image tube resolution. For a selected image tube and brightness of the dimmest star of interest, an effective aperture of the system necessary to give a desired signal/noise ratio can be determined.

Consideration of the space sextant application requirements emphasizes the desirability of the shortest folded system functionally practical. The short tube length reduces the weight of the structure necessary to ensure maintenance of proper optical alignment and adjustment; allows the use of a lighter, more compact gimbal; and reduces the size of any enclosure within which the sextant must be articulated.

The general class of system usually considered for a short telescope application is the Cassegrain telescope. Since the clear aperture and focal length are predetermined by the application and image tube characteristics, the problem is to design the shortest system which is consistent with the image quality requirements, and that can be produced to the necessary accuracy with a finite amount of effort.

The true Cassegrain[4] with parabolic primary mirror and hyperbolic secondary mirror has inherent coma to a degree which cannot be tolerated in this application. The Ritchey–Chretien modified form of Cassegrain corrects for coma by a different aspheric figuring of the mirrors. Astigmatism is still uncorrected and is the limiting aberration. The Schmidt–Cassegrain and Maksutov–Cassegrain forms offer advantages over the Ritchey–Chretien form in that the stop position and aspheric figuring are moved toward the center of curvature of the primary mirror, and the corrector can be used to support the secondary mirror. The Schmidt–Cassegrain form was chosen for this application because the corrector plate is less massive and occupies less space than the Maksutov corrector.

Since, to achieve compactness, the corrector plate of the Schmidt–Cassegrain is at a distance from the center of curvature of the primary mirror, astigmatism is not fully eliminated. The system is shortened until the residual astigmatism brings the image size up to the maximum tolerable amount as defined by the image tube characteristics. Although the Petzval sum is approximately zero, the residual astigmatism causes the field to be curved, and a field flattener is introduced adjacent to the focal plane. The resulting design has a spherical primary mirror, and aspheric corrector plate and secondary mirror.

The design of this system was carried out entirely (except for slide-rule calculations) on an IBM 7090 computer and much of the optimization was done by a semiautomatic lens design program.

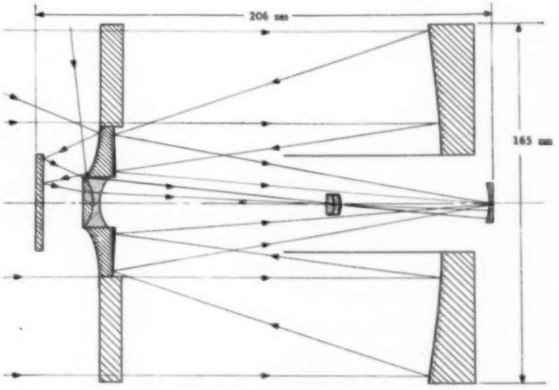

Fig. 4. Combined optical system.

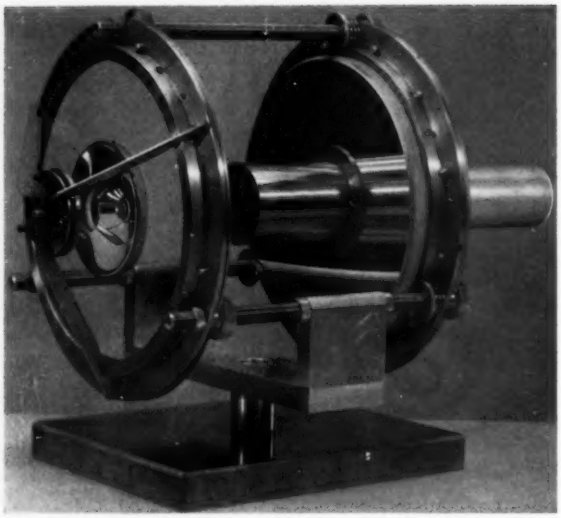

Fig. 5. Dual-field star tracker with image tube shield.

The lens optimization program was very useful in finding the best division of asphericity between the corrector and the secondary mirror of the Schmidt–Cassegrain. Although this is a relatively simple problem, the optimization program further reduced its difficulty. The eccentricity of the secondary mirror (conic section figuring) was allowed to vary while the corrector was figured to maintain axial stigmatism. Heaviest weighting was placed on obtaining the smallest possible images at the edge of the field. Although the only aberration appreciably controlled by this process was coma, the optimal solution was not the exact elimination of coma, but a balance between a small amount of coma and the residual astigmatism of the system. The Schmidt–Cassegrain was then shortened until the optimized system gave images at the edge of the field that just matched the tolerances. The optimization of the division figuring in any one case, would typically take from 1 to 2 min of computer time because of the extensive number of rays examined (45).

Combined Optical Systems

The problems of gimbaling the optical axes of the wide- and narrow-field systems in a space sextant application emphasize the desirability of coaxial combination and mechanical symmetry. Any fixed astrodome or window traversed by rays incoming to the systems should present a symmetrical and invariant aspect relative to the optical axes of the system, for any orientation permitted by the gimbal system. In a Cassegrain system the central zone of the aperture is blocked by the secondary mirror whose center, in turn, sees only its own shadow in the center of the primary. The wide-field system is arranged to occupy this vacant core with its aperture located just in front of the correcting plate, as shown in Fig. 4. With the two systems coaxial and the intersection of the gimbal motion axes located on this common optical centerline close to the plane of the rear surface of the corrector plate, the effect of an astrodome whose center of curvature also coincides with this common center will be symmetrical; and the optical axis will be normal to its surfaces in any gimbaled position.

An optical relay is provided to transfer the image, formed by the short focus wide-field system, to the image tube photoactive surface which is coincident with the narrow-field system focal plane.

Mode selection is accomplished by alternate insertion of masks in a plane just behind the optical relay where the ray bundle from the narrow-field aperture is small but still separate from the wide-field ray bundle passing through the relay lens. No optical elements are moved in a changeover. Thus, the danger of loss of alignment or adjustments is eliminated, and the masks located near the image plane are small and low in mass.

Performance

To verify the performance predicted for the system as a result of the optimization programs on the computer, a set of optical elements were constructed and assembled in a mount of laboratory breadboard construction. The dual-field star tracker with image tube shield is shown in Fig. 5 and has the following characteristics:

Narrow-Field System

Type	Schmidt–Cassegrain
Field of view	2°
Clear aperture	165-mm (6.25-in.) diam
Effective aperture	143-mm (5.62-in.) diam (equivalent)
Focal length	437 mm (17.2 in.)
Image plane	15.25-mm (0.6-in.) diam

Wide-Field System

Type	Annular field, "inside out"
Field of view	Solid angle included between two concentric cones with apex angles of 70° and 165°
f/number	f/8 average
Image plane	15.25-mm (0.6-in.) diam

Tests were conducted on the wide-field system to demonstrate the inside-out, point-to-point mapping of the annular toric reflector (Fig. 3). A plot of the angle transfer from object space to the image plane also demonstrated a very close-to-linear relationship.

It was expected that the nature of the toric reflector might result in an appreciable change in both focal length and effective aperture as a function of off-axis angular position. Measurements to determine this variation in terms of f/number ratio showed the system to have an average value of $f/8$ with a variation of less than $0.5f$ stop between points anywhere in the field of view.

The resolution of a point source onto the image plane was found to have a radial width of 0.025 mm and a tangential length of approximately 0.125 mm. This held true for any off-axis position within the field of view.

Tests were conducted to establish the linearity of the narrow-field system. Angular position in the field of view was determined to within 2 arc-sec, and the image position was measured to within 0.013 mm. Within the accuracy of the measurements, the system was linear which indicates a linearity of better than 0.1% full field. The image of a point source was less than 0.025 mm in diameter and of high quality throughout the field, showing only a trace of astigmatism at the extreme field edges.

The design and fabrication of the optical elements of the dual-field star tracker telescope was performed by the Willey Optical Research Lab and Development Service, Farmington, Connecticut, for the Armament and Control Products Section of the Light Military Electronics Department, General Electric Company, Johnson City, New York. Mounting, integration with the electron optics, and performance testing and evaluation were performed by Advance Engineering of the Armament and Control Products Section.

The automatic lens design program was developed by R. R. Willey, Jr., while at the Research Laboratories of United Aircraft Corporation. Continuation of the work reported in this paper is now being carried out under a National Aeronautics and Space Administration contract.

References

1. H. B. Haake and J. D. Welch, IRE Trans. Aerospace Navigational Electron. **ANE 8,** 28 (1961).
2. J. D. Welch, "Advanced Optical-Inertial Space Navigation System", paper presented at AIAA, Summer Meeting, 17 June 1963.
3. J. Killpatrick, Appl. Opt. **1,** 147 (1962).
4. R. R. Willey, Jr., Sky and Telescope **23,** 191 (1962).

Applied Optics Patents

Reviewing panel C. Shepard (Chairman) *Rochester*
R. Anwyl *Rochester*
J. J. Ball *National Bureau of Standards*
G. W. Cleek *National Bureau of Standards*
A. Danti *Texas A & M*
J. Fitzmaurice *Baird-Atomic*
F. F. Hall, Jr. *ITT Federal Labs*
R. S. Hunter *Hunter Assocs*
W. L. Hyde *University of Rochester*
S. F. Jacobs *TRG*
R. Kingslake *Eastman Kodak*
D. J. Lovell *University of Michigan*
D. L. MacAdam *Eastman Kodak*
A. Mann *Spectrolab*
T. K. McCubbin *Penn State University*
R. K. McDonald *Boeing*
J. R. Meyer-Arendt *NBS–Boulder*
G. W. Stroke *University of Michigan*
D. E. Williamson *Cordis*

The patents reviewed below have been issued by the U.S. Patent Office on the dates quoted except where otherwise mentioned. The patent number, date of issuance, and classification number are quoted in the first line. The filing date is that of the earliest patent application. The opinions stated in the reviews are those of the reviewers and are not meant to express the thinking either of the organizations with which members of the panel are associated, of the Optical Society of America, or of this journal. Normally, statements of fact are based upon the patents and not independently verified. Printed copies of American patents may be ordered from the Commissioner of Patents, Washington 25, D.C., for 25¢ each. A weekly subscription service to any selected subclass is also available from the Patent Office.

3,021,751 20 Feb. 1962 (Cl. 88-20)
Tachistoscopes.
G. C. BARNETTE. Assigned to Learning Through Seeing, Inc. Filed 26 May 1960.

Mechanical and electrical details of a projection tachistoscope to test reading ability are given. W.L.H.

3,021,754 20 Feb. 1962 (Cl. 88-61)
Light-polarizing apparatus or the like.
B. ROSS. Assigned to Hoffman Electronics Corporation. Filed 26 Sept. 1956.

The light reflected from a semiconductor at oblique incidence is polarized, and Ross points out that the polarization can be varied by injecting free carriers electrically or optically into the material. No quantitative results are given. W.L.H.

3,038,368 12 June 1962 (Cl. 88-1)
Co-ordinate theodolite.
L. FIALOVSZKY. Assigned to Gamma Optikai Muvek. Filed 8 Sept. 1959 (in Hungary 10 Sept. 1958).

A mechanical and optical arrangement is described that provides simple and direct data reduction when surveying by traversing. W.L.H.

3,039,356 19 June 1962 (Cl. 88-15)
Kaleidoscopes.
R. E. KNITTEL. Filed 4 Nov. 1959.

New and exotic kaleidoscopes complete with flowing liquids are revealed. W.L.H.

3,041,922 3 July 1962 (Cl. 88-14)
Optical device for a correct adjustment and reading of the slidable displacement of a carriage in a machine.
K. RANTSCH. Assigned to M. Hensoldt und Söhne Optische Werke, A. G. Filed 5 Mar. 1959 (in Germany 8 Mar. 1958).

This is a complex patent with 33 drawings showing optical systems that allow a tool to be positioned accurately on inaccurate ways. The position of the tool (or the work) is observed with reference to an accurate grid, and the optical systems are devised so that linear and angular errors in the optical train do not introduce reading errors. W.L.H.

3,041,923 3 July 1962 (Cl. 88-14)
Stress photometer.
F. T. GEYLING. Assigned to Bell Telephone Laboratories, Inc. Filed 14 Dec. 1959.

Describes a means for scanning photoelastic stress patterns along circular contours and measuring light intensity values therein to facilitate gathering of data from a photoelastic model under stress. The data so obtained are particularly suited to a new mathematical method of stress calculation developed for its compatibility with modern high-speed digital computers. R.D.A.

3,042,805 3 July 1962 (Cl. 250-207)
Light measuring apparatus.
S. L. BOERSMA. Assigned to N. V. Optische Industrie de Oude Delft. Filed 18 Apr. 1960 (in Netherlands 22 Apr. 1959).

A light-measuring device is described particularly suited to low illuminations encountered in x-ray photofluorography, wherein a photoelectric cell circuit is automatically standardized during brief periods (less than 0.1 sec) using a reference light source. This procedure yields a capacitor charged to a reference voltage which, in turn, permits accurate measurement of the fluorescent screen brightness and, hence, accurate determination of proper exposure. The system overcomes typically high variations in sensitivity of photomultiplier tubes and photoconductive cells. R.D.A.

3,044,349 17 July 1962 (Cl. 88-22.5)
Optical pyrometer apparatus.
D. L. Watrous. Assigned to General Electric Company. Filed 28 Dec. 1959 (Div. of Application 26 Feb. 1957).

A high-temperature pyrometer is described having great sensitivity, speed of operation, and accuracy which determines temperature by using a null-balancing principle for measuring the color temperature of a heated object. The device is insensitive to errors caused by changes in source emittance or absorption of the radiated energy. A flexible quartz rod transmits the radiation to a sensitive detector alternately through two narrow-bandpass filters, one of which is effectively an optical wedge. R.D.A.

3,046,830 31 July 1962 (Cl. 88-27)
Optical navigational device.
M. R. Pierce and J. S. Fassero. Filed 17 June 1958.

An optical and mechanical scheme for a navigational device is described in considerable detail that allows the coordinates of two stars to be determined simultaneously and two lines of position to be plotted directly on a Universal Plotting Sheet. The device would be useful for celestial navigation of an airplane by the pilot. W.L.H.

3,046,837 31 July 1962 (Cl. 88-40)
Condenser for increasing the resolving power of microscopes.
J. Barabas, L. Zselyonka, F. Kiss, and A. Libik. Filed 12 Jan. 1959 (in Hungary 22 May 1958).

A complicated condenser is described that allows the simultaneous use of dark-field, bright-field, and oblique illumination of the specimen. When properly adjusted, a distinct appearance of relief is given to the specimen. The instrument is now manufactured in Hungary and is available in the U.S.A. from National Instruments Lab., Washington, D. C. A paper in English describing the condenser and showing the results has been published in *Mikroskopie* 15, 3 (1961). W.L.H.

3,049,966 21 Aug. 1962 (Cl. 88-24)
Two-stage photogrammetric rectifier.
H. E. R. Gruner. Assigned to Bausch & Lomb, Inc. Filed 17 Apr. 1961.

A photogrammetric rectifier comprising a photographic projector, a first-stage easel, and a second projection lens which relays the first image to a second-stage easel of film holder permits two successive rectifying steps without an intermediate transparency. A unique illumination system provides substantially uniform exposure by programed brightness control of a long narrow lamp as it traverses the projector gate. Single-stage rectifications also benefit from the improved means for achieving uniform exposure. R.D.A.

3,049,972 21 Aug. 1962 (Cl. 88-33)
Binocular with improved system of optical adjustment.
T. Malinowski. Assigned to Ernest Leitz Canada Ltd. Filed 19 Apr. 1961.

A mechanical arrangement for simplifying the alignment of prism binoculars is described. W.L.H.

3,051,043 28 Aug. 1962 (Cl. 88-24)
Projection system.
G. V. Miller. Filed 31 Aug. 1959.

An improvement of illumination on a rectangular screen by decentering and tilting lenses in the condenser is described. W.L.H.

3,053,134 11 Sept. 1962 (Cl. 88-1)
Optical pulse echo system.
B. G. Bjornson. Assigned to Bell Telephone Laboratories. Filed 1 Apr. 1948.

The light sources for optical ranging systems usually generate exponentially decaying pulses with the result that the strong returns from nearby targets appear longer than those from distant targets. This invention equalizes the return-pulse shapes by applying a varying bias voltage across the photomultiplier detector. In addition a means for synchronizing the pulse indicator with pulse transmissions is described. R.K.M.

3,053,147 11 Sept. 1962 (Cl. 88-65)
Circular light polarizer.
E. R. Blout. Assigned to Polaroid Corp. Filed 16 Nov. 1959.

Linear polarizers can be made by dyeing a suitably oriented polymer; circular polarizers can be made by dyeing macromolecules with helical form, if a method can be found to orient the helices properly. This patent describes suitable macromolecules, particularly polypeptides, suitable dyes, and methods of orientation to give high circular dichroism. W.L.H.

3,053,984 11 Sept. 1962 (Cl. 250-203)
Star tracking system.
H. R. Hulett. Assigned to Hughes Aircraft Co. Filed 5 Jan. 1951.

A scheme is claimed for a star tracker using a "fan-bladed" chopper rotating at high speed in the focal plane, and a deviation wedge rotating slowly in the aperture. When the star is on axis, the wedge nutates its image slowly around the outer edge of the openings in the chopper, and a steady signal is given. When the star moves off-axis, it misses the openings in the chopper during part of the rotation cycle of the wedge, and the signal is modulated to show the direction of the pointing error. The signal can be proportional to the angular error over only a small zone comparable with the blur of the star image. W.L.H.

3,054,323 18 Sept. 1962 (Cl. 88-14)
Automatic optical measuring instrument.
D. E. Davidson. Assigned to Davidson Optronics, Inc. Filed 5 Jan. 1959.

An autocollimator particularly suited to aligning distant mirrors is rendered capable of continuous automatic operation by electronic detection of the reflected light emanating originally from two fluorescent lamps which are disposed parallel to each other and in near alignment, and transverse to the axis of mirror rotation. The lamps are energized out of phase to permit detection of the direction of deviation. Simultaneous visual observation is provided for. R.D.A.

3,054,898 18 Sept. 1962 (Cl. 250-83.3)
Infrared ranging system.
T. A. Westover and B. Rossett. Assigned to Servo Corp. of America. Filed 14 Mar. 1960.

A passive infrared ranging device is presented which basically depends on the shift of the systems focal-point with target range. The deviation is measured with the aid of two detectors and two prisms, the latter positioned side-by-side with apexes touching at a point between a common collecting lens and the focal point. A mechanical drive moves the prisms along the optic axis. Each detector collects energy through a different prism. Their outputs with prism displacement can be equated with target range. R.K.M.

3,055,259 25 Sept. 1962 (Cl. 88-14)
Optical measuring devices.
C. F. Dietrich. Assigned to Optical Measuring Tools Limited. Filed 3 Mar. 1958.

Describes a refined optical depth-measuring device wherein two marginal beams, limited by a Hartman diaphragm or equivalent means, are directed through a microscope having an objective with very long working distance. Substantial improvement in accuracy over a conventional microscope system using an objective of short focal length and high numerical aperture is claimed. The system is also applicable to determination of lens focal lengths. R.D.A.

3,058,389 16 Oct. 1962 (Cl. 88-23)
Photometers
R. D. Morrow. Assigned to Morrow Products, Inc. Filed 5 July 1955.

A simple, compact, relative intensity photometer, intended particularly for determining photographic exposure, comprising a diffuse field illuminated by scene light and a comparison field illuminated by a small standard light source, wherein both fields are rendered monochromatic through filtering, is described. The embodiments shown would appear to require substantial modification to provide the accuracy available in many inexpensive exposure meters or cameras incorporating automatic exposure control devices. R.D.A.

3,058,393 16 Oct. 1962 (Cl. 88-65)
Light-polarizing film material and the process of preparation.
W. H. Ryan and L. C. Farney. Assigned to Polaroid Corp. Filed 27 Mar. 1958.

A multilayer polarizing film suitable for stereoscopic pictures is described. W.L.H.

3,059,524 23 Oct. 1962 (Cl. 88-14)
Method and apparatus for the continuous colorimetric determination of the individual components of a mixture.
W. Grassmann and K. Hannig. Filed 2 June 1959 (in Germany 4 June 1958).

An accessory for use with any photocell or thermocouple-colorimeter consists of a filter disk which rotates different filters successively into the light beam, and a strip recorder. The filters are changeable so that the reading through each indicates predominately the concentration of only one of the known components of the mixture. Another element of the invention is a chromatographic sampling device for continuous dilution and buffering of dyeing solution, held at constant (100°C) temperature. D.L.M.

continued on page 1316

Analysis and Design of Plane-Mirror Systems

R. J. Pegis and M. M. Rao

A procedure is given for the analysis of systems of plane mirrors by matrix multiplication. The method suggests a design procedure which is illustrated by the unified synthesis of the Wollaston and pentaprisms.

Introduction

The first application of fourth-order matrices to plane-mirror problems appears to have been made by Smith.[1,2] At that time the relative merits of algebraic and trigonometric methods were very much in dispute, the strongest supporter of the trigonometric methods being Baker.[3] Smith's comments on p. 95 of the discussion following ref. 2 are well worth noting. More recently, Rosendahl[4] has come close to the matrix method by his use of quaternions in plane-mirror optics. The present work was occasioned by a course taught by one of the authors at the University of Rochester and thesis material presented by the other. The data for the examples are taken from Hopkins.[5]

Theory

Let (l,m,n) be the direction cosines of the normal to a plane whose perpendicular distance from the origin in a system of Cartesian coordinates is p. Then the equation of this plane is

$$lx + my + nz = p. \tag{1}$$

Let (x,y,z) be any point, and consider the problem of finding its image (x',y',z') when the plane is regarded as a mirror. The calculation of (x',y',z') has been shown by Smith[1] to take the simple matrix form

$$(x,y,z,1)\begin{pmatrix} 1-2l^2 & -2lm & -2ln & 0 \\ -2lm & 1-2m^2 & -2mn & 0 \\ -2ln & -2mn & 1-2n^2 & 0 \\ 2lp & 2mp & 2np & 1 \end{pmatrix} = (x',y',z',1)$$

which for convenience we abbreviate to

$$(x,y,z,1)(R) = (x',y',z',1). \tag{2}$$

If we have N mirrors instead of one we simply subscript the quantities l,m,n,p,R by defining reflection matrices

$$(R_j) = \begin{pmatrix} 1-2l_j^2 & -2l_jm_j & -2l_jn_j & 0 \\ -2l_jm_j & 1-2m_j^2 & -2m_jn_j & 0 \\ -2l_jn_j & -2m_jn_j & 1-2n_j^2 & 0 \\ 2l_jp_j & 2m_jp_j & 2n_jp_j & 1 \end{pmatrix}. \tag{3}$$

The calculation of the image point then proceeds by ordinary matrix multiplication and may be written

$$(x,y,z,1)(R_1)(R_2)\ldots(R_N) = (x',y',z',1). \tag{4}$$

We denote by (R) or $(R_{1,N})$ the product of the N reflection matrices

$$(R) = (R_1)(R_2)\ldots(R_N) \tag{5}$$

From the form of the matrices (R_j) it is easy to see that $(R_{1,N})$ always takes the form

$$(R_{1,N}) = \begin{pmatrix} a & d & g & 0 \\ b & e & h & 0 \\ c & f & j & 0 \\ \xi' & \eta' & \zeta' & 1 \end{pmatrix}, \tag{6}$$

where (ξ',η',ζ') is the image of the origin after reflections $1,2,\ldots N$. The quantities $a\ldots j$ have the added significance that if the direction cosines of the incident ray are (L,M,N) and those of the emergent ray are (L',M',N') then the transformation of these quantities by the system is

$$(L,M,N)\begin{pmatrix} a & d & g \\ b & e & h \\ c & f & j \end{pmatrix} = (L',M',N'). \tag{7}$$

It is helpful to define (r) to be the (R) matrix with its last row and column removed,

$$(r) = \begin{pmatrix} a & d & g \\ b & e & h \\ c & f & j \end{pmatrix}.$$

In like manner we may define a reverse reflection matrix

$$(R_{N,1}) = (R_N)(R_{N-1})\ldots(R_1)$$

R. J. Pegis is at Saint John Fisher College, Rochester, New York. M. M. Rao's present address is Madras Institute of Technology, Chromepet, India. He was formerly with Bausch & Lomb, Inc.

Received 1 August 1963.

and show that it will be

$$(R_{N,1}) = \begin{pmatrix} a & b & c & 0 \\ d & e & f & 0 \\ g & h & j & 0 \\ \xi & \eta & \zeta & 1 \end{pmatrix},$$

where (ξ,η,ζ) is the image of the origin after reflections $N, N-1, \ldots 1$.

Several important properties of the R matrices follow. By way of notation, (I) represents the unit matrix and vertical bars about a matrix, e.g., $|R|$ denotes the determinant of the matrix. Then

$$(R_j)(R_j) = (I), \tag{8a}$$

$$(R_{1,N})(R_{N,1}) = (I), \tag{8b}$$

$$|R_j| = -1, \tag{8c}$$

$$|R_{1,N}| = (-1)^N. \tag{8d}$$

The matrix (R), while extremely useful for the analysis of mirror systems, is of limited use in synthesis, since for more than one mirror the relations among $a,b, \ldots j$ are not obvious. Accordingly, Smith has used a second type of component and system matrix, called an S matrix, in an attempt to reduce the number of parameters requiring specification. The observation which makes the S matrix possible is that the reflection matrix (R_j) is the square of the matrix

$$\begin{pmatrix} 0 & in & -im & il \\ -in & 0 & il & im \\ im & -il & 0 & in \\ il & im & in & 0 \end{pmatrix},$$

where i is the imaginary square root of -1, as may be verified by direct matrix multiplication. In spite of the imaginaries, this matrix is far more convenient than (R_j), since it has but three distinct entries (apart from sign). However, it has the disadvantage of being *almost* antisymmetric, and it is far more convenient to change the sign of the last column and define

$$(S_j) = \begin{pmatrix} 0 & in & -im & -il \\ -in & 0 & il & -im \\ im & -il & 0 & -in \\ il & im & in & 0 \end{pmatrix}. \tag{9}$$

It is easy to see that the product of any number of matrices of the form (S_j) is always of the form

$$\begin{pmatrix} \kappa & \nu & -\mu & -\lambda \\ -\nu & \kappa & \lambda & -\mu \\ \mu & -\lambda & \kappa & -\nu \\ \lambda & \mu & \nu & \kappa \end{pmatrix},$$

so that even for a large system the S matrix has but four distinct elements. These elements will moreover always obey the relation

$$\kappa^2 + \lambda^2 + \mu^2 + \nu^2 = (-1)^N, \tag{10}$$

where N is the number of reflections. The relation between the component matrices (S_j) and the S matrix for the whole system is the same as that between the (R_j) and $(R_{1,N})$:

$$(S_{1,N}) = (S_1)(S_2) \ldots (S_N). \tag{11}$$

When the sign of the last column of $(S_{1,N})$ is changed and the matrix squared, the result gives the first three rows of $(R_{1,N})$. In fact

$$\begin{pmatrix} \kappa & \nu & -\mu & \lambda \\ -\nu & \kappa & \lambda & \mu \\ \mu & -\lambda & \kappa & \nu \\ \lambda & \mu & \nu & -\kappa \end{pmatrix}^2 = \begin{pmatrix} a & d & g & 0 \\ b & e & h & 0 \\ c & f & j & 0 \\ 0 & 0 & 0 & (-1)^N \end{pmatrix}. \tag{12}$$

The reverse calculation is equally simple. When (r) is symmetric it is easy to see that $\kappa = 0$ or $\lambda = \mu = \nu = 0$ and that the derivation of κ,λ,μ,ν by direct substitution in (12) is straightforward. In all other cases it is more convenient to use Smith's formulas[1]

$$\frac{1}{4\kappa} = \frac{\kappa}{a+e+j+|r|} = \frac{\lambda}{h-f} = \frac{\mu}{c-g} = \frac{\nu}{d-b}. \tag{13}$$

The utility of the R matrices will be demonstrated in an application to mirror system analysis, and that of the S matrices in an application to design.

Sample Calculations

As a first example of the application of the theory to practical matters we consider the reversion prism of Fig. 1. This prism inverts (or reverts) the image, leaving the line of sight undeviated. The number of reflections is three, and the mirror constants are given in Table I. The corresponding R matrices are

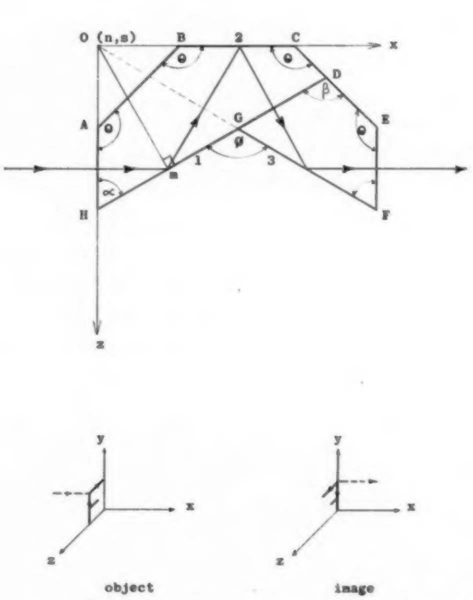

Fig. 1. Reversion prism: $OA = OB = 1$, $AB = BC = CE = 1.4142$, $CD = 0.5176$, $GF = HG = 2$, $\alpha = 60°$, $\beta = 105°$, $\theta = 135°$, $\phi = 120°$, $Om = p_1 = \sqrt{3}$, $On = p_2 = 0$, $Os = p_3 = 0$.

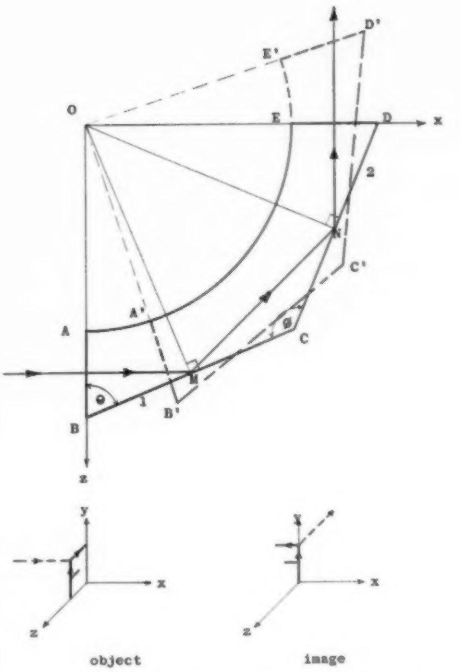

Fig. 2. Wollaston prism: $OA = 2.4142 = OE$, $BC = 2.6131 = CD$, $AB = ED = 1$, $OM = p_1 = 3.1544$, $ON = p_2, = 3.1544$, $\theta = 67° 30'$, $\phi = 135°$.

Table I. Mirror Constants of Reversion Prism

Surface	l	m	n	p
1	$^1/_2$	0	$^1/_2\sqrt{3}$	$\sqrt{3}$
2	0	0	1	0
3	$-^1/_2$	0	$^1/_2\sqrt{3}$	0

$$(R_1) = \begin{pmatrix} ^1/_2 & 0 & -^1/_2\sqrt{3} & 0 \\ 0 & 1 & 0 & 0 \\ -^1/_2\sqrt{3} & 0 & -^1/_2 & 0 \\ \sqrt{3} & 0 & 3 & 1 \end{pmatrix},$$

$$(R_2) = \begin{pmatrix} 1 & 0 & 0 & 0 \\ 0 & 1 & 0 & 0 \\ 0 & 0 & -1 & 0 \\ 0 & 0 & 0 & 1 \end{pmatrix},$$

$$(R_3) = \begin{pmatrix} ^1/_2 & 0 & ^1/_2\sqrt{3} & 0 \\ 0 & 1 & 0 & 0 \\ ^1/_2\sqrt{3} & 0 & -^1/_2 & 0 \\ 0 & 0 & 0 & 1 \end{pmatrix},$$

and their product is

$$(R_{1,3}) = \begin{pmatrix} 1 & 0 & 0 & 0 \\ 0 & 1 & 0 & 0 \\ 0 & 0 & -1 & 0 \\ -\sqrt{3} & 0 & 3 & 1 \end{pmatrix},$$

showing that an inversion of the z axis has taken place, while the x and y axes have been undisturbed. Having $(R_{1,3})$ we could now compute at once the image of any point (x,y,z) by means of (2).

As a second example we consider the problem of designing a prism to deviate the line of sight through 90° while neither inverting nor reverting the image. It should, however, be pointed out at the start that the example is only intended to illustrate the method, and that specific elementary solutions to this problem are very simple to find. We shall show that the analysis via the S matrix leads to solutions in both the Wollaston and pentaprism forms.

Consider a rectangular and right-handed system of coordinates and assume that the line of sight enters the system in the direction of the positive x axis and leaves in the direction of the negative z axis. The direction parallel to the y axis is undeviated and the negative z direction is deviated into the negative x direction.

From the relation

$$(L,M,N)(r) = (L',M',N'),$$

we have the equations

$$\begin{aligned} aL + bM + cN &= L', \\ dL + eM + fN &= M', \\ gL + hM + jN &= N'. \end{aligned}$$

From the fact that the number triplets (1,0,0), (0,0,−1), (0,1,0), respectively, for (L,M,N) are deviated into (0,0,−1), (−1,0,0), (0,1,0), respectively, for (L',M',N') we are able to solve for (r), obtaining

$$(r) = \begin{pmatrix} a & d & g \\ b & e & h \\ c & f & j \end{pmatrix} = \begin{pmatrix} 0 & 0 & -1 \\ 0 & 1 & 0 \\ 1 & 0 & 0 \end{pmatrix}.$$

From (13) we find for the components of the S matrix the values

$$\kappa = \pm 1/\sqrt{2},\ \lambda = 0,\ \mu = \pm 1/\sqrt{2},\ \nu = 0,$$

where in the choice of signs κ and μ must agree. We therefore have two sets of characteristic constants which correspond to the same r matrix, and this suggests that there are two optical systems to do the same transformation. The two S matrices are given below.

Case I.

$$(\kappa,\lambda,\mu,\nu) = (1/\sqrt{2},0,1/\sqrt{2},0)$$

$$(S) = \begin{pmatrix} 1/\sqrt{2} & 0 & -1/\sqrt{2} & 0 \\ 0 & 1/\sqrt{2} & 0 & -1/\sqrt{2} \\ 1/\sqrt{2} & 0 & 1/\sqrt{2} & 0 \\ 0 & 1/\sqrt{2} & 0 & 1/\sqrt{2} \end{pmatrix}.$$

Case II.

$$(\kappa,\lambda,\mu,\nu) = (-1/\sqrt{2},0,-1/\sqrt{2},0)$$

$$(S) = \begin{pmatrix} -1/\sqrt{2} & 0 & 1/\sqrt{2} & 0 \\ 0 & -1/\sqrt{2} & 0 & 1/\sqrt{2} \\ -1/\sqrt{2} & 0 & -1/\sqrt{2} & 0 \\ 0 & -1/\sqrt{2} & 0 & -1/\sqrt{2} \end{pmatrix}.$$

In both cases we may solve for the directions of the reflecting surface normals. The fact that the system under consideration has neither to invert nor to revert

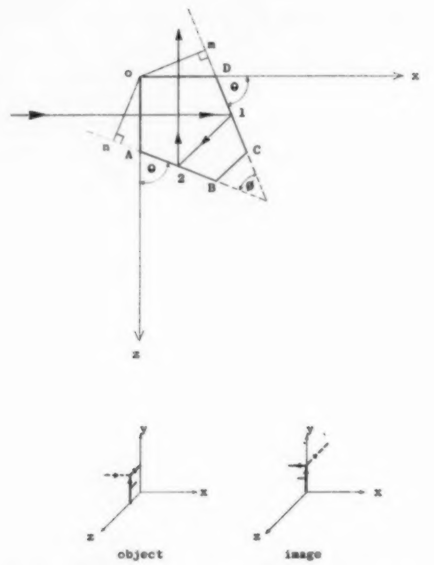

Fig. 3. Pentaprism: $oA = oD = 1$, $AB = CD = 1.0824$, $om = p_1 = 0.9239$, $on = p_2 = 0.9239$, $\theta = 67°\,30'$, $\phi = 45°$.

the image requires that the number of surfaces be even. Suppose two surfaces are considered, with normal direction numbers (l_1,m_1,n_1) and (l_2,m_2,n_2), respectively. Then the matrix equation for the design is

$$\begin{pmatrix} 0 & in_1 & -im_1 & -il_1 \\ -in_1 & 0 & il_1 & -im_1 \\ im_1 & -il_1 & 0 & -in_1 \\ il_1 & im_1 & in_1 & 0 \end{pmatrix} \begin{pmatrix} 0 & in_2 & -im_2 & -il_2 \\ -in_2 & 0 & il_2 & -im_2 \\ im_2 & -il_2 & 0 & -in_2 \\ il_2 & im_2 & in_2 & 0 \end{pmatrix}$$

$$= \begin{pmatrix} \kappa & \nu & -\mu & -\lambda \\ -\nu & \kappa & \lambda & -\mu \\ \mu & -\lambda & \kappa & -\nu \\ \lambda & \mu & \nu & \kappa \end{pmatrix}$$

together of course with the auxiliary equations

$$l_1^2 + m_1^2 + n_1^2 = l_2^2 + m_2^2 + n_2^2 = 1.$$

The matrix equation is of course redundant after its first line, so that this line alone needs to be used.

For case I we have

$$\begin{aligned} \kappa &= 1/\sqrt{2} = l_1l_2 + m_1m_2 + n_1n_2, \\ \lambda &= \quad 0 \quad\; = -l_2m_1 + l_1m_2, \\ \mu &= 1/\sqrt{2} = -l_1n_2 + l_2n_1, \\ \nu &= \quad 0 \quad\; = -m_1n_2 + m_2n_1. \end{aligned}$$

Trigonometric solution of these equations leads to the fact that if θ_1 and θ_2 are angles satisfying $\theta_1 - \theta_2 = 45°$, then

$$\begin{aligned} (l_1,m_1,n_1) &= (\cos\theta_1,0,\sin\theta_1), \\ (l_2,m_2,n_2) &= (\cos\theta_2,0,\sin\theta_2), \end{aligned}$$

the solutions for different values of θ_1 correspond to rotations of the same system about its y axis. The particular case $\theta_1 = 67.5°$, $\theta_2 = 22.5°$ corresponds to the Wollaston prism shown in Fig. 2.

For case II we have

$$\begin{aligned} \kappa &= -1/\sqrt{2} = l_1l_2 + m_1m_2 + n_1n_2, \\ \lambda &= \quad 0 \qquad = -l_2m_1 + l_1m_2, \\ \mu &= -1/\sqrt{2} = -l_1n_2 + l_2n_1, \\ \nu &= \quad 0 \qquad = -m_1n_2 + m_2n_1. \end{aligned}$$

This time trigonometric solution leads to

$$\begin{aligned} \theta_1 - \theta_2 &= 225°, \\ (l_1,m_1,n_1) &= (\cos\theta_1,0,\sin\theta_1), \\ (l_2,m_2,n_2) &= (\cos\theta_2,0,\sin\theta_2). \end{aligned}$$

Again the system is a constant deviating system, and we may write the solution corresponding to different values of θ_1 for different orientations. The value $\theta_1 = -22.5°$ corresponds to the orientation in Fig. 3, which is the pentaprism. There are no other cases.

Conclusion

The methods and examples presented here demonstrate that a sufficiently simple analysis technique for mirror systems may be turned to advantage in synthesis. There are further calculation problems when the number of reflections becomes high, and it is hoped to give a complete account of the algebra for such systems in a future paper.

References

1. T. Smith, Trans. Opt. Soc. (London) **30,** 68 (1928).
2. T. Smith, Trans. Opt. Soc. (London) **30,** 79 (1928).
3. T. Y. Baker, Trans. Opt. Soc. (London) **29,** 49 (1927).
4. G. Rosendahl, J. Opt. Soc. Am. **50,** 287 (1960).
5. R. E. Hopkins, Proposed MIL Handbook (privately circulated at Institute of Optics, Univ. of Rochester, Rochester, N.Y.

January Feature

Optics of the Photographic System

A Method for Localized Variation of the Paths of Two Paraxial Rays

Loyd E. Sutton

This paper treats lens systems which consist of spherical and plane refracting surfaces, and for which fixed values of the indices of refraction have already been assigned. Simple algebraic equations are derived which allow changes to be made in the curvatures of two consecutive surfaces, together with changes in two specified vertex separations, subject to the following invariance condition: the heights and slope angles of both the marginal and principal paraxial rays must be left unchanged at all surfaces of the system other than the two surfaces undergoing modification. These equations may be considered to constitute a generalized "bending", although no attempt is made to retain the Petzval contribution as an invariant. The use of a series of such "bendings", applied independently at separate elements of the system, for certain adjustments of the third-order aberrations is immediately evident. Lagrange's invariant allows a surprisingly concise formulation of the final equations. If the first surface of an element is located at the primary focal point of the second surface, a separate solution is derived in which only two lens parameters are to be changed. These results are apparently new, although similar results for single paraxial rays are well known. Tentative suggestions as to additional applications are made.

Introduction

The object of this paper is simply to present a straightforward generalization of one of the many procedures often used by the optical designer, thus adding one more tool to the set at his disposal. It appears likely that the invariance properties of this apparently new tool will suggest its use in a variety of applications. Thus, the tool developed here might eventually be found useful in some phase of the complex problem of automatic lens design. In this paper we will consider only systems consisting of spherical and plane refracting surfaces.

The ordinary procedure of bending a lens element, in which equal increments are given to the curvatures of both its refracting surfaces, has had extensive application in optical design. In its use, there are two main restrictions involved in retaining its desirable invariance properties accurately. First, if the refractive indices are the same on both sides of a given element, the procedure leaves the Petzval contribution invariant. Second, if the element is also a thin lens, strictly defined as a "blueprint lens" of zero thickness, the paths of the marginal and principal paraxial rays are left invariant. Just this second invariance property will be retained in our generalization to the case of a thick lens with arbitrary indices, in the sense that, except for a local variation at a given element, the two paraxial ray paths will be kept invariant. This invariance condition is explicitly described in the caption for Fig. 1 in terms of the symbols explained in the "Definitions" section.

Comments on the Equations to Be Derived

From inspection of the final expressions, Eqs. (34) and (35), for such a generalized "bending", it will be clear that the equations reduce to those of ordinary bending only when the first and second restrictions cited above are *both* fulfilled. (We will use quotes to distinguish the new four-parameter "bending" from an ordinary bending.) Dropping the Petzval sum as an invariant of the new "bending" when thick lenses are treated turns out to be less of a concession than might at first be apparent. In return, we acquire a means of varying the third-order aberrations arising from a single element in a way which is independent of the third-order contributions arising from succeeding elements of the lens system. Of course, the usual conditions of physical constructability must be observed. Thus, we have so far used this "bending" method only for fine adjustments, such as, for example, those ordinarily needed to balance the third-order aberrations against the results of full ray tracing. It might be noted at this point that special treatment would be required if the stop plane were located *inside*

The author is with the National Bureau of Standards, Washington 25, D.C.

Received 29 May 1963.

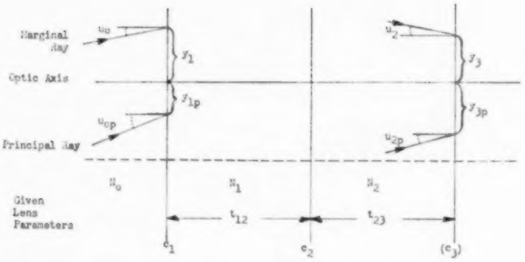

Fig. 1. In the text, formulas are derived for modified values of the parameters c_1, t_{12}, c_2, and t_{23} which will leave invariant the paraxial quantities shown here (above the dashed line). A family of solutions based on an arbitrary positive parameter, denoted by k, is obtained. (The short parallels to the optic axis are drawn only to depict slope angles of the two rays.)

an element which one found it imperative to "bend". On the other hand, referring to Fig. 1, the third surface depicted, c_3, might well represent the stop plane and the "bending" method would still apply. If c_3 represented the focal plane, a slight "bending" would produce a small change in t_{23}, which in this case is the back focal length of the lens system.

Since the marginal and principal paraxial rays are always taken to be two distinct rays, we will have a nonzero value for I, Lagrange's invariant. Also, in the course of deriving the results given by Eq. (35), we must assume a nonzero value for the quantity Q_1, defined by Eq. (34). The implications of removing this latter restriction are given in the section immediately following Eqs. (34) and (35). There we note that Q_1 is equivalent to $N_1(1 - \phi_2 Z_1)$, in the notation defined in Eq. (4).

Definitions

The symbols used here for the tracing of paraxial rays follow Feder.[1] However, we will also list these definitions below, referring the reader to Fig. 1 for examples of the subscripting convention used.

For the lens parameters:

c_1 is the curvature, that is, the reciprocal radius, of the first surface of a given element (positive for the center of curvature to the right of the surface);

N_0 and N_1 are the refractive indices to the left and right, respectively, of the first surface, and

t_{12} is the vertex separation between the first and second surfaces (two subscripts are helpful in specifying such separations unmistakably).

For the marginal ray:

y_1 is the height on the first surface (positive if above the optic axis);

u_0 is the slope angle on the left of the first surface (a slope angle is positive if the ray slopes downward from left to right), and

u_1 is the slope angle on the right of the first surface.

For the principal ray:

y_{1p}, u_{0p}, and u_{1p} are quantities corresponding to those just defined.

Derivation of the Generalized "Bending" Equations

For simplicity, a direct algebraic derivation of the equations will be given here, though the possibility of derivations based on matrices or Gaussian brackets[2] will be apparent to some readers. Feder's equations for paraxial ray tracing[1] are the starting point for the derivation and will be expressed here in terms of certain abbreviations which are quite common in the literature. We will first express u_2 as a function of u_0 and y_1, and to do this we will need equations for a refraction at the first surface, a transfer to the second surface, and then a second refraction. In essentially Feder's notation, these three operations are given by the equations

$$u_1 = c_1\left(1 - \frac{N_0}{N_1}\right)y_1 + \left(\frac{N_0}{N_1}\right)u_0, \tag{1}$$

$$y_2 = y_1 - t_{12}u_1, \tag{2}$$

$$u_2 = c_2\left(1 - \frac{N_1}{N_2}\right)y_2 + \left(\frac{N_1}{N_2}\right)u_1. \tag{3}$$

Using now the abreviations,

$$\left.\begin{aligned} \phi_1 &= c_1\,(N_1 - N_0),\\ \phi_2 &= c_2\,(N_2 - N_1),\\ Z_1 &= \frac{t_{12}}{N_1}, \end{aligned}\right\}. \tag{4}$$

Eqs. (1)–(3) become

$$u_1N_1 = \phi_1 y_1 + u_0N_0, \tag{5}$$

$$y_2 = y_1 - Z_1u_1N_1, \tag{6}$$

$$u_2N_2 = \phi_2 y_2 + u_1N_1. \tag{7}$$

On substituting Eqs. (6) and (5) into Eq. (7), we have

$$u_2N_2 = \phi_2 y_1 - \phi_2 Z_1 u_1 N_1 + u_1N_1,$$

or

$$u_2N_2 = \phi_2 y_1 - \phi_2 Z_1(\phi_1 y_1 + u_0N_0) + \phi_1 y_1 + u_0N_0.$$

Regrouping of this result gives the desired expression:

$$u_2N_2 = (\phi_1 + \phi_2 - \phi_1\phi_2 Z_1)y_1 + (1 - \phi_2 Z_1)u_0N_0, \tag{8a}$$

and similarly,

$$u_{2p}N_2 = (\phi_1 + \phi_2 - \phi_1\phi_2 Z_1)y_{1p} + (1 - \phi_2 Z_1)u_{0p}N_0. \tag{8b}$$

Note that, while Eq. (8a) refers to the marginal paraxial ray, the corresponding equation obtained by attaching the subscript p to u_2, y_1, and u_0 is valid for the principal paraxial ray. In what follows, this "p-subscripting" procedure will be used freely. We will also need to refer back to three expressions for Lagrange's invariant, denoted by I:

$$I = N_0(y_{1p}u_0 - y_1u_{0p}), \tag{9a}$$

$$I = N_1(y_{2p}u_1 - y_2u_{1p}), \tag{9b}$$

$$I = N_2(y_{2p}u_2 - y_2u_{2p}). \tag{9c}$$

In outline, we are seeking a family of "bendings" in which N_0, N_1, and N_2 are known constants of the original lens system and will not be changed. Certain conditions will be imposed on the "bendings" in two distinct steps. In the first step, any given member of our family of "bendings", as specified by the degree of "bending", must change the three parameters c_1, c_2, and t_{12} in such a way that u_2 and u_{2p} remain unchanged from their values in the original system. If we use the third parameter to specify the degree of "bending", we can replace t_{12} by a new numerical value $\bar{t}_{12}$ arbitrarily. Then the two disposable parameters, c_1 and c_2, will just suffice to hold u_2 and u_{2p} fixed. However, the heights of our two rays on the third surface (y_3 and y_{3p}) would naturally be changed by the first step alone. Thus, in the second step, we will have to solve for a new value of t_{23}, the distance to this surface, which will leave y_3 fixed. Here, it is essential to realize that y_{3p} will automatically remain fixed, since it is the fourth variable appearing in Lagrange's invariant and the other three will be held constant. Also, it is understood that when we make a change in the value of a given t, this alone will be done, and does not *imply* any change in the subsequent t's of the lens system. (The subsequent t's may of course be changed later in the process if the equations specify such changes explicitly.)

Proceeding to the solution of the first step, we will denote the modified values of the lens parameters and variables by using bars, for example, $\bar{c}_1$, $\bar{c}_2$, and $\bar{t}_{12}$.

It will be convenient to specify the degree of "bending" by using a positive constant k (usually assigned a value close to 1.0) and writing

$$\bar{t}_{12} = kt_{12}. \tag{10}$$

The modified values of the parameters in Eq. (4) are represented by

$$\left.\begin{aligned} \bar{\phi}_1 &= \bar{c}_1(N_1 - N_0), \\ \bar{\phi}_2 &= \bar{c}_2(N_2 - N_1), \\ \bar{Z}_1 &= \frac{\bar{t}_{12}}{N_1} = \frac{kt_{12}}{N_1} = kZ_1; \end{aligned}\right\} \tag{11}$$

where the last relation follows from Eq. (10). Thus, $\bar{Z}_1$ will be known in terms of k and a parameter of the original lens system, namely, t_{12} or the linearly related variable Z_1. However, $\bar{\phi}_1$ and $\bar{\phi}_2$ must be solved for by using the relations given in Eqs. (8a) and (8b). We will first express the solution in terms of k, ϕ_1, ϕ_2, and Z_1. Then Eqs. (4) and (11) will allow an easy transition back to the variables k, c_1, c_2, and t_{12}. The three refractive indices also appear in both forms as constants.

The parameters of the modified lens system, as given by Eq. (11), must satisfy Eqs. (8a) and (8b), because we are requiring that $\bar{u}_2 = u_2$ and $\bar{u}_{2p} = u_{2p}$. We may thus write

$$u_2N_2 - u_0N_0 = (\bar{\phi}_1 + \bar{\phi}_2 - \bar{\phi}_1\bar{\phi}_2\bar{Z}_1)y_1 - \bar{Z}_1u_0N_0\bar{\phi}_2, \tag{12a}$$

$$u_{2p}N_2 - u_{0p}N_0 = (\bar{\phi}_1 + \bar{\phi}_2 - \bar{\phi}_1\bar{\phi}_2\bar{Z}_1)y_{1p} - \bar{Z}_1u_{0p}N_0\bar{\phi}_2. \tag{12b}$$

To solve for $\bar{\phi}_2$, we write the equation resulting from

$$(-y_{1p})\cdot\text{Eq. (12a)} + (y_1)\cdot\text{Eq. (12b)},$$

making use of Eq. (9a) to obtain

$$N_2(y_1u_{2p} - y_{1p}u_2) + I = (\bar{Z}_1I)\bar{\phi}_2. \tag{13}$$

On the left-hand side of Eq. (13) we replace I by the expression given in Eq. (9c) and then use the relations implied by Eq. (2), which result in

$$\begin{aligned} &N_2[u_2(y_{2p} - y_{1p}) - u_{2p}(y_2 - y_1)] \\ &\qquad = N_2t_{12}(u_1u_{2p} - u_2u_{1p}) = (\bar{Z}_1I)\bar{\phi}_2. \end{aligned} \tag{14}$$

In Eq. (14) above, $(u_1u_{2p} - u_2u_{1p})$ can be further simplified by using Eq. (15) below, which is a consequence of Eq. (7):

$$\left.\begin{aligned} u_{2p} &= \frac{1}{N_2}(\phi_2y_{2p} + u_{1p}N_1), \\ u_2 &= \frac{1}{N_2}(\phi_2y_2 + u_1N_1). \end{aligned}\right\} \tag{15}$$

Thus,

$$(u_1u_{2p} - u_2u_{1p}) = \frac{\phi_2}{N_2}(y_{2p}u_1 - y_2u_{1p}) = \frac{\phi_2}{N_2}\left(\frac{I}{N_1}\right), \tag{16}$$

where the value of I is taken from Eq. (9b).

Substituting from Eq. (16) into Eq. (14) and then using an expression for $\bar{Z}_1$ given by Eq. (11), Eq. (14) becomes

$$\frac{t_{12}\phi_2}{N_1} = \bar{Z}_1\bar{\phi}_2 = \frac{kt_{12}\bar{\phi}_2}{N_1}. \tag{17}$$

Equation (17) thus yields a solution for the second of the two unknowns appearing in Eqs. (12a) and (12b) in the form

$$\bar{\phi}_2 = \frac{\phi_2}{k}, \tag{18}$$

while $\bar{Z}_1$ is known to be given by

$$\bar{Z}_1 = kZ_1. \tag{19}$$

We can now solve Eq. (12a) alone for the other unknown, $\bar{\phi}_1$. Substituting Eqs. (18) and (19) into Eq. (12a) and rearranging terms gives

$$\bar{\phi}_1y_1(1 - \phi_2Z_1) = [u_2N_2 - u_0N_0(1 - \phi_2Z_1)] - \frac{1}{k}(\phi_2y_1). \tag{20}$$

Here we note that Eq. (8a) can be written as

$$[u_2N_2 - u_0N_0(1 - \phi_2Z_1)] = \phi_1y_1(1 - \phi_2Z_1) + \phi_2y_1. \quad (21)$$

Thus, using Eq. (21) in Eq. (20), we have

$$\bar{\phi}_1y_1(1 - \phi_2Z_1) = \phi_1y_1(1 - \phi_2Z_1) + \phi_2y_1\left(1 - \frac{1}{k}\right), \quad (22)$$

and

$$\bar{\phi}_1 = \phi_1 + \frac{\phi_2\left(\frac{k-1}{k}\right)}{1 - \phi_2Z_1}. \quad (23)$$

Except for a change of variables, which will be deferred until after completion of the second step, Eqs. (18), (19), and (23) constitute the solution of the first step described in our outline of the derivation.

For the second step, we will again use bars to indicate quantities of the modified system, bearing in mind that u_0, y_1, and (because of the first step) u_2 will not need to have bars. Here, we will impose the condition $\bar{y}_3 = y_3$ on Eq. (28), in which $\bar{y}_3$ would otherwise appear. For the original system, we have, by using Eq. (5) in Eq. (6) and by advancing the subscripts of Eq. (6),

$$y_2 = y_1(1 - Z_1\phi_1) - Z_1u_0N_0, \quad (24)$$

and

$$y_3 = y_2 - Z_2u_2N_2, \quad (25)$$

where we define

$$Z_2 = \frac{t_{23}}{N_2}. \quad (26)$$

For the modified system, Eqs. (24)–(26) become

$$\bar{y}_2 = y_1(1 - \bar{Z}_1\bar{\phi}_1) - \bar{Z}_1u_0N_0, \quad (27)$$

and

$$y_3 = \bar{y}_2 - \bar{Z}_2u_2N_2; \quad (28)$$

where

$$\bar{Z}_2 = \frac{\bar{t}_{23}}{N_2}. \quad (29)$$

We are seeking a solution for $\bar{Z}_2$ in terms of k and the parameters of the original system. Substituting from Eqs. (25) and (27) into Eq. (28) and then using Eqs. (6), (5), and the relation $\bar{Z}_1 = kZ_1$, we have

$$\left.\begin{aligned}(y_1 - Z_1u_1N_1) - Z_2u_2N_2 &= y_1 - y_1\bar{Z}_1\bar{\phi}_1 - \bar{Z}_1u_0N_0 - \bar{Z}_2u_2N_2,\\ u_2N_2(\bar{Z}_2 - Z_2) &= Z_1(\phi_1y_1 + u_0N_0) - \bar{Z}_1(u_0N_0 + y_1\bar{\phi}_1),\\ u_2N_2(\bar{Z}_2 - Z_2) &= Z_1y_1(\phi_1 - k\bar{\phi}_1) + Z_1u_0N_0(1 - k).\end{aligned}\right\} \quad (30)$$

We know from Eq. (23) that

$$k\bar{\phi}_1 = k\phi_1 - \frac{\phi_2(1 - k)}{1 - \phi_2Z_1}.$$

Consequently, Eq. (30) can be written as

$$u_2N_2(\bar{Z}_2 - Z_2) = Z_1y_1\phi_1(1 - k) + Z_1u_0N_0(1 - k) + \frac{Z_1y_1\phi_2(1 - k)}{1 - \phi_2Z_1},$$

$$u_2N_2(\bar{Z}_2 - Z_2) = (1 - k)Z_1\left(\phi_1y_1 + u_0N_0 + \frac{y_1\phi_2}{1 - \phi_2Z_1}\right),$$

or

$$u_2N_2(\bar{Z}_2 - Z_2) = (1 - k)\,Z_1 \times \left(\frac{(\phi_1 + \phi_2 - \phi_1\phi_2Z_1)y_1 + (1 - \phi_2Z_1)u_0N_0}{1 - \phi_2Z_1}\right). \quad (31)$$

We can now reduce Eq. (31), by Eq. (8a), to

$$u_2N_2(\bar{Z}_2 - Z_2) = \frac{(1 - k)Z_1\,(u_2N_2)}{1 - \phi_2Z_1}. \quad (32)$$

The solution of the second step in our outline of the derivation thus follows from Eq. (32) in the form

$$\bar{Z}_2 = Z_2 - \frac{(k - 1)Z_1}{1 - \phi_2Z_1}, \quad (33)$$

and Eqs. (23), (19), (18), and (33) constitute the equations of our generalized "bending". Taken in that order, they prescribe (for a specified value of k) the new values to be assigned to the four consecutive parameters denoted by ϕ_1, Z_1, ϕ_2, and Z_2.

However, we will express the final results in terms of the original lens parameters. Substitution from Eqs. (4) and (11) into Eq. (23) yields

$$\bar{c}_1(N_1 - N_0) = c_1(N_1 - N_0) + \left(\frac{k - 1}{k}\right)\left(\frac{c_2(N_2 - N_1)(N_1)}{N_1 - t_{12}c_2(N_2 - N_1)}\right),$$

which leads directly to the expression for $\bar{c}_1$ given by Eqs. (34) and (35) below. By similar substitutions and simplifications, using Eqs. (4), (11), (26), and (29) in Eqs. (19), (18), and (33), we complete the derivation of the equations for generalized "bending". The results are given in the next section in a form convenient for computation. A secondary form for $\bar{c}_2$ is given to bring into evidence the fact that when $N_2 = N_0$ and $t_{12} = 0$, we obtain the ordinary bending equations for a thin lens.

Generalized "Bending" Equations

Using the abbreviation,

$$Q_1 = N_1 + t_{12}c_2(N_1 - N_2),^* \quad (34)$$

we have, for arbitrary positive values of k,

$$\left.\begin{aligned}\bar{c}_1 &= c_1 - \left(\frac{k - 1}{k}\right)\left(\frac{c_2N_1}{Q_1}\right)\left(\frac{N_1 - N_2}{N_1 - N_0}\right),\\ \bar{t}_{12} &= kt_{12},\\ \bar{c}_2 &= \frac{c_2}{k} = c_2 - \left(\frac{k - 1}{k}\right)c_2,\\ \bar{t}_{23} &= t_{23} - (k - 1)\left(\frac{t_{12}N_2}{Q_1}\right).\end{aligned}\right\} \quad (35)$$

---

* If $Q_1 = 0$, "bending" must be effected by Eq. (40) instead.

Interpretation of the Unique Singularity

The implications of a zero value for Q_1 are of some interest in themselves and call for further comment. By solving for t_{12}, we see that, in that case, the first surface of the given element would be located exactly at the primary focal point of the second surface. We must derive special "bending" equations for this type of element, where $Q_1 = N_1(1 - \phi_2 Z_1) = 0$, because any attempt to use Eq. (35) obviously leads to singularities, for all values of k different from unity. However, large sections of our original derivation remain valid and can be used to shorten this rederivation.

First, it may be verified that Eqs. (1) through (19) are formally valid whatever the value of Q_1, since we did not require $(1 - \phi_2 Z_1)$ to be nonzero in obtaining them. In the case when $Q_1 = 0$, however, we will be able to deduce that the value of k must be restricted to unity. We can use Eqs. (18) and (19) to obtain

$$(1 - \bar{\phi}_2 Z_1) = (1 - \phi_2 Z_1) = 0.$$

Thus, Eqs. (8a) and (8b) can now be written as

$$\left.\begin{aligned} u_2 N_2 &= \phi_2 y_1, \\ u_{2p} N_2 &= \phi_2 y_{1p}. \end{aligned}\right\} \tag{36a}$$

Similarly, Eqs. (12a) and (12b) become

$$\left.\begin{aligned} u_2 N_2 &= \bar{\phi}_2 y_1, \\ u_{2p} N_2 &= \bar{\phi}_2 y_{1p}. \end{aligned}\right\} \tag{36b}$$

Consequently, we have, from Eqs. (36a) and (36b),

$$\begin{aligned} \bar{\phi}_2 y_1 &= \phi_2 y_1, \\ \bar{\phi}_2 y_{1p} &= \phi_2 y_{1p}. \end{aligned}$$

Note that y_1 and y_{1p} cannot both be zero, because the invariant I would vanish, contrary to our choice of two independent paraxial rays. We must therefore conclude that $\bar{\phi}_2 = \phi_2$. Now, Eqs. (18) and (19), in turn, require that $k = 1$ and $\bar{Z}_1 = Z_1$. Thus, the values of t_{12} and c_2 must remain unchanged by the equations expressing "bending" for the special case of $Q_1 = 0$. It then follows that the value of Q_1 must also remain zero. Clearly, these conclusions are in no way dependent on the division by $(1 - \phi_2 Z_1)$ by which we previously obtained Eq. (23) from Eq. (22), in the course of solving for $\bar{\phi}_1$. By Eq. (36b), we see that now u_2 and u_{2p} are independent of $\bar{\phi}_1$, so we can assign $\bar{\phi}_1$ any value we wish. It will be convenient to express $\bar{\phi}_1$ in terms of an arbitrary parameter, denoted by j, in the form

$$\bar{\phi}_1 = \phi_1 + jN_1\phi_2. \tag{37}$$

(Note that ϕ_2 is always nonzero for $Q_1 = 0$, since otherwise an element of infinite thickness would be implied.)

To solve for $\bar{Z}_2$, we simply repeat the reasoning leading from Eq. (24) to Eq. (30), verifying that Eq. (30) is still valid although, since $Q_1 = 0$, k must be restricted to the value unity. Thus Eq. (30) becomes

$$u_2 N_2 (\bar{Z}_2 - Z_2) = Z_1 y_1 (\phi_1 - \bar{\phi}_1).$$

Using Eq. (37), we have

$$u_2 N_2 (\bar{Z}_2 - Z_2) = Z_1 y_1 (-jN_1\phi_2),$$

and, by Eq. (36a),

$$\phi_2 y_1 (\bar{Z}_2 - Z_2) = \phi_2 y_1 (-jN_1 Z_1). \tag{38}$$

We know that ϕ_2 is nonzero, and thus it may be divided out of Eq. (38). Since y_1 and y_{1p} cannot both be zero, and Eq. (38) could also be written with y_{1p} substituted for y_1, we conclude that

$$\bar{Z}_2 = Z_2 - jN_1 Z_1. \tag{39}$$

After an obvious change of variables is applied to Eqs. (37) and (39), the "bending" equations for the case $Q_1 = 0$ may be written, for arbitrary values of j, as

$$\left.\begin{aligned} \bar{c}_1 &= c_1 - j(c_2 N_1)\left(\frac{N_1 - N_2}{N_1 - N_0}\right), \\ \bar{t}_{12} &= t_{12}, \\ \bar{c}_2 &= c_2, \\ \bar{t}_{23} &= t_{23} - j(t_{12} N_2). \end{aligned}\right\} \tag{40}$$

We see that "bending", for this special category of lens elements, is effected by changing only the first and fourth parameters of the usual four, and that this category cannot arise if either t_{12} or c_2 is zero. Incidentally, it may be of some interest to observe that a similar special category arises, however, when one uses $c_1 = c_2 = 0$ in Eqs. (34) and (35).

It might be noted at this point that, provided ϕ_1 and ϕ_2 have differing numerical values, the unique singularity requiring Eq. (40) occurs at a different location of the first surface of the given element when one applies the equations of Corollary 1, described below.

Suggested Corollary Equations and Applications

There are certain corollaries to Eqs. (34) and (35) which can be expressed in an obvious way in additional equations, if they are to be used frequently. We will only indicate here how these corollaries could be expressed algebraically, since they represent simply special uses of the basic Eqs. (34) and (35).

Corollary 1. We can consider the path of the light as proceeding from right to left and then apply Eqs. (34) and (35) to the resulting reversed system. The effect of this reversal is that the distance to the (normal) left of the given element is varied, rather than that to the right. Equations involving a relabeling of variables result, but the variation in ray paths is still local, because the angles and heights occurring at other elements are unchanged.

Corollary 2. Another form can be derived in two steps. In the first step, we apply Eqs. (34) and (35), and the value which we choose to assign to k may be denoted by k_0. In the second step, we apply Corollary 1 to the parameters which resulted from the first step, and the value assigned to k in this second step is the reciprocal of k_0. It turns out that the element thickness is left unchanged by this double transformation. Thus, we obtain variation of the two curvatures of the given element and the distances on both its left and right. This form retains the same local variation property that its two components possess. It is applicable only when Eq. (40) is not needed.

We might mention possible additional areas of application for these "bending" procedures. First, in theoretical studies of the fifth and higher order aberrations, two lens systems may have to be adjusted slightly so as to have exactly the same values for certain of the third-order aberrations, meanwhile keeping certain of the first-order characteristics invariant. Conversely, it might be necessary to increase a thickness or change a curvature slightly to bring it to a specified value (for reasons of economical lens production), in a way which would minimize readjustment of the aberrations in an already well-corrected design. This latter comment suggests a second possible area of application—in the problem of introducing a constructable thickness into a thin lens design.[3] However, if this is to be done in a single step, it will probably be limited to certain cases in which the original curvatures would not be greatly altered by the "bending" process. For cases in which the original curvatures are quite small, one might try a "bending" as applied to a so-called "air-space" lens. For such a lens, referring to Fig. 1, only the index N_1 is unity, t_{12} has a value greater than zero, and the distance t_{23} could have an original value of zero. In this case, a "bending", by Eqs. (34) and (35), could be applied so as to increase the value of t_{23}. Again, an otherwise similar situation could be handled, in which only the index N_0 is unity. This would correspond to obtaining a nonzero value for the thickness of the second glass of a cemented doublet, when the first glass already has a nonzero thickness. Only further experience will indicate whether practical solutions of the thin-to-thick lens problem can be obtained through generalized "bending" or through some more elaborate procedure based upon it. Third, the techniques used in obtaining the results of this article might be found helpful in obtaining algebraic solutions of somewhat similar problems not considered here, such as those involving small changes in the indices of refraction.

Conclusions

We have shown that the final results of the generalized "bending" procedure derived here are expressible in concise algebraic equations which are well within the scope of modern computing methods. Special use of Lagrange's invariant in treating the two paraxial rays simultaneously results in a simpler formulation of the generalization than one might anticipate otherwise. So far, it appears that the chief advantage of the generalized "bending" is in making possible changes in the third-order aberrations of a given element, independently of third-order contributions from succeeding elements of a lens system. This property suggests a number of applications.

Readers who are interested in other recent results in the general field of invariants in geometrical optics are referred to a paper by Unvala.[4]

References

1. D. P. Feder, J. Opt. Soc. Am. **41,** 630 (1951).
2. M. Herzberger, J. Opt. Soc. Am. **33,** 651 (1943).
3. M. Herzberger, J. Opt. Soc. Am. **34,** 114 (1944).
4. H. A. Unvala, Optik **19,** 551 (1962).

General Motors

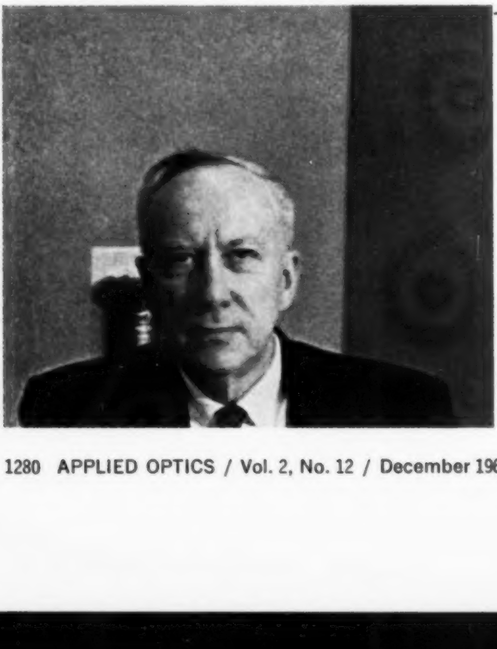

Gerald M. Rassweiler who was recently appointed Technical Director of Basic Applied Sciences for GM Research Laboratories.

Automatic Lens Design for Nonexperts

Berlyn Brixner

Automatic lens design by nonexperts is practical with the 1962 LASL lens-designing code, a general-purpose iterative program for evaluating and designing optical lens and mirror systems with surfaces generated by conic sections. Using skew ray traces, it analyzes lens performance statistically, finds differences resulting from design-parameter alterations, and computes a linear combination which will improve performance. Program characteristics, lens parameters, ray sampling, image evaluation, lens-performance weights, merit calculation, and parameter interactions are briefly described. Sample calculations are given in detail for a Lister-type lens and in summary for a special-purpose zoom lens.

The purpose of this paper is to describe a lens-designing program for the IBM 7090 which is in use at the Los Alamos Scientific Laboratory and to call attention to the fact that instrument designers with special optical problems can now learn to design their own lenses. The paper is not aimed at the optical specialist.

For the optical specialist it may be well to mention that this computer program does not follow classical designing methods. It does not make use of Gaussian and third-order optics or diffraction theory. It does two main things: it evaluates lens performance and improves lens prescriptions. The method is so powerful that the starting prescription need be no more than sheets of glass with plane surfaces. The possibilty of making lens designs practically from scratch in this way has apparently not been recognized by previous workers[1-3] who have used the same least-squares technique to minimize spot sizes. These workers based their solutions on the assumption that it is necessary to have a partially corrected prescription before starting designing. But actually the cruder the starting prescription the more rapid the rate at which the program converges on a solution.

To evaluate performance, the program analyzes image defects precisely by calculating the sizes and positions of image spots produced by bundles of skew rays traced through the lens. The size of the ray bundle at the focal plane of interest is the main criterion of lens performance. The image spot is evaluated from the rms radius of the rays from the centroid of the ray-bundle intersection on a plane normal to the optical axis. To improve the lens, the program obtains a sharper focus by changing the parameters of the lens system to make the bundles of rays intersect the image surface at the desired positions in patterns of the smallest size. The program performs this operation by first determining differences in lens performance resulting from design parameter alterations. Then it applies a least-squares technique to compute a linear combination* which will give an improved lens prescription. At the conclusion of each design cycle a merit number is obtained. The smaller this number, the better the performance. A perfect lens would have a merit number of zero. To obtain this number the average deviation of the rays from each image point is first obtained. Next, each average deviation is multiplied by the assigned weight. The merit number is the sum of these products.

In addition to evaluating performance and improving the prescription, the program has an automatic meridional rim-ray trace, which gives the ray-intersection coordinates at each optical surface, and an automatic scaling routine, which gives the scaled ray-intersection coordinates at any focal plane of interest. These coordinates are useful for preparing lens drawings and spot diagrams.

The program can investigate lens systems with as many as 98 surfaces. Although the most used lens or mirror surfaces are either spheres or right-circular cylinders, surfaces generated from any conic section may be used. Any of the surfaces of revolution may be displaced or tilted as desired. There is a wide

---

The author is with the University of California, Los Alamos Scientific Laboratory, Los Alamos, New Mexico.

Received 15 July 1963.

This work was done under the auspices of the U.S. Atomic Energy Commission.

* This is a linearization procedure similar to that outlined by D. P. Feder, J. Opt. Soc. Am. **52,** 180 (1962).

choice possible in the number and distribution of the rays which may be traced through the lens. The positions and sizes of the entrance and exit pupils can be readily controlled. The lens focus may be fitted to a specified focal surface, or the shape of the best focal surface may be determined. Simultaneous design for seven image points, six wavelengths, and five conditions of use is possible. An example of different conditions of use would be the positions of a zoom lens.

The rest of this paper will briefly give some characteristics of the program, will outline the method for using it, and, in more detail, will give examples of two lenses designed by means of the program.[4,5,*]

Selecting the Design

The instrument designer may find that one of the many standard lenses will be adequate for his needs. With the program he can readily evaluate a likely prescription. Or, if the standard lens is not entirely adequate, the machine can indicate minor alterations of the surface radii and in the spacing of the elements which will give the best performance in his situation. If still better performance is required, he can let the machine determine the lens design most suitable for his problem. One starts the design by making monochromatic runs on a series of air-spaced glass sheets. After making runs on a series of lenses of increasing complexity, he can then choose the lens which best suits his needs. The monochromatic design is achromatized by substituting crown and flint glasses in the prescription and readjusting by means of additional runs on the machine.

Preparing the Problem for the Machine

To evaluate an existing lens one needs, in addition to the prescription, the following information: the distance from the object, the angle of view, the entrance pupil location, the relative aperture (*f*/number), the image distance, and the shape of the focal surface (plane or curved). In the absence of specific conjugates, the object distance is assumed to be infinity. To find the angle of view, one traces a series of ray bundles from object points at increasing angles. The entrance pupil distance may be specified or it may be determined by the designing program. If the image distance is specified, the ray-tracing program can set the plane of interest at that distance. If the image field is curved, the additional values of the sagitta for the image points are also used. If the image distance is unknown, the ray-tracing program will set the plane of interest at the back focus calculated from the automatic meridional ray trace with the first refractive index selected (plus the sagitta plus a fine-adjustment increment if these are assigned nonzero values).

Table I. Summary of Lister Lens Designing Sequence and Progress

Operation performed	Ray pattern	Increments used: Total	Increments used: Per cycle	Cycles run	Figure of merit	Computation time (sec)
Start	2	—	—	—	904.7	73
Designing	2	4	1	29	24.9	18
Designing	2	6	1	25	18.0	17
Designing	2	6	2	25	0.26	22
Designing	2	8	2	25	0.23	22
f/2.0	2	—	—	—	4.9	<1
Designing	2	9	3	28	0.30	35
Designing	2	9	4	28	0.22	45
Ray change	6	—	—	—	4.0	<1
Designing	6	9	4	28	0.31	106
Designing	6	9	5	28	0.27	123
Designing	6	9	6	28	0.26	148
Ray change	12	—	—	—	0.84	<1
Designing	12	9	6	28	0.41	281

For evaluating performance, the choice of input rays is very important. Since the rays traced through the lens represent the behavior of light, they should be selected to function efficiently as agents for lens performance evaluation. Each ray may be considered as a sample of the focusing ability of the lens region

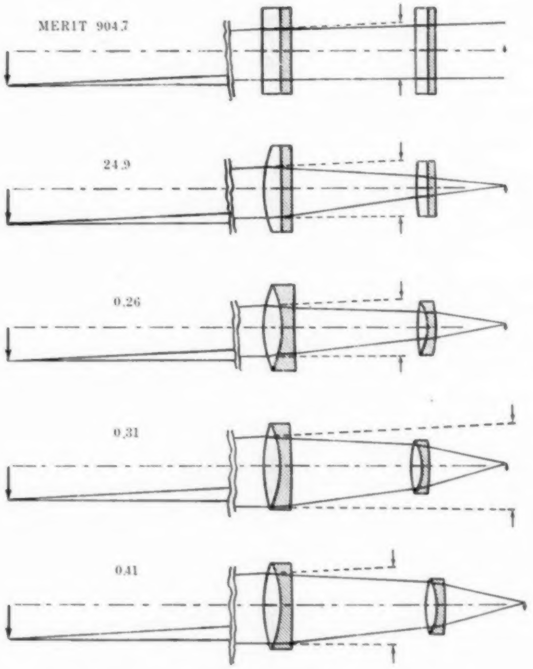

Fig. 1. Five lenses in the Lister lens-design series.

---

* These reports are available at nominal cost from the Office of Technical Services, Department of Commerce, Washington 25, D.C. They are also available for reference use by the general public in 85 United States libraries and in 84 foreign libraries.

Table II. Prescriptions for the Lister Lens Designs

Glass type	Figure of merit									
	904.7		24.9		0.26		0.31		0.41	
	t	r	t	r	t	r	t	r	t	r
	170.0		170.0		170.0		170.0		170.0	
518 596	2.7	∞	2.7	15.14	2.7	14.42	2.7	19.76	2.7	20.555
621 362	1.5	∞	1.5	∞	1.5	−14.20	1.5	−13.63	1.5	−14.568
	18.0	∞	18.0	1513	18.0	219.4	17.32	−94.52	19.299	−154.06
518 596	1.8	∞	1.8	43.62	1.8	16.85	1.8	13.94	1.8	12.183
621 362	1.0	∞	1.0	∞	1.0	−6.310	1.0	−7.072	1.0	−8.0225
	10.0	∞	10.0	−144.2	10.0	−15.75	11.12	−22.50	11.525	−27.126
Entrance pupil	−20.0		−20.0		−20.0		−36.0		−18.8	

which surrounds the ray path. The larger the surrounding region, the less typical this sampling will be. The pattern of rays to be traced is placed in a unit-radius entrance pupil. The ray-tracing program scales the unit-pupil dimensions to the actual pupil dimensions to obtain the coordinates of each ray to be traced. The rays usually sample the entrance pupil with a grid-pattern array, but as many as 25 rays may be positioned in any pattern desired. In this program, up to 100 rays can be traced from each object point for each color.

When designing lenses, the designer can weight the deviations of the rays from the desired image points to emphasize specific aspects of lens performance. The more important the aspect, the higher the weight assigned. Optimum lens performance requires minimum image-spot sizes on the focal surface. These image spots are made up of a maximum of six colors, each from a maximum of seven object points. The weights for the sizes of these spots are assigned individually. Weights on the deviations caused by the variation of magnification with color for each of these seven images are also assigned individually. The seven desired image heights, the individual weights for each of these image heights, and the sagitta (for a curved field) are assigned by the programmer. The required principal focal length and the weight on the reciprocal focal length may be specified. The exit-pupil position is calculated from a ray traced from an object point at a height selected by the programmer. The desired distance of the exit pupil from the last optical surface and the weight on this distance are also specified by the programmer. The above weights are the total number which control the design program. Another factor of importance to lens performance is the entrance pupil aperture radius or the operating relative aperture of the lens, one of which may be fixed for designing.

Choosing the Design Program

The lens characteristics are specified by parameters, i.e., numbers which correspond to the physical characteristics of the lens. The designing program can calculate a better number for a parameter by evaluating the effect of small changes of that parameter on the performance of the lens. If two parameters are changed and the effects computed simultaneously, there is an interaction which produces a much greater improvement of lens performance than that obtained with each taken alone. Up to a certain point, the more effects of parameter changes computed simultaneously, the faster the improvement of lens performance. However, if too many parameters are changed at once, the progress becomes erratic because of the program's inability to evaluate precisely the too complex problem. This program can work with a maximum of ten simultaneous parameter changes.* With ten simultaneous changes, forty-five interacting pairs are present. To arrive at the minimum merit number obtainable with a specific set of variable parameters, it is necessary to work with all possible pairs as often as possible. An iterative sequencing procedure accomplishes this result.

Boundary Conditions

Any variable parameter which shows a tendency to exceed its boundaries is manually fixed at the boundary. Since most problems have only a few boundary violations and since the code is mainly used for short machine runs, this manual operation is not cumbersome.

---

* The selection of the ten-simultaneous-parameters maximum in this code was an arbitrary decision based on our experience that a larger number would not produce useful solutions at the present stage of the art. This conclusion is similar to that of J. Meiron.[3]

Table III. Weights for Images of Lister Lens Designs

Performance feature to be weighted	Image point			
	First	Second	Third	Other
Focal length	—	—	—	0
Exit pupil distance	—	—	—	0
rms spot size	100	100	100	
Lateral chromatism	0	0	0	
Image height	0	0	100	
(Image height desired	0.12	0.36	0.60)	
(Object height given	1.0	3.0	5.0)	

Table IV. Analysis of Lister Lens Performance by Twelve-Ray Traces

Image point	Light color	Height of centroid	rms image-spot sizes		
			Sagittal	Tangential	Radius
First	*C*	0.1202	0.0011	0.0011	0.0015
First	*d*	0.1201	0.0007	0.0007	0.0010
First	*F*	0.1199	0.0009	0.0009	0.0013
Second	*C*	0.3606	0.0009	0.0010	0.0014
Second	*d*	0.3603	0.0009	0.0007	0.0011
Second	*F*	0.3595	0.0010	0.0010	0.0014
Third	*C*	0.6007	0.0008	0.0009	0.0013
Third	*d*	0.6002	0.0013	0.0007	0.0015
Third	*F*	0.5989	0.0012	0.0013	0.0018

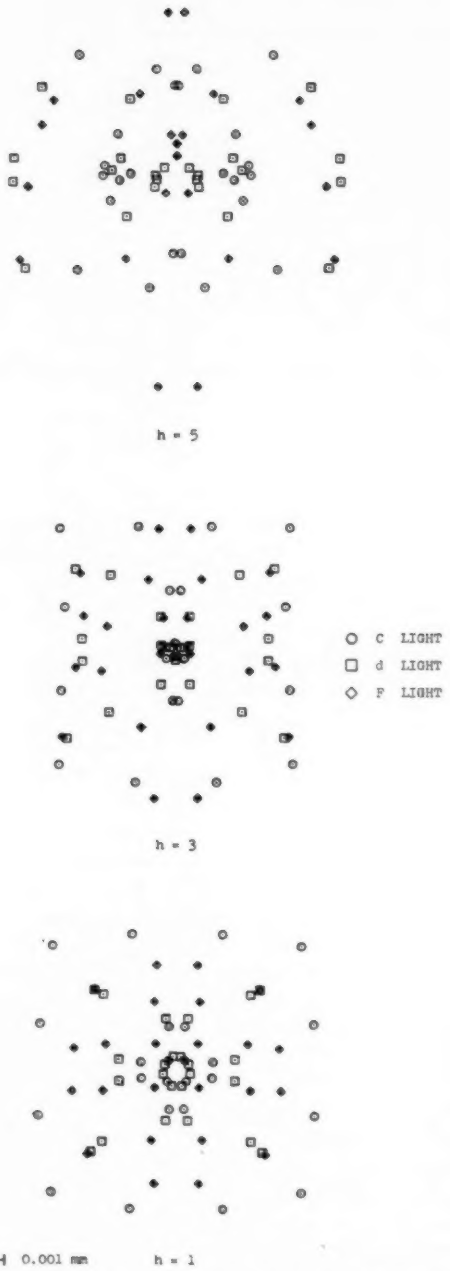

Fig. 2. Spot diagrams of three images made by the Lister lens.

Sample Calculation

The lens to be designed in the following sample calculation consists of two cemented doublets in series which produce an $f/2$ Lister-type lens[6] set to work at a magnification of about one eighth. The objects are at an axial distance of 170 mm from the first lens surface and 1, 3, and 5 mm from the optical axis. The images are on a flat field which is started with the back focal distance held at 10 mm. After the lens has been stabilized, this distance is made a design parameter. The design was started with two cemented sheets of 518 596 and 621 362 glass spaced 18 mm apart. The entrance pupil distance was fixed at -20 mm and the aperture radius at 4 mm. Designing was started with three colors (C, d, F), a two-ray pattern, and a series of twenty-nine single increments to the four glass–air surfaces. As a result, the prescription's figure of merit went from 905 to 25. A summary of the complete 15-min series of runs used to design this lens is shown in Table I. Figure 1 illustrates five of the prescriptions in the series to show the changes being made during the progress of the design. The prescriptions for five designs are given in Table II. The weights used for all stages of the design are shown in Table III.

These runs produced an $f/2.0$ lens of 20.884-mm (C-light) focal length, which should give 700-lines/mm resolution over most of the 1.2-mm diam focal surface at 11.525-mm distance. There is a maximum of 0.0018-mm variation of lateral magnification with color at the edge of the 1.7° half-field of view. Table IV shows the details of the twelve-ray-trace analysis of lens performance. The spot diagrams of the three images are shown in Fig. 2.

Table V. Prescription for the Zoom Lens

Glass[a] type	Thickness or space for zoom position					Radius of curvature
	One	Two	Three	Four	Five	
	9000	9000	9000	9000	9000	
						504.64
517 645	10	10	10	10	10	
						295.86
617 366	15	15	15	15	15	
						350.59
	10	110	210	310	410	
						350.75
517 645	20	20	20	20	20	
						−462.72
617 366	10	10	10	10	10	
						5912.7
	500	400	300	200	100	
						45343.0
517 645	10	10	10	10	10	
						118.46
617 366	15	15	15	15	15	
						218.67
	10	110	210	310	410	
						581.80
517 645	20	20	20	20	20	
						−224.34
617 366	10	10	10	10	10	
						−678.84
	1000	900	800	700	600	
						449.38
517 645	20	20	20	20	20	
						−221.69
617 366	10	10	10	10	10	
						−649.20
	376.532	376.532	376.532	376.532	376.532	
Entrance pupil	−800.0	−800.0	−800.0	−800.0	−800.0	

[a] The indexes used are 1.000206, 1.000206, 1.000208, 1.51521, 1.51966, 1.52769, 1.61176, 1.62069, and 1.63839.

A Complex Design

An example of a complex design which can be made with this program is a special-purpose zoom lens. This lens is an objective for a high-speed camera used to photograph explosions through the 10.2-cm-diam viewing port of a concrete bunker. 20-mm images of 150- to 450-mm explosive objects are required, with the objects 9000 mm from the front lens element. To obtain this range of magnification, a zoom ratio of approximately 3.6:1 is needed. Between the viewing port and the objective's image, there is a distance of more than 2000 mm, which can be used for any desired arrangement of lens elements.

In the search for a solution to this difficult imaging problem, it was decided to let the lens-designing program find the optimum design for lens systems with three or four or more elements so that we could select the simplest design which would give the required resolution. Using the program's substitution capability, we let the machine design each lens system simultaneously for five equally spaced positions of the moving elements. Several monochromatic designs were made with zoom arrangements which previous workers had found to be useful.[7] The so-called four-lens system, which has five elements, was found to be the minimum which would give the desired image quality. The entire available length was used because a long lens nearly always gives the best performance. The design was then restarted with five cemented sheets of 517 645 and 617 366 glass (*C*, *e*, and *g* melt indexes adjusted for 2135-m elevation) in a zoom system consisting of two coupled sliding lenses which move between three fixed lenses. These paired components quickly assumed shapes to give negative,

Table VI. Weights for Images of the Zoom Lens

Performance feature to be weighted	Image point			
	First	Second	Third	Other
Focal length	—	—	—	0
Exit pupil distance	—	—	—	0
rms spot size	100	100	100	
Lateral chromatism	0	50	100	
Image height	0	0	100	
(Image height desired	0	5	10)	

Table VII. Analysis of Zoom Lens Performance by Six-Ray Traces

Characteristic feature	Zoom position				
	One	Two	Three	Four	Five
Element shift	0.0	100.0	200.0	300.0	400.0
Object size, maximum	150.000	197.128	259.716	342.248	450.000
Magnification	0.133	0.101	0.077	0.058	0.044
Relative aperture	12.0	10.0	8.0	7.0	6.5
Focal length, C	1592.04	1097.30	790.76	583.51	436.86
Focal length, e	1595.01	1098.04	790.70	583.15	436.40
Focal length, g	1592.16	1097.13	790.55	583.32	436.72
Mean spot size, image 1	0.013	0.014	0.015	0.014	0.017
Mean spot size, image 2	0.014	0.015	0.015	0.014	0.018
Mean spot size, image 3	0.017	0.017	0.017	0.015	0.018
Lateral chrom., image 2	0.009	0.006	0.005	0.005	0.006
Lateral chrom., image 3	0.017	0.012	0.010	0.010	0.011

positive, negative, positive, and positive powers. Before the final design was achieved, we made several readjustments of the movements and spacings of the elements. Ten parameters were incremented simultaneously during the final stages of the design. The parameters consisted of all the radii of curvature, the sizes of the three intermediate objects, and the back focal distance.

The prescription data for five zoom positions are shown in Table V. The weights used for designing are shown in Table VI. Table VII shows the details of the six-ray trace analysis of lens performance for five positions. For each of these five positions the spot sizes and focal positions for C, d, e, F, g, and h light were determined. There was no discernible shift of the optimum focal plane for any of the positions tested, possibly because the variation of focus with color is the principal defect of this lens. Except for h light, the maximum spot sizes on the focal plane at the 376.532-mm back focus did not go above 0.027 mm, and the average is about 0.013 mm. A visual white-light resolution of about 100 lines/mm is predicted for most of the zoom range.

Thanks go to John C. Holladay for developing our automatic lens-designing program and instructing me in its use, to Charles A. Lehman for developing this faster enlarged program, and to William C. Davis for helpful criticism of this paper.

References

1. F. Wachendorf, J. Opt. Soc. Am. **43,** 325 (1953).
2. S. Rosen and C. Eldert, J. Opt. Soc. Am. **44,** 250 (1954).
3. J. Meiron, J. Opt. Soc. Am. **49,** 293 (1959).
4. C. A. Lehman, Los Alamos Scientific Laboratory Report LA-2837 (1963).
5. B. Brixner, Los Alamos Scientific Laboratory Report LA-2877 (1963).
6. A. E. Conrady, *Applied Optics and Optical Design*, R. Kingslake, ed. (Dover, New York, 1960), Part 2, pp. 662–678.
7. R. Kingslake, J. Soc. Motion Picture Televison Engrs. **69,** 1 (1960).

THE SCIENCE OF COLOR

THIS DEFINITIVE BOOK ON COLOR, prepared by OSA's Colorimetry Committee and setting forth the history, physics, physiology, psychology, and technology of color vision and color measurement, has been reprinted.

LIMITED EDITION. Twenty-five color plates make this book uniquely beautiful, and when the original supply of color sheets is exhausted, they cannot be reproduced. Therefore, this edition is limited.

AUTHORITATIVE DATA, mostly unavailable in other books, 39 tables, 102 figures, 340 pages of text, 22 pages of bibliography, and 23 pages of glossary-index have all been critically reexamined and corrected. The new **SCIENCE OF COLOR** is therefore the most up-to-date as well as the most complete source book for color science.

ORDER NOW **See Page A18**

FROM OSA **SEND CASH WITH ORDER** **PRICE $10.00; OSA MEMBERS $8.50**

A New Method for High-Speed Motion-Picture Photography of Transparent Drops

Albert Pfeiffer

A new method applicable to high-speed motion-picture photography of moving transparent drops is described. Previous methods have not considered the optical properties of drops as image-forming, spherical convex lenses. By taking advantage of this property of transparent drops, it has been possible to produce sufficient light contrast between the drop and its illuminated background to enable drops to be photographed. It is concluded that high-speed motion-picture photography of transparent drops can be accomplished where it is possible to produce sufficient light contrast between the drop and its background to make the drop visible. Two highly satisfactory methods of producing this contrast were tested experimentally and found to produce an excellent technique that could be used for a variety of investigations in the aerosol field.

Drop photography is a very useful tool for investigations in the fields of evaporation, condensation, coating, stability, settling (mass subsidence), impaction, fluid dynamics, and production of aerosols. Only drops that are visible in a general optical sense, however, can be photographed.

The following methods have been used previously in an attempt to produce sufficient light contrast to make transparent drops optically distinguishable: dark-field illumination,[1] Schlieren,[2] shadow,[3] and silhouette.[4] The latter method shows the silhouette of the drop in direct light. In these older methods, the drop usually photographs black against a bright background. When the background is a dark color, it is impossible to obtain satisfactory photographs. Furthermore, these methods will work only if the optical axis of the camera and the illuminating light beam form a narrow limited angle with each other.

All previous methods have failed to consider that the transparent drops are actually image-forming, spherical convex lenses. When these properties of the drop were studied, it was found possible to produce a sharp contrast between a drop and its surroundings by diffused reflected light.

Basic Optical Principles

Elements of Optical System

The basic optical system consists of the (1) light source, (2) drop, (3) limited background, (4) unlimited or general background, and (5) objective lens and ground glass of the camera (Fig. 1). Light rays from the light source incident upon the general background are reflected diffusely through the drop and objective lens, and the resultant image is brought into focus on the ground glass of the camera. As explained later, the transparent drop in this system acts as an image-forming optical lens; thus, the basic laws of optics as applied to lenses may be applied to this drop.

Experimental Method

Visibility of Drop

A drop can be photographed only if it is visible, i.e., optically distinguishable from its surroundings. If a convex lens is used to look at some object, e.g., a page of print, a reverse picture of a certain area of the page can be seen in the lens (Fig. 2) when the lens, the eye, and the print are at certain distances from one another. If the object is large enough, it is possible to see two images simultaneously—a direct image of the print (seen around the outside of the lens) and an inverted image of the print within the lens.

This contrast between images enables the viewer to distinguish the lens itself. Since a transparent drop is also a lens, it too can be distinguished under similar

---

The author is with the U.S. Army, Chemical Corps Research and Development Command, Physicochemical Research Division, Chemical Research and Development Laboratories, Army Chemical Center, Maryland.

Received 14 September 1962.

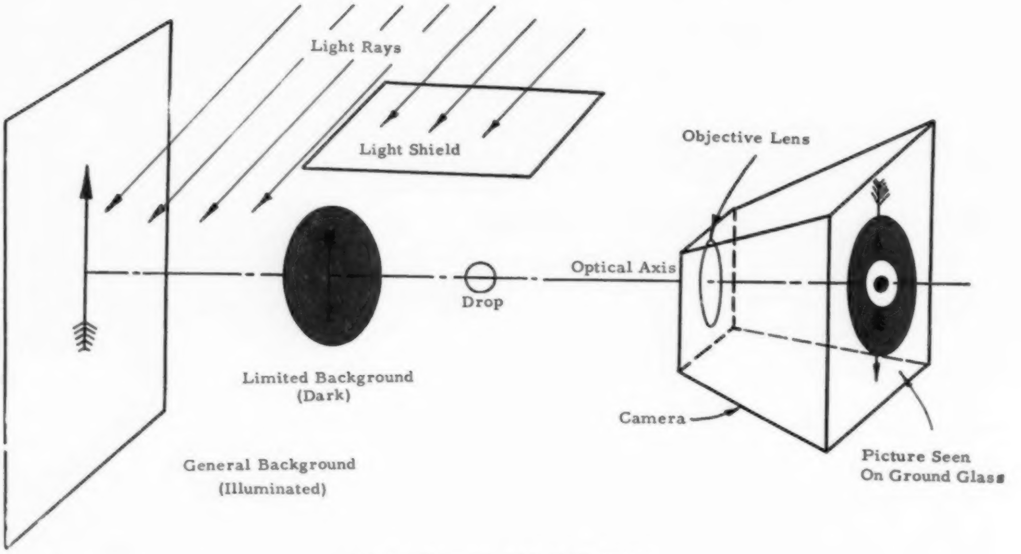

Fig. 1. Elements of optical system.

conditions. Furthermore, the drop can be photographed when these images are in contrast (Fig. 3).

Image Formation of Drop and Background on Ground Glass of Camera

In order to develop a method by which sufficient light contrast could be produced for satisfactory drop photography, first it was necessary to determine how images of the drop and background relate to each other. By first substituting transparent glass spheres 5 mm in diameter for drops, it was possible to develop and test contrast techniques at the optical bench on a large scale.

Figure 4 shows the normal relationship between the glass sphere and the background elements. A white test body with a groove on its left side was placed upon the dark opaque surface. Figure 5 shows how the background appears when photographed through the drop. Although the background and sphere now appear in an inverted position, the position of the white test body remains unchanged. (The groove remains on the left side.)

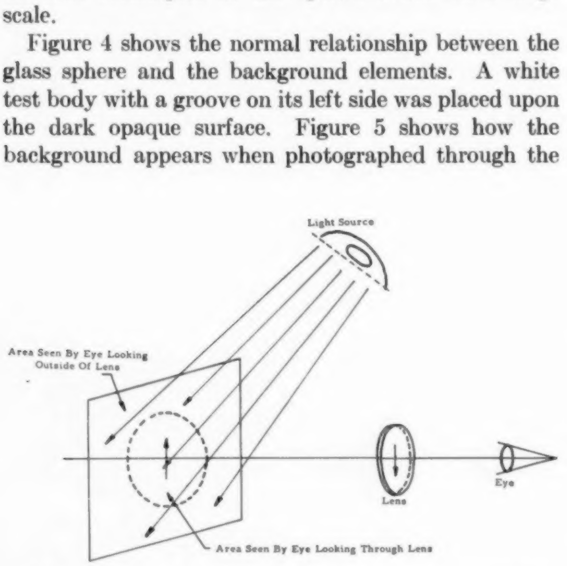

Fig. 2. Diagram of object viewed in and around convex lens.

This phenomenon can be explained graphically (Fig. 6): From any point on the white object AB, any number of light rays can be constructed. For purposes of illustration, consider two such rays leaving point B on the white object. The first ray passes through the R-point of the drop as a chief ray; it is refracted by the drop and passes on through the center of the objective lens. The second ray leaving point B passes through the focal point F of the drop, is refracted by the drop into a path parallel to the optical axis, strikes the objective lens where it is again refracted, and passes on through focal point F''' of the lens. The two rays will intersect at a point behind the objective lens within the camera. To obtain a sharp image of the white object, the ground glass must be positioned at this exact point.

Next, consider two rays leaving point X on the darker background. The first ray passes directly through the center of the objective lens. The second ray passes through the focal point F'' of the objective lens and is refracted by the lens into a path parallel to the optical axis. These rays will also intersect. Their point of intersection, however, is in a different image plane from the one in which the image of the white object is located. This is a desirable factor in the photography of the white object.

The inversion of the darker background with respect to the position of the white object within the camera can be easily seen now from this graphical construction.

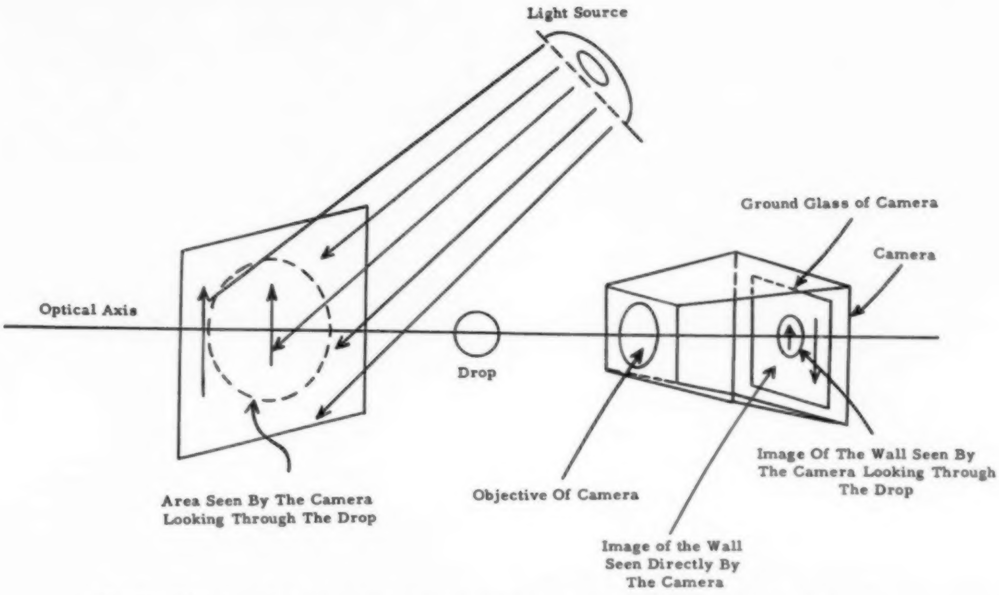
Light Source
Ground Glass of Camera
Camera
Optical Axis
Drop
Image Of The Wall Seen By The Camera Looking Through The Drop
Area Seen By The Camera Looking Through The Drop
Objective Of Camera
Image of the Wall Seen Directly By The Camera

Fig. 3. Diagram of object viewed through drop and background viewed directly by camera.

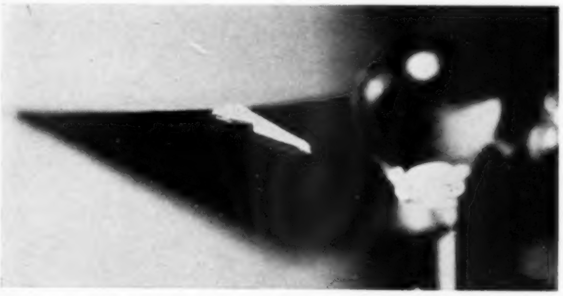

Fig. 4. Glass sphere, opaque surface, and white test body viewed directly.

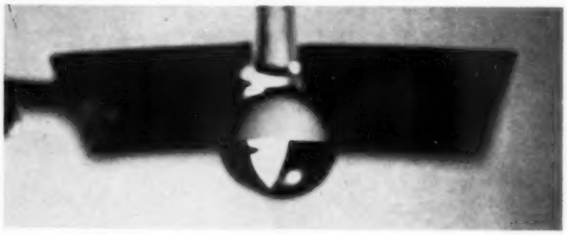

Fig. 5. Glass sphere with opaque surface and white test body viewed through ground glass.

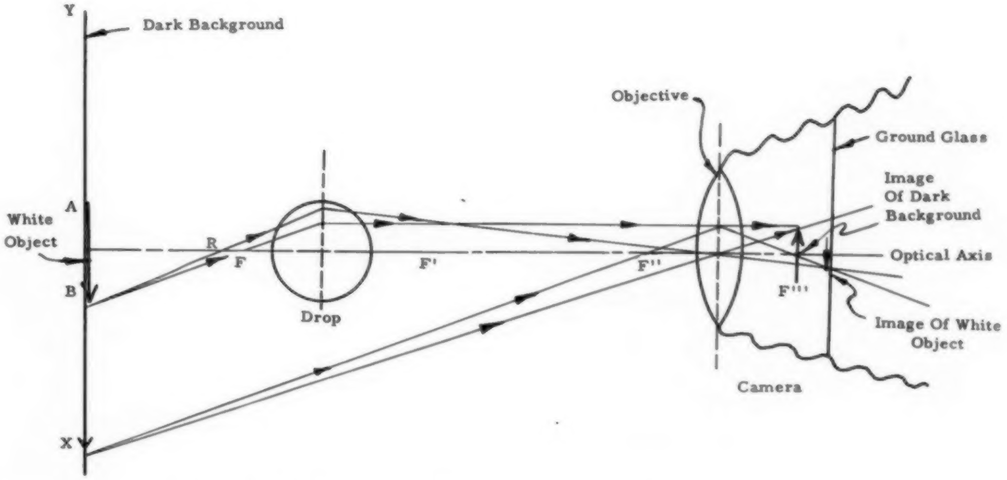
Y
Dark Background
Objective
Ground Glass
A
White Object
R
F
F'
F''
Image Of Dark Background
Optical Axis
B
Drop
F'''
Image Of White Object
Camera
X

Fig. 6. Image formation of white object and dark background within camera.

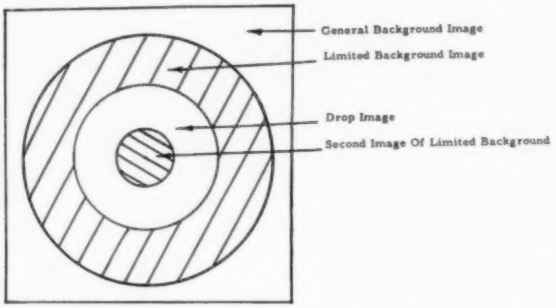

Fig. 7. Typical picture of drop and backgrounds seen on ground glass of camera.

With the light source available in this work, pictures of moving drops could be obtained having a radius as small as 30 μ. It should not be difficult to obtain pictures of drops as small as 3 μ if the light source were 100 times more intense, but for drops as small as 3 μ, the geometrical optics analysis would not be expected to be sufficiently rigorous.

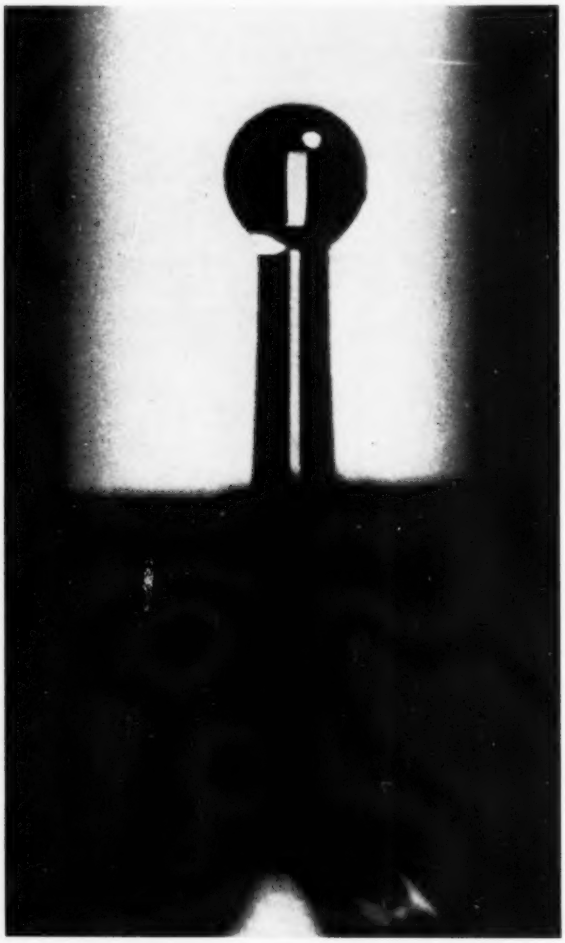

Fig. 8. Photograph of glass sphere viewed against illuminated limited background and dark general background.

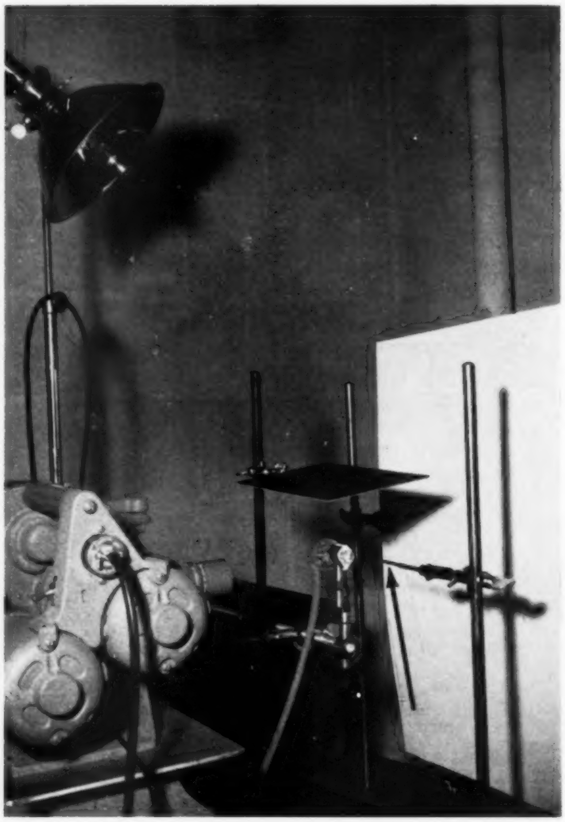

Fig. 9. Experimental setup used to photograph transparent drops against dark limited background and illuminated general background: high-speed motion-picture camera, light source, light shield, atomizer, limited background shown by arrow, general background.

To calculate the actual drop size from the picture of a drop, one has to measure the magnification at the point, in the field of view, where the drop will appear. This measurement can be made by using a calibrated scale. The optical justification for this procedure of determining the magnification can be derived from a consideration of Fig. 6 and the depth of field of the particular camera used.

Procedure

In this method, the drop is photographed with two backgrounds contrasting in either color or intensity of illumination (Fig. 1). The general background is unlimited in size. The limited background, however, must be large enough to give an image on the ground glass of the camera somewhat larger than the image of the drop. At the same time, this limited background must be small enough to give a second complete image framed within the circumference of the drop image.

A well-defined contrast in light intensity or color is most essential between the two backgrounds; the sharper the contrast produced, the sharper the image of the drop. This image always assumes the color and light intensity of the general background and, therefore, becomes visible because of its contrast with the limited background. When all of these conditions are fulfilled, a picture as in Fig. 7 appears on the ground glass of the camera.

The limited background can be of any shape. If, for instance, a tape or metal strip is used as a limited background and is positioned parallel to the path taken by a moving drop, high-speed motion pictures can be taken of the drop along its entire path of motion.

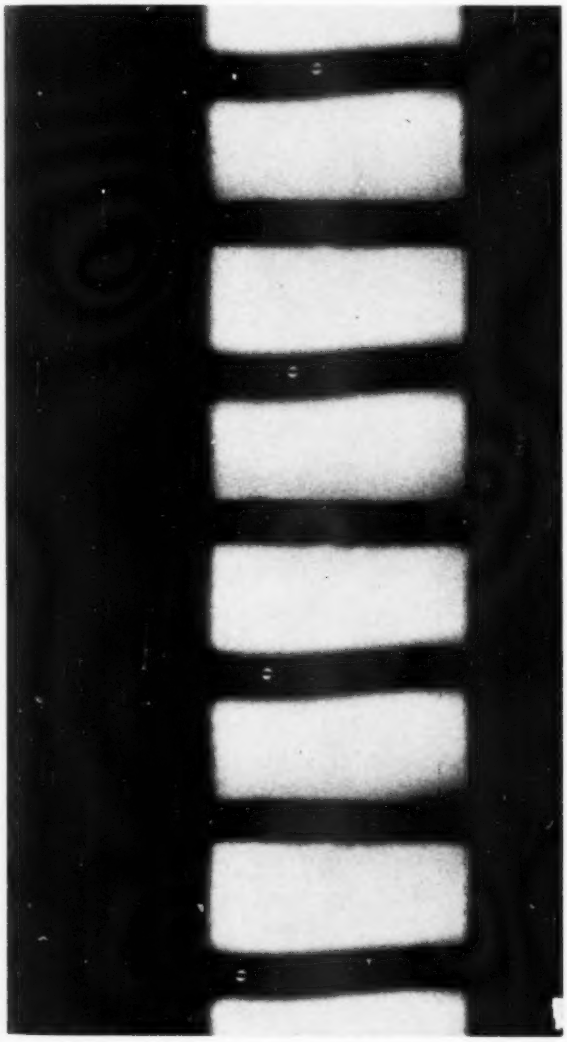

Fig. 10. Enlarged portion of a high-speed, 16-mm motion-picture film of a 50 μ drop (magnification, 60×; 4000 frames/sec.)

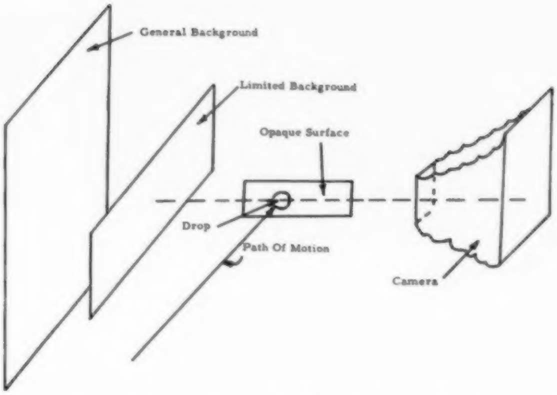

Fig. 11. Experimental setup for photographing drops moving very close to an opaque surface.

This procedure was first verified experimentally at the optical bench. Glass spheres were substituted again for transparent drops. In photographing Fig. 8, the limited background was illuminated, and the general background was kept devoid of light. The sphere, assuming the same color as the general background, is dark in this photo and can be seen in sharp detail against the illuminated limited background. The second image of the limited background also can be seen within the sphere.

High-speed photography of actual drops was attempted using the setup shown in Fig. 9. A narrow metal strip, shielded from all illumination, was used as the limited background. Drops were produced from liquid bis(2-ethylhexyl) hydrogen phosphite by an atomizer. Photographs were taken in a darkened room; the only light entering the objective of the camera was that reflected by the illuminated general background.

Figure 10 is an enlarged portion of a 16-mm high-speed film of a 50-μ drop taken at a speed of 4000 frames/sec (magnification, 60×). The drop appears

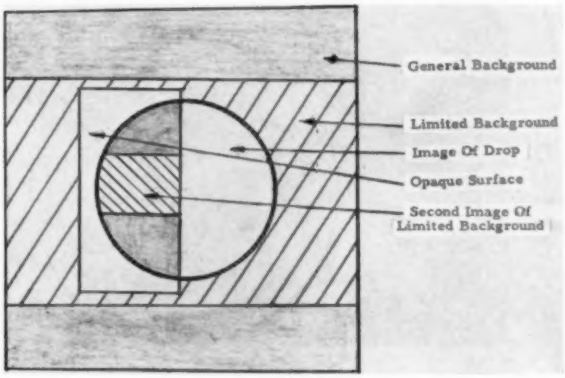

Fig. 12. Typical picture of drop near an opaque surface on ground glass of camera.

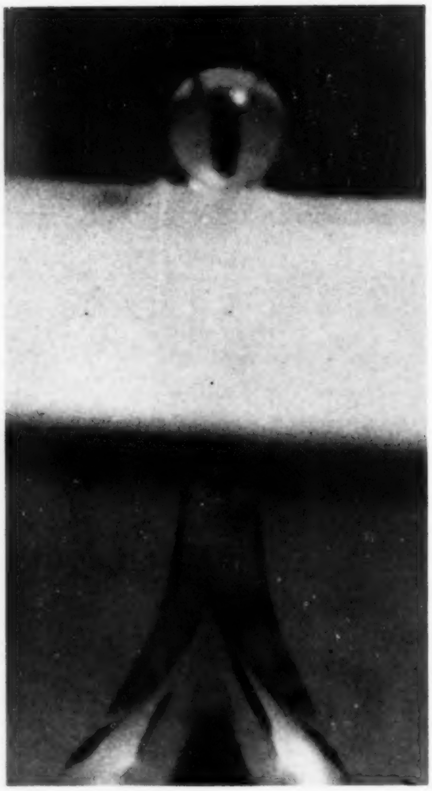

Fig. 13. Glass sphere contacting opaque surface photographed against dark limited background and dull general background.

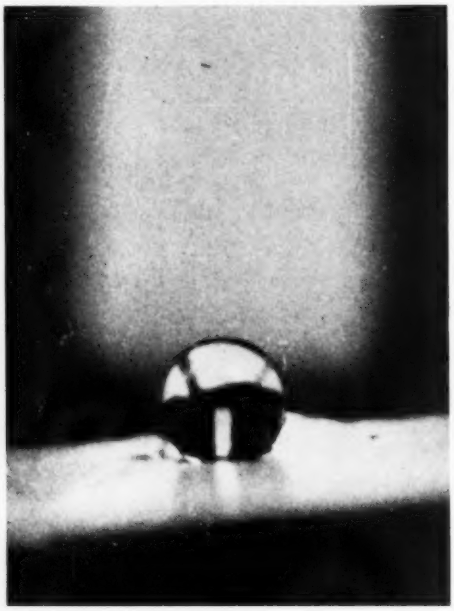

Fig. 14. Glass sphere contacting opaque surface photographed against dark general background and bright limited background.

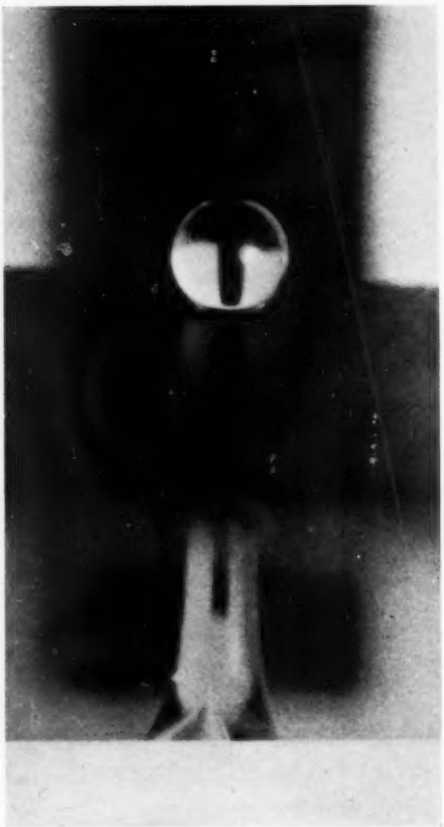

Fig. 15. Glass sphere contacting opaque surface photographed against dark limited background and bright general background.

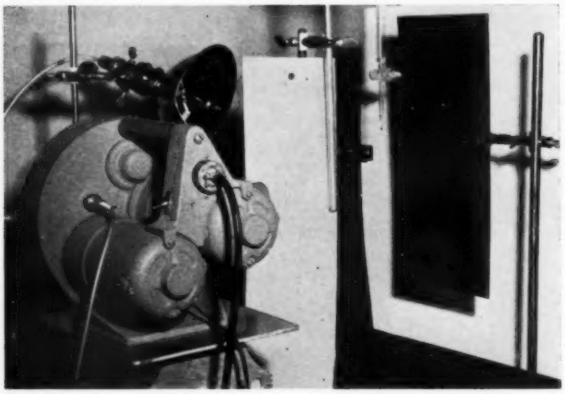

Fig. 16. Experimental setup: high-speed motion-picture camera, source of illumination, burette, light shield, reservoir, limited background, general background.

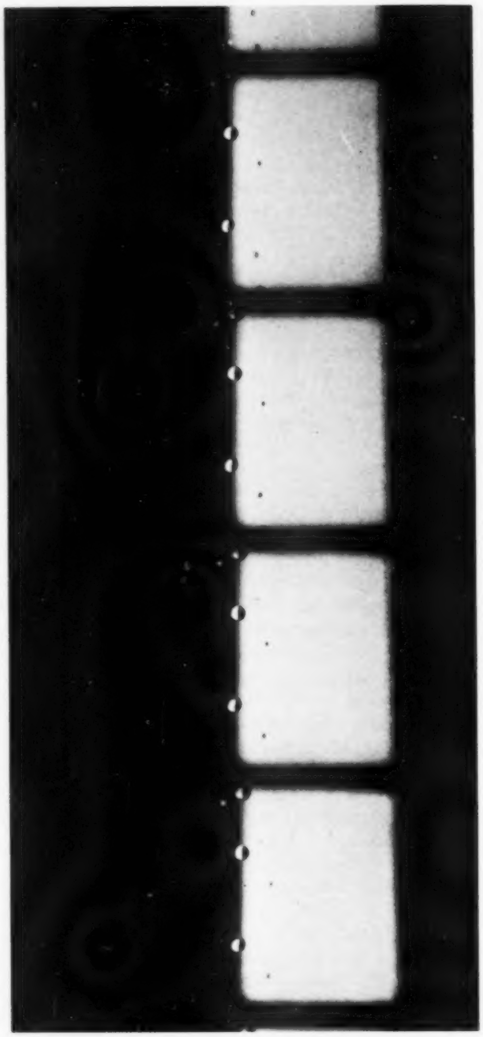

Fig. 17. Enlarged portion of high-speed, 16-mm motion-picture film of a stream of falling drops (magnification, 7×; 4000 frames/sec).

illuminated against the dark limited background, i.e., the metal strip. A second image of the limited background can be seen within the drop.

It is often desirable to photograph transparent drops on, or moving very close to, an opaque surface or target under certain experimental conditions. This can be accomplished quite satisfactorily if the opaque surface is positioned at about 90° to the limited background and contrastingly illuminated, compared with the general and limited backgrounds. Figure 11 is a diagram of such an experimental arrangement. Figure 12 shows how this setup would appear on the ground glass of the camera. This setup can be simplified somewhat for high-speed photography in this special situation.

Figures 13, 14, and 15, photographed under alternative conditions of lighting, show a glass sphere in contact with an opaque surface. In each of these three figures, a second image of the limited background appears within the sphere. In addition, the lower half of the sphere always is illuminated in the same manner as the general background, while the upper portion of the sphere is illuminated in the same manner as the opaque surface. The reason for this additional contrast in drop lighting is the additional image the drop produces from the opaque surface.

Figure 16 is a photo of the experimental setup used in preparing Fig. 17. In this setup, the drops were produced by a fine-tipped burette and allowed to fall by gravity. The optical axis of the camera was aligned so that it fell directly upon the left-hand edge of the dark limited background.

Figure 17 is an enlarged portion of a high-speed 16-mm film taken at 4000 frames/sec. Shown in this photo are two drop streams, one along the edge of the limited background (the larger drops) and one within the region of the limited background (the smaller drops).

Conclusions

High-speed motion-picture photography of transparent drops can be accomplished where it is possible to produce light contrast between the drop and its background sufficient to make the drop visible. Two highly satisfactory methods of producing this contrast were tested experimentally and found to produce an excellent technique that could be used for a variety of investigations in the aerosol field.

The author is indebted to James Ebaugh for his invaluable assistance in all scientific photographic work and to Richard Cogswell and Thomas Purcell for their technical assistance.

References

1. H. Schardin, J. Soc. Motion Picture Engrs. **61**, 273 (1953).
2. N. F. Barnes, J. Soc. Motion Picture Engrs. **61**, 487 (1953).
3. H. L. Green and W. R. Lane, *Particulate Clouds, Dusts, Smokes, and Mists* (Spon, London, 1957).
4. National Defense Research Committee, Division 10, *Handbook on Aerosols*, AEC Report (Government Printing Office. Washington, D.C., 1950).

November 1964 features High-Speed Photography

Applied Optics

Optical Activities in Industry

reported by FRANK COOKE, 66 Summer Street, North Brookfield, Mass.
Mr. Cooke welcomes news and comments for this column which should be sent to him at the above address

In place of Mr. Cooke's column this month, the following is reprinted from Commerce Digest [Vol. V, No. 12 (July 1963)] by kind permission of its Editor and of the Commissioner of Commerce of the Commonwealth of Massachusetts:

American Optical Is World Leader

133-Years Old Firm Has Top Role in Important Space Age Projects

Spectacular space age things are happening in an unspectacular way at the venerable, 133-years old American Optical Co., Southbridge. Little did William Beecher, a jeweler and inventor, dream when he started a little shop to manufacture spectacles in 1833 his enterprise would have worldwide significance in the field of better vision and undisputed leader in the industry. Today American Optical is firmly entrenched in almost every nation of the globe. It has subsidiaries in Chelsea, Buffalo, and Rochester, N.Y., Brattleboro, Vt., Putnam, Conn., Keene, N. H., Frederick, Md., and Pittsburgh, Pa. in the U.S. Its foreign operations include plants in Belleville and Nicolet, Canada, three in Great Britain, one each in Austria, Mexico, Argentina, and Brazil.

People of a century ago did not take as kindly to spectacles as in more recent decades, so the one-man business grew slowly for the first 30 years. Then in 1864 a group of 12 apprentices were hired, including the late George W. Wells. Five years later, Wells' initiative resulted in incorporation, the company did $50,000 worth of business and employed 85 workers. Today it requires more than 10,000 men and women to conduct its $100 million plus annual operation. Up to the turn of the century American Optical turned out spectacle frames and lenses. Even today, the bulk of American Optical products are designed to extend and protect man's physical senses. These products alone number more than 2000 with a range from tiny screws to huge missile trackers, from safety clothing to complex scientific instruments.

Research has played an increasingly important role, and countless new developments which have markedly aided the ophthalmic professions in vision correction, improved industrial safety, and contributed to medical and scientific research. A leading research center of the optical industry of the world is located in Southbridge with a staff of more than 100 scientists and technicians.

One of the newest and most amazing developments is that of fiber optics, a concept permitting the transfer of a complete image or light directly from one place to another without requiring the transmission to be in a straight line. In simple terms, by means of a bundle of hair-fine glass strands encased in a metal tubing, one can "bend" light rays—and a completely undistorted picture—in tight arcs. The company has hardly begun to scratch the surface of the applications of fiber optics, but it is already playing an important part in the medical and research fields. The latest major research and development field in which American Optical, and other American firms, have entered into with almost unprecedented enthusiasm and hope for the future, is the laser. Its potential may have a far greater impact on civilization than is even now suspected and while it is capable of fostering much in human progress it can also be channeled into the science-fiction death ray. While fiber optics is in its infancy and already being used extensively in certain fields, the laser is just beginning to get its eyes open. The laser converts a jumble of helter-skelter light waves into an intense unified narrow band of powerful light. Originally, lasers used ruby crystals, but American Optical's laboratory pioneered and developed an optical glass in which neodymium is a major ingredient which can be cast into any length desired in cylindrical form. The belief is held in some official quarters that within a decade the laser will have been developed into a $100 to $150 million industry in its various forms. According to one American Optical Scientist, "In spectroscopy, if even half what we imagine turns out to be true, lasers will turn, the whole field upside down." The laser's principal promise, even though distant, appears to be in the data processing and communications areas. The intensity and coherence of its light appear to offer media for sending message pulses far superior to any in use today, whether electrical, radar or microwave.

In the medical field, the Lown cardioverter is becoming of great importance in dealing with certain heart ailments. The American Optical oximeter measures the oxygen saturation in the blood in a matter of seconds rather than hours. The Hb-meter is a revolutionary, pocket-sized instrument providing laboratory accurate hemgolobin determinations in less than three minutes. The American Optical microtome slices biological tissues so thin that 254,000 layers would be only 1 inch high.*

In industrial safety, American Optical turns out thermogarb, clothing that withstands molten metal splash at 3000°F, while there are many types of safety goggles, respirators, helmets, and shields.

A wide range of space age products are being turned out in one of American Optical's subsidiaries, such as astronomical observatory equipment, missile range instrumentation, inertial guidance test equipment, aerial reconnaissance equipment, optical systems and components, and analytical test equipment.

The range of manufactured products continues with ophthalmic lenses and frames, eyewear cases, refracting equipment, orthoptic instruments, diagnostic instruments, optical machinery, microscopes and accesories, measuring instruments, projection equipment, field charting instruments, a long list of military products, personal leather goods, artificial eyes.

Thus it is, in the south central part of the Commonwealth lies an industry that is proud of its quality products, its far seeing vision of new things beneficial to all people and the ability of its scientists and workers to compete successfully in many phases of this increasingly scientific world. Visitors are ever welcome to visit the company's new exhibit hall adjacent to the main office and see for themselves some of the hundreds of products. It is open from 8.30 a.m. to 4.30 p.m. each weekday for individual visitors and arrangements can be made for tours by larger groups.

---

* *Ed. note:* This was presumably "100,000 layers would be only 1 cm high" before it was translated into English.

A Universal Spectrophotometer

Wilbur Kaye

By placing the sample between the monochromator of a prism-grating spectrophotometer, considerable versatility is obtained. Absorption, emission, fluorescence, excitation, polarized fluorescence, polarized excitation, phosphorescence, light scattering, and other types of spectral data may be obtained. Readily interchanged accessories fitting into the sample compartment are utilized. The instrument may be used in three modes—single-beam, double-beam time-shared, or double-beam space-shared. The monochromators may be used independently or simultaneously. High-brilliancy mercury and xenon sources are provided in addition to the standard hydrogen and tungsten lamps.

Introduction

Demands are being placed on spectroscopists to make many spectral observations besides absorption. Few spectrophotometers are designed for universal use and the spectroscopist must resort to the assembly of modules. Recently, Beckman Instruments designed a custom spectrophotometer for the University of Southern California that is unusually versatile and can be easily used to collect absorption, emission, fluorescence, excitation, polarized fluorescence, phosphorescence, light scattering, and other types of spectral data. This instrument model (DK-U) consists of a far ultraviolet prism monochromator (DK-1A) and a grating monochromator mounted end-to-end on a rigid base. The sample compartment is located between the two monochromators. Figure 1 is a photograph of the basic instrument. It consists of a spectrophotometer mounted on a desk and a floor-mounted relay rack containing the electronics and recorder. The principle of operation can be seen in the schematic diagram, Fig. 2. Source radiation modulated at 480 cps is dispersed by a synthetic quartz prism monochromator. This monochromator has very low stray light and, of course, does not suffer from overlapping orders. The dispersed radiation is optionally split into sample and reference paths by a rotating mirror then recombined with a second rotating mirror. The space between these two mirrors has been enlarged over that in a standard DK spectrophotometer in order to accept the necessary accessories. The recombined beam passes through an LiF field lens to a three-position mirror. In one position the beam can be deflected to the standard detector compartment, and in this position the instrument operates as a standard far ultraviolet DK-1A spectrophotometer. The second position of the mirror reflects the dispersed radiation out the front of the instrument for special applications. A third position rotates the mirror out of the beam, and the radiation falls on the entrance slit of a grating monochromator. The radiation is then dispersed and is detected by a photomultiplier. The wavelength of the two monochromators may be scanned independently or simultaneously. The amplified signals from any one of several detectors is recorded on a Brown strip chart recorder.

Sources

The 30-W Beckman tungsten and hydrogen lamps are supplied as standard parts. High pressure xenon and mercury lamps are mounted on a special backplate and operated from a dc power supply located in the central part of the desk on which the spectrophotometer rests (Fig. 1). PEK X-75 xenon and PEK 109 super high-pressure mercury lamps are used. Figure 3 shows the comparative outputs of these lamps. While these lamps are of relatively low-power dissipation, they are the most brilliant lamps available. They are located as close on axis of the spherical source condensing mirror as possible and fill the entrance slit to a height of 10 mm. Other lamps in wattages up to 1 kW have been tried in this instrument without yielding any more light through the monochromator. All of the high-intensity xenon and mercury lamps are subject to flicker (arc wander at constant current). When flicker occurs the instrument must be operated in a double-beam mode.

The author is with Beckman Instruments, Inc., Fullerton, California.

Received 28 February 1963.

Presented at the 14th Pittsburgh Conference on Analytical Chemistry and Applied Spectroscopy, March 1963.

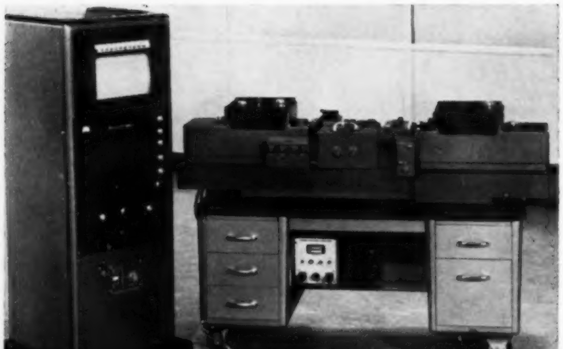

Fig. 1. Photograph of the DK-U universal spectrometer.

The tungsten, xenon, and mercury lamps are mounted on interchangeable air-cooled backplates. The hydrogen lamp (with far-ultraviolet transmitting window) is permanently mounted in the forward part of the source compartment and is engaged by a two-position mirror.

In some instances the Beckman low-pressure mercury lamp is desired. It is mounted on a special backplate and operated by the hydrogen lamp power supply located at the bottom of the relay rack (Fig. 1).

Prism Monochromator

This is a standard far uv DK-1A monochromator with a 30° prism of hydrothermally grown crystalline quartz. The face of the prism is 2.5 × 5 cm. The collimator is 50 cm in focal length and is coated with MgF_2 over aluminum. The slits are of 61-cm radius of curvature, 10 mm high, and with a maximum width of 2 mm. Apertures limiting slit height to 1.5 and 4 mm are mounted on a slide. The wavelength range of this monochromator extends from 160 to 3500 mμ. Specifications on this monochromator have been published.[1]

Grating Monochromator

The grating monochromator uses a Littrow mounting with a 50-cm focal length collimator. The grating measures 52 × 52 mm with 600 lines/mm blazed at 500 mμ in the first order. It is calibrated for use between 300 and 1000 mμ in the first order and between 200 and 350 mμ in the second order. The readout is linear in wavelength with dial markings every 5 Å in the first order and 2.5 Å in the second order. The slits have a radius of curvature of 335 cm, a maximum height of 10 mm, and a maximum width of 5 mm. The dispersion is 33 Å/mm in the first order and 17 Å/mm in the second order.

Modulators

The modulators are in the form of disks containing 8 openings. The disks are rotated by hysteresis synchronous motors at 3600 rpm resulting in 480-cps modulation. They are located immediately in front of the entrance slits of the two monochromators. Switches permit the use of either or both modulators. A phase adjustment control (variable capacitor on the motor) allows one to set the two modulators out-of-phase. For most studies the modulator over the prism slit is used and the second modulator is stopped at a position allowing light to pass into the grating monochromator. The second modulator is used only when studying phosphorescence spectra. The two modulators are then operated out-of-phase. The time lapse between the end of excitation and the beginning of observation is about 250 μsec. Thus phosphorescence from samples with a lifetime longer than about 200 μsec can be measured and distinguished from fluorescence.

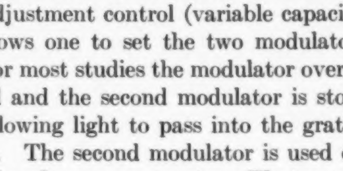

Fig. 2. Schematic diagram of the Beckman DK-U spectrometer.

Beam Splitter

The conventional 15-cps beam splitter of the DK-1A instrument is retained. The cage about the sample compartment has been enlarged to approximately 18.3 × 12.7 cm.

Filters

Holders for 2 × 2 in. (5 × 5 cm) filters are located in front of the 7200 and PbS detectors and before the entrance slit of the grating monochromators. Filters or screens may be needed to attenuate light, sort orders of the grating, or simply to reject exciting light. Corning filters 0-52, 0-53, 3-74, 3-72, 3-68, and 7-54 are most useful.[2] Electroplated screens with conical holes and transmissions from 0.1 to 22.5% are used for attenuation.[3]

Detectors

The 7200 photomultiplier and PbS detectors are located at the rear of the instrument and are used to monitor only the light from the prism monochromator. A 1P28 detector is used to measure light from the grating monochromator. A special backplate is available for an FW-118 photomultiplier with an S-1 surface. Other 1P28 detectors are located in accessories. All the photomultipliers except the FW118 are operated at 600 V across the dynode string.

Amplifiers

The electronic amplifiers are separated into preamplifiers and power amplifiers. Two sets of these amplifiers are provided. One preamplifier (standard) is located in the rear detector compartment. It amplifies only the signal from the 7200 photomultiplier and PbS detectors. The second (auxiliary) preamplifier serves all the other detectors. Separate gain controls for these two amplifiers are provided as well as a 20:1 attenuation on the photomultiplier load resistors. This allows a continuous control of gain by a factor of 500:1. The frequency response of the auxiliary preamplifier has been extended for phosphorescence measurements.

Recorder

A modified Brown ratio recorder with a 1-sec response is used. Linear and absorbance slidewires are furnished.

Modes of Operation

There are three basic modes for operation of this instrument: single-beam, double-beam time-shared, and double-beam space-shared. In the single-beam or energy mode, the beam splitter is stopped and a fixed voltage is placed across the ends of the recorder slidewire. This mode is often used for scanning emission, phosphorescence, and fluorescence spectra. In the double-beam, time-shared mode the beam splitter is rotated and the output from any one of the detectors is sorted into sample and reference signals by the commutator on the beam-splitter shaft. Either amplifier may be used. The recorder plots the ratio of sample and reference signals. This mode is most often used in absorption, fluorescence, and excitation spectroscopy.

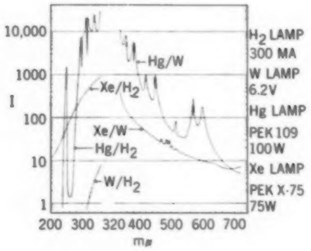

Fig. 3. Relative intensity of sources.

In the double-beam space-shared mode two detectors and two amplifiers are used. The recorder plots the ratio of these two signals. This mode is used for polarized fluorescence.

Scanning

Synchronous motors are used to drive the wavelength scrolls of the two monochromators, the recorder, and the accessories. A switch permits the simultaneous engagement of the recorder with either or both monochromators or with any accessory. The recorder can be operated at chart speeds from 0.75 to 22.5 cm/min. The prism readout is linear in wavelength with a tenfold change in scale expansion at 360 mμ. Scanning speeds from 0.075 to 225 mμ/min below 360 mμ and 0.75 to 2250 mμ/min above 320 mμ are provided. The grating wavelength drive is similar to that of the prism drive with an added 2:1 gear for second-order operation.

Purging

The source housing, prism monochromator, sample compartment, and 7200 detector housing may be purged with nitrogen. This is necessary for operation below 200 mμ.[1] It may also be necessary to prevent water condensation on cooled components. AR-3 cylinders of liquid nitrogen (with heat exchanger for evaporation of nitrogen at the demand rate) are preferred. Nitrogen is consumed at rates from 0.1 to 2 liters/sec.

Resolution

Since the prism and grating monochromators may be used separately or jointly, their resolution must be similarly known. Figure 4 shows the dispersion of the prism and the grating in first and second orders. The resolution of the prism monochromator varies drastically with wavelength. It is superior to that of the grating monochromator below 240 mμ. The limiting resolution of the grating in the first order is about 0.50 Å and in the second order is about 0.25 Å. Figure 5 shows the shape of the slit function for the prism monochromator alone and both monochromators as evidenced by scanning the emission spectrum of the 2536-Å line of a low-pressure (Beckman) mercury lamp.

The emission spectrum of the hydrogen lamp provides a convenient test of resolution and also of wavelength calibration in the far ultraviolet and visible

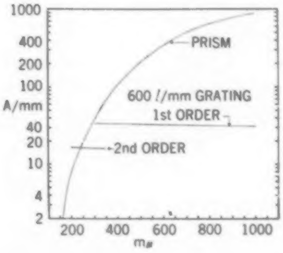

Fig. 4. Reciprocal dispersion of the 50-cm monochromator.

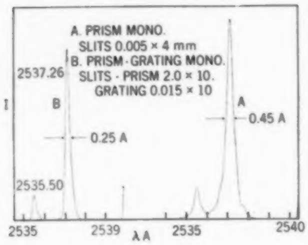

Fig. 5. Limiting resolution of the prism and grating monochromators.

regions. Figure 6 is a portion of this spectrum. The far-ultraviolet spectrum was obtained with the prism monochromator only when purged with nitrogen (and the half-intensity width of the lines is about 0.15 Å). The visible spectrum was obtained with both monochromators.

Stray Light

The stray light of any instrument is a function of the source and detector as well as the monochromator and the type of operation. Considering the three (or more) detectors, the four sources, and three distinctly different types of operation, absorption, fluorescence, and phosphorescence, the measurement of stray light will be complicated. The stray-light level of the prism monochromator for absorption work in the far ultraviolet region has been studied. The stray light above 210 mμ is less than 0.01%.[1] Figure 7 shows the stray-light level in the grating monochromator for a line source and the 1P28 detector. In order to obtain this spectrum the prism monochromator (slit-width 0.070 × 10 mm) was used to sort the 365-mμ emission from the high-pressure mercury lamp. The prism monochromator wavelength was fixed while the grating monochromator (slit-width 0.10 mm) was scanned. The gain and slit-width was such as to place the primary line well off scale. The ordinate figures are percentages of the intensity of the primary line ascertained by placing a screen of known transmittance in the beam. The intense line at "730" mμ is the 365-mμ radiation dispersed in the second order. When wavelengths shorter than 365 mμ are used for exciting fluorescence spectra it is usually desirable to use a filter (Corning 0-53, 0-52, or 3-74) to remove the second-order exciting line.

Between 400 and 700 mμ the stray light arising from a line source at 315 mμ is less than 0.003% of the 365 mμ line. The second order of the 365 mμ line has 10% the intensity of the first-order line due to the ratio of grating blaze efficiency at these wavelengths. The apparent increase in stray light between 365 and 400 mμ in Fig. 7 is due to the slit function of the prism monochromator rather than the grating monochromator.

Transmission Measurements

For most transmittance measurements, the prism monochromator alone should be used. However, where high resolution above 240 mμ and very low stray light is needed, both monochromators may be employed. Correction for defocusing effects may be necessary when using both monochromators for transmittance measurements.

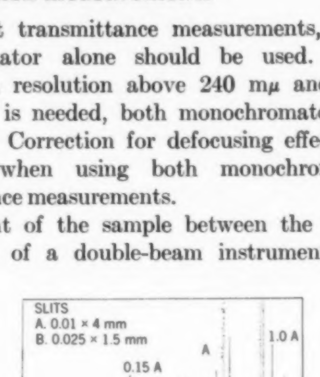

Fig. 6. Emission spectrum of the hydrogen lamp using both monochromators.

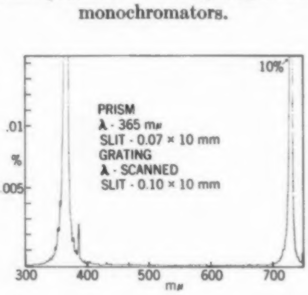

Fig. 7. Stray-light test of the grating monochromator for emission measurements.

Placement of the sample between the two monochromators of a double-beam instrument can pose problems for transmittance measurements with a servo-controlled slit system. If the sample and reference optical paths between the two intermediate slits are not equal, the apparent transmittance changes, due to defocusing of the prism exit slit image on the entrance slit of the grating monochromator by the field lens in the sample compartment. This condition will be produced by placing sample cells of unequal length or different refractive index in sample and reference paths. If the image of the exit slit of the prism monochromator is smaller than the entrance slit of the grating monochromator this effect will be negligible.

Figure 8 is a transmittance spectrum of a didymium filter and a 100% (air-air) background curve. While the slits of the prism monochromator were servo operated and ranged from 0.3 to 0.02 mm, the 100% line varied by only ±1 %. The didymium filter does not test the resolution or low stray-light possibilities of the double monochromator. The grating slits were set at 3.0 mm so the resolution is determined by the prism monochromator.

Fluorescence Spectroscopy

Fluorescence measurements may be made in any of the three modes with one or both monochromators and with any one of several accessories. The accessory ordinarily used for fluorescence measurements is outlined in Fig. 4. It fits into the sample compartment and consists of two pairs of mirrors and two water-jacketed cell holders. The mirrors reflect the exciting light onto sample and reference cells and then return the light fluorescing at 90° into the light path of the instrument. When using this accessory the instrument can be operated in the single-beam (energy) mode or the double beam, time-shared mode.

In the single-beam mode, the recorder plots the spectral energy as detected by the photomultiplier. Consequently the pen motion is a function of: (a) The source intensity, (b) the bandpass of the exciting monochromator, (c) the transmittance of the optics, (d) the quantum efficiency of the sample, (e) the absorbance of the sample at the exciting wavelength, (f) the absorbance of the sample at the fluorescing wavelength, (g) the bandpass of the grating monochromator (or filter), and (h) the sensitivity of the detector at the fluorescing wavelength. Figure 9 is a single-beam fluorescence spectrum of a solution containing 10 ppb of quinine sulfate in 0.025*N* sulfuric acid along with a spectrum of the solvent obtained in the single-beam mode. Excitation was obtained using the high-pressure mercury lamp with the prism monochromator set at 338 mμ. The fluorescence spectrum was scanned with the grating monochromator without a filter. Three peaks are evident. The peak at 338 mμ is due to Rayleigh scattering of the exciting radiation. Raman scattering from the water is responsible for the 375-mμ peak. The fluorescence of the quinine sulfate exhibits a maximum intensity at 445 mμ.

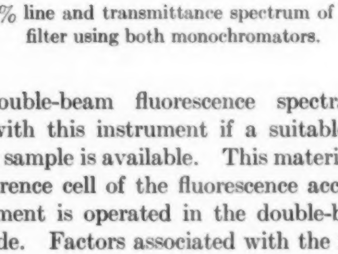

Fig. 8. 100% line and transmittance spectrum of a didymium filter using both monochromators.

True double-beam fluorescence spectra can be obtained with this instrument if a suitable reference fluorescing sample is available. This material is placed in the reference cell of the fluorescence accessory and the instrument is operated in the double-beam time-shared mode. Factors associated with the instrument are canceled leaving only the absorbance and quantum efficiency of the sample relative to the reference material. Considerable research remains to be done to select ideal reference materials. Quinine sulfate has been studied as a standard[4] and may be used as a reference fluorescing material; however, its fluorescent intensity at concentrations producing negligible self-absorption is weak and it is useful over only a narrow wavelength interval. Figure 10, curve A, shows the fluorescence spectrum of solid uranium acetate obtained in the single-beam mode. Curve B is the single-beam fluorescence (and phosphorescence) curve for a magnesium tungstate phosphor No. 1027 obtained from the National Bureau of Standards. Curve C is the double-beam record obtained by placing the uranium acetate in the sample channel and the phosphor in the reference channel. The 480-cps modulator on the grating monochromator was used in all three spectra. There is an obvious intensity variation among the emission peaks of uranium acetate between the curve A and C. The phosphor compensates for the sharp decrease in sensitivity of the 1P28 detector at wavelengths greater than 500 mμ. The emission peak at 590 mμ evident in curve C is almost absent in curve A. If the emission spectra of this phosphor were known in absolute units all instrumental parameters varying with wavelength and time could be compensated.[5]

By using the polarized fluorescence accessory (with the polarizer removed) described below, it is possible to make fluorescence measurements in the double-beam, space-shared mode. In this case the 7200 detector serves to monitor the exciting radiation transmitted through the sample. The recorder plots the ratio of fluorescent radiation (filtered) relative to the exciting (transmitted) radiation.

Double-beam operation wherein the reference channel monitors the exciting radiation has been reported before.[6–8] It is useful in compensating for source fluctuations; however, this is not a "true" double-beam mode because the wavelength of sample and reference beams are different. Strictly speaking, wavelength scans should be made in a double-beam space-shared mode only when employing wavelength invariant detectors.

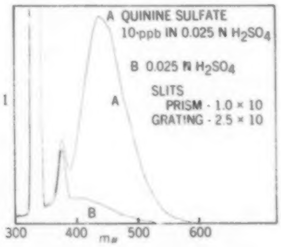

Fig. 9. Fluorescence spectrum of quinine sulfate in the single-beam modes.

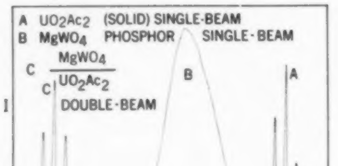

Fig. 10. Single- and double-beam fluorescence spectra of uranyl acetate and magnesium tungstate.

Excitation Spectroscopy

Excitation measurements allow the determination of absorption spectra of fluorescent materials at concentrations that produce negligible absorption. The same accessory is used for both fluorescence and excitation measurements. The wavelength of exciting light is scanned with the prism monochromator. Discrimination between exciting and fluorescing radiation may be made with either a filter or the grating monochromator. Figure 11 illustrates the excitation spectrum of quinine sulfate using both of these methods. The xenon lamp was used as a source in the single-beam mode. Curve A was obtained using a Corning 3-72 filter and the 7200 detector while curve B utilized the grating monochromator. The bandpass character of the grating monochromator is evidenced by the off-scale peak around 450 mμ. The peaks at 250 and 350 mμ correspond to the absorption maxima of quinine sulfate. Considerably more sensitivity is obtained using the filter than the grating monochromator in this application.

If a material of known quantum efficiency is available the excitation spectra may be obtained in the double-beam mode and the data reduced to absolute terms.

Phosphorescence Spectroscopy

Phosphorescence, emission, and excitation spectra may be obtained using the fluorescence accessory and both 480-cps modulators. The fluorescence accessory is designed to accept cryogenic cells; however, these have not yet been fabricated. Measurements may be made with either or both modulators on. Phasing of the second modulator is accomplished by varying the motor capacitor while observing the recorder output (single-beam) when both monochromators are set to the same wavelength. Figure 12 shows the spectra obtained in the single-beam mode of a magnesium arsenate (containing Mn) phosphor obtained from the National Bureau of Standards. The phosphor was mounted on a piece of white paper using Duco cement as a binder. The 365-mμ radiation from the high pressure mercury lamp served for excitation. The upper (A) curve was recorded using only the modulator in front of the grating monochromator. The sharp emission peaks around 650 mμ are due to the phosphor. The broad peak at 460 mμ arises from fluorescence of the paper on which the phosphor is mounted. The off-scale peak at 365 mμ is reflection of the exciting light.

Curve B of Fig. 12 was obtained when both modulators were rotating in an out-of-phase condition. The phosphor peaks at 650 mμ are present but weakened. The paper fluorescence and reflected exciting radiation have a negligible lifetime, hence, they are completely rejected. The phasing of the grating modulator is adjusted using the exciting radiation.

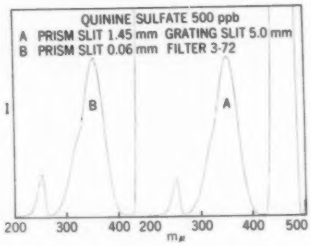

Fig. 11. Excitation spectrum of quinine sulfate.

Phosphorescence excitation spectra may be obtained by scanning the wavelength of exciting radiation with the prism monochromator.

Polarized Fluorescence

The optical diagram for this accessory is drawn in Fig. 2. The polarizer consists of a special Glan Thompson prism. The calcite for this prism is specially selected for transmission down to 215 mμ. The prisms are cemented with glycerol and are demountable. A small constant speed motor rotates the polarizer at 4 rpm. The polarizer and motor are on a subassembly that can be placed either before or after the sample or removed completely. A 1P28 photomultiplier detector is mounted on this accessory. The holder for this detector is water jacketed to allow an interchange with the high pressure xenon or mercury lamp. Space is provided between the sample and the detector for apertures and a filter. Controls are provided for power to the motor and a two-step gain and off control to the photomultiplier. In order to provide sufficient space, the sample is located in the reference channel of the instrument. A switch disengages the beam-splitting motor and commutator when using this accessory.

This accessory is capable of operation in the single-beam or double-beam space-shared modes. In the single-beam mode the output of the 1P28 detector is recorded directly. In the double-beam space-shared mode the ratio of signals from the 1P28 detector and 7200 detector (transmitted light) is recorded. The accessory can be used for 90° fluorescence, excitation, or light-scattering measurements in the single-beam or double-beam space-shared modes with or without the polarizer.

Figure 13A illustrates the behavior of this accessory for polarized light-scattering measurements. A dilute solution of collodion was used as the sample. Light scattered at 90° from this sample is highly polarized. For these measurements light of 550 mμ was used and no filter was employed between the sample and the detector. The single-beam mode was used.

Figure 13B shows the polarized fluorescence obtained from a solution of α naphthol in ethanol when excited at 365 mμ. The polarization ratio

$$p = \frac{I_{\parallel} - I_{\perp}}{I_{\parallel} + I_{\perp}}$$

measured from this curve is 1.6%. The low polarization can be interpreted as caused by a long fluorescence lifetime relative to the rotational mobility of the α naphthol molecule. A polarization ratio, p, of 20% was obtained when the α naphthol was dissolved in a viscous glycerine solvent and excited by 365-mμ radiation.

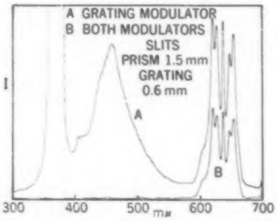

Fig. 12. Fluorescence and phosphorescence spectra of magnesium arsenate phosphor on paper.

Polarization spectra are often valuable and have been obtained by manual computation of the polarization, p, as a function of the wavelength of exciting or fluorescing radiation.[9] It is possible to obtain the necessary spectral information in a much less time-consuming manner with this accessory. Figure 14 is a single-beam excitation spectrum of a dilute solution α naphthol in glycerine obtained while the polarizer was continuously rotating. A Corning 3-72 filter with a cutoff of 430 mμ was inserted between the sample and the detector. The xenon lamp was used as a source.

The highly modulated spectra at wavelengths longer than 430 mμ are due to scattered light from dust particles and molecules. Random motion of these particles introduces some noise into the scattering portion of the spectrum. Exciting light between 340 and 430 mμ produces a fluorescence having a polarization of about 20%. This fluorescence may be partly due to fluorescence of the filter employed. Another transition occurs at 315 mμ having a polarization of only about 4%. A third transition produced by light of 240 mμ exhibits no detectable polarization. Presumably these varying polarizations reflect the lifetime of the transition between singlet and triplet states of the α naphthol molecule.[10]

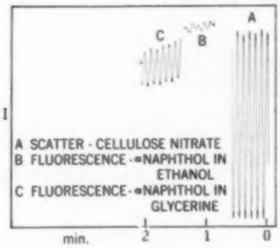

Fig. 13. Behavior of accessory for polarized light-scattering and polarized fluorescence measurements.

Other Accessories

Accessories have been designed for light scattering, fluorescence at small angles of incidence, and refractive index measurements. Other accessories for chromatogram plate scanning, and phosphorescence lifetimes are under study. In addition, existing Beckman components such as the flame and reflectance accessories may be attached to this instrument with a minimum of effort.

The following people have made important contributions to the design and construction of this instrument: F. Aladjem of the University of Southern California, D. Bishop, G. Keahl, M. Lu, J. McDaniel, B. Roeder, and C. Ronkes, all of Beckman Instruments.

References overleaf

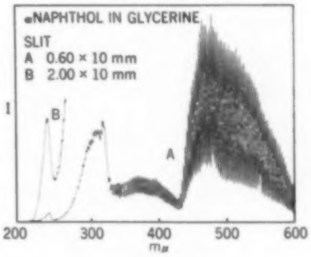

Fig. 14. Polarization modulated excitation spectrum of α-naphthol in glycerine.

References

1. W. I. Kaye, Appl. Spectry. **15,** 89 (1961).
2. Corning Glass Works, Corning, N.Y.
3. Pyramid Screen Corp., 181 Harvard St., Brookline 48, Boston, Mass.
4. W. H. Melhuish, J. Phys. Chem. **64,** 762 (1960).
5. C. A. Parker, Nature **182,** 1002 (1958).
6. F. R. Lipsett, J. Opt. Soc. Am. **49,** 673 (1959).
7. D. W. Moss, Clin. Chim. Acta **5,** 283 (1960).
8. W. H. Melhuish and R. H. Murashige, Rev. Sci. Instr. **33,** 1213 (1962).
9. G. Weber, Biochem. J. **75,** 335 (1960).
10. R. J. Keirs, R. D. Britt, Jr., and W. E. Wentworth, Anal. Chem. **29,** 202 (1957).

Meetings Calendar

December

1–3	Assoc. for Research in Ophthalmology, Ann. Mtg., Iowa City, Iowa
4	OSA Natl. Capital Sect. Mtg., Georgetown U., Indian Dyes by W. R. Brode *H. K. Hammond III, NBS, Wash. 25, D.C.*
11	ARPA Lecture, the Pentagon, Semiconductor Research by W. Shockley *E. Haynes, ARPA, Washington 25, D. C.*
9–12	1963 Fall URSI Mtg., U. of Wash., Seattle *M. G. Morgen, Dartmouth Col., Hanover, N.H.*
17	OSA Rochester Sect. Mtg., Cutler Union, Correlation Interferometry with Applications to Lasers and Astronomy by H. Gamo *J. H. Altman, Research Labs, Eastman Kodak Co., Rochester, N.Y. 14604*
19–21	APS, Pasadena, Calif. *W. A. Nierenberg, U. of Calif., Berkeley 4, Calif.*
26–31	AAAS, 130th Ann Mtg., Cleveland, Ohio *AAAS, 1515 Mass. Ave. N.W., Wash. 5, D.C.*

1964

—	Colloquium on Magnetism, Nottingham, England *IUPAP, Institut d'Optique, 3 boul. Pasteur, Paris 15e, France*

January

9	OSA Rochester Sect. joint mtg. with SPSE, Dryden Theater, Fiber Optics by J. W. Hicks *J. H. Altman, Research Labs, Eastman Kodak Co., Rochester, N.Y. 14604*
19–24	ACS Natl. Mtg., Denver, Colo. *ACS, 1155 16th St. N.W., Wash. 6, D.C.*
21	OSA Rochester Sect. Mtg., Cutler Union, Some Unusual Optics by H. Polster *J. H. Altman, Research Labs, Eastman Kodak Co., Rochester, N.Y. 14604*
22–25	12th Ann. Physics Show, Statler-Hilton Hotel, N.Y.C. *T. Vorburger, AIP, 335 E. 45 St., N.Y., 17, N.Y.,* APS *K. K. Darrow, 538 W. 120 St., N.Y. 27, N.Y.,* and AAPT *E. U. Condon, Univ. of Colorado, Boulder, Colo.*
29–31	Am. Meteorological Soc., Ann. Mtg., Los Angeles *AMS, 45 Beacon St., Boston 8, Mass.*

February

19	OSA Natl. Capital Sect. Mtg., Johns Hopkins Homewood Campus, Baltimore, Spectroscopic Research at JHU by G. H. Dieke *H. K. Hammond III, NBS, Wash. 25, D.C.*
19	OSA Chicago Sect. Mtg., Axicons and Their Uses by J. H. McLeod *C. R. Lambrecht, 7729 N. Ashland Ave., Chicago 31, Ill.*
27–29	APS, Tucson, Ariz. *K. K. Darrow, 538 W. 120 St., New York 27, N.Y*

March

2–6	15th Pittsburgh Conf. on Analytical Chem. and Appl. Spectroscopy, Pittsburgh, Pa. *J. O. Frohliger, Duquesne U., Pittsburgh 19, Pa.*
4–6	Thermal Radiation of Solids Symp., Sheraton-Palace Hotel, San Francisco *W. D. Harris, Eng. & Sci. Ext., U. of Calif., Berkeley 4, Calif.*
15–21	Am. Soc. of Photogrammetry, Am. Cong. on Surveying and Mapping, Washington, D.C.

April

—	OSA Natl. Capital Sect. Mtg., Georgetown U., Far Infrared Optics by R. C. Lord *H. K. Hammond III, NBS, Wash. 25, D.C.*
—	Internatl. Measurements and Instruments Conf., 3rd, Stockholm *G. Ljungberg, Royal Swedish Acad. of Engin. Science, Box 5073, Stockholm, Sweden*
—	Am. Ceramic Soc. Glass Div. Chicago *J. Rood, Bausch & Lomb, Rochester 2, N.Y.*
1–3	**Optical Society of America Spring Meeting, Sheraton-Park Hotel, Washington, D.C.** *M. E. Warga, OSA, 1155 16th St. N.W., Wash. 6, D.C.*
5–10	ACS Natl. Mtg., Phila., Pa. *ACS, 1155 16th St. N.W., Wash. 6, D.C.*
5–10	Asia-Pacific Acad. of Ophthalmology, 2nd Cong., Melbourne *R. N. Mellor, 82 Collins St., Melbourne, C1, Australia*
11–13	ISA Instrumentation Div. 4th Ann. Symp. on Measurement and Control, Tampa, Fla.
12–17	SMPTE, 95th Semiann. Conv., Los Angeles, Calif. *SMPTE, 55 W. 42 St., New York 36, N.Y.*
17–18	APS N.Y. State Sect. Spring Mtg. and Symp. on Modern Aspects of Resonance Physics, Corning Glass Center *J. T. Kerr, Corning Glass Works, Corning, N.Y.*
28–May 2	SPSE Internl. Conf. of Photographic Science and Engineering, American Hotel, N.Y.C.

May

—	Soc. of Technical Writers and Publishers, 11th Ann. Conv., San Diego, Calif.
4–5	Inter-Soc. Color Council, Statler-Hilton Hotel, NYC *R. M. Evans, Eastman Kodak Co., Rochester 4, N.Y.*
5–9	15th Natl. Science Fair-Internatl., Baltimore, Md. *Science Service, 1719 N St. N.W., Wash. 6, D.C.*
2nd week	French Soc. of Ophthalmology, 71st Cong., Paris *M.-A. Dollfus, Soc. Française d'Ophthalmologie, 27, rue du Faubourg-St.-Jacques, Paris 16, France*
19–21	PTG Microwave Theory & Techniques Internatl. Symp., Internatl. Hotel, Idlewild Airport *L. Swern, Sperry Gyroscope Co., Gt. Neck, L.I., N.Y.*
20–23	Acoustical Soc. of Am. NYC *W. Waterfall, 335 E. 45 St., New York 17, N.Y.*
25–29	French Soc. of Physical Chem., 14th Ann. Mtg., Bordeaux *G. Emschwiller, Soc. de Chimie Physique, 10, rue Vauquelin, Paris 5, France*
26–28	CIBA Found. Symp. on Physiology & Experimental Psychology of Color Vision, London *41 Portland Pl., London W. 1, England*
26–28	AFIPS, Spring Joint Computer Conf., Washington, D.C. *P. Huggins, AFIPS, P.O. Box 55, Malibu, Calif.*

June

—	APS, summer mtg., Denver, Colo. *K. K. Darrow 538 W. 120 St., New York 27, N.Y.*
7–13	European Opthalmological Soc., 2nd Cong., Vienna *J. François, 15 place de Smet de Naeyer, Ghent, Belgium*
8–10	PIB Symp. on Quasi-Optics, Statler-Hilton Hotel, N.Y.C. *L. Felsen, Polytechnic Inst. of B'klyn, 55 Johnson St., B'klyn 1, N.Y.*
15–26	AFOSR Seminar on Communications and Cybernetics, Cloudcroft *J. R. Foote, P.O. Box 1053, Holloman AFB, N.M.*
16–18	Conf. on Precision Electromagnetic Measurements, Boulder, Colo. *NBS Office of Technical Information, Wash. 25, D.C.*
21–26	ASTM Ann. Mtg., Conrad Hilton Hotel, Chicago *ASTM, 1916 Race St., Philadelphia 3, Pa.*

Photometric Accuracy of Infrared Spectrophotometers

James E. Stewart

A method for photometric calibration of infrared spectrophotometers is based on the use of a secondary transmittance standard of calcium fluoride whose transmittance has been established with a rotating sector. The transferability of intensity data among Beckman IR-7's has been studied by measuring the absorption bands of indene. The average deviation from the mean values of 10 indene bands measured on five calibrated instruments is 0.8% transmittance. It is suggested that the residual differences after calibration are due to small variations in slit function among the instruments.

Introduction

It is generally recognized by infrared spectroscopists that band intensities measured with different prism instruments differ by amounts too large to permit transfer of data. This unfortunate state of affairs has been attributed to the use of instruments having effective bandwidths wider than the bands being measured. It has long been the hope of spectroscopists that, one day, instruments providing high resolution would be readily available and that through their use, absolute, or at least transferable, intensity data could be recorded. Today, there are available at least one-half dozen varieties of grating spectrophotometers capable of at least 2 cm^{-1} resolution with signal-to-noise ratio adequate for quantitative measurements. This paper* is a report of a study on transfer of intensity data among several specimens of one of these grating instruments, the Beckman IR-7.

Experimental

Five IR-7 spectrophotometers were studied. Two of these were new instruments ready for shipment to their new owners; the other three had been used for periods of six months to a year in the laboratories of Beckman Instruments. They were standard instruments in all respects pertinent to this experiment and had received only routine maintenance. One of the instruments, however, had been used in a study of reference-beam attenuators, and its attenuator comb had been removed and reinstalled numerous times. The experiment was designed to obtain maximum information with minimum instrument time to avoid extended delays in the shipment of new instruments and to permit the extension of the study to instruments in other laboratories, including instruments of other types.

Each instrument was used to record spectra of a calcium-fluoride plate 1.19-mm thick, a silver-chloride plate 0.49-mm thick, and a sample of indene in a 0.025-mm cell. A typical record is shown in Fig. 1. In each case, the slits were programmed with the same slit-width, 1 mm, set at 1000 cm^{-1} corresponding to about 2-cm^{-1} resolution. Slit-widths at other frequencies varied slightly from instrument to instrument, and these were recorded. The effects of scanning speed and finite response time on apparent band frequencies and intensities should be well known to spectroscopists.[1,2] It was determined that the scanning speed selected for the measurements was well below the speed at which band distortions became apparent.

Frequency Calibration

The accuracy of frequency settings of most commercial grating instruments is at least as good as ±0.5 cm^{-1} near 1000 cm^{-1}. The photometric-calibration procedure described below makes use of a secondary transmittance standard and requires an accurate knowledge of the frequencies at which transmittance measurements are made. An error of 0.5 cm^{-1} at 900 cm^{-1} can introduce a photometric error of about 0.2% transmittance.† The absorption bands of indene

---

The author is with Beckman Instruments, Inc., Fullerton, California.

Received 18 September 1962.

* Some of this work was reported at the Pittsburgh Conference on Analytical Chemistry and Applied Spectroscopy, February 27-March 3, 1961.

† In this report, unless stated otherwise, errors are given relative to 100% transmittance rather than as percentage of observed transmittance.

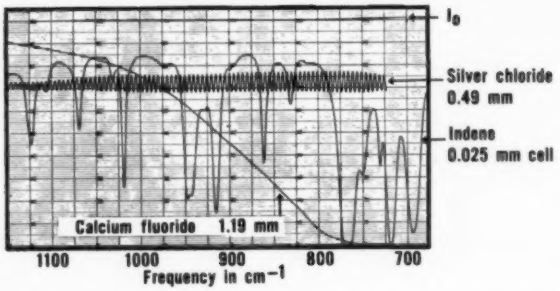

Fig. 1. Typical spectra of indene, silver chloride, and calcium fluoride.

have been proposed[3] for use in the frequency calibration of infrared spectrophotometers, and their values are known within ±1 cm^{-1}. The indene bands at 1122.7, 1067.9, 1018.6, 914.8, 861.3, and 830.5 cm^{-1} together with a superposed interference fringe pattern produced by the silver-chloride plate were used in establishing mutually consistent calibrations for the five instruments. The positions of the maxima in the silver-chloride fringe pattern occur at wave numbers given by

$$n\nu = a + bk, \tag{1}$$

where n is the refractive index relative to air, and k is the number of the fringe counted from an arbitrary starting point. The indene-band positions were measured relative to the fringe system to hundredths of a fringe, giving six corresponding pairs of values for ν and k. These values and National Bureau of Standards refractive-index data[4] were introduced into Eq. (1) and treated by least squares to obtain a and b. Subsequent frequency measurements were made relative to the fringe pattern and converted to wave numbers by using Eq. (1). In this way, the 10 indene bands discussed below were measured on five instruments with an average deviation of only 0.07 cm^{-1}.

Photometric Calibration

Photometric calibration was done by means of the fluorite-absorption spectrum. The transmittance of the calcium-fluoride plate was determined with a probable error of no more than ±0.07% of full scale using a rotating sector attenuator in a manner previously described.[5] Near the most sensitive transmittance level of about 40% T, the transmittance of fluorite decreases by less than 0.2% of full scale for a 1° temperature rise.[5] Care was taken that all specimens had reached the proper temperature before spectra were recorded. In addition, as a check on proper focusing of the optical paths preceding the entrance slit, a thick CaF_2 plate was inserted in the sample beam with the instrument set at 1500 cm^{-1}. Improper focus can result in abnormally high or low apparent-transmittance readings.

The IR-7 operating in its double-beam mode is an optical-null spectrophotometer using a comb-type reference-beam attenuator. Because the attenuator is imaged on the monochromator slit, photometric errors due to accidental comb irregularities or the inherent discontinuities occurring near the opaque end of the comb[6] are, to some extent, dependent on slit-width. This effect is minimized by the relatively wide geometric slit-widths used in high-dispersion grating instruments. No slit-width dependence was observed in the photometric calibrations used in these experiments.

The calibration data show that, at the transmittance values of the 10 indene bands discussed in the next section, corrections ranging up to 2.9% transmittance must be applied. The average corrections to the 10 bands for four of the IR-7's are 0.37, 0.53, 0.57, and 0.87% transmittance. The fifth IR-7 had an average correction of 1.82% transmittance, for the 10 indene bands which might reflect the excessive handling of its comb.

The transmittance of fluorite was measured at a series of frequencies along the absorption edge with each of the five instruments. Average values of transmittance agree with the standard values obtained by the rotating-sector method within 0.02% transmittance. The average deviation from the mean values is about 0.9% transmittance. When the instruments were operated in the single-beam mode and, therefore, were not dependent on the properties of the reference-beam attenuator, the average deviation from the mean values was only 0.14% transmittance.

Photometric Accuracy

The spectrum of indene between 675 and 1150 cm^{-1} provides a variety of bands having transmittances from 4% to 70%, half-bandwidths from 2.4 to 8.5 cm^{-1}, and various degrees of overlap. With the instrumental resolving power (effective bandwidth) employed, the ratio of effective bandwidth to half-bandwidth varies from 0.25 to 0.62. It is recognized that the resolving power employed is not high enough to provide absolute transmittance data. As a general rule, a ratio of effective bandwidth to half-bandwidth of about 0.2 is required if errors in absorbance are not to exceed about 2%. The indene bands were observed with a series of effective bandwidths, and the absolute absorbance was obtained by extrapolation to zero slit-width.

The transmittance of the indene sample and cell was calculated from the records and corrected for photometric error using the calibration data. No attempt was made to correct for cell absorption and reflection, because the same cell was used in all cases. Results are given in Table I. The probable uncertainty in reading off transmittance values from the recordings is estimated to be about 0.2–0.4% transmittance.

Table I. Measured Transmittance of Indene Corrected for Photometric Error

	Instrument, IR-7 No.							
Band	1	2	3	4	5	$\bar{T}$[a]	$\overline{\Delta T}$[b]	$T_{max} - T_{min}$
692.8 cm^{-1}	4.7%	4.4%	4.6%	4.8%	4.5%	4.6%	0.1%	0.4%
730.1	33.5	33.8	36.0	35.0	33.4	34.3	0.9	2.6
830.5	62.2	62.9	64.1	61.9	62.0	62.6	0.7	2.2
861.3	34.7	35.0	38.2	36.7	36.0	36.1	1.2	3.5
914.8	12.2	11.7	13.6	13.1	12.9	12.7	0.6	1.9
942.3	18.1	18.5	20.3	19.6	19.7	19.2	0.8	2.2
1018.6	24.6	24.5	26.3	24.8	23.9	24.8	0.6	2.4
1067.9	53.2	53.8	53.1	50.6	50.2	52.2	1.4	3.6
1106.4	68.9	70.4	70.3	67.1	66.8	68.7	1.4	3.6
1122.7	45.5	46.5	46.5	46.6	44.9	46.0	0.6	1.7
		Mean					0.8%	2.4%
		Mean before photometric correction					1.2	3.3

[a] $\bar{T}$ = mean value of transmittance.
[b] $\overline{\Delta T}$ = average deviation from mean.

Hence, the calibration procedure is seen to remove from one-third to one-half of the variation in measured transmittance, leaving an average deviation from mean values of 0.8% transmittance for the 10 bands and an average range of values of ±1.2% transmittance. When expressed as percent error in either observed transmittance or absorbance, the average for the 10 bands is about 2.7%. The remaining errors are too great to be due to variations in indicated slit program from one to another of the instruments, nor do they correlate well with sensitivities to slit-width. To some extent, within the precision of measurement, the deviations associated with a given instrument are systematic. For example, IR-7 No. 3 generally gives high values while IR-7 No. 5 reads low. This suggests that the differences are associated with differences in the slit function of the instruments, that is, differences in the spectral-energy distribution at the exit slit. There is another puzzling feature displayed by the data of Table I. The very sharp band at 1018.6 cm^{-1}, which might be expected to be quite sensitive to differences among instruments, was, in fact, one of the more repeatable bands, although its sensitivity to effective bandwidth was found to be large. Similarly, the sharp 730.1 cm^{-1} band is not as variable as some broader bands. The mean deviations are plotted in Fig. 2. The ordinate is expressed as mean deviation in transmittance divided by the extrapolated absorptance $(1 - T_0)$ at zero slit-width, while the abscissa is the ratio of bandwidth measured at one-half maximum absorptance divided by the effective bandwidth of the monochromator. The reason for the strange choice of coordinates will become clear in the next section.

Slit Function and Band Intensity

Physically, a slit function describes the radiant power of wave number ν passed through the exit slit of a monochromator which is set for a nominal wave number ν_0. The effect of the slit function on apparent peak intensities of bands has been studied theoretically numerous times.[2] Various analyses have been based on assumed slit functions and bands having rectangular, triangular, Gauss (Doppler), and Cauchy (Lorentz) shapes. The effect of defects in spectrometer alignment does not seem to have been treated, however. As it seems likely that variations in intensity data obtained from nominally identical instruments are due to differences in alignment, focus, and perfection of optical components, it seemed worthwhile to investigate this problem. The geometric slit function of an ideal monochromator having identical entrance and exit slits is a triangle of half-width s given by the product of the geometrical slit-width and the dispersion. To this must be added the contribution of diffraction to the geometrical slit-width, which is nearly the f/number of the monochromator multiplied by the wavelength. The diffraction contribution also rounds off the apex of the triangle and adds some rolling wings at the base of the slit function, but this effect is expected to be small in the case under study where the diffraction slit-width is only about 10% of the geometrical slit. The presence of aberrations in the optical system will also widen the slit function, as will mechanical imperfections such as nonparallel slits and improper focus. These effects, lumped under the term "defocusing," are included in the slit function by modifying the triangle to a trapezoid of width $2(s + \sigma)$ at the base and $2\,\sigma$ at the top, symmetric about a central frequency ν_0. Mathematically, this becomes

$$\begin{aligned} \text{slit function} = S &= A\, s/(2\sigma + s) && \xi \leqq \sigma \\ &= A\,(\sigma + s - \xi)/(2\sigma + s) && \sigma \leqq \xi \leqq \sigma + s \\ &= 0 && \xi \geq \sigma + s, \end{aligned} \tag{2}$$

where $\xi = \nu - \nu_0 \geq \sigma$, and A is a normalizing factor. A suitable modified expression represents the slit function for $\xi < 0$. Some aberrations, such as slit-

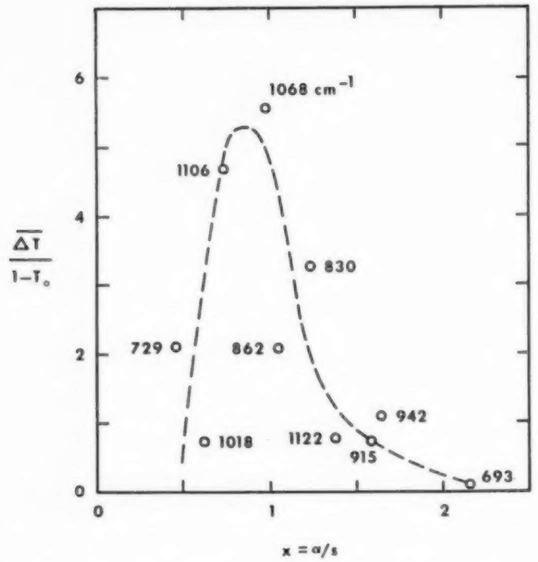

Fig. 2. Deviations in measured peak intensity of indene bands recorded on five IR-7 spectrophotometers. The ordinate is mean deviation divided by absorptance at zero slit-width (extrapolated). The abscissa is one-half the ratio of bandwidth at one-half maximum absorptance to effective bandwidth of the monochromator.

image curvature, result in a skewed slit function which can be treated by writing Eq. (2) with different values of s for $\xi > 0$ and $\xi < 0$.

It is known that the apparent peak height of a band, even when scanning very slowly, depends on band shape as well as bandwidth and slit-width. To include the effects of band shape in this study of defocusing, absorption bands having both Lorentz and Gauss shapes were studied:

$$\text{Lorentz:}\quad B_L = \frac{1 - T}{1 - T_0} = \frac{\alpha^2}{\alpha^2 + \xi^2},$$

$$\text{Gauss:}\quad B_G = \frac{1 - T}{1 - T_0} = \exp\left(\frac{-\xi^2 \, ln\, 2}{\alpha^2}\right). \qquad (3)$$

Notice that these expressions define the *absorptance* of the bands, not *absorbance*, and that the half-width 2α is defined as the width at one-half maximum absorptance, rather than one-half maximum absorbance. No theoretical significance is claimed for these expressions. They are merely mathematically convenient descriptions of band shapes similar to those often found in absorption spectra.

The apparent peak intensities were obtained in the form

$$\beta = \frac{1 - T_a}{1 - T_0} = \frac{1}{As} \int_{-(\sigma + s)}^{\sigma + s} S(s, \sigma, \xi) B(\alpha, \xi) d\xi. \qquad (4)$$

Integrations were carried out for a variety of values of the resolution parameter $x = \alpha/s$ and the defocusing parameter $y = \sigma/s$ with the aid of a Bendix G-15 digital computer. Equation (4) with trapezoidal slit function can be integrated in closed form for a Lorentz band, but must be treated as a finite summation for a Gauss band.

The relative error in observed transmittance can be found from β by observing that

$$\frac{T_a - T_0}{T_0} = \frac{\Delta T}{T_0} = \frac{1 - T_0}{T_0}(1 - \beta). \qquad (5)$$

The sensitivities of the band intensities to changes in σ are found by calculating

$$\frac{1}{s}\frac{\partial \beta}{\partial y} = \frac{\partial \beta}{\partial \sigma} = \frac{1}{As} \int_{-(\sigma + s)}^{\sigma + s} B(\alpha, \xi) \frac{\partial}{\partial \sigma} S(s, \sigma, \xi) d\xi. \qquad (6)$$

Figure 3 shows the calculated values of β for Lorentz and Gauss bands as functions of resolution for various degrees of defocusing. It is seen that Gauss bands are recorded slightly less faithfully than Lorentz bands for small values of x and somewhat more faithfully for large x.

The sensitivity of peak heights to defocusing, $\partial\beta/\partial y$ is plotted in Fig. 4 for Lorentz bands and in Fig. 5 for Gauss bands. The behavior of the two sets of curves is similar, although the peak heights of the Gauss bands are somewhat more sensitive to defocusing than those of the Lorentz bands at lower values of x and less sensitive at large x values. It is interesting to note the maxima in these curves falling at values of x ranging from 0.3 for triangular-slit functions to 1.3 for trapezoidal-slit functions having $\sigma = 2s$. If the effective bandwidth is taken as $s + 2\sigma$, then the apparent intensity is most sensitive to defocusing for bands having a width at one-half maximum absorptance of about one-half the effective bandwidth of the monochromator.

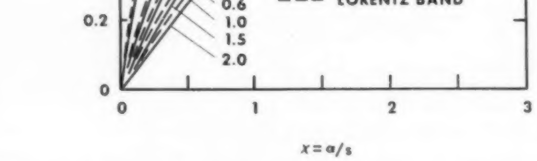

Fig. 3. Calculated relationship between apparent absorptance, 1-T_a, and actual absorptance, 1-T_o, of Gauss- and Lorentz-shaped bands for various values of the resolution parameter x and the defocusing parameter y.

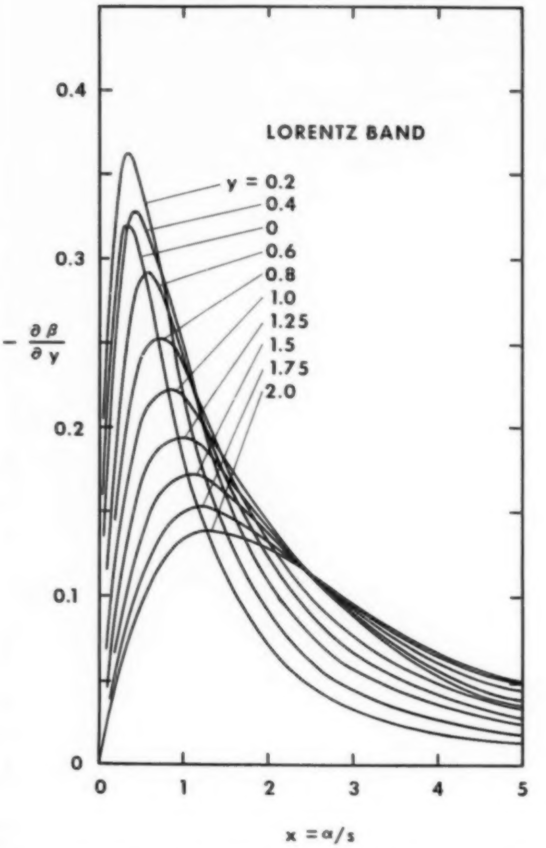

Fig. 4. Sensitivity of the apparent peak intensity of a Lorentz-shaped band for various values of the resolution parameter x and defocusing parameter y.

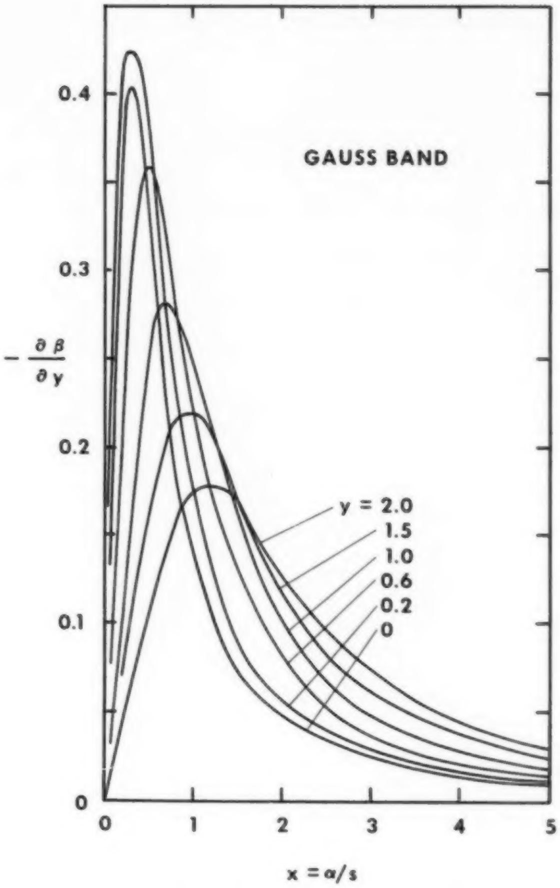

Fig. 5. Sensitivity of the apparent peak intensity of a Gauss-shaped band for various values of the resolution parameter x and defocusing parameter y.

The experimental data plotted in Fig. 2 show a dependence on the resolution parameter $x = \alpha/s$. The error $\overline{\Delta T}/(1 - T_0)$ appears to be small at both large and small values of x, reaching a maximum in the neighborhood of $x \sim 0.8$. There is a striking qualitative resemblance between the experimental data and the computed curves of Figs. 4 and 5. Although no definite conclusion can be drawn from this resemblance, it is not inconsistent with the postulate that the residual disagreement among the instruments is due to differences in slit function.

Conclusion

The agreement in measured band intensities from five IR-7's, particularly after photometric calibration, is encouraging. It must be remembered that all measurements were made by the same operator under carefully specified conditions of resolving power, scanning speed, and response period, and that the same sample cell was used throughout. It is hoped that, in the near future, similar experiments will be performed including spectrophotometers of other types. It is expected that the effects of variations in slit function will be more pronounced in comparisons of instruments of different design.

The author gratefully acknowledges many helpful discussions with W. I. Kaye and W. S. Gallaway during the course of this study.

References

1. S. Brodersen, J. Opt. Soc. Am. **43,** 1216 (1953).
2. K. Frei and Hs. H. Gunthard, J. Opt. Soc. Am. **51,** 83 (1961). Other references are cited in this article.
3. R. N. Jones, P. K. Faure, and W. Zacharias, Rev. Univ. Mines **15,** 417 (1959); R. N. Jones, N. B. W. Jonathan, M. A. MacKenzie, and A. Nadeau, Spect. Acta **17,** 77 (1961); IUPAC *Tables of Wavenumbers for the Calibration of Infrared Spectrometers* (Butterworths, Washington, 1961).
4. L. W. Tilton, E. K. Plyler, and R. E. Stephens, J. Opt. Soc. Am. **40,** 540 (1950).
5. J. E. Stewart, Appl. Opt. **1,** 75 (1962).
6. K. Kudo, Sci. of Light **4,** 85 (1955).

Papers to appear in subsequent issues

Correspondence to these authors will be forwarded if addressed in care of the Managing Editor

Infrared Transmission through Fogged Salt Windows—*Morrow and Turk*

A Simple Grating Calibrator for the Visible and Vacuum Ultraviolet—*Hammer, Arakawa, and Birkhoff*

The Use of Polarized Infrared Radiation in Magneto-optical Studies of Semiconductors—*Palik*

A Photomultiplier Circuit for Precision Spectrophotometry—*Budde*

The Probability Distribution of Camera Resolution—*Rosenau*

Transmission of Isotropic Radiation Across an Interface Between Two Dielectrics—*Stern*

Test of Theoretical Absorption Band Model Approximations—*Burch and Williams*

Optics in Norway—*Hisdal and Omholt*

Use of an Analog Computer in Side-on Arc Spectroscopy—*Shumaker and Yokley*

Attenuation by Ozone and the Earth's Albedo in the Middle Ultraviolet—*Green*

Observations of Near Infrared Radiation from the Solar Atmosphere—*Taylor and MacQueen*

Irradiance on a Flat Object Underwater—*Tyler and Shaules*

Kirchhoff Diffraction Pattern Calculations—*Moore*

Interference Filter Spectrometer for Low Intensity Extended Sources—*Carter, MacRae, Nelson, Birkhoff, and Arakawa*

Measurement of Energy Flux Density Distribution in the Focus of an Arc Image Furnace—*Beyer, McCulley, and Evans*

Irradiance Linearity Corrections for Multiplier Phototubes—*Baker and Wyatt*

Optics in Australia—*Steel*

Dispersion in the Vicinity of an Optical Resonance—*Fork and Bradley*

Design for a Wide-Angle, Linear-Output, Horizon-Sensor Optical System—*Palser*

Test Methods in Spectrophotometry: Stray Light Determination—*Poulson*

The Scattering of Infrared Radiation from Clouds—*Bauer*

Temperature Measurements with an Optical Pyrometer under Adverse Conditions—*Paul*

An Absolute Reflectometer for Use at Low Temperatures—*Hartman and Logothetis*

Field Photometer with Nine-Element Filter Wheel—*Frentress, Young, and Edwards*

Jet-Controlled Arc II: Excitation of Third Spectra—*Moore, Thygesen, Derwin, and Eward*

Optical Properties of "Liumogen": A Phosphor for Wavelength Conversion—*Kristianpoller and Dutton*

Exfocal Pumping of Optical Masers in Elliptical Mirrors—*Roess*

Optical Harmonic Generation in Two Ferroelectric Crystals—*Smith*

Refractive Gradient Effects in Proposed Liquid Lasers—*Winston and Gudmundsen*

A Method for Performing the Analog Fourier Transform for Interference Modulation Spectroscopy—*Vogel and Genzel*

Electro-Optics Effects in Optically Active Crystals—*Buhrer, Ho, and Zucker*

Photographic Instrumentation for Triangulation Studies of Luminous Clouds in the Upper Atmosphere—*Cooksey, Frentress, and Edwards*

The Modulation Transfer Function in Photography—*Frieser*

The present State of the Art with Regard to Detection—*Scott*

Spectroscopy Applied to Hypersonic Atmospheric Penetration—*Planet*

A New Grazing Incidence Spectrometric Mounting—*Landon*

Spectral Emittance of Refractory Materials—*Blau and Jasperse*

The Infrared Transmittance of Carbon Dioxide—*Stull, Wyatt, and Pluss*

An Automatic Calibrating Apparatus for Standard Scales by Counting Interference Fringes—*Doi, Shimizu, Tsuboi, and Kouno*

Data Processing System for the Automatic Transformation of Observed Plasma Intensities into Their Radial Distribution—*Paquette and Wiese*

The Modulation Transfer Paradox—*Hempenius*

Thermal Radiation Characteristics of Xenon Flashtubes—*Lincoln*

Conversion of a Double-Beam IR Spectrometer to Grating Operation—*Evans and Afremow*

Transmittance of Some Optical Materials for Use between 1900 and 3400 Å—*Pellicori*

The Use of a Single-Plane Parallel Plate as a Lateral Shearing Interferometer with a Visible Gas Laser Source—*Murty*

IR Transmittance of Water Vapor—*Wyatt, Stull, and Plass*

Electrostatic Fields in Xerography—*Neugebauer*

Dynamics of the Giant Pulse Laser—*Frantz*

Solid Backed Evaporated Thermopile Radiation Detectors—*Astheimer and Weiner*

Variation of the IR Spectral Radiance near the Limb of the Earth—*Wark, Alishouse, and Yamamoto*

Design Study of Air-Spaced Triplets—*Wallin*

Image of the Optical Grating Modulated by the Signal and Its Application of the Measurement of Strain Distribution—*Suzuki, Mino, and Shinoda*

A Double-Pass Pfund Spectrograph for Solar Research—*Mitchell and Mohler*

Zeeman Effect at 3.39 μ in a Helium–Neon Laser—*Bell and Bloom*

Microscopic Observation of Film Cross Sections Having Steep Contours—*Frieden*

Moiré Fringes as Visual Position Indicators—*Vargady*

Analysis of Fine-Detail Reproduction in Photographic Systems—*Simonds, Kelch, and Higgins*

The Sensitivity and Accuracy of Double-Beam Spectrophotometers—*Rikmenspoel*

Optical System Design for Telescopes—*Patrick and Scidmore*

Balanced Optical Discriminator—*Kaminow*

Dependence of Absorption Frequency on Intensity—*Krolik, Mandelberg, and Condell*

Collodion Technique of Mirror Cleaning—*McDaniel*

Laser Action in Neodymium Doped Glass at 1.37 μ—*Mauer*

The Total Band Absorptance of CO near 4.7 μ—*Shaw and Houghton*

Absolute Solar Spectra 3.5 to 5.5 μ. Part II—Theoretical Spectra for Altitude Range 15–30 km—*Bradford, Farmer, and Todd*

Absolute Solar Spectra 3.5 to 5.5 μ. Part I—Experimental Spectra for Altitude Range 0–15 km—*Farmer and Todd*

Some Qualitative and Quantitative Results on Spatial Filtering of Granularity—*Thiry*

The Twentieth Century Microscope—*Benford*

Method for Engineering Photographic Systems—*Higgins*

Argon Tube Pumped Laser—*Long and Conger*

An Automatic Retardation Meter for Automatic Polarimetry by Means of an ADP Polarization Modulator. Part I—*Takasaki et al.*

Image Evaluation for Reconnaissance—*Brock*

On Determination of Absorption and Reflection Coefficients—*Kahan*

Spectroscopic Research on the major Planets—*Spinrad*

An Optical Null Double-Beam Double-Pass Infrared Spectrophotometer

Shigeo Minami

A novel signal treatment for an optical null double-beam double-pass system is developed and used in a vacuum-type prism infrared spectrophotometer. A feature of this instrument is the arrangement of the specially-shaped beam switch and the second chopper working in conjunction with the phase-sensitive rectifier. The beam switch is made so that the lower half of the reference beam and the upper half of the sample beam are sent to the monochromator optics during one half of the cycle; the other parts of reference and sample beams reach the monochromator optics during the other half of the cycle. The second chopper alternately blocks the upper and lower halves of the image formed at the focal point of single-pass beam in proper synchronism with the beam switch. Fairly good cancellation of the scattered radiation was achieved through adjustment of the phase relation between the beam choppers and the phase-sensitive rectification system. In addition to reporting the general design and construction, detailed descriptions of the control and recording systems which provide the unique features are also included.

Introduction

In using the double-pass monochromator system developed by Walsh[1] in an optical null double-beam spectrophotometer, radiation from a source should be chopped with two rotating sectors before arriving at a detector; one chopper is a so-called beam switch for the double-beam system; the second chopper is in the monochromator for the double-pass system. In order to achieve a signal-to-noise ratio as high as possible with a given spectral slitwidth and scanning speed, and a detector, such as a thermocouple or bolometer, having rather slow response, there are rather severe limitations on the frequencies of the chopping systems and the frequency difference between the two. Accordingly, conventional electronic arrangements composed of an ac amplifier and a rectifier cannot be simply used to solve this problem.

In recent years, several methods have been proposed from the signal processing point of view, and further discussions of their relative advantages are made by Golay on the basis of signal-to-noise ratios.[2-4] In treating such a system from the standpoint of signal processing, the relationships between beam switch, double-pass beam chopper, and synchronous rectifier have to be appropriately selected, taking into consideration the chopping frequencies and relative phases for the detector to be used. The instrument reported here is a vacuum-type prism spectrophotometer, in which a new signal processing arrangement using a specially-shaped beam switch and a second chopper in conjunction with a synchronous rectifier for achieving optical null is employed. A detailed discussion of the principle, the design and construction, and the performance of the instrument follows.

Principle of Operation

Both a reference beam I_0 and a sample beam I are focused on opposite sides of the specially-shaped beam switch after passing through a reference cell and a sample cell respectively. At all times the beam switch sends half of the reference beam and half of the sample beam toward the monochromator. During one half of the rotation of the switch, it sends the upper half of the reference beam and the lower half of the sample beam to the monochromator at the same time; during the other half of the rotation the other halves of the sample and reference beams are passed. This switch is mechanically coupled to the second chopper which is located between corner mirrors in the double-pass

---

The author was at the Laboratory of Molecular Spectroscopy and Infrared Studies, Department of Physics, The Ohio State University, Columbus, Ohio. His present address is: Department of Applied Physics, Faculty of Engineering, Osaka University, Osaka, Japan.

Received 14 September 1962.

This investigation was supported in part by the Office of Naval Research through a contract with The Ohio State University Research Foundation.

monochromator and which alternately blocks the upper or the lower parts of the once-passed beam during each half rotation of the beam switch.

Figure 1 contains diagrams indicating the shapes of the beam switch and the second chopper, and their chopping operation with monochromatic beam images at the exit slit position. Accordingly, if the upper and the lower beams are well balanced the detector provides an output signal proportional to the intensity difference between the double-passed I_0 and I beams as a chopping-frequency component. After amplification, the signal is rectified with a phase-sensitive rectifier which is synchronized with the effective signal from the double-pass radiation. Even if the upper and the lower beams are not well balanced, since signals due to the unbalanced portion of the single-pass beam and scattered radiation are 90° out of phase with the effective double-pass signal, any spurious signals are completely eliminated.

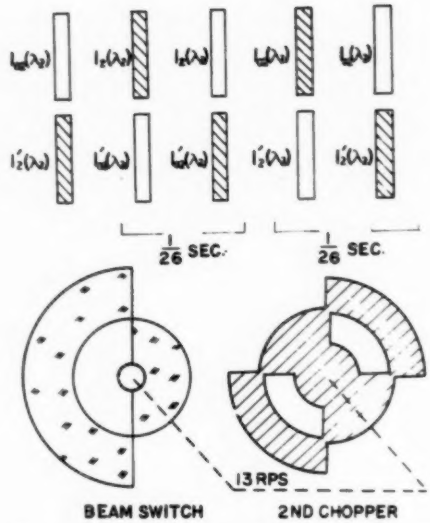
$I_{02}(\lambda_2)$
$I_2(\lambda_2)$
$I_2(\lambda_2)$
$I_{02}(\lambda_2)$
$I_{02}(\lambda_2)$
$I_2'(\lambda_2)$
$I_{02}'(\lambda_2)$
$I_{02}'(\lambda_2)$
$I_2'(\lambda_2)$
$I_2'(\lambda_2)$
1/26 SEC.
1/26 SEC.
13 RPS
BEAM SWITCH
2ND CHOPPER

Fig. 1. Shapes of beam switch and second chopper, and their chopping operation for double-pass beam.

The waveforms of each component in the radiation signal are shown in Fig. 2. In the figure the following notation is used: $I_{01}(\lambda_1)$ and $I_{01}'(\lambda_1)$ are the amplitudes of single-pass reference beams which come from the upper and the lower halves of the slit respectively; $I_1(\lambda_1)$ and $I_1'(\lambda_1)$ of the upper and lower sample beams; $I_{02}(\lambda_2)$ and $I_{02}'(\lambda_2)$ of the upper and lower double-pass reference beams; and $I_2(\lambda_2)$ and $I_2'(\lambda_2)$ of the upper and lower double-pass sample beams. S and s represent intensities of scattered radiation due to the undispersed incident radiation corresponding to the beam switching cycle. Since it is difficult to maintain the upper and lower beams balanced throughout the entire wavelength region in practice, Fig. 2 shows the signal waveforms in an off-balanced condition. After perfect adjustment of the phase-sensitive rectifier, only the double-pass signal waveform is effective. This may be expressed by the Fourier series:

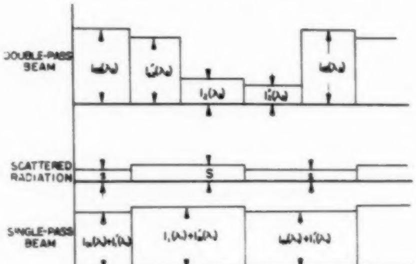

Fig. 2. Waveforms of component in radiation signal.

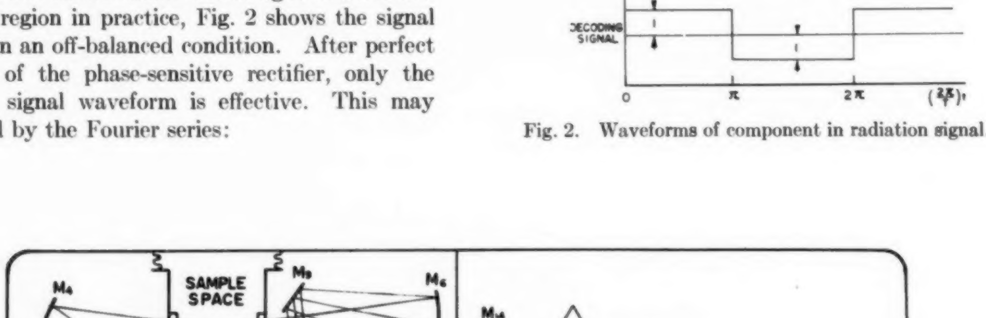
M₄
SAMPLE SPACE
M₉
M₆
M₂
E
SOURCE
M₁
M₁₀
M₁₁
A₂
M₁₂
CH-1
A₁
M₅
M₃
SAMPLE SPACE
M₈
M₇
M₁₄
NaCl or KBr PRISM
M₁₇
M₁₅
L
S₁
CH-2
4
1
2
3
M₁₆
S₂
M₁₃
M₁₈
R
M₁₉

Fig. 3. Arrangement of optical components of spectrophotometer M = mirror; CH = chopper; R = detector.

$$\begin{aligned} f(\omega t) = \frac{a_0}{2} + \frac{1}{\pi} [(A - B) \cos\omega t - \frac{1}{3} (A - B) \cos3\omega t \\ + {}^1/_5(A - B) \cos5\omega t - \ldots \\ + (C - D) \sin\omega t + (A + B) \sin2\omega t \\ + {}^1/_3(C - D) \sin3\omega t + {}^1/_2(A + B) \sin4\omega t + \ldots] \end{aligned} \quad (1)$$

where

$$\begin{aligned} A &= I_{02}(\lambda_2) - I_{02}'(\lambda_2) \\ B &= I_2(\lambda_2) - I_2'(\lambda_2) \\ C &= I_{02}(\lambda_2) + I_{02}'(\lambda_2) \\ D &= I_2(\lambda_2) + I_2'(\lambda_2). \end{aligned}$$

The Fourier series expressing the decoding signal in the phase-sensitive rectifier is

$$F(\omega t) = \frac{4}{\pi} (\sin\omega t + \frac{1}{3} \sin 3\omega t + \frac{1}{5}\sin5\omega t + \ldots). \quad (2)$$

Combining Eqs. (1) and (2) with Perseval's theorem, the dc output of the phase-sensitive rectifier becomes

$$\begin{aligned} E_0 = \frac{2}{\pi^2} \{[I_{02}(\lambda_2) + I_{02}'(\lambda_2)] - [I_2(\lambda_2) + I_2'(\lambda_2)]\}(1 + \frac{1}{3^2} + \\ \frac{1}{5^2} + \ldots) = \frac{1}{4} \{[I_{02}(\lambda_2) + I_{02}'(\lambda_2)] - [I_2(\lambda_2) + I_2'(\lambda_2)]\}. \end{aligned} \quad (3)$$

As the output signal from the rectifier provided by Eq. (3) has just the same form as that of the conventional double-beam spectrophotometer, the signal E_0 is used for completing the servo loop through the beam attenuator, in this case a comb-shaped wedge. However, one has to keep in mind that the value of E_0 in this system is half of that of the conventional double-beam system, as are other double-beam and double-pass spectrophotometers using optical null principle.[4]

Design and Construction

Optical System

As shown in Fig. 3, the optical arrangement is similar to that of conventional spectrophotometers, the chopper arrangement representing the major difference. All optical components and part of the electromechanical system are mounted on a steel plate and are in a tank that can be evacuated. Radiation from a Nernst glower E is reflected by mirrors M_1 and M_2, and M_3 and M_4 to form images at the centers of the two sample spaces. Sample spaces, enclosed in brass cylinders which have 15.3 cm effective path lengths, are separated from the large evacuated chamber by KBr windows, and may be evacuated individually if desired. After passing through the sample spaces, reference and sample beams are focused on opposite sides of the beam switch CH-1. A comb-shaped beam attenuator A_1 is located in the reference beam just in front of the chopper. This attenuator is placed as close as possible to the beam switch disk, but in a manner such that no disturbances result from reflection of the sample beam from it. By mirrors M_{10}, M_{11}, and M_{12} the combined beams from the switch are focused on the entrance slit S_1 of the monochromator. A KBr cylindrical lens L is located in front of the entrance slit and serves as a field lens.

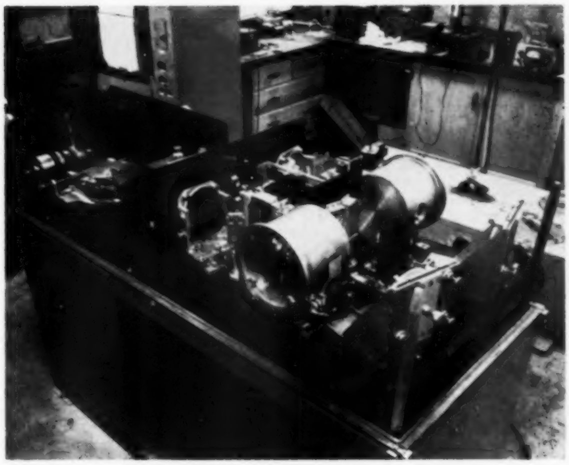

Fig. 4. Photograph of spectrophotometer with cover removed.

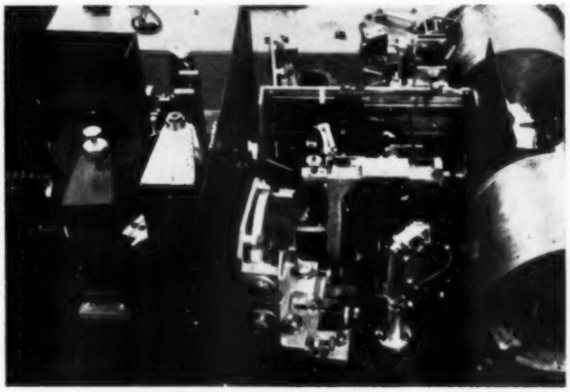

Fig. 5. Close-up view around beam switch and second chopper.

A Littrow type monochromator with a Walsh type double-pass arrangement is used for NaCl or KBr dispersing elements which have faces 160 × 110 mm and 60° apex angle. As a collimator, a 12° off-axis paraboloidal mirror M_{13} of 700 mm focal length is used. The image of the exit slit S_2, which has 16 × 1.6 mm maximum area, is focused on a Reeder thermocouple R after a 1:8 image reduction by the ellipsoidal mirror M_{19}.

Mechanical Construction

All optical components are mounted on a 19 mm thick steel plate with part of the driving mechanism in the vacuum tank, of which the outside dimensions are about 178 × 74 × 44 cm.* In obtaining spectro-

---

* The base plate, vacuum tank and some other components discussed by R. A. Oetjen[5] are utilized in this instrument.

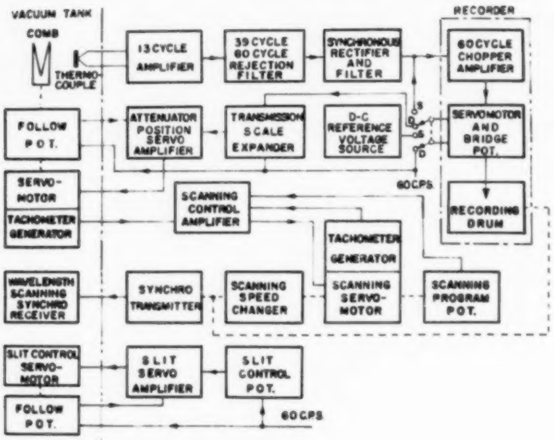
VACUUM TANK
COMB
THERMO-COUPLE
13 CYCLE AMPLIFIER
39 CYCLE 60 CYCLE REJECTION FILTER
SYNCHRONOUS RECTIFIER AND FILTER
RECORDER
60 CYCLE CHOPPER AMPLIFIER
FOLLOW POT.
ATTENUATOR POSITION SERVO AMPLIFIER
TRANSMISSION SCALE EXPANDER
D-C REFERENCE VOLTAGE SOURCE
S
D
S
D
SERVOMOTOR AND BRIDGE POT.
60CPS
SERVO-MOTOR
TACHOMETER GENERATOR
SCANNING CONTROL AMPLIFIER
RECORDING DRUM
TACHOMETER GENERATOR
WAVELENGTH SCANNING SYNCHRO RECEIVER
SYNCHRO TRANSMITTER
SCANNING SPEED CHANGER
SCANNING SERVO-MOTOR
SCANNING PROGRAM POT.
SLIT CONTROL SERVO-MOTOR
SLIT SERVO AMPLIFIER
SLIT CONTROL POT.
FOLLOW POT.
60CPS

Fig. 6. Block diagram of control and recording system.

scopic data, the inside of the tank is maintained at a pressure between 0.1 and 0.3 mm Hg with a rotary pump.

The vacuum system and a portion of the electronic system involving the preamplifier, main amplifier, slit drive servo amplifier, and the Nernst glower power pack are located underneath the evacuated chamber. The main electronic system including a recorder is mounted in a rack separated from the vacuum tank. An outside view of the spectrophotometer is shown in Fig. 4.

For the sample spaces, brass cylinders of 20.3 cm inside diameter which have KBr windows are so bolted to the base plate that the open end of each cylinder is aligned with a hole bored in the tank wall. Sylphon bellows with flanges are used to connect the cylinders to the tank wall and maintain the volume near the sample space evacuated. This construction makes it easy to put samples into the sample spaces without disturbing the vacuum.

For both slit drive and wavelength scanning systems, conventional mechanisms were adopted. The slit jaws are caused to slide along V-shaped guides by turning screws driven by a two-phase servomotor. A Littrow mirror mounted behind the prism is rotated by a lever 480 mm long in conjunction with a mechanical cam driven by a worm and gear. The worm is rotated with a synchro receiver mounted on the base plate.

The beam switch and the second chopper are connected together by gear trains and universal joints to ensure constant synchronization. The center heights of both rotating shafts are readily adjustable to make the upper and the lower beam intensities equal. Figure 5 is a close-up view of the photometer section and a part of the monochromator, which shows the detailed construction of the beam switch, comb-shaped attenuator and the second chopper.

Control and Recording Systems

The principal parts of the control and recording systems, which include a commercial electronic recorder, are housed in a console separated from the vacuum tank. Controls are centralized on one panel of the console. The remote operation of the mechanisms inside the tank is carried out using a synchro pair and positioning servo units. Figure 6 is a block diagram of the control and recording systems.

Radiation Signal Amplifier and Beam Balancing Servo System

The output of the thermocouple is connected to a Perkin-Elmer Model 107 amplifier, of which the output circuit is modified for either double-beam or single-beam use. After rectification by a phase-sensitive combination of components, the signal is fed to the recorder. The use of the slide wire in the commercial electronic recorder is modified according to whether single-beam or double-beam operation is desired. For the former operation, the reference dc voltage is provided by flashlight batteries connected to the slide wire; for the latter operation, 60 cps ac voltage is so connected that the slide wire serves as a master potentiometer in the beam-attenuator positioning servo loop. The comb-shaped attenuator is mechanically coupled with a slave potentiometer and a two-phase servo motor.

A transmission scale expander makes possible recorder deflections five or ten times as large for a given transmittance, and thus permits more accurate measurement of extremely weak absorption bands. This operation is based on applying 5× or 10× the original voltage across the slave potentiometer, the pen position adjustment, in conjunction with the expander, being accomplished electrically. Figure 7 shows the circuit diagram of the transmission scale expander and pen position adjuster.

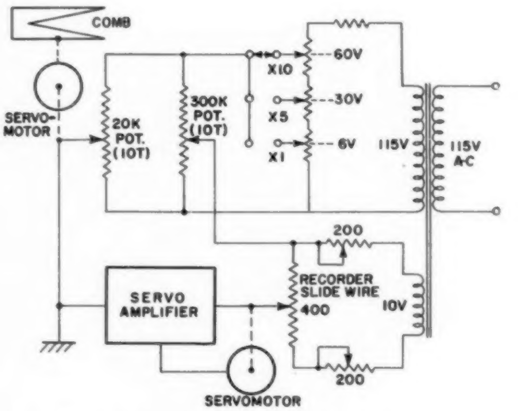
COMB
SERVO-MOTOR
20K POT. (10T)
300K POT. (10T)
X10
X5
X1
-60V
-30V
-6V
115V
115V A-C
200
RECORDER SLIDE WIRE
400
10V
200
SERVO AMPLIFIER
SERVOMOTOR

Fig. 7. Circuit diagram of transmission scale-expander and pen position adjuster.

Wavelength Scanning System

In order to provide continuous scanning speed control readily, and to maintain proper synchronization between the Littrow mirror rotation and the chart drive of the remote recorder, a synchro transmitter and receiver pair (Bendix Aviation Corp., 115 V, 60 cps, single phase) is used. A two-phase servomotor (Ford Instruments, 10 W, 60 cps, high voltage unit) controlled electronically rotates the synchro transmitter and recorder drum. Gear trains allow the scanning speed to be changed in 12 steps so that the complete spectral range may be scanned in periods varying from 3 to 770 min; moreover, continuous variation between steps is provided electronically. A modified Leeds and Northrup Speedomax G recorder is used as the recording device. The abscissa of the recorded spectrogram may be varied from 6.4 to 254 mm per micron. Manual scanning is also available through a differential gear train.

Suppression of wavelength scanning speed in the vicinity of deep absorption bands, and programming of speed so that it is related to the spectral slitwidth are characteristic of most modern spectrophotometers. Both are incorporated in the instrument described here, although the methods used here differ from others described previously.

Both types of speed control are accomplished using the servo-system shown in Fig. 8. The upper half of the drawing relates to the error signal detection and the lower to the servomotor drive. A two-phase ac tachometer generator (Kollsman Instru. Corp., 60 cps, induction generator) is coupled with the scanning motor for monitoring the rotating speed. First of all, for the constant speed scan, the ac output voltage of the generator, which is proportional to its rotating speed, is compared with the constant dc voltage after rectification. The reference dc voltage is supplied from the plate side of the parallel 12AU7 triode of which grid voltages are kept constant. The unbalanced signal is supplied to a 6BJ7 variable-μ pentode in order to modulate the 60 cps signal which is applied to the cathode as the signal source for the two-phase motor driving circuit. As a result, the feedback loop for the scanning motor control is completed. Secondly, the programmed scan is readily accomplished by using a voltage that is gradually varied rather than that of constant value as the reference. This voltage is generated with the above triode circuit and a nonlinear potentiometer, the shaft of which is connected with the scanning motor. In the vicinity of deep absorption bands, a crystal diode rectifier and a tachometer generator connected to the beam balancing servomotor gives a dc voltage proportional to the rotating speed to the grid of the triode in which the reference voltages are generated. Consequently, speed suppression related to the slope of the absorption curve is available throughout either the "constant speed" or the programmed scan.

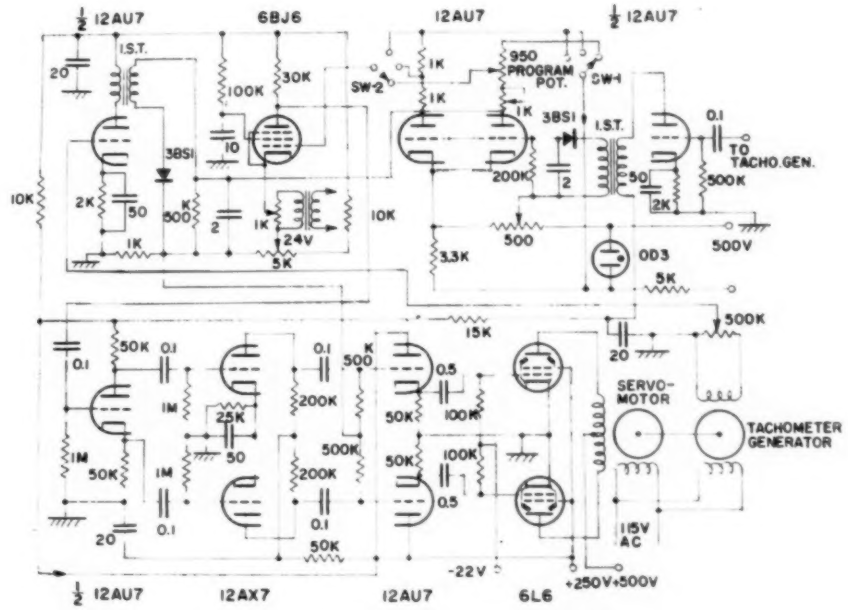
½ 12AU7
6BJ6
12AU7
½ 12AU7
20
I.S.T.
100K
30K
SW-2
1K
1K
950
PROGRAM POT.
SW-1
1K
3BS1
I.S.T.
0.1
TO TACHO.GEN.
10
3BS1
200K
2
50
500K
10K
2K
50
K 500
2
1K
24V
10K
2K
1K
5K
500
500V
3.3K
OD3
5K
15K
500K
0.1
50K
0.1
0.1
K 500
0.5
20
SERVO-MOTOR
1M
25K
200K
50K
100K
TACHOMETER GENERATOR
1M
50
500K
50K
100K
1M
50K
1M
200K
0.5
20
0.1
0.1
50K
115V AC
-22V
+250V
+500V
½ 12AU7
12AX7
12AU7
6L6

Fig. 8. Circuit diagram of wavelength scanning system.

Performance

As discussed in the first part of this paper, according to the theory, any spurious signals from the receiver due to the single-pass beam and scattered radiation in the monochromator can be completely eliminated by balancing the upper and lower beams and by precise adjustment of the synchronous rectifier.

In practice, since the radiation that passes through the exit slit contains a relatively large component that is once-passed, initial positioning of the slits is critical. Failure to do this properly may result in inferior results in the short wavelength region. In the instrument constructed here, in order to avoid any ill effects that would result from mismatched portions of the single-pass beam, the optical alignment in which the single-pass beam is focused in a position just above the slits has been used.[6] That the effect of scattered radiation is fairly well eliminated is shown in Fig. 9. This shows the polystyrene bands around 14 μ. It also indicates how the effect of the scattered radiation is influenced by changing the phase of the phase-sensitive rectifier.

Figure 10 shows polystyrene and glass absorption as recorded at a rapid rate, such as might be used in survey work. The ammonia absorption bands in the 11 μ region are shown in Fig. 11 as recorded at a medium scanning rate.

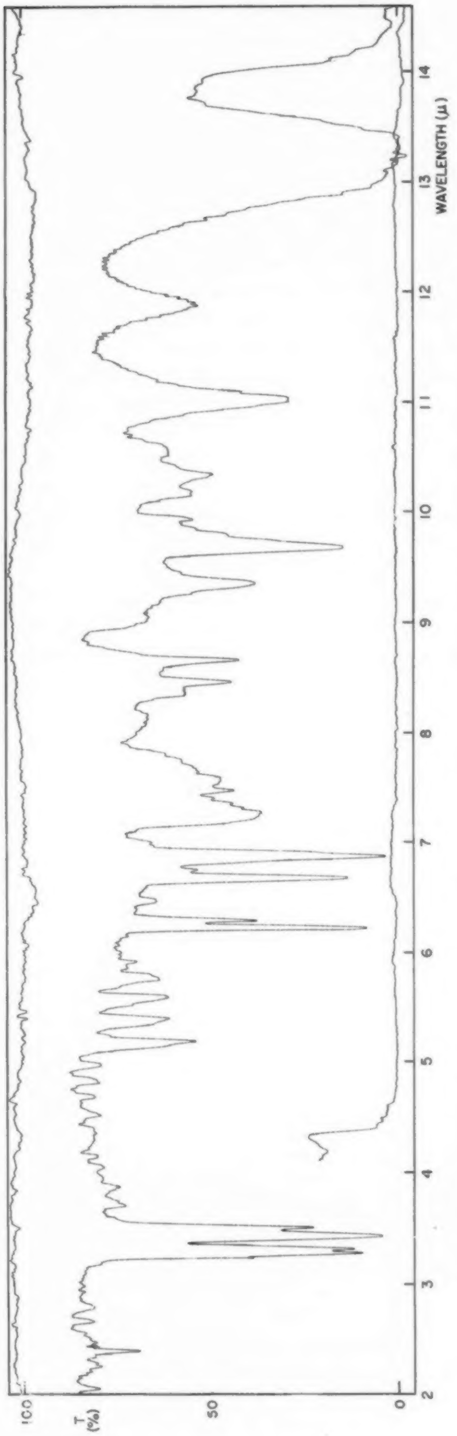

Fig. 10. Transmission curves for air, polystyrene, and glass (scanning rate: approximately 13 min for entire region).

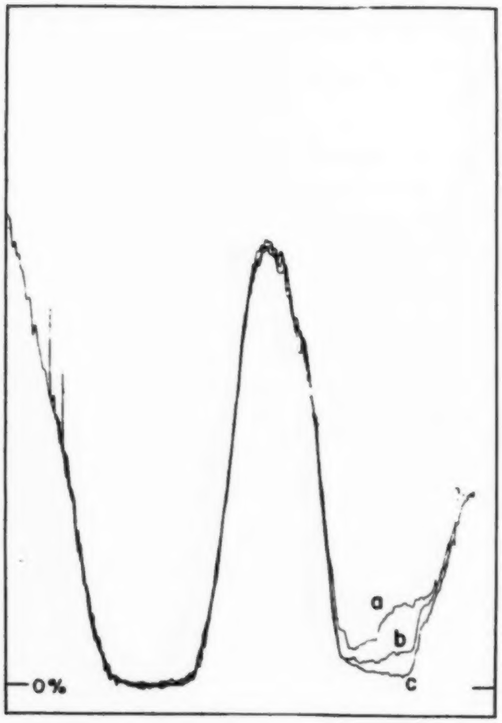

Fig. 9. Polystyrene bands around 14μ. Changes from a to c through b, bringing the phase-sensitive rectifier adjustment to the optimum position, shows how the effect of scattered radiation can be minimized (scanning rate: 0.25μ/min).

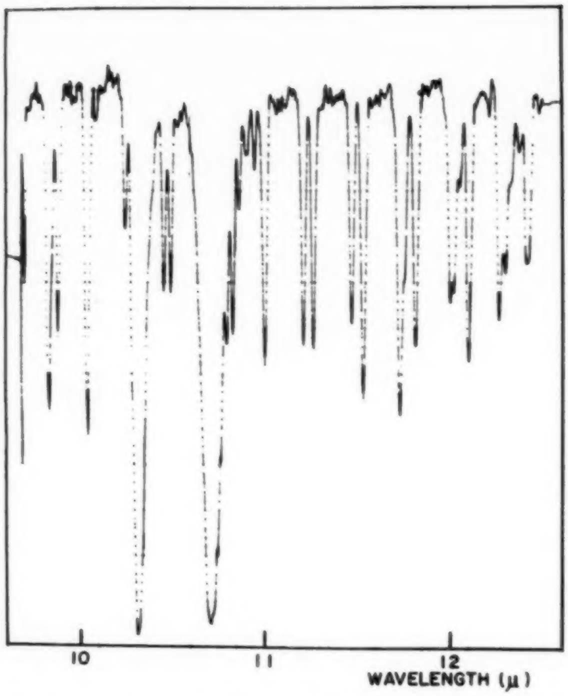

Fig. 11. Ammonia bands around 11μ (scanning rate: 0.25μ/min).

Conclusion

A principle for a double-beam and double-pass system using the optical-null method was developed and reduced to practice in a vacuum-type prism spectrophotometer. The objective was to eliminate the effect of scattered radiation, and to achieve resolution and signal-to-noise ratio as nearly as possible equaling that of a single-pass instrument.

If it is assumed that the amplitude of the signal on the entrance slit is the same in any system, the signal-to-noise ratio of this instrument should be one half that of the conventional double-beam and single-pass instruments. However, as the double-pass system allows the use of slits double the width of that of the single-pass instrument, the signal-to-noise ratio should be the same except for losses due to absorption and reflection, the spectral slit width being the same in both instances. The absorption records indicate that the resolution and signal-to-noise ratio are almost the same as that of the single-pass instruments. Elimination of the effect of scattered radiation is quite well accomplished.

The instrument has many features in the electronic and control systems that make for convenience in use. Especially, the flexible wavelength scanning control system gives efficient and easy scheduling of the scanning program and speed selection. Easy change from double-beam to single-beam operation is an additional advantage.

The author wishes to express appreciation to Harald H. Nielsen and Robert A. Oetjen for constant guidance and encouragement. Thanks are due Carl McWhirt and his staff for shop work in completing this instrument. Sung Mook Lee assisted considerably in assembling and adjusting the instrument during a period when it was necessary for the author to be in Japan. Acknowledgment is made of the generosity of the Bakelite Corporation in donating to the University an infrared spectrograph containing many of the major components used in this investigation.

References

1. A. Walsh, J. Opt. Soc. Am. **42,** 94 (1952).
2. S. F. D. Orr, J. Opt. Soc. Am. **43,** 709 (1953).
3. E. F. Daly, Nature **171,** 560 (1953).
4. M. J. E. Golay, J. Opt. Soc. Am. **46,** 422 (1956).
5. R. A. Oetjen, J. Opt. Soc. Am. **35,** 743 (1945).
6. J. C. O. Rochester and A. E. Martin, Nature **168,** 785 (1951).

I. G. Ross *Sydney* (left), K. H. Illinger *Tufts*, and M. K. Wilson, editor of the March 1964 feature on Chemical Optics, during the International Symposium on Molecular Structure and Spectroscopy, Tokyo, September 1962.

Patents *continued from page 1270*

3,060,019 23 Oct. 1962 (Cl. 96-1)
Color electrophotography.
S. W. Johnson and J. P. Lauriello. Assigned to Radio Corporation of America. Filed 22 July 1958.

A photoconductive coating of zinc oxide in resin binder, dye-sensitized so as to be slightly sensitive in one portion of the spectrum (e.g., blue) somewhat more sensitive in a second (e.g., green) and highly sensitive in a third (e.g., red), is used to make three-color electrostatic prints without filtering or registration difficulties. For the example proposed, a color transparency is imaged on the charged surface for a relatively long time during which all areas except those which correspond to black or blue in the original are discharged. Those remaining charged areas are developed with a blue powder which has sufficient conductivity that the areas thus developed cannot subsequently hold a charge in the dark. The sheet is then recharged and re-exposed for a shorter time, sufficient to discharge all areas except those illuminated with green light. Those still remaining charged areas are developed with a conducting green powder and the process is repeated, with a slight exposure sufficient to discharge all areas except those illuminated with red, which are then developed with a red powder. All other combinations of sensitivities and powder colors are covered in the claims, for two or more colors. It may be noted that all blacks in the original will be rendered blue, in the example, and yellows, pinks, pastels, and middle tones, in general, will be rendered white. Use of the process for printing multicolor line drawings and maps is suggested. C.S.

3,060,020 23 Oct. 1962 (Cl. 96-1)
Method of electrophotographically producing a multicolor image.
H. G. Greig. Assigned to Radio Corporation of America. Filed 2 Nov. 1959 (Div. of Application 20 Mar. 1958).

Electrostatic developing powder consisting of finely divided photoconductive, dye-sensitized zinc oxide coated with film-forming material and suitably colored is proposed, to produce either overlapping or nonoverlapping deposits of differently colored images on photoconductive zinc oxide sheets. Printing from color transparencies is proposed, by successive filtered exposures with intervening development of overlapping colored images. Exposure using "filters capable of transmitting all colors except yellow" is followed by development with a yellow powder. After development and recharging of the whole sheet, both where developed with the yellow powder and where such yellow is not present, "a second exposure is made through filters transmitting all colors except blue, and the development carried out with the blue-colored developer powder. In the same way, red light is filtered out and a red developer powder over-printed over the yellow and blue." Although this procedure is claimed "to provide a composite image in natural colors" it cannot do so because, for instance cyans, pinks, and all pastels would be reproduced white. Use of the nonoverlapping variations of the printing powders would suffer all the limitations of color-rendering described in the abstract for U.S. patent 3,060,019 above. C.S.

3,060,021 23 Oct. 1962 (Cl. 96-1)
Method for electrophotographically producing a multicolor picture.
H. G. Greig. Assigned to Radio Corporation of America. Filed 2 Nov. 1959 (Div. of Application 20 Mar. 1958).

Electrostatic developing powder, consisting of semiconductive zinc oxide coated with a heat-sensitive, film-forming material, such that the developed image has volume resistivity not greater than $10^{12}\ \Omega$ per cm and therefore cannot hold an electrostatic charge in the dark, is used to print two or more nonoverlapping, differently colored images on a dye-sensitized zinc oxide resin coated sheet. Although this process is proposed for reproduction of color transparencies, and although the sequence of exposure colors and developer colors differ from those described in the abstracts for U.S. patents 3,062,019 and 3,062,020 the limitations are essentially the same as for U.S. patent 3,062,019. C.S.

3,060,790 30 Oct. 1962 (Cl. 88-14)
Colorimeter and color sorting apparatus.
J. W. Ward. Assigned to Specialties, Inc. Filed 2 Feb. 1959.

A four-filter colorimeter is combined with electrical networks for analog computation of CIE tristimulus values and chromaticity coordinates and comparison of same with pre-set standard values and tolerances on each of three of those quantities. Conformance with the standard values, or classifications according to which one or combinations of tolerances is violated, is indicated by the glowing of one of twenty-seven pilot lamps. The samples are carried to the reading position by a continuously moving belt, and the indications of conformance or manner of violation of tolerance is delayed until the sample emerges to where it can be picked up manually. D.L.M.

3,062,087 6 Nov. 1962 (Cl. 88-14)
Apparatus for investigating polarized-light phenomena.
F. Zandman and J. Avril. Assigned to The Budd Co. Filed 2 Apr. 1957 (in France 9 Apr. 1956).

A polariscope specially adapted to the observation of photoelastic phenomena in surface coating is described. W.L.H.

3,062,088 6 Nov. 1962 (Cl. 88-14)
Null-type radiation analysis system.
H. M. Bolz. Assigned to Bodenseewerk, Perkin-Elmer and Co. Filed 9 Apr. 1959.

For instruments such as double-beam spectrometers, a concept for null-type radiation analysis is presented which utilizes a mechanical attenuator in both sample and reference beams. Both attenuators are coupled to each other but have different transmission characteristics. This method enhances the detection of weak absorption bands because the reference beam attenuator is forced to move to greater displacements. R.K.M.

3,062,095 6 Nov. 1962 (Cl. 88-24)
Projector optical scanning system.
J. Rutkus, Jr., D. W. Shepardson, and A. W. Griswold. Assigned to Xerox Corp. Filed 2 July 1959.

This complicated patent covers a xerographic-type reproducing machine. An optical image of the original copy is projected onto a rotating drum comprised of a photoconductive insulating-layer backed by a charged electrical conductor. The presence of illumination causes an electrostatic latent image to develop on the outer drum surface. As the drum rotates, an electroscopic ink pigment is transferred to the drum surface in correspondence with the original image. The drum next moves against a paper surface and prints a copy. The apparatus to charge the drum, dispense the powder, project an image, handle the paper, and deliver the prints is shown in some detail. The machine disclosed appears to be similar to the Xerox 914 copying machine which has recently gone into widespread use. R.K.M.

3,063,332 13 Nov. 1962 (Cl. 88-2.4)
Angle measuring mechanism.
J. Fajans. Assigned to Electrokinetics Corporation. Filed 28 Apr. 1960.

The angular separation of two distant objects, such as stars, is conveniently determined using a device comprising coaxial inner, middle, and outer members. The inner member is substantially a telescope having a pivoted reflector in front of the objective. Rotation of the reflector is mechanically coupled to the relative rotation of two of the coaxial members. The several relative rotations are coupled to potentiometers which, in an appropriate electrical circuit, yield a direct angular indication. R.D.A.

3,064,526 20 Nov. 1962 (Cl. 88-32)
Dual image reflecting telescope.
W. N. Lindsay. Filed 23 June 1958.

Lindsay has devised a variation of the Cassegrain-Galilean reflecting telescope for visual use: the primary mirror converges the light onto a convex secondary adjusted to make it parallel again. The stray-light problem is claimed as an advantage, that is, the user sees most of the field directly and unmagnified with a small portion highly magnified in the middle. All of the claims include the simultaneous presentation of the magnified and unmagnified fields. W.L.H.

3,064,534 20 Nov. 1962 (Cl. 88-84)
Reflector for space vehicle.
J. W. Tumavicus. Assigned to United Aircraft Corp. Filed 13 Apr. 1960.

A lightweight, collapsible, parabolic reflector is described which is useful for space applications. The sectors of the mirror are compactly stored with their long axis parallel to the mirror base and the fixed focal point (a detector on a tripod). Each mirror sector has a shaft at one end that fits into individual holes located about the base circumference. When actuated by a common drive-mechanism in the base, all sectors simultaneously swing out into open position. R.K.M.

3,066,222 27 Nov. 1962 (Cl. 250-83.3)
Infrared detection apparatus.
R. M. Poorman, G. C. Haettinger, and R. F. O'Connell. Assigned to Union Carbide Corporation. Filed 18 Nov. 1959.

This invention relates to an improved refrigerated mounting means for an infrared detection cell utilizing cryogenic liquids. The improvement is related to the technique for filling and venting the refrigerant liquids. A device built to the specification of the invention has successfully maintained the desired operating temperature for an infrared detector for 6 to 7 hr without refilling. This device was 12.5 cm in length and 6 cm wide. It is intended to be applied primarily to missile use where small size and long life are necessary. D.J.L.

3,074,317 22 Jan. 1963 (Cl. 88-57)
Zoom lens.
A. Cox and W. J. Johnson. Assigned to Bell and Howell Co. Filed 24 Dec. 1959.

A 3:1 zoom lens of 11 elements (*f*/1.8 aperture) is described, the front positive 3-element group being cam-driven to hold focus and is also adjustable for focusing the system; the middle negative 3-element group is movable linearly for zooming; and the fixed positive element yields parallel light in the stop space. There is also a 4-element fixed positive system in the rear. One example is given, dominated by a set of 8 inequalities. R.K.

continued on page 1322

A Large-Stage Photoelectric Planimeter for Leaves

P. D. Carman

A number of possible designs of photoelectric planimeters are examined with special attention to uniformity of response over the stage area. A design is developed in which four photocells are positioned to make their total response uniform over a large stage. The principle is illustrated by the construction of one such instrument.

A large variety of photoelectric planimeters have been made to measure the areas of objects by measuring their obstruction of light.[1–5] One such device[1] with a 14.5-cm diameter stage was constructed by Donovan, Magee, and Kalbfleisch with some advice from the author. Experience with it showed that a much larger stage, about 30 cm by 45 cm, would be useful, if it could be designed without increasing the instrument size. The design of such a large-stage area photometer is described here.

The measuring stage in a simple photoelectric planimeter with a diffusing stage and a single photocell is limited in area by basic photometric principles. If a uniform diffuse source S (Fig. 1) of luminance B candelas/cm^2 is viewed by a small photocell of area P from a distance D on the axis of the source, the light flux reaching the photocell from a small area Δ_S of the source at a distance r from the center of the source is given by

$$\Delta F_r = \frac{B\Delta_S P \cos^4\theta}{D^2}, \text{ where } \tan\theta = \frac{r}{D}\cdot$$

The flux from a small area at the center of the source is given by

$$\Delta F_0 = \frac{B\Delta_S P}{D^2}\cdot$$

The percentage difference between these two, that is, the error at distance r is given by

$$\begin{aligned}\delta_r &= \frac{\Delta F_0 - \Delta F_r}{\Delta F_0} \times 100\% \\ &= (1 - \cos^4\theta) \times 100\% \\ &= 200\left(\frac{r}{D}\right)^2\% \text{ approximately, for small values of } \theta.\end{aligned}$$

Hence if the error is to be limited to 1%, $\frac{r}{D}$ must not exceed 0.0707. Hence if D is 90 cm, r should not exceed 6.35 cm, and at a radius of 7.2 cm[1] the theoretical error is 1.28%. This is for a small photocell. For a large photocell, calculation is much more involved. A formula suitable for numerical computation is given by Walsh.[6] It shows that, for a 15-cm diameter receiver at 90 cm from the stage, the sensitivity for an object 7.2 cm off center is down 1.24%. Thus the gain in uniformity achieved by the use of a large photocell is negligible.

The need for a large-stage photometric planimeter inspired a general re-examination of design problems.

The basic requirement for a photometric planimeter is that over its working stage area, the product of the illumination and the receiver sensitivity should be essentially constant. In practice it is usually best to make each of these constant individually.

Illumination and collection may each approach either a totally diffuse or a unidirectional condition. Intermediate conditions are also possible though more difficult to design.

A fully directional system, in which a lens is used to provide a collimated light flux at the stage and a second lens focuses this light on the receiver, is very attractive because it will measure accurately on samples which scatter light even if they do not absorb it. Unfortunately, to give basically uniform sensitivity, at least one of the lenses must be aplanatic. This makes the cost high for a large-stage instrument. An economical variant of this system has been described by Miller *et al.*[7] in which plastic Fresnel lenses are used and their errors are compensated by empirically graded shading. The difficulty of obtaining accurate and permanent correction by shading makes such a system attractive only for specimens which do not have enough absorption to make simpler systems satisfactory.

The author is in the Division of Applied Physics, National Research Council, Ottawa, Canada.

Received 24 September 1962.

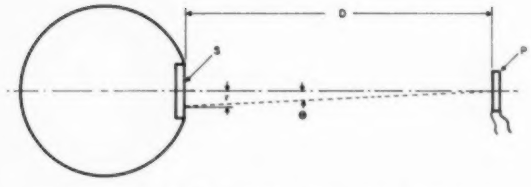

Fig. 1. Principle of a simple photometric planimeter.

If at least one diffusing system is to be used it should be the illumination system and should consist of an integrating sphere or cube. As a lamp ages, the distribution of its output changes. If several lamps are used their outputs will depreciate unequally. Both effects would reduce illumination uniformity without the corrective mixing action of an integrating device. Thus an integrating illuminator has a major advantage over either a unidirectional illuminator or an intermediate arrangement such as multidirectional illumination.

An integrating system might also be used as the collecting system. However, two integrating devices make access to the stage difficult.

Since both unidirectional and diffuse collecting systems had practical disadvantages an intermediate or multidirectional collecting system was considered. It seemed likely that several photocells at a convenient distance above a uniform diffuse-source stage could be arranged so that the sum of their responses was nearly constant for a small area moved anywhere on the stage. Since such an arrangement was economical and convenient, its design was studied theoretically.

A. Marriage[8] has shown that uniform illumination can be obtained along a line by adding the illumination from two well-spaced lamps. The similar case of two photocells added to provide uniform sensitivity along a line was first studied. The significant difference between the two situations is that the lamp was treated as a source radiating equally in all directions, whereas the photocell approximates a Lambert's law receiver. This raises the cosine from the third to the fourth power.

From Fig. 2, the light flux on photocell P_1 of area "a" from a small surface at Q of area A and luminance B is

$$F_1 = \frac{BAa}{D^2}\cos^4\theta = \frac{BAa}{D^2}\,\frac{1}{1 + 2\dfrac{x_1^2}{D^2} + \dfrac{x_1^4}{D^4}}.$$

If B is constant and A, a, and D are the same for both photocells the sum of the light fluxes on P_1 and P_2 is

$$F_1 + F_2 = \frac{BAa}{D^2}\left(\frac{1}{1 + 2\dfrac{x_1^2}{D^2} + \dfrac{x_1^4}{D^4}} + \frac{1}{1 + 2\dfrac{x_2^2}{D^2} + \dfrac{x_2^4}{D^4}}\right).$$

The variable bracketed term can be evaluated for various source positions and for various values of the photocell separation d using $d = x_1 - x_2$. Results are shown in Fig. 3. Gains in the length of source positions covered with adequate uniformity are not as great as for lamps, due to the additional cosine factor, but are promising.

To extend the uniform coverage to an area, four photocells placed at the corners of a square were tried. Taking the height of this square above the diffuse source as unity, squares were tried with sides of 1.00, 1.04, 1.06, 1.08, 1.10, and other values. That is, in a coordinate system with center at the center of the diffuse source and z axis vertical, photocell positions were as shown in Table I, in which the last position is an additional rectangular arrangement. Selected results

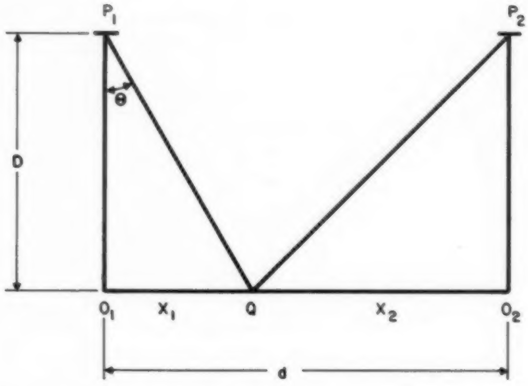

Fig. 2. Calculation of uniformity of sensitivity along a line.

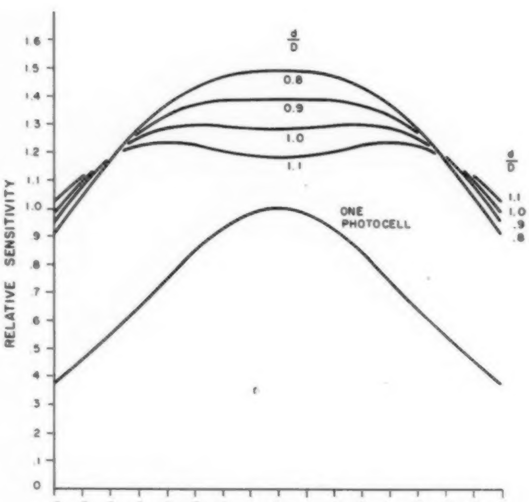

Fig. 3. Uniformity of sensitivity along a line with two photocells.

Table I. Positions for Four Photocells

x	y	z	Fig. 4
±.50	±.50	1.00	a
±.52	±.52	1.00	b
±.53	±.53	1.00	c
±.54	±.54	1.00	d
±.55	±.55	1.00	e
±.54	±.52	1.00	f

of the calculations are shown in Fig. 4 as relative sensitivities and contours of equal sensitivity for the first quadrant of the source. Sensitivities are symmetrical about both the x and the y axes. The approximate position of maximum sensitivity is indicated and the value of the variable term there is shown.

A square stage area of side 0.81 is covered with a uniformity of ±1%, or 2% total variation, for photocell positions $x = y = \pm 0.53$. Larger values of x and y extend the uniformity along the diagonal but reduce the uniformly covered square. A long narrow rectangle might advantageously be placed along the diagonal, except for mechanical difficulties, but for the 45 cm by 30 cm shape desired the diagonal is not useful. Some attempt was made to improve the coverage of a 3:2 rectangle, and Fig. 4f shows that $x = \pm 0.54$, $y = \pm 0.52$ slightly extends the x dimension covered from 0.81 to 0.85 while reducing the y dimension to 0.66.

To scale this arrangement to cover the desired 45 cm by 30 cm, multiplying x, y, and z by 45/0.8 provides a small safety factor and gives for the photocell position

$$x = \pm 30.4 \text{ cm}, \quad y = \pm 29.3 \text{ cm}, \quad z = 56.2 \text{ cm}.$$

This arrangement, with some space for adjustments, fits conveniently in a 75-cm cube (Fig. 5). Photocells used were Weston 856YR.

The diffuse source stage was provided by a 75-cm integrating cube with a window of 040 White Diffusing Opal Perspex 3 mm thick protected by 6-mm plate glass. Light is from eight 20-W, 59-cm fluorescent lamps arranged as shown in Fig. 6. Brightness uniformity was well within 1% without any lamp selection or adjustment. The lamps were operated at their rated voltage from a regulating transformer. Fluorescent lamps have an advantage over tungsten lamps in that their output varies only as the first power of the voltage rather than the 3.38th power. In addition, they produce light of the desired spectral quality with greater efficiency and hence with less heating of the cabinet.

The photocells were first placed in their calculated positions. Uniformity of sensitivity was measured by placing a 5-cm diameter aperture at each of forty stage positions. It was found that reflections from the black painted walls of the compartment were causing serious departures from the calculated sensitivity distribution. This was corrected by lining the walls with black velvet. Small adjustments were then made to the photocell positions to allow for departures from the $\cos^4$ law and for differences in sensitivity. The desired ±1% accuracy was readily achieved.

The instrument was originally constructed using pink fluorescent lamps and Wratten 29 filters in accordance with earlier practice. However, a test made by covering the whole stage with sugar-beet leaves showed that for this spectral distribution the leaves had a transmission of about 1%. A 1% transmission would make leaf area measurements appear to be 1% smaller than their true values. This seemed an undesirably large persistent error.

In a search for better spectral conditions a number of leaves were spectrophotometered. Typical results, in Fig. 7, showed that the blue region below 500 mμ is much more desirable than the red region. This is in accordance with the work of Petrov and Gavrilov.[4]

A change was made to blue fluorescent lamps and to Corning filters CS5-57. The red and the blue spectral arrangements are shown in Fig. 8. Calculations based on manufacturers' data and the leaf transmissions of Fig. 7 showed important reductions in the effective leaf transmissions with the blue system (Table II). It seems reasonably safe to expect that all leaves which are predominantly green in color can be measured with errors in area due to transmission of less than 1%.

Table II. Effective Leaf Transmissions for Various Leaves in Two Spectral Conditions

		Transmission %	
Leaf	Curve (Fig. 7)	Blue	Red
Sugar beet	1a	0.05	0.8
Sugar beet (worst)	1b	0.25	1.8
Trefoil	2	0.4	1.7
Coleus	5	0.6	2.8
Perilla (red)	6	3.0	12

For the final adjustment of the instrument the uniformity of sensitivity was as shown in Fig. 9. The stage brightness was about 400 cd/m² and the total photocurrent for the uncovered 30 cm by 45 cm stage was about 50 μA.

A general view of the instrument is shown in Fig. 10. The Kipp A70 galvanometer is set to full-scale reading on the unobstructed aperture by the use of its internal range switch plus a coarse and a fine shunt located on top of the cabinet.

The author wishes to thank L. S. Donovan for suggesting the requirement, C. Dodd for the spectrophotometry of leaves, and B. Norton for making the sensitivity calculations and for carrying out the final stages of construction and adjustment of the planimeter.

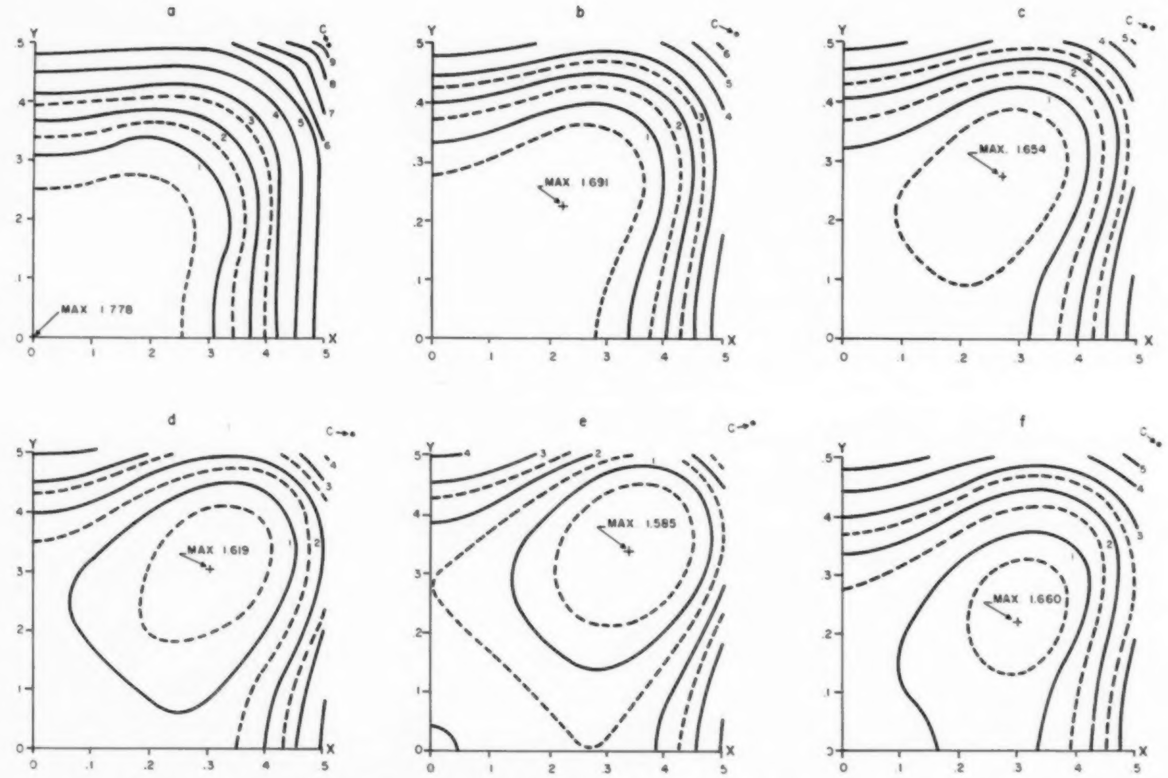

Fig. 4. Uniformity of sensitivity over an area using four photocells. Contours indicate percentage below maximum sensitivity. C designates plan position of photocell.

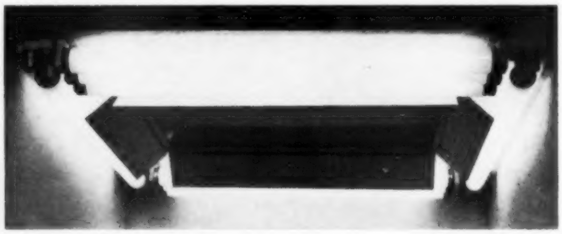

Fig. 6. Arrangement of fluorescent lamps in integrating cube. Note baffles between lamps and window.

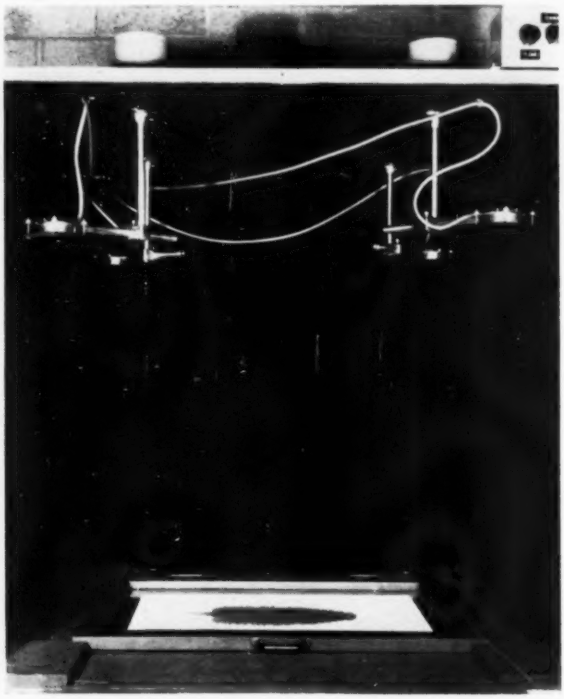

Fig. 5. Arrangement of four photocells in planimeter.

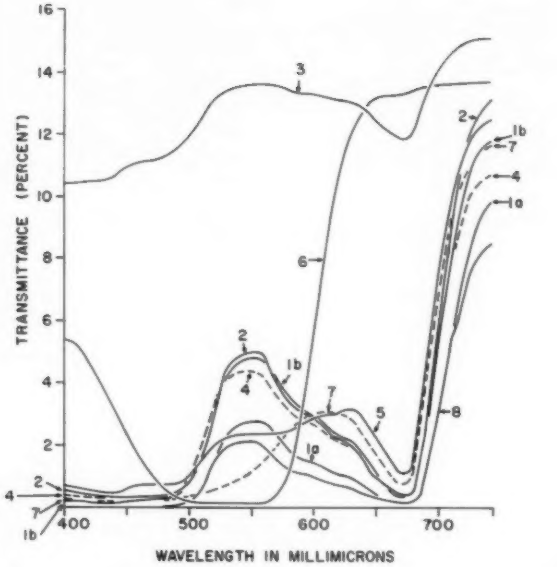

Fig. 7. Spectrophotometric curves of a number of leaves. Measured with normal illumination and nearly diffuse pickup. 1a—Sugar beet (minimum). 1b—Sugar beet (maximum). 2—Trefoil (red clover similar). 3—Begonia (white). 4—Begonia fibrous. 5—Coleus. 6—Perilla (red). 7—Rex begonia. 8—Orange (philodendron similar).

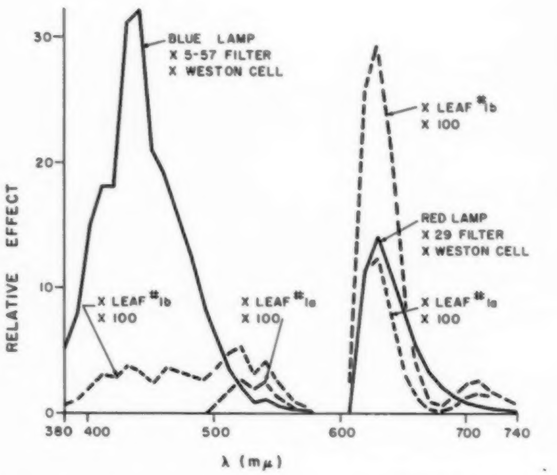

Fig. 8. Blue and red spectral arrangements. Lamp × filter × cell curves are computed from manufacturers' data.

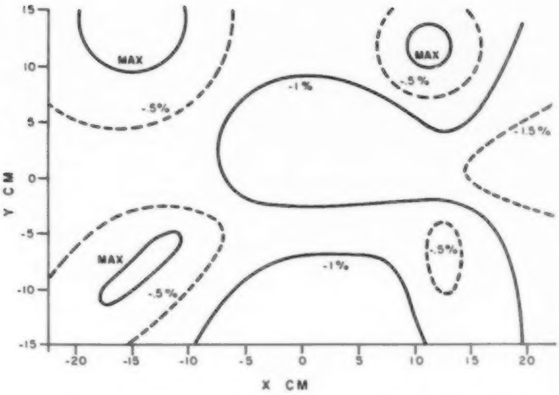

Fig. 9. Uniformity of sensitivity measured after final adjustment.

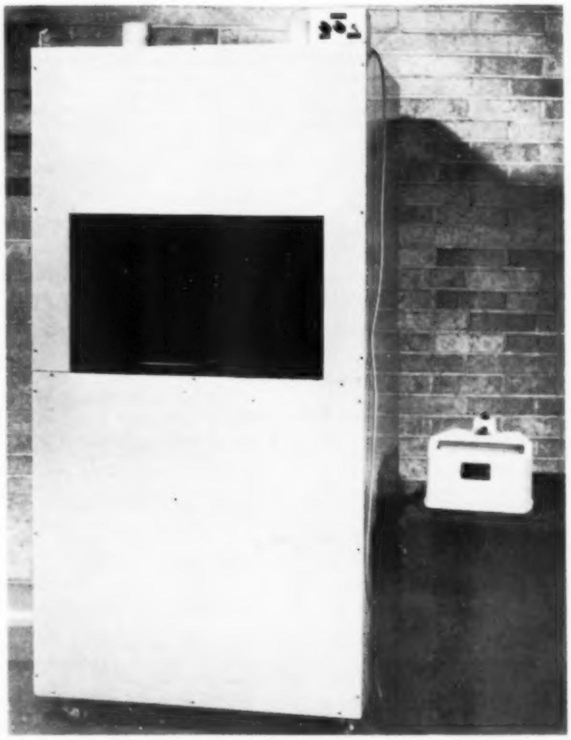

Fig. 10. General view of photoelectric planimeter.

References

1. L. S. Donovan, A. I. Magee, and W. Kalbfleisch, Can. J. Plant Science **38,** 490 (1958).
2. See also bibliography in ref. 1.
3. R. W. Gerdel and Robert M. Salter, J. Am. Soc. Agronomy **20,** 635 (1928).
4. E. G. Petrov and N. I. Gavrilov, Compt. rendus (Doklady) de l'Académie des Sciences de l'URSS **24,** 499 (1939).
5. B. Orchard, J. Experimental Botany **12,** 36, 458 (1961).
6. J. W. T. Walsh, *Photometry* (Constable & Co. Ltd., London, 1953), 2nd ed., p. 142.
7. E. E. Miller, C. A. Shadbold, and L. Holm, Plant Physiology **31,** 484 (1956).
8. A. Marriage, *Even Illumination from a Pair of Lamps* (Royal Photographic Society of Great Britain, Science and Applications of Photography, 1953), p. 220.

Patents *continued from page 1316*

3,074,318 22 Jan. 1963 (Cl. 88-57)
Zoom lens system.
Keizo Yamaji. Assigned to Canon Camera Co. Filed 2 Sept. 1960 (in Japan 5 Sept. 1959).

A 13-element mechanically compensated zoom lens of high quality is described, with an aperture of $f/2.8$ and a focal-length range from 45 to 200 mm (4.1:1). The maximum angular field is ±25°. The fixed front component is positive, of three elements; the sliding negative component has four elements; the cam-driven third component is a single negative element; and the fixed rear component contains a positive doublet, a positive singlet, a thick negative singlet, and a rear positive singlet. One example is given which is covered by a set of 15 inequalities. R.K.

3,079,507 26 Feb. 1963 (Cl. 250-217)
Optical pyrometers.
H. J. C. George. Assigned to Quartz and Silice S. A. Filed 29 Jan. 1959.

An optical pyrometer of the disappearing filament type is described, wherein a single light-sensitive element monitors a cyclically scanned field which includes the filament image. The ac component of the detected signal may be used to measure or to control automatically the temperature of the heat source. R.D.A.

3,079,834 5 Mar. 1963 (Cl. 88-14)
Spectrometers.
A. E. Martin. Assigned to C. A. Parsons and Co., Ltd. Filed 28 June 1955 (in Great Britain 1 July 1954).

This invention is concerned with improvements in the operation of optical spectrometers especially applicable to infrared spectra with ruled diffraction gratings. The object is to provide a means (3 alternative arrangements are pictured in figures) whereby the grating may be rotated by a screw in such a way that a linear relation is obtained between the wavelength of spectral lines and the number of turns of the screw. By calibration of the screw or use of a micrometer screw, the reading of the screw indicates the wavelength directly in microns. This idea seems to be akin to the older application of calibrated wedges in absorption photometers attached to calibrated dials. G.L.C.

3,087,062 23 Apr. 1963 (Cl. 250-83.3)
100 in. (2.54 m) radiometer.
H. L. Clark. Filed 13 May 1960.

The radiometer of the present invention was designed to provide a system for measuring slight temperature differences, such as required in investigating sea states. It utilizes a 2.54-m diam mirror of 1.77-m focal length. A thermopile is placed at the focal point to provide an electrical output. The incident radiation is mechanically chopped at about 5 cpss and the electrical signal is synchronously rectified. Changes in radiant intensity equivalent to 500-μ degrees can be observed with a possible error of about 5% D.J.L.

3,088,368 7 May 1963 (Cl. 88-57)
Variable-magnification Optical System.
R. W. Tripp, E. B. Brown, and M. Shenker. Assigned to Farrand Optical Co. Filed 15 Jan. 1959.

A two-member projection system is described which is capable of giving a wide range of image magnification between a fixed pair of conjugate planes. Lens group A forms a reduced real image of the object, and lens group B reprojects this image on the screen, both lens groups being moved to vary the magnification. To maintain correct stop imagery, the lens groups are telecentric at the real image lying between them. Several examples are given, some of which are simple and some very complex. R.K.

3,088,369 7 May 1963 (Cl. 88-57)
Projection lens system.
J. R. Miles. Assigned to F. E. Aufhauser. Filed 12 Feb. 1960.

A reversed Galilean afocal attachment is described for use in front of the lens of a motion-picture projector to shorten the equivalent focal length and hence enlarge the projected image. The attachment contains four elements in two widely spaced groups. Two specific examples are given, both of which magnify the image by a factor of 2. R.K.

3,088,370 7 May 1963 (Cl. 88-57)
Adjustable lens mount.
O. Erbe and O. Weiss. Assigned to C. Zeiss, Oberkochen. Filed 20 June 1960 (In Germany 11 July 1959).

For moving a lens relative to a mount, an inner sleeve is provided between lens and mount; one rack is mounted on the inside of the mount, another rack on the outside of the lens, and a pinion is attached to the intermediate sleeve meshing with both racks. A longitudinal motion of the intermediate sleeve produces twice as great a longitudinal motion of the lens. R.K.

3,088,371 7 May 1963 (Cl. 88-57)
Symmetrical 6-element objective.
H. Lowenthal. Assigned to General Scientific Corp. Filed 5 Aug. 1960.

A picture claim is made for a symmetrical 6-element lens intended to cover ±28° at $f/5.6$. Each half contains three uncemented meniscus elements in the order plus-minus-plus, with their concave sides facing the stop. R.K.

3,090,278 21 May 1963 (Cl. 88-14)
Automatic means for aligning spectrometer components.
J. L. Saunderson. Assigned to Baird-Atomic, Inc. Filed 22 Mar. 1960.

A direct reading spectrometer is susceptible to small variation in temperature, barometric pressure, etc., causing misalignment and consequent errors in quantitative analysis. This invention uses a servo control to adjust the grating for small displacements. The servo is actuated by a divided and chopped central image or spectral line falling on a photomultiplier tube. J.J.B.

3,090,279 21 May 1963 (Cl. 88-14)
Interferometer using a diffraction grating.
J. J. Chisholm. Assigned to Bausch & Lomb, Inc. Filed 13 May 1960.

This interferometer contains a diffraction grating for dividing, and recombining, the light. Advantages are claimed to be lower cost (as compared with flats of interferometer quality) and ease of adjustment. As shown in the figure, light coming from source 12 is collimated by lens 16, split by transmission grating 10, passed through two channels 30 and 32, and returned by two reflection type diffraction gratings 22 and 24. J.M.A.

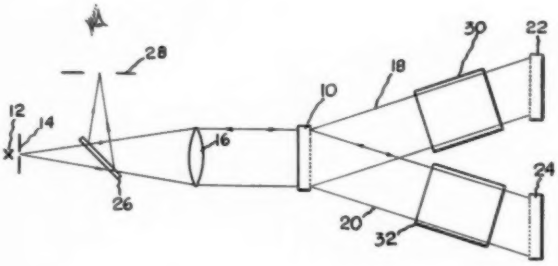

3,090,282 21 May 1963 (Cl. 88-57)
Mechanism for controlling the axial displacement of optical elements.
P. Angénieux. Filed 3 March 1959 (in France 28 Jan. 1959).

A mechanism for a zoom lens is described in which free balls replace the "pins" in a "pin-and-slot" mechanism. The slots are shaped in accordance with the desired law of motion, and by using three pre-stressed balls at each end of the lens barrel, a very precise yet freely operable zoom mechanism can be obtained. R.K.

3,090,863 21 May 1963 (Cl. 250-43.5)
Monochromator adapted for use in the ultraviolet region.
P. M. McPherson. Assigned to McPherson Instrument Corporation. Filed 31 Jan. 1962.

The patent covers several schemes for constructing an ultraviolet concave grating monochromator having stationary entrance and exit slit apertures. In such monochromators, the grating is translated to maintain the focus as it rotates to scan the spectrum. Mechanisms, cams, and linkages to provide such motion are described. T.K.M.

3,094,580 18 June 1963 (Cl. 88-57)
Afocal focal-length changer.
R. Rosier. Assigned to SOM Berthiot. Filed 3 Aug. 1960 (in France 6 Aug. 1959).

A thick afocal telephoto converter is described in which the outside surfaces are perpendicular either to the principal or to the marginal ray. Plano interfaces, and two other "buried" achromatizing surfaces, are added for the correction of aberrations. One example is given, for converting a 50 mm $f/2.8$ lens to 75 mm focal length. R.K.

3,094,581 18 June 1963 (Cl. 88-57)
Zoom projection lens.
F. G. Back. Filed 29 Dec. 1960.

An optically compensated zoom projection lens is described, of the type in which two coupled sliding positive components have a fixed negative component between them, and a fixed positive component in the rear. The diameter of the fixed negative component is made such that the entrance pupil diameter remains substantially constant during a zoom in order to maintain a reasonably constant screen brightness. The focal length is varied by pulling out the front flange of the complete lens, and the system may be focused for use with different screen distances by rotating the same front flange. Two examples are given: one covers a focal length range of 15 to 25 mm for use with 8 mm film, and the second covers a range of 91 to 156 mm for use on a slide projector. R.K.

Optical Excitation of Mercury Vapor for the Production of Isolated Fluorescence

R. Zito, Jr., and A. E. Schraeder

Empirical data are presented for the preliminary intensity and resolution measurements made in the multiple-step induced fluorescence of mercury vapor. The primary application contemplated for such a process is the production of an isolated source of visible radiation in three-dimensional space. A dual optical excitation process is employed in conjunction with inelastic foreign gas molecule collision for the resultant spontaneous, visible fluorescence of excited mercury atoms. Details of the experimental apparatus and techniques employed are also given.

Introduction

Preliminary studies were made to examine the possible application of dual excitation of mercury vapor as a usable source of fluorescence. In particular, the experiments were directed at the production of an isolated region of fluorescing vapor for three-dimensional purposes. Many approaches[1–4] to the problem of achieving the display of information in real three-dimensional space have been taken. The two general types of approaches involve either the use of complex switching matrices for activating appropriate circuits in a three-dimensional array or the use of mechanically moving components within the display volume. In the former type of system, such phenomena as localized electrical discharges in a gaseous medium between a predetermined set of wire electrodes results in a "glowing region" of gas within a larger volume.[3] The fluorescence or electroluminescence of appropriate phosphor elements by dual electrical or combined electrical and optical excitation has also been employed.[2]

In the second variety of devices, a rotating or oscillating screen is employed to sweep out a volume in space. This screen is either a passive, diffuse reflector for an appropriately programmed external source of light, a phosphor screen within a cathode-ray tube[5] which fluoresces when impinged upon by an electron beam, or an electroluminescent panel whose segments are activated at the "correct times" to display a point of light at some location in space.

To produce a visual image in three-dimensional space, a number of conditions must be satisfied. The image space must be transparent to visible radiation and, at the same time, possess such properties to cause a near-point source of light to appear within its interior. The location of the near-point source must be controllable by some means external to the image space. Consequently, a threshold or multiple-excitation phenomenon of some sort is required whereby no visible light is produced at a limited region of the image space until a minimum-excitation level is reached or until two or more stimuli are present.

Step-wise excitation[6,7] of mercury vapor at low pressures exhibits properties readily applicable, in principle, to obtaining an isolated, visible region of fluorescence in space. The excitations employed are optical.

Figure 1 illustrates the technique that was studied. Two beams of radiation, excitations 1 and 2, are introduced into the absorbing-gas region and result in fluorescence of the mercury vapor at the volume of intersection. Neither excitation by itself will cause visible fluorescence of the mercury if appropriately filtered.

Figure 2 is a partial energy-level diagram for mercury showing the energy states utilized by these processes. The first excitation is the resonance line 2536.52 Å, ultraviolet region, and the second excitation is the 4046.66 Å line that raises the excited 6^3P_0 atom to the 7^3S_1 state. The mechanism for producing the green fluorescence at the region of beam intersection is basically the following:

Excitation 1 raises the normal ground state, 6^1S_0,

R. Zito is a consulting physicist with General Electric Company, MSVD, Philadelphia, Pennsylvania. A. E. Schraeder is a senior research engineer with the Instrumentation Section, Research Division, Jones & Laughlin Steel Company, Pittsburgh, Pennsylvania.

Received 25 September 1962.

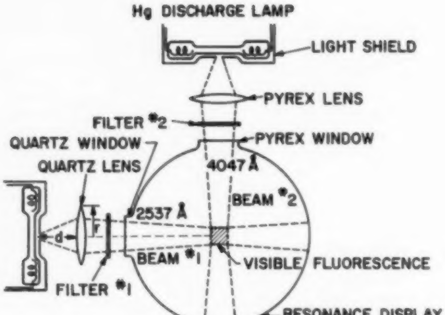
Hg DISCHARGE LAMP
LIGHT SHIELD
PYREX LENS
FILTER #2
QUARTZ WINDOW
PYREX WINDOW
QUARTZ LENS
4047 Å
2537 Å
BEAM #2
d
f
BEAM #1
VISIBLE FLUORESCENCE
FILTER #1
RESONANCE DISPLAY CHAMBER

Fig. 1. Dual excitation chamber containing mercury vapor and nitrogen gas.

atom to the first resonance, 6^3P_1, level. Subsequent collisions between these resonant-state Hg atoms and diatomic nitrogen molecules also present in the medium result in the creation of metastable, 6^3P_0, state Hg atoms. Excitation 2 then raises these 6^3P_0 atoms formed along beam 1 to the 7^3P_1 state. Spontaneous decay to the lower 6^3P_2 state produces the green 5460.74 Å line. Other processes are also possible, depending upon the spectral characteristics of the excitations and the conditions in the absorption chamber.

Experimental Procedure

Construction and Processing of Chambers

Three designs of absorption chambers were used in this investigation: an all-quartz Raman tube and two all-pyrex tubes with multiple-window flats. Figure 3 shows the construction of the cell that was used for most of the experiments performed. The cell is a pyrex cylinder about 15 cm in length and 11.5 cm in diameter, with one quartz window cemented to the side wall. Due to the window mounting, it was not possible thoroughly to outgas the chamber walls, and it became necessary to flush the system periodically with nitrogen. A cemented quartz window was used rather than a graded seal because of the increase in optical path length encountered with the seal. Processing of this cell consisted simply of introducing a few drops of mercury, connection to the vacuum system, and pumping down to about 10^{-4} mm pressure. At this pressure, the contamination due to hydrogen and oxygen is quite serious; therefore, the entire system is flushed with nitrogen a number of times. It was noted that the fluorescence intensity was appreciably diminished 10 or 15 min after the flushing procedure compared to the intensity immediately following the processing. This may be attributed largely to the outgassing of the inside walls of the system. The gas used was reagent-grade nitrogen, with an impurity analysis as follows:

neon	0.6 mole%
argon	0.02 mole%
helium	0.02 mole%
hydrocarbons	0.002 mole%
hydrogen	0.002 mole%
hydrogen cyanide	0.01 mole%
oxygen	0.002 mole%
carbon dioxide	0.002 mole%

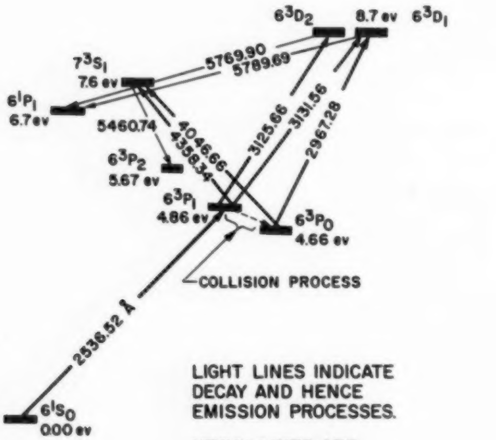
6^3D_2
8.7 ev
6^3D_1
7^3S_1
7.6 ev
5769.90
5789.69
6^1P_1
6.7 ev
5460.74
4046.56
4358.34
3125.66
3131.56
2967.28
6^3P_2
5.67 ev
6^3P_1
4.86 ev
6^3P_0
4.66 ev
COLLISION PROCESS
2536.52 Å
6^1S_0
0.00 ev
LIGHT LINES INDICATE DECAY AND HENCE EMISSION PROCESSES.
HEAVY LINES ARE ABSORPTION PROCESSES.

Fig. 2. Mercury energy-level diagram. Light lines indicate decay and, hence, emission processes. Heavy lines are absorption processes.

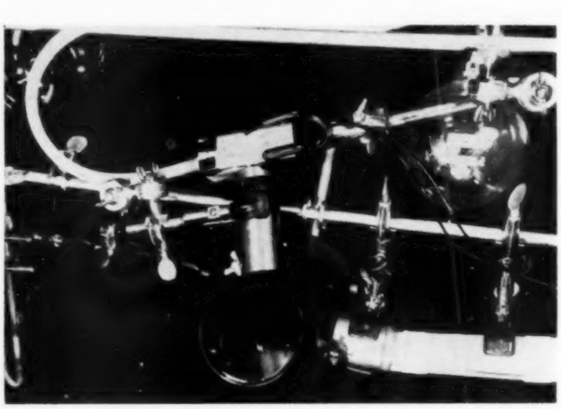

Fig. 3. Display chamber, dual excitation.

Light Sources

The source used initially was a dc-operated Cooper-Hewitt lamp[8] constructed in the laboratory. This lamp is started by tipping the tube, causing the mercury to run along the walls to the anode to establish an arc. The large diameter of the lamp, about 19 mm, necessitated deflecting the arc to the light exit wall of the tube by a magnetic field for maximum unreversed 2537 Å line. When this lamp is run hot, the lines are badly broadened; consequently, it was found necessary to water-cool continuously the lower portion of the lamp during operation. A search was made for more efficient, readily available mercury-discharge sources. It was found that an electrodeless rf-excited capillary is quite effective in exciting the mercury lines.[9]

A variation of the Hootermans lamp[8] was employed, in which the tube is constricted so that the discharge will take place closer to the walls, and was operated at 35 W. Calibration of this source was done by comparison with an incandescent lamp. The method used was the following: A 100-W incandescent lamp was mounted in a nonreflecting, telescoping tube, one end of which had a circular opening of 0.64-cm diam. Over the opening were placed one Wratten No. 73 filter (Fig. 4) and diffusing white paper whose transmission over the visible frequency range is flat. The distance of the bulb filament from the aperture was adjusted until the diffusely illuminated Wratten filter appeared to be the same brightness as an identical filter arrangement against the surface of the mercury lamp. This distance was found to be 7.6 cm. The total radiated energy from a 100-W filament between 5000 Å and 6000 Å and operated at about 2900°K is found (see Fig. 5) from Planck's law as

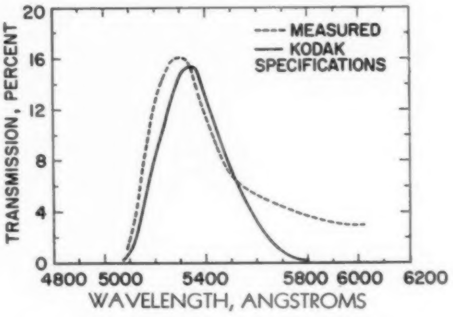

Fig. 4. Wratten No. 73 filter spectral transmission.

$$E_B = 8.4 \times 10^{12}\ \text{erg/cm}^3\text{-sec at } \lambda = 5500\ \text{Å},$$

$$E_{B\lambda}\Delta_\lambda = 8.4 \times 10^{7}\ \text{erg/cm}^2\text{-sec}.$$

The total radiation is

$$\sigma T^4 = 3.8 \times 10^{9}\ \text{erg/cm}^2\text{-sec}.$$

Since the total electrical input is 100 W, the ratio of the radiation between 5000 Å and 6000 Å and the total output is taken to find the power in this wavelength interval, or

$$100 \times \frac{E_{B\lambda}\Delta_\lambda}{\sigma T^4} = 8.4/3.8 = 2.2\ \text{W}.$$

Correcting for the inverse square law:

$$\frac{2.2}{4\pi(7.6)^2} = \frac{2.2}{720} = 3 \times 10^{-3}\ \text{W/cm}^2.$$

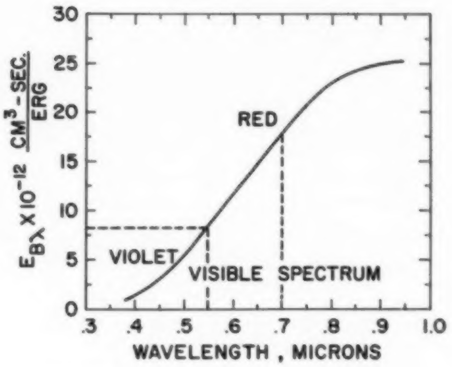

Fig. 5. Incandescent lamps pectral energy distribution. Planck's curve for $T = 2870°$ K.

Since filtering on both lamps is the same, the lowering of the light level due to their attenuation may be ignored. However, it is necessary to account for the response characteristic effects of the Wratten filter on the line emission of the mercury lamp. Table I gives some relative intensities of the mercury-arc lines.[10] Of the light transmitted from the mercury lamp through the filter,

$$\frac{98(10)}{9.8(10) + 5(1.2) + 10(0.2) + 10(0.2)} = \frac{98}{108} = 91\%$$

is the green, 5461 Å, line. Thus, the radiated intensity of 5461 and, consequently, 4047 and 2537 Å is about 2.8×10^{-3} W/cm^2 at the lamp surface. This corresponds approximately,

$$\text{for 2537 Å:}\quad 2.8 \times 10^{-3} \times 5.05 \times 2537 \times 10^{-8} \times 10^{22} = 14.1 \times 0.254 \times 10^{15} = 3.6 \times 10^{15}\ Q/\text{sec-cm}^2,$$

$$\text{for 4047 Å:}\quad 14.1 \times 0.405 \times 10^{15} = 5.7 \times 10^{15}\ Q/\text{sec-cm}^2,$$

$$\text{for 5461 Å:}\quad 14.1 \times 0.546 \times 10^{15} = 7.7 \times 10^{15}\ Q/\text{sec-cm}^2.$$

Optical Filters

In order to produce an isolated region of fluorescence within the chamber, it is necessary to separate the two wavelengths, 2537 Å and 4047 Å, in the excitation

Table I. Relative Intensities of Some Mercury Arc Lines[11]

Wavelength (Å)	Arc intensity	Wratten-filter transmission	Human eye response (1%)
2536.5	10	—	—
4046.56	10	—	0.1
4358.34	10	—	2
5460.73	10	9.8	99
5675.8	5	1.2	96
5769.60	10	0.2	89
5790.66	10	0.2	87
6072.63	5	—	54
6123.47	6	—	47
6234.35	8	—	32

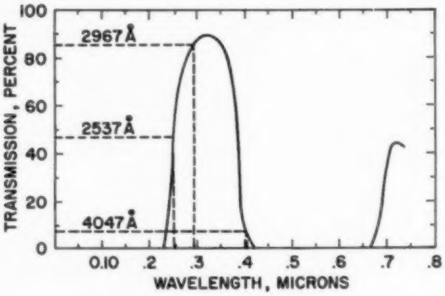

Fig. 6. Spectral transmission, Corning glass filter No. 9863, 2.9–3.1 mm thickness.

beams. Removal of the ultraviolet 2537 Å line from beam 2 is simple. The glass lenses and pyrex windows of the chamber have sufficient attenuation in this region. However, the problem becomes quite serious for the removal of 4047 Å in beam 1. Due to the possibility of exciting the 6^3P_0 level by 2967.28 Å, a rather sharp cut-off filter is required. If 2967 Å was present in beam 1, it was noted that a marked yellow fluorescence of 5789.69 Å was given off along its length, emitted by the 6^3P_1 level atoms undergoing a transition to the 6^1P_1 level.

A Corning No. 9863 transmission filter was first employed for beam 1. From Fig. 6, it can be seen that even though the relative transmission of the 2537 and 4047 Å lines are in the ratio of about 5:1, the presence of the 2967 Å line, which is 97% transmitted by the filter, will cause visible fluorescence[7,11,12] along the length of beam 1. Interference filters are available that have characteristics in the ultraviolet region approaching those needed for this application. Figure 7 shows a reflectance response for incident angles of 47° and 35° to the normal of the filter plane for a Bausch & Lomb experimental reflectance filter No. 6933. However, some difficulty is encountered because of the ratio of less than 3:1 in attenuation of the 2967:2537 Å lines.

Fluorescence Intensity and Resolution

Contamination Effects

The presence of such other gases as H_2, O_2, or CO_2 gives rise to serious quenching of the visible resonance radiation within the chamber. Unless the chamber is flushed a number of times, the fluorescence is either extremely low or completely quenched.

Lamp Operating Conditions

Increasing the lamp input power gives a noticeable increase in the excitation of the fluorescence. None of the lamps employed, however, was capable of being run at much higher power input than 30 W because of their design. Varying the air flow over the lamps was found to affect grossly the emitted line shapes. If the lamps were operated hot, i.e., uncooled or overcooled, no excitation of fluorescence was observed in the chamber. In the first case, the effect may be attributed to pressure broadening of the lines at higher temperatures; and in the case of overcooling, the overall intensity was greatly reduced and created a cool layer of mercury vapor close to the walls of the lamp, thus increasing the self-reversal of the lines.

Variation of the Color of Fluorescence

A marked change in the color or emitted wavelengths of fluorescence took place as the nitrogen pressure was varied in the absorption chamber. Immediately after flushing with nitrogen and admitting the gas at intermediate pressures, 3–15 mm, the fluorescence along beam 1 with no filter present was a deep yellowish-green in color. As the pressure of N_2 was decreased, the color changed to bluish-green and finally to a light blue at very low N_2 pressures. This may be attributed to the decreasing number of 6^3P_0 and 6^3P_1 atoms with decreasing N_2 pressure,[12] causing a corresponding reduction in the reabsorption of the 4047 and 4358 Å emitted by decaying 7^3S_1 atoms. A reduction of this reabsorption results in more of this visible light escaping the chamber to the observer. Since the 7^3S_1 level emits 5461, 4047, and 4358 Å upon spontaneous decay, we find that the population density of 6^3P_0 affects not only the absorption rate of primary 4047 but also the intensity of re-emitted 4047, thus changing the color of visible fluorescence.

Diffusion as a Function of N_2 Pressure

The diffusion of the metastable 6^3P_0 atoms at low N_2 pressures is quite pronounced. It was found that, at N_2 pressures of 5 mm or below and with beams 1 and 2 present, resolution of the region of fluorescence was quite poor. At these pressures and below, beam 2 was visible as fluorescence almost along its entire length, even though only wavelengths above 4000 Å were present in its path. This is due to diffusion of metastables from their volume of production, i.e., along beam

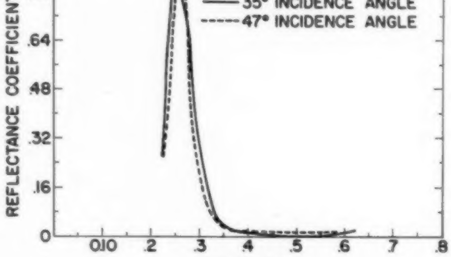

Fig. 7. Bausch & Lomb reflectance filter No. 6933.

1 to the region along the length of beam 2. As the pressure of N_2 was increased to 20 mm or greater, the visible portion of beam 2 contracted toward the intersection volume of both beams. These initial observations appear to verify those of earlier experiments. If the effective radii of both Hg atoms and N_2 molecules are taken as $\sigma \approx 3 \times 10^{-8}$ cm, and since the population density of 6^3P_0 is so much smaller than that of 6^1S_0 and N_2, the approximate relationship

$$Z = N\pi\sigma^2 C_{(6^3P_0)} \text{ collisions/sec}$$

may be used. $C_{(6^3P_0)}$ = average speed of 6^3P_0 atoms $\approx 2 \times 10^4$ cm/sec, and N = population density of other colliding bodies. At 25°C, the density of nitrogen is 6.5×10^{16} molecules/cm³, and of the 6^1S_0 atoms about 4×10^{13} atoms/cm³. Foote[13] and Stuart[14] give experimental values of 3.8×10^{-14} cm^{-3} and 2×10^{-12} cm^{-3} for 6^3P_0 destructive collision cross sections between N_2 and 6^1S_0, respectively. These were obtained at a nitrogen pressure of 2 mm.

By suitable calculations, it may be shown that about one collision in 120 of N_2 and 6^3P_0 and one in 2.5 with 6^1S_0 are inelastic. These calculations give

$$Z(N_2, 6^3P_0) = 3.6 \times 10^5 \text{ collisions/sec},$$

$$Z(6^2S_0, 6^3P_0) = 221 \text{ collisions/sec},$$

resulting in a mean time between inelastic collisions, for the greater rate, of about 3×10^{-4} sec. This gives an average total distance of 7 cm traveled by metastable mercury atoms. Pool[15] also obtained lifetimes, τ, of 6^3P_0 between 2×10^{-4} and 5×10^{-4} sec at N_2 pressures in the 2–40 mm range.

Penetration of Radiation

Under most conditions, the fluorescence due to beam 1 with all wavelengths present was visible along its entire length through the chamber. The beam entered the chamber through a window in the wall at right angles to the axis of the cylindrical chamber, thus making the path length about 10.8 cm.

Absorption of Reradiated 2537 Å

Resolution of the beam intersection within the chamber is partially a function of the reabsorption rate of the 2537 Å line emitted by atoms returning from the 6^3P_1 to the 6^1S_0 level.[16] Since this reradiation is essentially isotropic, 6^3P_1 and, consequently, 6^3P_0 atoms are created outside the volume occupied by beam 1. However, due to the relatively low level of intensity of reradiated 2537 as compared to the primary source of beam 1, this effect is secondary to that of 6^3P_0 diffusion and beam collimation.

Summary

Measurements were made of the fluorescence intensity of the green 5461 Å line by means of the dual-excitation process. The lamp source analyzed earlier was employed as both beam 1 and beam 2 inputs. A simple, single-lens geometry for achieving an unfiltered, slowly convergent beam of radiation gave an input level of about 5×10^{-5} W/cm² for both the 2537 Å and 4047 Å lines. Both wavelengths were present in beam 2 (see Fig. 1), and beam 2 was omitted. Absorption of both wavelengths through the chamber was such that a reduction of fluorescence level by a factor greater than 2 over 5 cm path length was observed. The nitrogen pressure was 12 mm.

A visual-comparison technique similar to that employed for the lamp output calibration was used to determine the level of 5461 Å radiation from a section of the dually excited gas about 2 cm down from the chamber entrance window. The total radiated energy (principally 5461 Å) was approximately 1.1×10^{-8} W/cm² of fluorescing-gas area. Correcting for the human-eye response, this corresponds to an illumination level of 6.7×10^{-6} lm/cm², or 6×10^{-3} lm/cm².

The light intensities in terms of photon density are—

Incident 2537 Å line:	6.4×10^{13} Q/sec-cm²,
Incident 4047 Å line:	10.2×10^{13} Q/sec-cm²,
Fluorescent 5461 Å line:	2.7×10^{10} Q/sec-cm².

If the destruction rate of 6^3P_0 atoms due to their mutual collisions is considered very small, then as a first approximation the radiated 5461 Å is proportional to the product of the intensities of 2537 Å and 4047 Å input.

Both experimental and theoretical results indicate that an N_2 pressure in the range of 5–20 mm is needed for maximum intensity of the green 5461 Å radiation. However, to reduce the diffusion of 6^3P_0 atoms, it is desirable to use a pressure upwards of 20 mm of either N_2 or a rare gas such as helium for which metastable quenching is a minimum. Better ultraviolet filters for line separation are required. Percentage transmission of 2537 Å greater than the 20% figure so far obtained is desirable. It is imperative that both the 4047 Å and 2967 Å lines be eliminated from beam 1 in order for this beam to be invisible except at the intersection with beam 2. The filters that were employed approach the type of response necessary, but are still inadequate for complete isolation of the fluorescence region.

Most important parameters to control are undoubtedly the intensity, line shape, and size of the light sources. So far, the intensity of fluorescence is lower, by a factor greater than the 100, than is desirable for easily visible levels.

References

1. H. Cheshire, Control Engineering **9** (No. 1), 21 (1962).
2. J. R. Alburger, New Electroflor Materials, Electronic Industries & Tele-Tech **16**, 50 (1957).
3. D. W. Perkins, Space Aeronautics **38** (No. 4), 64 (1962).

4. C. D. LaFond, Missiles and Rockets **9** (No. 16), 49 (1961).
5. J. L. Coddington and R. J. Schipper, "Practical Solid State Three-Dimensional Display", Paper presented at IRE International Conference, New York City, 28 March 1962.
6. C. Fuchtbauer, Physik. Z. **21,** 635 (1920).
7. R. W. Wood, Proc. Roy. Soc. (London) **106,** 679 (1924).
8. H. Cotton, *Electric Discharge Lamps* (Chapman & Hall, London, 1946).
9. L. M. Ashenbrand and M. Zelikoff, J. Opt. Soc. Am. **42,** 11, 818 (1952).
10. C. D. Hodgman ed.-in-chief, *Handbook of Chemistry and Physics,* 29th ed. (Chemical Rubber Publishing Co., Cleveland, 1945), p. 2072.
11. A. C. G. Mitchell and M. W. Zemansky, *Resonance Radiation and Excited Atoms* (Cambridge U. Press, New York, 1962).
12. M. J. E. Golay, Phys. Rev. **37,** 821 (1931).
13. P. D. Foote, Phys. Rev. **30,** 288 (1927).
14. H. Stuart, Z. Physik. **37,** 619 (1926).
15. M. L. Pool, Phys. Rev. **33,** 22 (1929).
16. M. W. Zemansky, Phys. Rev. **29,** 521 (1927).

Applied Optics
Of Optics and Opticists

This column is compiled partly from information sent by our Reporters in various centers of optics across the continent, but the Managing Editor welcomes news from any source

With the kind permission of the Editor of *The Optical Journal and Review of Optometry,* we are reprinting an editorial which appeared in the 1 August 1963 issue under the heading of **The Life of a Word**.

Very few dictionaries, either ophthalmic, medical, or general, carry the word "opticist". Its use occurs in the heading of a column "Of Optics and Opticists" in *Applied Optics.* This is a monthly publication of the Optical Society of America. Its readers are mostly physicists.

"Opticist" was once offered as the logical name for the nonmedical refractionist. The word was coined by Charles F. Prentice of New York, generally regarded as the father of American optometry. This goes back to 1886, the year Prentice had the word copyrighted.

Prentice felt there was a vacancy to be filled by the introduction of the name "opticist". He gave it peculiar significance, holding it to have greater fitness in distinction from its relative "optician". At the time, those who tested sight and fitted glasses were known as "opticians", as were the ophthalmic dispensers.

Prentice cited two conflicting definitions of "optician" from Webster: (1) one who makes or sells optical glasses and instruments; (2) a person skilled in the science of optics. Webster qualified the latter definition in 1886, calling it "rare", and in an earlier edition, in 1860, termed it "little used".

Prentice spoke of applied optics as a specific department of practice. He described it as "prescribing, according to scientific principles in physics, the lenses required to correct optical defects in the human eye—as an opticist, in the light of my meaning and definition of the word."

"A person qualified in the latter practice", he said, "would not be distinguished in his line of specialty under the general term, Optician, nor could he rightfully assume the title, Oculist, and I, therefore, advance the word, 'Opticist', in the absence of a better one having the same significant root, ops, as being the appellation best chosen to convey the idea of one making a specialty of fitting glasses or lenses, i.e., spectacles, to correct anomalies of refraction and accommodation of the human eye, in accordance with the science of Physiologic Optics, while at the same time wholly neglecting the practice of medicine and surgery".

To encourage the public to place confidence in the nonmedical vision specialist, Prentice issued ornate booklets under the title "Opticist". He had the word on his office door and projected it however he could. But he was alone in this.

Although he coined, copyrighted, and used "opticist" himself, Prentice recognized that his new creation would fail to meet with approval, much less adoption, unless it could be shown to be of benefit as an addition to the English vocabulary. In this he was right, up to a point.

None of the sight-testing opticians of his day accepted his term. More and more, they spoke of their work as "optometry". In 1904, the American Optometric Association adopted "optometrist" as the proper name for their specialty.

This must have been a bitter pill for Prentice. Who knows? Now he may be resting easy in the knowledge that his word "opticist" survives, even though it relates to specialists in physical optics and not ophthalmic optics.

HAVE YOU RENEWED
YOUR SUBSCRIPTION?

T. Matrai *Central Research Institute for Physics* at the Budapest Second Optical Conference 6–10 May 1963, organized by the Hungarian Society for Optics, Acoustics and Film Techniques.

Applied Optics — Letters to the Editor

Letters to the Editor should be addressed to the Editor,
APPLIED OPTICS, AFCRL, Bedford, Mass.

Effect of Pre-excitation on Flash Lamp Optical Quality

H. G. Heard

Energy Systems, Inc., Palo Alto, California.
Received 24 June 1963.

Twelve-inch (30.5-cm) flash lamps, having a 13-mm bore and filled with 60 cm of xenon, have been observed to exhibit poor focal properties when operated at 10,000- to 25,000-J input. This anomaly was believed to be a result of the failure of the discharge to fill the flash tube; it was traced, in part, to the tendency of the plasma to be confined to a path along the inner surface of the flash lamp, as first established, where the 0.25-mm tungsten trigger wire contacts the quartz envelope. Figure 1 shows the flash lamp luminous output when a 60,000-Ω resistor was placed between the flash lamp and the 8-μF capacitor bank, using the circuit of Fig. 2. Only the pre-excitation trigger was fired to permit observation of the trigger discharge. Figure 1 is a 1-sec time exposure which shows that (a) the spirally wrapped trigger wire is responsible for initiating the irregular discharge; (b) the discharge column eventually becomes a small diameter axial filament of minimum length.

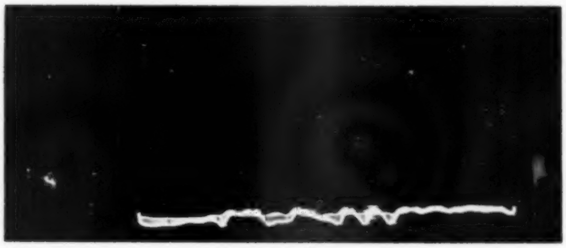

Fig. 1. Time-dependent luminosity variation of a 13-mm bore, 30.5-cm flash lamp triggered with a spiral tungsten trigger wire. Exposure time: 1 sec.

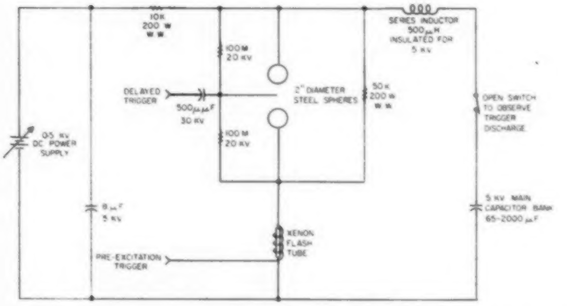

Fig. 2. Circuit for flash lamp pre-excitation. The delayed trigger was applied 100–1000 msec after the flash tube was triggered with the pre-excitation pulse.

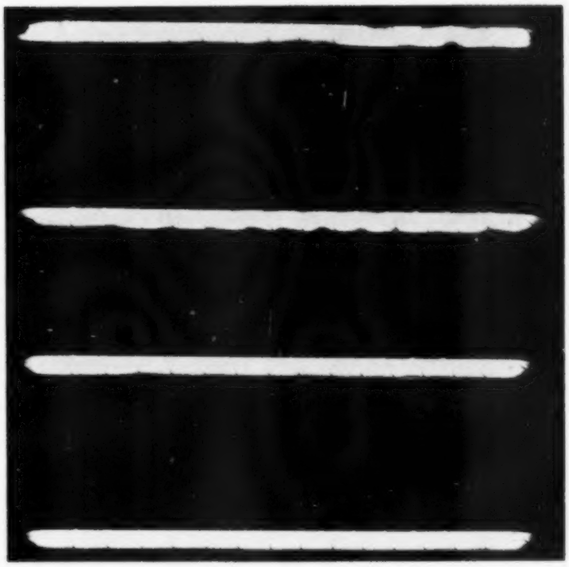

Fig. 3. Irregularities in luminous output of 13-mm bore, 30.5-cm flash lamp. From top to bottom: capacitor bank triggered at 0, 100, 200, and 500 msec after pre-excitation of the discharge. Multiple exposure time: 1 sec each.

The above observations lead to the hypothesis that improved line source optical quality could be achieved if the energy stored in the capacitor bank were not delivered until after the minimum length plasma develops. Figure 3 confirms the validity of this assumption. The 1-sec time exposure displays the attenuated green light output obtained when a circuit shorted the 50,000-Ω series resistor after 0, 100, 200, and 500 msec, respectively. An improvement was observed in the optical quality of the discharge for delays of 500 msec or greater. Similar results were observed in other 30.5-cm flash tubes having bores of 7, 9, and 11 mm. No improvement was observed for 3- and 5-mm bore tubes. The flash lamp fill pressure was 60 cm. This pressure necessitates a high voltage trigger, but has been found to improve markedly tungsten electrode life, reduce flash-tube bore discoloration, and increase lamp brilliance. Measurements of lamp brightness current, voltage current, and time-dependent current characteristics show that, for the usual damped discharge, the flash lamp parameters remain essentially unchanged.

Letters *continued overleaf*

CHANGES OF ADDRESS

Changes of address should be sent to Applied Optics, Subscription Handling, American Institute of Physics, 335 East 45th Street, New York 17, New York *as far in advance as possible, preferably* **eight weeks.**

Precise Automatic Readout on Comparator with Photoelectric Detection

Jean M. Bennett

Michelson Laboratory, China Lake, California.
Received 15 July 1963.

The comparator with photoelectric detection reported previously[1,2] has been modified with an automatic readout so that the settings may be recorded rapidly with no loss of accuracy. A photograph of the comparator (Type 300 manufactured by David W. Mann Company, Lincoln, Mass.) and some of the associated electronic components is shown in Fig. 1. The comparator has a 200-mm single-thread leadscrew with a 1-mm pitch which has been completely immersed in an oil bath to eliminate the effects of variable-thickness oil films and dust. The least count on the divided head attached to the screw is 1 μ, and tenths of a micron can be estimated on the vernier. The photoelectric setting attachment (a commercial model is now available from the David W. Mann Company) makes possible a setting precision of $\pm 0.2\ \mu$ on all symmetric objects ranging from sharp spectral lines to broad sinusoidal interference fringes. The automatic readout is accomplished by means of a 5000-count pulse generator (Type 8603, 5000-count manufactured by W. and L. E. Gurley, Troy, N.Y.) which is connected by means of a set of ultraprecision gears with a 2 to 1 gear ratio to the leadscrew, so that one rotation of the leadscrew gives 10,000 counts (each count thus corresponding to 0.1 μ). The output of the pulse generator is amplified by a wide band (dc to 150 kc/sec) amplifier (Model 102 B decade isolation amplifier manufactured by Keithley Instruments, Inc., Cleveland, Ohio) and fed into a 7-place counter (Model 8360 universal EPUT and timer manufactured by Beckman/Berkeley Division, Richmond, Calif.). A Model 1453 printer manufactured by Beckman/Berkeley Division, Richmond, Calif., actuated by command from a tap key, records readings from the counter. (As the printer and counter are delivered from the factory, only six of the seven digits shown on the counter are recorded by the printer. A minor factory modification of the counter must be made in order to have the seventh digit print out.) When the output of the pulse generator was checked against the reading on the divided head, it was found that at each setting one or two spurious counts were added to the reading, probably because of backlash (there was no sense of polarity in the pulse generator so that both forward and reverse counts added to the reading). In order to eliminate the spurious counts, it was found necessary to drive the leadscrew with a variable-speed motor (Type V10R 208 rpm motor manufactured by Bodine Electric Company, Chicago, Illinois, the speed of which on 115 V ac is actually around 400 rpm under load) which was geared down with a 22 to 1 gear ratio and attached to the leadscrew through a backlash-free, multijaw coupling. The motor, seen in the lower right in Fig. 1, was mounted on a dovetail slide, so that it could be easily engaged and disengaged. A speed control unit[3] was added between the variac and the motor to prevent stalling at slow speeds. With this system it was possible to obtain rotations of 0.03 rpm to 18 rpm of the comparator leadscrew.

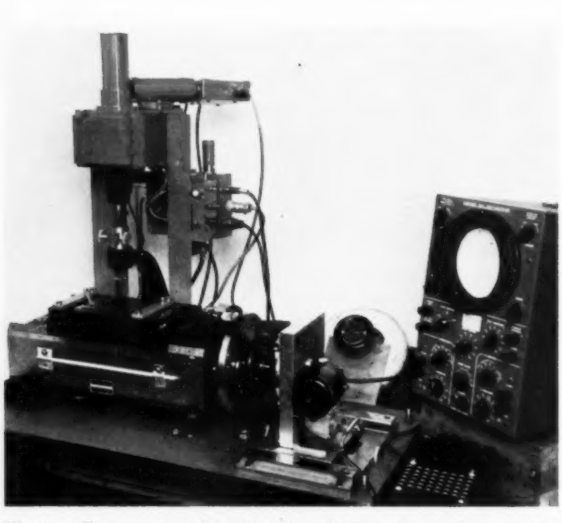

Fig. 1. Comparator with photoelectric detection and automatic readout. The power supplies, amplifier, counter, and printer are not shown.

The pulse generator was checked against the divided head by clearing the counter at the 0.0000 mm reading on the head and recording the pulse generator readings at intervals of 0.005 mm on the head for one complete rotation of the leadscrew (1 mm). During this time the leadscrew was driven continuously at a very slow rate (approximately 0.03 rpm), and the readings were recorded by pressing the tap key while the system was in motion. Using this procedure, the readings from the pulse generator checked with those on the divided head within ±1 count (0.1 μ), showing that the small periodic error found previously[2] was in the leadscrew or the bearings but *not* in the divided head. Also the pulse generator was checked over leadscrew distances of several centimeters and the readings agreed within ±1 count with the readings on the divided head. Hence, the *pulse generator gives a reading which is the same as that on the divided head to within ±1 count* (0.1 μ). Settings may therefore be made with the same precision, using the motor drive as is possible with manual setting, $\pm 0.2\ \mu$.

The author is indebted to Burton W. Wheeler, Jr., of the David W. Mann Company for obtaining the pulse generator, gears, and fittings for the comparator. She would also like to thank Vernon O. Jones of the Physics Model Shop for the precision mounting of the pulse generator and for making the reduction gearbox for the variable speed motor

References

1. J. M. Bennett and W. F. Koehler, J. Opt. Soc. Am. **49**, 466 (1959).
2. J. M. Bennett, J. Opt. Soc. Am. **51**, 1133 (1961).
3. J. R. Jacques, Electronics Illustrated **6**, 34 (1963).

Note on the Paper[*] "Tilted-Plate Interferometry with Large Plate Separations"

H. W. Moos, G. F. Imbusch, L. F. Mollenauer, and A. L. Schawlow

Department of Physics and W. W. Hansen Laboratories of Physics, Stanford University, Stanford, California.
Received 19 July 1963.

A. Hermansen has kindly drawn out attention to the work of E. Rasmussen, *Physica* **XII**, 656 (1946) and *Dan. Mat. Fys. Medd.* **23**, 3 (1945), and his own work reported at the conference on "Modern Systems for Detecting and Evaluating Optical Radiation", Fifth Meeting and Conference of the International

---

[*] Published in Appl. Opt. **2**, 817 (1963).

Commission for Optics (1959), on the use of tilted-plate interferometry in testing interferometer plates and in high-resolution spectroscopy. The paper by A. Hermansen has a very useful discussion of resolution and maximum plate separation as a function of reflectivity.

The Symposium Lens Improved

Berlyn Brixner

University of California, Los Alamos Scientific Laboratory,
Los Alamos, New Mexico.

Received 12 July 1963.

The initial design of the $f/1.5$ Symposium Lens[1] was tried on the Los Alamos Scientific Laboratory program for the IBM 7090.[2] This program uses the least-squares technique to minimize spot sizes. Image evaluation and designing was done with three off-axis object points on the 6° half field of view, with three colors (*C*, *d*, *F* refractive indexes from the Bausch & Lomb optical glass catalog), and with 2-, 6-, 12-, and 26-ray patterns as the design was refined. Because of the symmetrical behavior of the two halves of a lens, these rays are traced through only one half of the lens and are equivalent to twice the number of rays through the whole lens. No attempt was made to determine a better choice of glasses.

By means of a series of short machine runs, the surface radii, glass thicknesses, and air thicknesses were made into variables. Between these runs the design progress was studied in relation to the Symposium specifications, and any undesirable features that had developed were manually corrected. After nine runs, which used approximately 35 min of machine time, the figure of merit for the initial design, 3.8, was reduced to 0.154. With five additional runs (25 min) the figure of merit was reduced to 0.068. By this time design progress was so slow that further designing seemed unprofitable. Table I gives the prescriptions and Table II the performance characteristics of the initial design and of these two lenses. In Table II the 2-ray figure of merit for the initial design, 3.8, is deceptively small when compared with a more realistic evaluation by the 26-ray pattern, which shows the figure of merit to be 11.0 at 0.582 back focus and the average rms spot radius to be 0.0334. The three designs are illustrated in Fig. 1, which shows the paths of the outer rays of the 6° off-axis bundle, the entrance and exit pupils, and a possible trim of the lens elements.

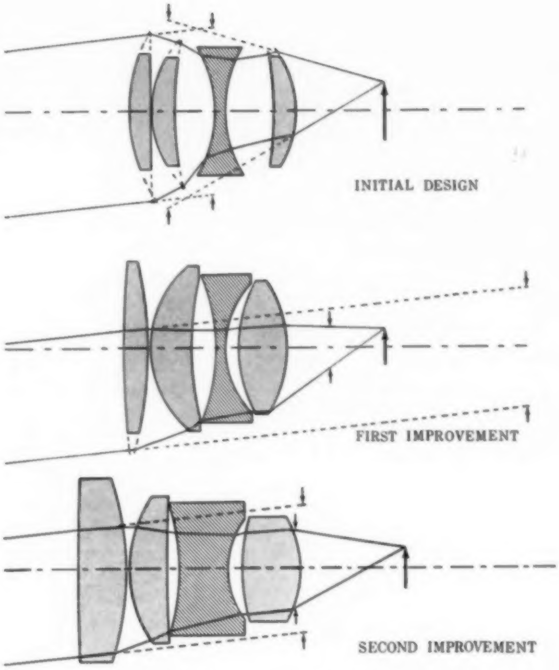

Fig. 1. Illustrations showing three of the Symposium Lens designs.

Table II. Optical Characteristics of the Symposium Lens Designs

Performance feature	Initial	First	Second
Entrance pupil distance	0.450	2.210	1.144
Exit pupil distance	−0.685	0.235	−0.025
Focal length (*d*)	1.254	1.0022	1.0012
Back focus	0.475	0.5253	0.5405
Ray pattern	2	12	26
Figure of merit	3.8	0.154	0.068
Average rms spot radius	0.0058	0.00046	0.00021
Lateral chromatic range	0.0022	0.00060	0.00011

Table I. Prescriptions for the Symposium Lens Designs

Glass type		Initial		First		Second	
N	V	*t*	*c*	*t*	*c*	*t*	*c*
			1.150		0.19288		0.08897
1.6200	60.3	0.120		0.1402		0.2500	
			0.000		0.47398-		0.65924-
		0.001		0.0100		0.0144	
			1.800		1.73197		1.52235
1.6200	60.3	0.120		0.2200		0.1900	
			0.500		0.59546		0.11886
		0.210		0.1300		0.0568	
			1.500-		0.97762-		0.88381-
1.6490	33.8	0.050		0.0500		0.2500	
			1.500		2.00000		2.32270
		0.250		0.0700		0.0696	
			0.500-		1.35036		1.03268
1.6200	60.3	0.120		0.2635		0.2941	
			1.800-		1.52526-		1.85689-

This work was done under the auspices of the U.S. Atomic Energy Commission.

References

1. D. P. Feder, Appl. Opt. **2**, 272 (1963).
2. B. Brixner, Los Alamos Scientific Laboratory Report LA-2877 (1963).

Correction of Phase Errors in Interferograms

Lawrence Mertz

Block Associates, Inc., Cambridge 39, Massachusetts.
Received 10 August 1963.

There are several points in the recent communication of Loewenstein[1] with which the author disagrees. First, in his interpretation of the influence of an error in the choice of center of an interferogram, he attributes the resulting depression of the continuum to the nonsymmetry of his scanning function. Connes[2] has given the correct interpretation, which is that the shape of the scanning function changes along the spectrum, and the depression is a result of the diminution of the integrated scanning function for wavelengths where $\delta = [(2n - 1)/4]\lambda$ (n integral). It is well known that, if $I(\tau)$ and $\mathcal{S}(\nu)$ are a Fourier transform pair, then $I(\tau - \delta)$ and $\mathcal{S}(\nu)e^{-2\pi i\nu\delta}$ are also a Fourier transform pair. The real part of $e^{-2\pi i\nu\delta}$ gives the continuum suppression. Furthermore, the numerical values of Fig. 3 of the Loewenstein paper appear to be inconsistent. The continuum has been depressed to zero at about 96 cm^{-1} (104 μ), corresponding to a δ of $^1/_4(104) = 26\ \mu$. If his δ refers to mirror motion error rather than path difference, the mirror motion would still be 13μ.

Next, he described two methods of restoring the symmetry to the scanning function, the second of which requires some method (not given) to ascertain the position error δ. The first method involves calculating the amplitude spectrum (square root of the power spectrum) rather than the cosine spectrum of the interferogram. This method has been analyzed by Connes.[2] Loewenstein has however applied the method to the interval O to D, for which the method is not valid, instead of the interval $-D$ to $+D$. Although he illustrates a broadened total scanning function, in reality no single scanning function exists for the nonsymmetric interval, not even for a local spectral region. This lack of existence stems from the nonlinear process of taking the square root of the sum of the squares. The present author contends that two scanning functions are necessary and sufficient for the interpretation of nonsymmetrically truncated interferograms.

Let us define the center of the interferogram as a place of stationary phase of the fringes, i.e., the fringes of all wavelengths of a local region of the spectrum have the same phase and so add constructively at the center of the interferogram.

Such a definition is more relaxed than a definition relating to symmetry, since symmetry implies stationary phase in addition to specifying that phase as zero. Furthermore, it is difficult to compensate perfectly an interferometer for symmetric fringes, so stationary phase is really more appropriate for defining the center.

Further, if we define

$C(I) \equiv$ cosine Fourier transformation of a function I,
$S(I) \equiv$ sine Fourier transformation of the function I,
$A(I) \equiv$ amplitude Fourier transformation of the function I
$= [C^2(I) + S^2(I)]^{1/2}$,

$I(\tau)$ and $T(\tau)$ as functions of τ, which may be identified with the interferogram and the truncating (apodizing) functions, respectively, with no restrictions on their symmetry, it can be proved (although the author has not seen this theorem in the literature) that if $\tau = 0$ is a place of stationary phase for $I(\tau)$, and $\star$ denotes convolution, then

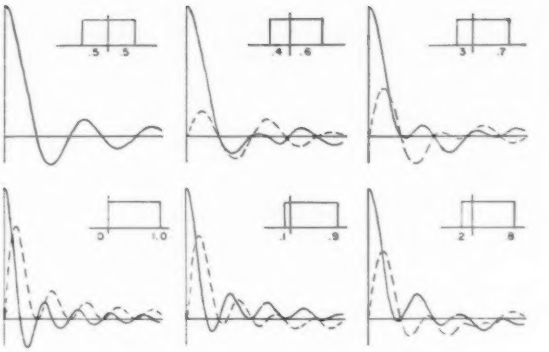

Fig. 1. Instrumental profiles.

$$A^2(I\cdot T) = [A(I) \star C(T)]^2 + [A(I) \star S(T)]^2.$$

The left-hand side is the power spectrum calculated from a truncated interferogram; the right-hand side involves two instrumental profiles $C(T)$ and $S(T)$. Examples of these profiles are shown in Fig. 1 for varying amounts of decentering of the interferogram within the measurement interval. $C(T)$ are shown as solid lines, $S(T)$ as dashed lines.

In these notations Loewenstein's application of the amplitude method would involve the following questionable relation

$$A(I\cdot T) \overset{?}{=} A(I) \star A(T).$$

There are actually three circumstances for which this simpler relation is valid. If $A(I)$ is a Dirac delta function or even several widely spaced delta functions, such as an emission spectrum, or if $S(T) = 0$ corresponding to symmetric truncation, or if $C(T) = 0$ which is of no special significance.

The author would like to add that the desired term $A(I) \star C(T)$ in the correct relation can in fact be isolated from the spurious term $A(I) \star S(T)$ by at least two methods, though their description is not *apropos* in this Letter.

References

1. E. Loewenstein, Appl. Opt. **2**, 491 (1963).
2. J. Connes, Rev. optique **40**, 68 (1961).

Author's Reply

E. V. Loewenstein

AFCRL, Bedford, Massachusetts.
Received 29 August 1963.

Mertz's first point is that the author did not understand the change in the shape of the scanning function as it is moved along the spectrum. This is not so, as it was stated[1] in the paragraph below Eq. (5) that the amount of asymmetry (of the scanning function) depends on the ratio δ/λ, the phase error to the center wavelength of the scanning function. This point was repeated in the conclusion.

As for the continuum depression (which was referred to as distortion of the base line), the depression to zero takes place not where the integrated scanning function is zero but where the convolution of the scanning function with the true spectrum is zero. Further, the shapes of the spectral lines reflect the symmetry of the scanning function. If the scanning function is very asymmetric, the spectral lines will also be asymmetric, particularly if the lines are narrow. In Fig. 3 of the previous paper,[1] it will be seen that there is a narrow line near 90 cm^{-1}. If the scanning function had been much more asymmetric when computing one curve than it was when computing the other, that fact would have shown up as a change in the shape of the line. The value of 7 μ given for the phase error is correct.

No method was given for computing the phase correction, ϵ, as that may depend to some extent on the apparatus. It is possible, when a digital record is produced, to take the first few data points on either side of the central maximum, find the position of the peak by fitting these points with a polynomial of appropriate order, and thus determine the phase error δ. We take then $\epsilon = \delta$.

As for Mertz's second point, it is true that $T = \sqrt{C^2 + S^2}$ is not a true scanning function, for the reason that he gives. Therefore, in the case of symmetric interferograms, the desirable method for correcting a phase error is to correct the cosine functions in the transformation, as was stated in the conclusion.

Finally, we would like to draw attention to two transcription errors in the previous paper, in Eqs. (4) and (5). The second term on the right-hand side of Eq. (4) should read:

$$-\delta\left[1 - \frac{\sin(\omega - \omega_0)D}{(\omega - \omega_0)D}\right]\frac{\sin(\omega\epsilon - \omega_0\delta)}{(\omega - \omega_0)\delta}$$

and the second term on the right-hand side of Eq. (5) should read:

$$+\delta\left[1 - \frac{\sin(\omega - \omega_0)D}{(\omega - \omega_0)D}\right]\frac{\sin\omega_0\delta}{(\omega - \omega_0)\delta}.$$

Reference

1. E. V. Loewenstein. Appl. Opt. **2**, 491 (1963).

A Precision Chopper Disk

Hans R. Rottmann

Owens-Illinois Technical Center, Toledo, Ohio.

Received 28 June 1963.

As part of an investigation concerning the problem of chopping light, a precise semicircular rotary shutter was required. The purpose of this letter is to describe an inexpensive method of making such a shutter.

Figure 1 gives a front view of the chopper disk. The hub H is press-fit into an aluminum base plate P. The extended straight edges E of the plate P pass below the center line of the hub. Balancing was obtained by drilling numerous holes into the large semicircular portion of the plate P, and by a steel plate attached to the small semicircular portion. These are not shown in the drawing. A thin sheet of opaque material covers all holes. The optically effective edges are two injector razor blades RB fixed to supporting blocks B. The blocks have elongated slots through which they are screwed onto the base plate.

To achieve adjustment of the knife edges a small accessory plate AP is screwed tightly on the base plate P below each block B. Each plate AP has two threaded holes supporting long adjustment screws S, which allow minute displacements of the injector blades in a plane perpendicular to the axis of the hub in order to obtain adjustment.

Figure 2 shows the method of mounting the shutter for adjustment. All parts of the shutter except the blades RB are omitted. A small hollow cylinder C serves to locate the axis of the hole in the hub. The cylinder fits smoothly into the hole so that its axis coincides with the axis of the hole. The pin P, which is pressed into the cylinder, serves as a pointer. Its point lies approximately on the axis. The collar is positioned to keep the point in the plane of the blades when the cylinder is rotated. Adjustment is obtained when both knife edges are aligned, and when the axis of the hub hole intersects the straight line formed by extension of the edges.

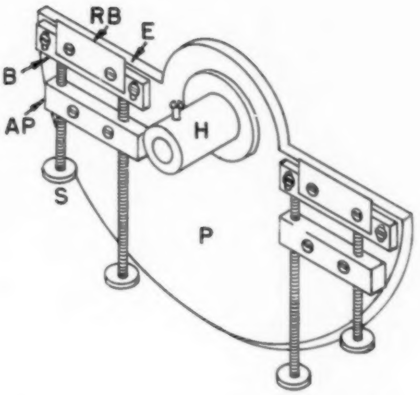

Fig. 1. Chopper disk and adjustment devices. E is the radial edge of the base plate P, H is the hub, block B supports the blade RB, AP is an accessory block, and S is an adjustment screw.

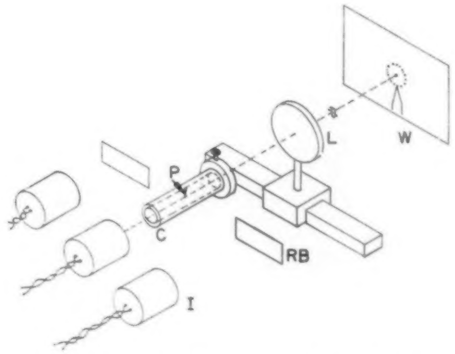

Fig. 2. Optical setup for adjustment of the blades RB. I is an incandescent lamp, C is a hollow cylinder, P is a pin, L is an objective lens, and W is a white screen.

In principle the adjustment is achieved by focusing magnified images of the blades and the pin onto a white screen W. The two blades RB and the hole in the hub are illuminated from the left by the incandescent lamps I. The blades RB and the pin P can be focused individually on the screen by simply shifting the lens L. The use of only one lens for all three projections ensures that the focusing of the blades and the pin occur under the same conditions. The lens is placed in front of the hollow cylinder C which is supported by the hub. The cylinder is now rotated by hand. The image of the pinpoint on the screen is marked by pencil for each step of rotation. This results, after one revolution, in a circle. The center of the circle represents the intersection of the hub axis with the screen. The lens is now placed in front of the first blade. The adjustment by the two threaded screws is completed when the image of the sharp edge of the blade passes through the center of the small circle. The plate B (Fig. 1) supporting the injector blade RB is then screwed tightly to the base plate P.

The procedure is essentially the same with the second knife edge. It is adjusted when its image on the screen coincides with the image of the first edge. After the adjustments are completed the accessory plates AP and the hollow cylinder C are removed and the disk is ready for use.

The accuracy obtained was better than ±15 sec. The axis of the hub was in level alignment with the extended knife edges by ±0.0025 mm.

A Simple Method for Preparing Layers of Sodium Salicylate

R. A. Knapp

Institute of Optics, University of Rochester, Rochester, New York.

Received 9 August 1963.
This research was supported by the National Aeronautics and Space Administration (Goddard Space Flight Center).

The widespread use of a sodium salicylate sensitized photomultiplier as a photon detector in the near and vacuum ultraviolet has resulted in the development of various techniques for the preparation of layers of the phosphor. One of the most widely used methods consists of spraying a solution of the phosphor, in alcohol or other solvent, from some sort of atomizer. The chief defects of this method, however, are that it is time consuming and the danger exists of the formation of voids in the film, due to large drops reaching the surface, which result in nonuniform spatial response and increased sensitivity to longer wavelength scattered light. The method described below has been developed in our laboratory to remedy these defects. It provides a rapid and convenient method of producing fine-grained and uniform layers over as wide an area as is desired.

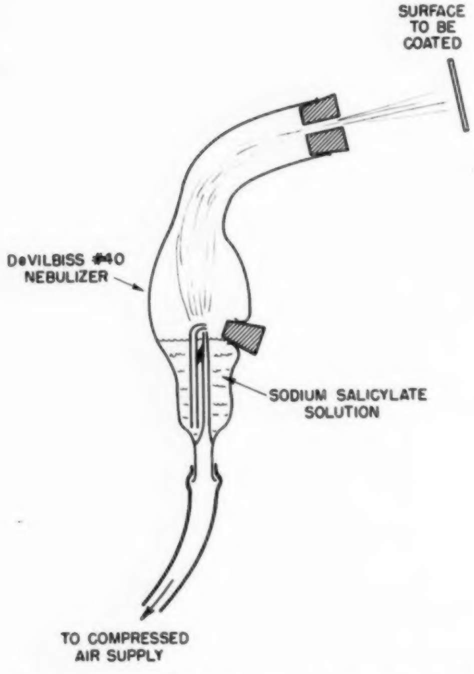

Fig. 1. Nebulizer modified for preparing sodium salicylate layers.

A commercially available nebulizer for aerosol therapy (DeVilbiss Glass Nebulizer #40, the DeVilbiss Company, Somerset, Pennsylvania, available in most drug stores) is modified as shown in Fig. 1 by the addition of a small aperture at the output end. The nebulizer was chosen because of the extremely fine, i.e., small droplet size, mist produced by it. This mist is then directed through the exit hole onto the surface to be coated. We have found that, depending on the speed desired, holes of 1.6 to 0.8 mm are adequate. The use of a very low air pressure 1 to 2 lb/in.^{2} (50–100 mm Hg) avoids the possibility that any large drops, which may be accidentally formed, will reach the surface being coated which is held 2.5 to 5 cm away from the nozzle. Since the mist dries on contact, the coating may be applied continuously, and uniform layers of any desired thickness may be produced in a matter of minutes. The method is, of course, not limited to the material discussed here and should prove useful for preparing coatings of other materials for which similar methods have been previously used.

Index of Refraction of KDP

Jane H. Dennis and R. H. Kingston

Lincoln Laboratory, Massachusetts Institute of Technology, Lexington, Massachusetts.

This laboratory is operated with support from the U.S. Army, Navy, and Air Force.
Received 26 July 1963.

Since KDP (potassium dihydrogen phosphate) has become of great importance in nonlinear optical experiments, we have measured the indices of refraction over most of its transmission range.

The large variety of detectors needed to cover the range of wavelengths from 0.2 to 1.5 μ made measurement on a goniometer very difficult. Instead, a comparison method of measurement using a Perkin–Elmer model 12C spectrometer was used. The KDP prism, of 19 mm dimensions, was supplied by Clevite Corporation. It was mounted in a Perkin–Elmer model 98 prism in the same position as the original prism. The spectrum of an Hg lamp with a quartz envelope was run with this prism with and without polarizers and also with a standard fused quartz prism. The Littrow mirror in the spectrometer was left in the same position for both prisms. There is then a one-to-one correspondence between the index of refraction and the spectrometer drive calibration.

Both the ordinary and extraordinary indices were measured to 1.5 μ, and these figures are good to about 0.4%. In the ultraviolet, the extraordinary index has been measured to 0.2536 μ. The ordinary index values have only been obtained to 0.4048 μ because the corresponding indices in the fused quartz

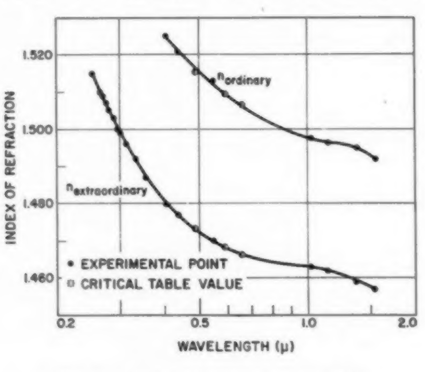

Fig. 1. Index of refraction of KDP.

prism lie in the upper ultraviolet around 0.1800 μ and the Hg lines in this region are too weak for absolute identification. The accuracy of the measurement in the ultraviolet is about 0.2%. The curves in Fig. 1 also include the four points in the visible given in the *International Critical Tables*.[1]

Reference

1. *International Critical Tables* (McGraw-Hill, New York 1930), Vol. 7, p. 27.

A Low-Pressure Arc Source for the Emission Spectrum of the FeO Molecule

R. K. Dhumwad and Arnold M. Bass

National Bureau of Standards, Washington, D. C.

R. K. Dhumwad was a guest worker at the National Bureau of Standards. He is now with the Atomic Energy Establishment, Trombay, Bombay, India.

Received 31 July 1963.

This work was supported in part by the National Aeronautics and Space Administration.

A low-pressure arc source, based on a design suggested by Davis,[1] has been developed for the excitation of FeO (Fig. 1). The arc between iron (spec-pure) electrodes operated at 0.6 A dc, in flowing oxygen at a pressure of 7 cm Hg. The arc gap was 6.35 cm with a potential difference of 450 V. The appearance of the arc was flamelike and yellowish in color. Under these conditions of the source, the line spectrum of iron was found to be suppressed. It has thus been possible to obtain emission spectra of the FeO molecule completely free of overlapping atomic iron lines which were present in previously reported FeO spectra.[2–5] Figure 2 shows typical portions of the FeO spectrum indicating the absence of Fe lines. The spectrum has been photographed in the second and third order (0.8 and 0.5 Å/mm, respectively) in the region of 5400–9000 Å on the 9.15 m grating spectrograph (Paschen–Runge mounting) at the Argonne National Laboratory. Work on the analysis of the band systems is in progress.

Our observations with the low-pressure arc confirm the suggestion by Davis[1] and by Grinfeld *et al.*[6] that this source may provide a very efficient method for exciting the spectra of molecules at relatively low excitation temperatures.

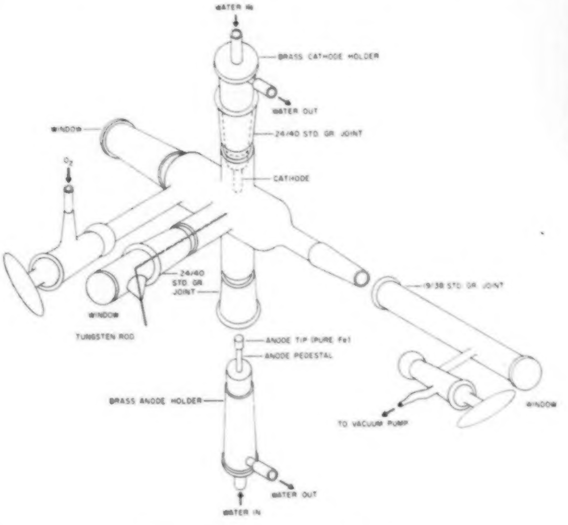

WATER IN
BRASS CATHODE HOLDER
WATER OUT
WINDOW
24/40 STD. GR. JOINT
O_2
CATHODE
24/40 STD GR JOINT
19/38 STD. GR. JOINT
WINDOW
TUNGSTEN ROD
ANODE TIP (PURE Fe)
ANODE PEDESTAL
BRASS ANODE HOLDER
TO VACUUM PUMP
WINDOW
WATER OUT
WATER IN

Fig. 1. Low-pressure arc source.

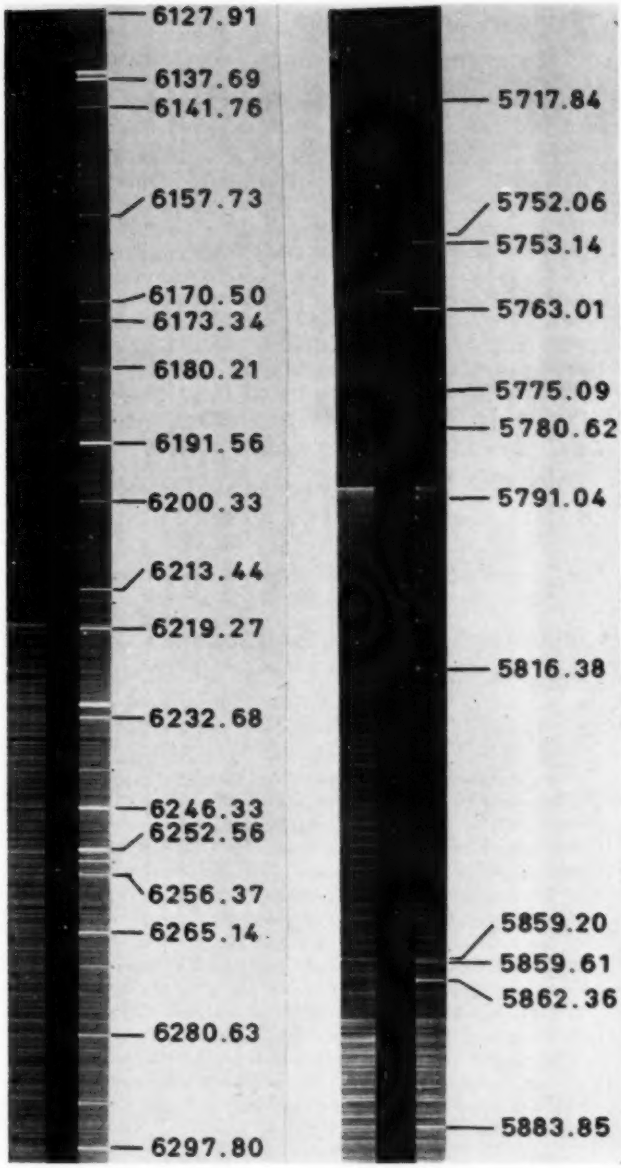

6127.91
6137.69
6141.76
6157.73
6170.50
6173.34
6180.21
6191.56
6200.33
6213.44
6219.27
6232.68
6246.33
6252.56
6256.37
6265.14
6280.63
6297.80
5717.84
5752.06
5753.14
5763.01
5775.09
5780.62
5791.04
5816.38
5859.20
5859.61
5862.36
5883.85

Fig. 2. Suppression of iron lines in low-pressure arc. In each set of spectra a thorium spectrum is in the middle, with the spectrum of an iron arc in air to the right and that of the low-pressure arc to the left.

References

1. S. P. Davis (private communication).
2. A. Delsemme and B. Rosen, Bull. Soc. Sci. Liège, 70 (1945).
3. B. Rosen, Nature, **156,** 570 (1945).
4. L. Malet and B. Rosen, Bull. Inst. Coll. Belg. 377 (1945).
5. A. M. Bass and W. S. Benedict, Astrophys. J. **116,** 652 (1952).
6. R. Grinfeld, M. A. Poggio, J. H. Elias, and E. J. Bertomeu, J. Opt. Soc. Am. **52,** 591 (1962).

Artificial Green Flashes

D. Deirmendjian

The RAND Corporation, Santa Monica, California.

Received 25 July 1963.

We would like to make two comments on the recent paper by Feibelman on "Low Sun Phenomena".[1] First, artificial prominences, whether green, red, or indifferent, produced by jet plane exhausts and contrails crossing a low sun *are not* the same phenomenon as the green flash. The former are produced by forward scattering on different types and sizes of the particles in the local cloud of exhaust or condensation products. On the other hand, although no complete theory is yet available, it appears that the green flash is mainly due to clear atmosphere dispersion when the sun appears as a quasi-point source.

Second, the appearance or not of the man-made green flashes described by Feibelman should give *no* indication of the quality of astronomical seeing.

Reference

1. W. A. Feibelman, Appl. Opt. **2,** 199 (1963).

Immersion Null Test for Aspherics

Robert T. Holleran

American Optical Company, Keene, New Hampshire.

Received 5 July 1963.

An interesting and apparently novel method of testing aspherical surfaces employs an immersion liquid. The surface is made level and covered with a liquid which assumes the form of a plano-convex aspheric lens in contact with the surface. The liquid's index of refraction is so chosen that a spherical wavefront is returned to an axial point source. It is found that for each eccentricity over a wide range of conic sections there corresponds an index for the immersion liquid which produces a null test. This index is given by the simple formula, $n = (1 + e^2)^{1/2}$, for a very thin liquid layer.

A typical test arrangement is shown in Fig. 1. The formula is derived with the aid of the geometrical abstract, Fig. 2.

The vertex radius of curvature R of conic sections is equal to b^2/a in the standard notation. A general equation for conic sections symmetrical about the coordinate axes can, therefore, be written in the form

$$x^2(1 - e^2)^2 + y^2(1 - e^2) = R^2, \tag{1}$$

where e is the eccentricity. Letting $y = kR$, this equation yields the sagitta

$$s = a - x = \frac{R}{1 - e^2}\left\{1 - [1 - k^2(1 - e^2)]^{1/2}\right\} \tag{2}$$

and the slope of the normal to the conic surface:

$$\tan i' = dx/dy = k/[1 - k^2(1 - e^2)]^{1/2}. \tag{3}$$

In the immersion test, the axial distance d for which a ray striking the conic at height y returns upon itself after refraction and reflection is given by

$$d = \frac{y_{-1}}{\tan i} = \frac{y - (t - s)\tan i'}{\tan \arcsin(n \sin i')}, \tag{4}$$

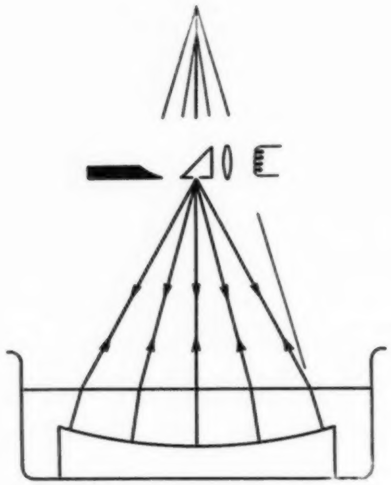

Fig. 1. The knife-edge test becomes a null test by immersion.

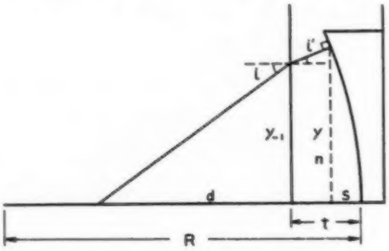

Fig. 2. Immersion null test geometry.

when n is the index of the immersion medium and t is its thickness. Replacing t by cR, and y, s, and $\tan i'$ by their equivalents, Eq. (4) can be transformed into

$$d = \frac{R}{n}\left\{\left(\frac{1}{1 - e^2} - c\right)[1 - k^2(1 - e^2)]^{-1/2} - \frac{e^2}{1 - e^2}\right\} \times [1 - k^2(n^2 - e^2)]^{1/2}. \tag{5}$$

Expanding the one-half power quantities, the equation may be expressed as

$$d = \frac{R(1 - c)}{n}\left\{1 + \frac{k^2}{2}\left(1 + \frac{e^2}{1 - c} - n^2\right) + \frac{k^4}{8}\left[(3 - e^2 - 2n^2)\left(1 + \frac{ce^2}{1 - c}\right) - (n^2 - e^2)^2\right] + \ldots\right\} \tag{6}$$

For $k = 0$, the distance is

$$d_{\text{paraxial}} = \frac{R}{n}(1 - c). \tag{7}$$

The k terms of Eq. (6) form a convergent series of aberration coefficients. Inspection shows that the k^2 term becomes zero when the test index is chosen so that

$$n^2 = 1 + \frac{e^2}{1 - c} \tag{8}$$

d then becomes d_{paraxial} and null test conditions obtain over the appreciable aperture for which the higher power terms may be

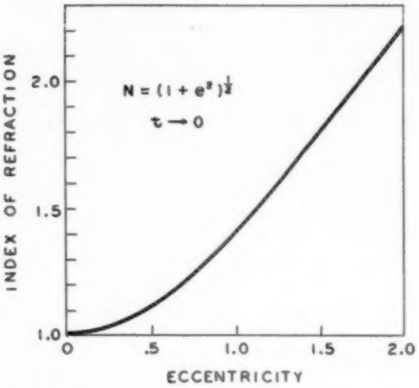

Fig. 3. Index of immersion medium required for null test as a function of eccentricity of a conic.

neglected. For zero thickness, $c = 0$, and the null test index becomes (see Fig. 3)

$$n = (1 + e^2)^{1/2}. \tag{9}$$

The accuracy of this test, like that of other compensation lens tests, is extremely good for shallow curves but decreases rapidly with the speed of the surface and its size. The error along the axis may be determined from Eqs. (5) and (7) as

$$\Delta d = d_{\text{paraxial}} - d. \tag{10}$$

Δd may then be related to the error imparted to the surface when figured to null. The departure from the true conic, assuming any values whatever for the test parameters of Eq. (8),

$$\Delta s = \int di'\,dy \cong \frac{1}{d}\int_0^y k\,\Delta d\,dy. \tag{11}$$

The ultimate error in nullity, when the index is exactly correct and Δd is due only to the neglected terms of Eq. (6), is given for small values of c with sufficient accuracy by

$$\Delta s = \frac{Rk^6e^2}{16} = \frac{y^6e^2}{16R^5\lambda}\ \text{wavelengths.} \tag{12}$$

The computed error for a paraboloid of vertex radius 100 cm at a focal ratio of 2.5 is 0.11 wavelength.

For shallow curves considerable parameter errors may be tolerated. A surface immersed in water and figured to null will be 77% corrected from sphere to parabola. At $f/8$ this error is 0.13 wavelength for a 15.2-cm diam mirror imaging from infinity.

When the immersion medium cannot be freely chosen, the index required for a null test may be varied by adjusting thickness, in accordance with Eq. (8), or by the use of unequal conjugate distances for light source and image.

The author has used the immersion method successfully in testing an accurate parabola of 20.3-cm diam and 152.5-cm focal length. Null test conditions were obtained with an immersion oil of index 1.41. Spheres tested in this manner showed increasing knife-edge shadow depth and Ronchi line curvature as the immersion index was increased in several steps.

An advantage of the method lies in the ease and assurance of alignment of liquid lens to aspherical surface. Also, the double pass of light through the liquid lens permits some transverse separation of the light source and image for convenient observing.

The principle may also be applied to convex surfaces. A particularly simple application occurs in the case of a convex aspheric observed through its plane back surface, when the material of the aspheric element itself replaces the immersion medium and by virtue of its own index and thickness provides correct compensation with no need for any liquid layer. Many variations suggest themselves making use of a plane or spherical back surface with or without an immersion liquid, often requiring additional analysis to determine parameters for a null test, and always requiring material of good optical quality for the convex aspheric.

Application of the immersion test to surfaces other than conics is a matter for individual computation. There are, of course, many surfaces whose zonal aberrations cannot be compensated by the action of a replica lens alone.

A Note on the Testing of Homogeneity of Large-Aperture Parallel Plates of Glass

M. V. R. K. Murty

Institute of Optics, University of Rochester, Rochester, New York.

Received 22 July 1963.
This work was supported by a contract from the National Aeronautics and Space Administration.

Recently, there has been a great need for large pieces of glass having a high degree of homogeneity. Some of these pieces of glass may be as large as 30 in. (76.25 cm) in diam and 6 in. (15.25 cm) thick. Usually, the homogeneity requirements vary depending on the application. Sometimes it is required to make measurements so that variations of the order of 10^{-7} in the refractive index should be detected. If the variation in the refractive index is ΔN and the thickness of the glass is T, then the following simple relationship may be written,

$$T\,\Delta N = n\lambda, \tag{1}$$

where n is the fraction or multiple of the wavelength λ. The expression in (1) gives the excess optical path difference introduced by the glass plate as a result of a small variation ΔN in the refractive index. If the light is made to pass twice through the glass, as for instance in some autocollimating arrangement, the expression in (1) may be written as,

$$2T\,\Delta N = n\lambda. \tag{2}$$

The expression in (2) is plotted in Fig. 1 for different values of ΔN (10^{-5} to 10^{-7}) taking the value 5.5×10^{-4} mm for the wavelength λ. Thus a casual examination of Fig. 1 indicates that to detect variations of the order of 10^{-7} in refractive index in reasonably thick pieces of glass, one should be able to detect optical path differences of the order of $\lambda/20$. The expression in (2) is valid only when we assume that the thickness is constant. Usually, the surfaces are not finished to the required accuracy and as such an independent method is used to find the variation of the physical thickness of the glass plate over its entire surface. In the general situation, therefore (2) should be modified as

$$2T\,\Delta N + 2(N - 1)\Delta T = n\lambda. \tag{3}$$

Any method of testing a lens or a mirror could be adopted to the testing of homogeneity of a thick parallel glass plate. Typical arrangements are shown in Figs. 2–4. Figure 2 shows an arrangement where the light from a point source is autocollimated by means of a large lens and a plane mirror. The region between the lens and the plane mirror is traveled essentially by parallel

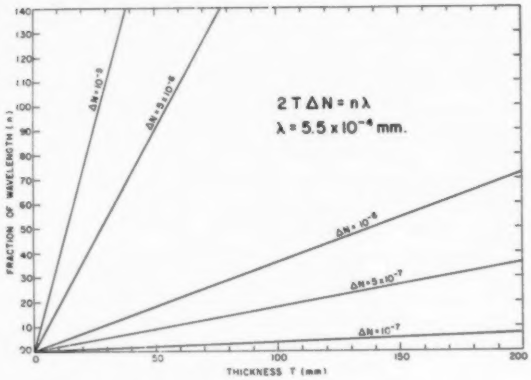

Fig. 1. Plot of fraction or multiple of wavelength of optical path difference (n) due to various amounts of small variations of refractive index (ΔN) vs the thickness (T) of the parallel plate of glass. The wavelength (λ) is taken as 5.5×10^{-4} mm.

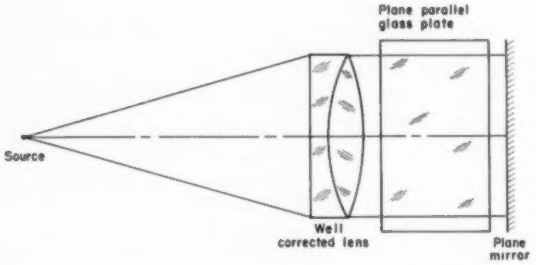

Fig. 2. A possible arrangement for homogeneity testing using a well-corrected lens and a plane mirror.

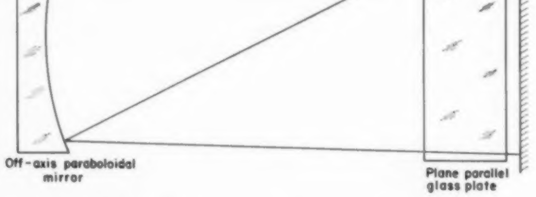

Fig. 3. A possible arrangement for homogeneity testing using an off-axis paraboloidal mirror and a plane mirror.

light and the block of glass is placed in this region. Figure 3 shows a slightly different arrangement wherein the lens of Fig. 2 is replaced by an off-axis paraboloidal mirror. Figure 4 shows an arrangement in which the paraboloidal mirror is used on-axis. In this case, we have to tolerate some amount of central obscuration. In all the above-mentioned arrangements, one feature is common. This is the collimation of light by one element and the reversal of the light by the use of the large plane mirror. As one can see, the methods shown in Figs. 2–4 are quite difficult and probably very expensive because of the need of fabrication of the large paraboloidal mirror or the lens and a large plane mirror. An alternative method is suggested in which the function of the two main elements of Figs. 2–4 is taken over by a single element. This single element is a large spherical mirror the expense of which is much less than the schemes shown in Figs. 2–4.

A schematic diagram of the method of testing the homogeneity of a large piece of plane parallel glass using a large spherical mirror is shown in Fig. 5. The spherical mirror can be tested independently by any of the usual methods. The parallel plate of glass is placed close to the spherical mirror. The only objection that may be raised against this method is the fact that the light is not strictly collimated and, in fact, convergent and divergent light is passing through the glass plate. There are mainly two effects due to the introduction of a parallel plate of glass in front of the spherical mirror as shown in Fig. 5. One effect is the simple displacement of the apparent center of curvature of the spherical mirror. This shift is away from the mirror, and its magnitude is given by the following expression:

$$\text{Apparent shift of center of curvature} = T(N-1)/N, \quad (4)$$

where T is the thickness of the glass plate and N is the refractive index. This means simply that the point source of light, instead of being placed at the actual center of curvature of the spherical mirror, should be placed at the apparent center of curvature whose distance from the actual center of curvature is given by the expression in (4). The second and more important effect of the parallel plate in front of the spherical mirror is the small amount of spherical aberration introduced. This is a more serious limitation, and the purpose of this letter is to establish the limits of validity of this method. For our purposes, we need only consider the primary spherical aberration of the glass plate. This is because of the fact that we try to limit the primary

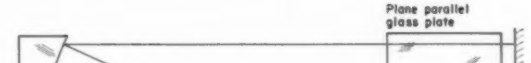

Fig. 4. A possible arrangement for homogeneity testing using a paraboloidal mirror on axis and a plane mirror. A small central obscuration is unavoidable.

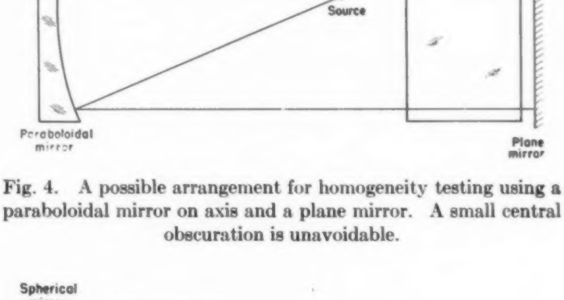
Spherical mirror
Actual center of curvature
Source at apparent center of curvature
Plane parallel glass plate

Fig. 5. Proposed arrangement for homogeneity testing using a single spherical mirror.

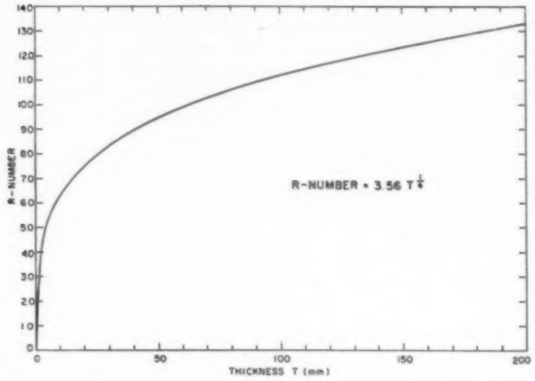

Fig. 6. A plot of the R-number of the spherical mirror vs the thickness T of the glass plate such that the amount of the spherical aberration is insignificant.

spherical aberration to a small fraction of a wavelength and as such the higher-order aberration would be extremely small.

The primary spherical aberration of a glass plate of thickness T and index N is given as an optical path difference by the following expression:

$$\text{Primary spherical aberration} = T(N^3 - 1)\theta^4/4N^3, \qquad (5)$$

where θ is the semiangular aperture of the spherical mirror. By proper focusing, the value of the primary spherical aberration can be reduced to one-fourth the value given in (5). Thus one has as the maximum primary spherical aberration one-fourth of the value given in (5) and one should set this at some upper limit. This upper limit is quite arbitrary, but some guidance may be obtained from examining Fig. 1. One can see that optical path differences of the order of $\lambda/20$ are involved when one tries to detect variations of the order of 10^{-7} in refractive index in reasonably thick glass plates. Thus we may set for the effect of the primary spherical aberration an upper limit of $\lambda/32$. Taking $N = 1.5$ and $\lambda = 5.5 \times 10^{-4}$ mm we get the following relationship between the thickness T and the allowable semiangular aperture θ,

$$T\theta^4 = 3.91 \times 10^{-4}. \qquad (6)$$

Here T is in mm and θ is in rad. One may note that θ may be replaced by a more convenient number which we call R-number using the relation $\theta = D/2R$, where D is the diameter of the mirror and R is the radius of curvature. Thus (6) may be rewritten as

$$R\text{-number} = R/D = 3.56\ T^{1/4}. \qquad (7)$$

The relationship given in (7) is plotted in Fig. 6. Using this plot one can easily estimate the smallest possible R-number that could be used for a spherical mirror to be set up in the test scheme indicated in Fig. 5. As an example, let us assume that a spherical mirror of 30.5-cm diam and radius of curvature of 305 cm is available. Thus the mirror has an R-number of 10 and, using (7), we arrive at the important conclusion that one can check the homogeneity of a parallel plate of glass of thickness up to about 62 mm. If the R-number is increased to 12 so that the radius of curvature is now 366 cm, glass thickness could be increased up to about 132 mm.

Nondestructive Laser Pumping by High Explosives

John K. Crosby and R. C. Honey

Stanford Research Institute, Menlo Park, California.

Received 15 July 1963.

Pumping lasers by the light from a shock wave caused by detonation of high explosive has been suggested as a way of achieving high laser output power and energy without the necessity of a large primary power storage system. The very high powers available from high explosives make this an attractive source for many applications, particularly when low total mass is a requirement. Unfortunately, the excess power, not used for light production, usually results in destruction of the laser and its surroundings so that only one burst of radiation can be obtained for each laser. This is a disadvantage not only for many applications, but also when research is being conducted on the subject since a new laser for each experiment makes the research very expensive. To avoid this difficulty, a technique has been developed which allows the light from an explosive light source to pump a laser material without destroying the material. This technique has been demonstrated by pumping a neodymium-doped glass laser from a distance of 3.5 m without damaging the laser. This letter describes this technique and shows the results of the trial shot.

Figure 1 shows the basic setup used. The explosive light source is placed behind a concrete wall pointing up into a mirror. This mirror directs the light horizontally into a plastic Fresnel lens which images the light source aperture, A, on the 60-cm diam paraboloidal mirror of a surplus Navy signaling searchlight. This searchlight mirror then forms an image of the Fresnel lens upon the laser rod. The focal length of the mirror is 24.5 cm and if it were a good image-forming system, the final image on the laser would be about 2.8 cm in diam. With this mirror, however, aberrations due to the large aperture and off-axis errors cause a 50% increase in this figure so that nearly the entire 5-cm length of the rod is irradiated. Since the laser is only 0.635 cm in diam, the full height of the Fresnel lens image is not required to cover it. Part of this excess is eliminated by moving the Fresnel lens and the explosive down farther behind the concrete wall so that more protection is provided for the searchlight. An attempt to use some of the remaining light is made by placing a plane, steel mirror with aluminized surface directly in front of the laser to provide some additional irradiation from that side.

The light source consists of a block of Composition B explosive,

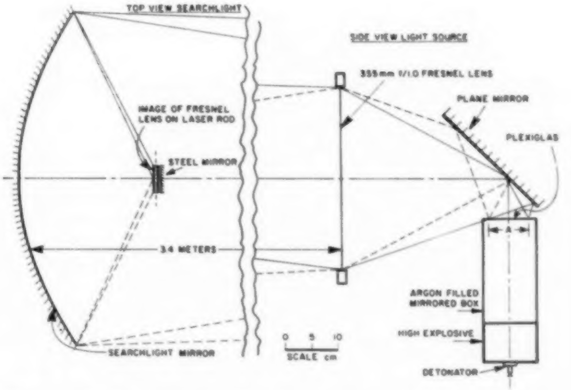

Fig. 1. Optical arrangement for explosive light source laser pumping.

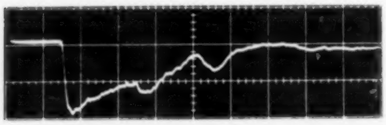

(a) PUMP PULSE – HORIZONTAL SWEEP SPEED – 10 microseconds/div.

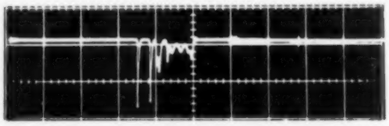

(b) LASER OUTPUT – SAME SWEEP SPEED AND SWEEP TRIGGER AS PUMP PULSE

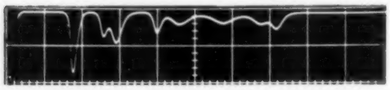

(c) LASER OUTPUT – EXPANDED TIME SCALE – 2 microseconds/div.

Fig. 2. Oscilloscope records.

10 × 10 × 7.5 cm placed at the end of a 10 × 10 × 20-cm box made of front surface mirrors. The end of the box away from the explosive is closed by a sheet of 0.6-cm Plexiglas. Small holes in the Plexiglas allow argon to flow through the box for several minutes before the shot.

The laser is mounted in the searchlight on the pedestal normally used for the arc lamp. The laser output beam is directed out the side of the searchlight housing and into the port of a bombproof shelter where it is recorded by a suitably filtered photomultiplier. Another photomulitplier with a filter transmitting in the green observes part of the light from the explosive light source via a mirror placed slightly to one side of the searchlight.

Optical alignment is checked by replacing the laser with a clear projection bulb with a fairly small filament. The Fresnel lens is placed where the best image of this filament is formed by the searchlight mirror. The explosive light source is then placed so that the image of the searchlight mirror formed by the Fresnel lens is sharp and centered on the Plexiglas-covered end of the mirror box.

Although explosive light sources have been used and roughly calibrated at least since 1937,[1] only recently have detailed theoretical calculations and experimental measurements of their output been made.[2–4] These measurements show that, for the light source geometry given above, the shock wave should initially appear to be a blackbody source at 30,000°K and is then expected to attenuate during the 25 μsec it is on so that the average intensity is about half of the initial intensity. If a neodymium-glass laser were placed inside a completely enclosed mirror box with perfect mirrors, the maximum energy stored in the metastable state at the end of the light pulse should be 0.23 J for each cm^2 of laser surface neglecting spontaneous emission losses. For the 0.635-cm diam, 5.1-cm long rod used here, this amounts to $10.2 \times 0.23 = 2.35$ J. When the laser is moved away to the focus of the searchlight and the reflection losses of all the mirrors are taken into account, this maximum energy stored per cm^2 of surface is reduced to 0.08 J. Since only one side of the rod is irradiated with this full intensity, the total stored energy should not be more than about 0.4 J.

For this experiment, the Eastman Kodak Company kindly supplied the laser complete with multilayer coatings to give 97% reflection at the output end and 100% at the other end. The rod had a threshold of about 15 J when closely coupled[5] to a linear xenon flash lamp with a comparably short pump pulse. If the xenon lamp is assumed to have an effective blackbody temperature of 5000°K and to have 50% conversion efficiency from electrical to light energy, the energy stored in the metastable level by a 15-J pulse should be about 0.5 J, but the inefficiencies in the optical coupling, spontaneous emission losses, cavity losses, and other losses reduce this to the threshold level. Some of these sources of loss are the same for the explosively pumped laser; others are not.

Figure 2 shows the oscilloscope records of photomultiplier output during a shot. These records show that the pump pulse is indeed strong enough to cause this laser to oscillate above threshold. Figure 2(a) shows the output of the light source. There is a 15-μsec delay between the detonator pulse, which triggered all the 10-μsec/cm traces, and the breakout of the shock wave into the argon. The intensity then falls slowly for about 20 to 25 μsec until a short pulse signals the shock arrival at the Plexiglas. The light output after this time may be from an air shock colliding with the plane mirror. Figure 2(b) shows laser output beginning about 19 μsec after the start of the light source output. Figure 2(c) of this picture shows a self-triggered record of this output at a faster sweep rate.

The only unexpected damage resulting from the shot was the fracture of the soft glass tube which was placed around the laser to protect it from shock and to filter out the strong ultraviolet portions of the pumping light. This tube was fractured either by the thermal shock from the large amount of energy absorbed or by mechanical shock from the steel mirror which was unexpectedly found to be loose after the shot. The laser itself was undamaged, however, as was the searchlight and its mirror.

The success of this shot not only lends credence to the calculations which have been summarized earlier, but also shows conclusively that research into ways of improving efficiency and increasing power output of explosively pumped lasers can be performed without sacrificing a laser in each experiment.

The authors are very grateful to Wayne McKusick of Eastman Kodak Company for supplying the laser rod on very short notice.

References

1. A. Michel-Lévy and H. Muraour, Compt. Rend. **204**, 576 (1937).
2. J. W. Bond, "The Structure of a Shock Front in Argon", Los Alamos Scientific Laboratory, LA 1893 (1954).
3. I. Sh. Model, Zhur. Ekspt1. i Teoret. Fiz. **32**, 714 (1957), Soviet Phys.—JETP **5**, 589 (1957).
4. J. Roth, "Research Study on the Surface Initiation of Explosives", Final Report, AFSWC TDR 63-49, Stanford Research Institute, Menlo Park, Calif. (1963).
5. P. A. Miles and H. E. Edgerton, J. Appl. Phys. **32**, 741 (1961).

A Carbon Furnace as a Source of Continuous Infrared Radiation

Robert Spanbauer, Phillip E. Fraley, and
K. Narahari Rao

Laboratory of Molecular Spectroscopy and Infrared Studies, Department of Physics, The Ohio State University, Columbus, Ohio. Captain Spanbauer is a student under the AFIT program.

Received 26 September 1963.

The construction of this furnace was supported by a contract between the Office of Naval Research and The Ohio State University Research Foundation.

During the past decade, the techniques of obtaining high resolution in infrared regions progressed tremendously. Excellent gratings have been produced recently, and highly sen-

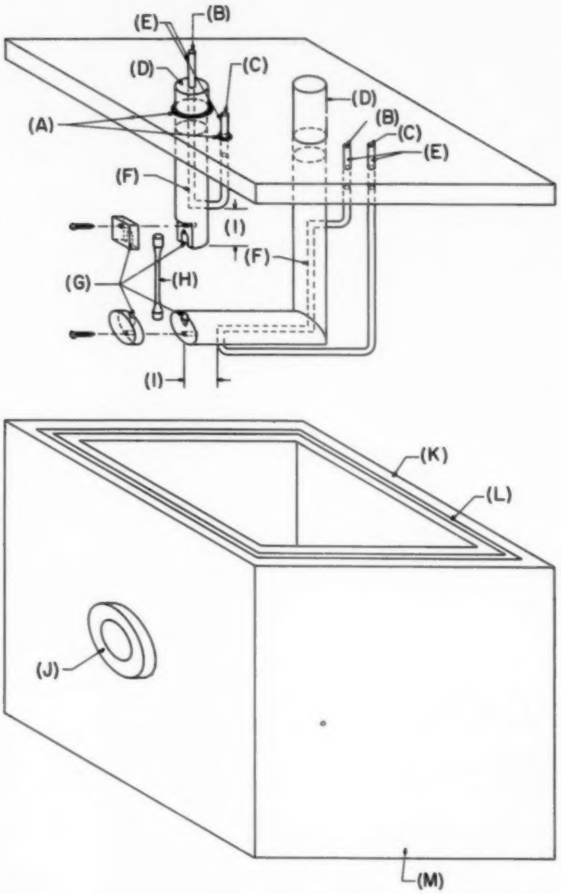

Fig. 1. The components of the carbon furnace. (A) The hole through which the water-cooled electrode is inserted. It is made 1.6 mm oversize and the space is filled with a ceramic adhesive for electrical insulation. (B) Inlet for water. (C) Outlet for water. (D) 2.5-cm diam copper rods which serve as electrodes. (E) 6.3-mm copper tubing. (F) 6.3-mm hole. (G) Cutouts of clamps are made slightly smaller than the radius of the carbon rod so as to ensure good electrical contact when clamps are inserted in position. (H) Carbon rod: 7 cm long; the ends measure about 12.7-mm diam and are copper-plated; the body measures about 6.3-mm in diam; 3.2–4.8-mm diam cavity has been drilled through the center along the length. A slot 2.5 mm wide has been cut on the side of the graphite rod to enable viewing the cavity. (I) This dimension is kept to about 1.9 cm to prevent the cooling of the graphite rod. (J) Infrared transmitting window. (K) Holes in lid and tapped holes in box are not shown. (L) 3.2-mm O-ring groove. (M) 25 cm × 25 cm × 25 cm steel box which has been water-cooled and interior porcelainized.

sitive detectors are available for use in the near infrared region. Since much of the work done with high-resolution infrared spectrographs pertains to the study of the absorption spectra of small polyatomic molecules, it is important to develop improved sources of continuous infrared radiation. The pioneering work of Rupert and Strong[1] demonstrated that the carbon arc is by far the best source of continuous infrared radiation. In this laboratory, the carbon arc (a movie projector source unit) proved to be very suitable in the regions not interfered by atmospheric absorptions. Edse *et al.*[2] considered the possibility of using the strong infrared continuum from an aluminum powder oxygen flame for absorption studies in infrared. However, in day-to-day work, it is rather important to have a source which is simple to operate, and at the same time have high intensity. We have now tried a carbon furnace operating in an atmosphere of argon, and it proved to be one of the best sources of continuous infrared radiation. The details of the furnace employed by us are furnished in Fig. 1. The main element is a carbon rod 7 cm long. A 3.2-mm diam cavity had been drilled through the entire length, and observations were made into this cavity through a slot cut on the side of the rod. The carbon rod was surrounded by an atmosphere of argon and it was heated electrically by passing a current of nearly 225 A at about 4 V. Thus far, we have been able to operate this source continuously for a period of nearly twelve hours. The design permits use of any infrared transmitting window, and, therefore, this source is useful in the entire region between 1–40 μ. Our studies indicated that the source compares excellently with the carbon arc, but has the advantage that it can be used with vacuum spectrographs even in the regions of atmospheric absorption.

Our thanks are due to John Phillips for valuable discussions about the method of viewing the cavity of the carbon furnace.

References

1. C. S. Rupert and J. Strong, J. Opt. Soc. Am. **39,** 1061 (1949).
2. R. Edse, K. N. Rao, W. A. Strauss, and M. E. Mickelson, J. Opt. Soc. Am. **53,** 436 (1963).

K. Bernolák *Hungarian Optical Works* during the Budapest Second Optical Conference of the Hungarian Society for Optics, Acoustics and Film Techniques, 6–10 May 1963.

T. Barna and J. Molnar, secretary and president, respectively, of the Hungarian Society for Optics, Acoustics and Film Techniques.

photos F. S. Harris, Jr.

A Publication of the Optical Society of America

ANNUAL SUBSCRIPTIONS

OSA members	$ 6.00
Other AIP societies' members	$ 8.00
Non-members and libraries	$10.00
Single copies	$ 3.00

Subscriptions should be addressed to APPLIED OPTICS Subscription Handling, American Institute of Physics, 335 East Forty-Fifth Street, New York 17, New York. **Eight weeks should be allowed for order processing.**

ADVERTISING

Advertising inquiries, orders, plates, and correspondence should be addressed to the APPLIED OPTICS Advertising Office, 1155 Sixteenth Street, N.W., Washington, D.C. 20036 • 202-DI 7-4131 • Mrs. Boraks

Applied Optics

A monthly publication of the
Optical Society of America

John N. Howard, Editor
Patricia R. Wakeling, Managing Editor

INDEX TO
VOLUME 2
1963

Subject 1344
Author 1355

Names of people and companies occurring in filler photograph captions have not been included in this index.

Published monthly by the Optical Society of America, Inc., in cooperation with the American Institute of Physics, at 20th and Northampton Streets, Easton, Pa. Editorial and advertising offices: 1155 16th St. N.W., Washington, D.C. 20036. 202-Di7-4131. Supported in part by a grant from the National Science Foundation. Subscription rates: $6.00 to OSA members, $8.00 other AIP Societies' members; nonmembers and libraries: $10.00 per year. Single copies $3.00. Second class postage paid at Easton, Pa. © Copyright 1963 by the Optical Society of America.

1963 Feature Editors:

January	**James G. Baker**
February	**James G. Baker**
March	**W. Lewis Hyde**
April	**F. Dow Smith**
May	**R. A. Woodson**
July	**Mary E. Warga**
September	**Mary E. Warga**
October	**Seymour Rosin**
November	**Earle K. Plyler**
December	**Donald P. Feder**

Subject Index to Volume 2*

Key to Index Use

1. Subjects, not titles, have been indexed.
2. Principal subjects are given in boldface type. Cross-referenced subjects which should be consulted for more thorough coverage are given in italics after the principal subject.
3. (L), (N), (B), (P) indicate: (L) Letter to the Editor; (N) from notes in one of the departments and not in a regular article; (B) book, or book review; (P) patent. (E), (T), (E/T) (T/E) indicate that the article is experimental, theoretical, or both.

Aberrations
- Catadioptric flat-field camera (T), 1081
- Measurement of distortion in photographic objectives (E), 759 (L)
- Null corrector for paraboloidal mirrors (T/E), 153

Absorption, Adsorptance, Adsorption
- Atmospheric infrared bands at nonuniform pressures (T), 605
- Beer's law and optimum transmittance in measurements (T/E), 937
- Cell for multiple pass (E), 764 (L)
- Coefficients of krypton in 600–886Å region (E), 947
- Infrared
  - Far, at liquid helium temperature from chromium ions in ruby (E), 977 (L)
  - Spectral, of solids 2–25 μ (E), 1169
  - Water, on walls as source of measurement errors (E), 1196
- Mercury vapor of resonance radiation (E), 1323
- Muscovite spectrum, alteration by KBr pellet preparation (E), 177 (L)
- Ozone in 4.75-μ region of solar spectrum (E), 581
- Solar, ordinates for calculations (T/E), 109, 810
- Spectra
  - Band for atmospheric slant paths (T), 515
  - Infrared, of thin films, 652 (P)
  - Magnesium hydroxide and calcium hydroxide (E/T), 1147
  - Water
    - In 2.7-μ band (T/E), 1117
    - Total by vapor in near infrared (E), 585
- Spectrophotometer, atomic (E), 931
- Spectroscopy at high resolution, application to simple molecules (E), 909

Aerosols
- Optical measurements in cloud chamber (E), 207

Alignment
- Interferometer (T), 541 (L)
- Optical instrument, 1168 (P)

Aluminum
- Surface, appearance of uncolored anodized (E), 448 (L)

Amplifier
- Simple voltage, for photovoltaic cells (E), 249

Angle Measurements (see also *Measurements*)
- Interferometer for precision (E), 762 (L)
- Mechanism, 1316 (P)

Arcs
- Imaging furnace, kaleidoscope to obtain uniform flux (T/E), 265
- Jet-controlled, excitation of second spectra (E), 635
- Vacuum, spectral line profiles in magnetically confined (E), 699

Aspherics
- Catadioptric optical system aberrations in flat-field cameras (T), 1081
- Fabrication of surfaces, 328 (N), (E) 1181
- Immersion null test (T/E), 1336 (L)

Astrometry
- Correction of measured star positions to standard coordinates (E/T), 17
- Problems of long-focus photographic (E), 9
- U. S. Naval Observatory 60-in. reflector (E), 1

Astronomy (see also *Image Formation, Photometry, Telescopes*)
- Cameras for, 549 (P)
- Correction of photographically measured star positions (E/T), 17
- Image orthicon at Dearborn Observatory (E/T), 157, 810
- Infrared, 8–14 μ, photometer (E), 749
- Limitations of image quality of large telescopes (E/T), 23
- Photomultipliers for pulse-counting applications (E), 181
- Solar observatory on Long Island (E), 93
- Solution of Kirkwood gaps in asteroids, 1100 (N)
- Spectrophotometer, dual-channel pulse-counting (E), 165

Astrophysics
- Contributions of W. W. Coblentz (E), 1101

Atmosphere
- Ground-level abundance of nitrous oxide, methane, and carbon monoxide (E), 176 (L)
- Infrared
  - Absorptances of bands at nonuniform pressures (T), 605
  - Transmission
    - Slant paths (T), 561
    - Solar radiation (E/T), 887
- Low sun solar phenomena (E), 199
- Spectral band absorptance for slant paths (T), 515

Atomic Spectra (see *Spectra*)

Beam Splitter
- Autocollimator, automatic, 1270 (P)
- Continuously variable (E), 1203 (L)

Beer's Law
- Optimum transmittance in absorption measurements (T/E), 937

Binoculars
- Improved mechanical adjustment, 1270 (P)
- Optical system for zoom, 1180 (P)

Blackbody
- Spectral variation of radiation (T), 1113

Bolometers
- Characterization of detectors (T/E), 1201
- Detectivity of cryogenic (T), 649 (L)

Books Received, 219

Books Reviewed
- *Advances in Glass Technology.* American Ceramic Society. Reviewed by N. J. Kreidl, 589
- *Advances in Spectroscopy,* Vol. 2. Edited by H. W. Thompson. Reviewed by D. A. Ramsay, 740
- *Advances in X-Ray Analysis,* Vol. 5. Edited by William M. Mueller. Reviewed by George L. Clark, 806
- *Annotated Bibliography on Soft X-Ray Spectroscopy.* H. Yakowitz and J. R. Cuthill. Reviewed by M. Parker Givens, 885

---

* Prepared by Franklin S. Harris, Jr., Aerospace Corporation.

Atlas of Optical Phenomena. Michel Cagnet, Maurice Françon, and Jean Claude Thrierr. Reviewed by A. I. Mahan, 908
Atmospheres of Mars and Venus; A Report of the Space Science Board. William W. Kellogg and Carl Sagan. Reviewed by Robert M. Chapman, 297
Classical Electrodynamics. John David Jackson. Reviewed by George Shortley, 480
Color in Business, Science and Industry. Deane B. Judd and Gunter Wyszecki. Reviewed by Henry Hemmendinger, 1108.
Elsevier's Dictionary of General Physics, in Six Languages. W. E. Clason. Reviewed by Erik Ingelstam, 908.
Diffuse X-Ray Reflections from Crystals. W. A. Wooster. Reviewed by C. A. Taylor, 885
Direct Observations of Imperfections in Crystals. J. B. Newkirk and J. H. Wernick, editors. Reviewed by W. C. McCrone, 298
Electroluminescence. H. K. Henisch. Reviewed by H.-E. Gumlich, 886
Elements of Infrared Technology: Generation, Transmission and Detection. Paul W. Kruse, Laurence D. McGlauchlin, and Richmond B. McQuiston. Reviewed by J. S. Garing, 358
Fifty Years of X-Ray Diffraction. P. P. Ewald. Reviewed by Dan McLachlan, Jr., 832
Flammenphotometrie. Second Revised Edition. R. Herrmann and C. Th. J. Alkemade. Reviewed by H. G. Wolfhard, 490
Fundamentals of Infrared Technology. Marvin R. Holter, Sol Nudelman, Gwynn H. Suits, William L. Wolfe, and George J. Zissis. Reviewed by William G. Langton, 364
Fundamentals of Theory Design and Application of Electronic Computers. V. A. Zimin. Reviewed by H. G. Cohen, 1231
Instrumental Optics. G. A. Boutry. Reviewed by R. M. Scott, 584
Introduction to the Methods of Optical Crystallography. F. Donald Bloss. Reviewed by Thomas P. R. Gibb, Jr., 282
ISA Transactions. Volume 1, Number 1. Instrument Society of America. Reviewed by Donald E. Williamson, 290
Japanese Journal of Applied Physics. Reviewed by Bryce Crawford, Jr., 489
Lasers, Generation of Light by Stimulated Emission. B. A. Lengyel. Reviewed by J. Weber, 806
Masers and Lasers. C. A. Hogg and L. G. Sucsy. Reviewed by O. S. Heavens, 479
Mechanism of Glass Polishing. D. C. Cornish. Reviewed by Given W. Cleek, 590
Molecular Spectroscopy. International Union of Pure and Applied Chemistry, Physical Chemistry Section, Royal Netherlands Chemical Society, and Netherlands Physical Society. Reviewed by H. Stammreich, 740
National Catalog of Patents, 223(N)
On the Broadening and Shift of Spectral Lines in the Plasma of a Gaseous Discharge. M. A. Mazing. Reviewed by J. H. Jaffe, 734
On the Spectral Excitation in a Spark Discharge. N. K. Sukhodrev. Reviewed by Cyrus Feldman, 734
Optical Methods of Measuring Plasma Jet Temperatures. H. C. Hottell, G. C. Williams, and W. P. Jensen. Reviewed by R. H. Tourin, 298
Optics publications in *Radio Propagation.* Section D, *Journal of Research of the National Bureau of Standards.* Selected by David M. Gates, 1068
Optics of Flames. F. J. Weinberg. Reviewed by Bernard Lewis, 886
Organic Chemical Crystallography. A. I. Kitaigorodskii. Reviewed by F. W. Cagle, Jr., 282
Photographic History of Mars, 1905 to 1961. E. C. Slipher. Reviewed by Andrew T. Young, 1060
Physik und Technik der Ultrarotstrahlung. Werner Brügel. Reviewed by J. N. Howard, 378
Publications of W. W. Coblentz on Infrared Spectroscopy, 1111(N)
Radioluminescence Yield of Organic Scintillators. Z. A. Chizhikova. Reviewed by J. B. Birks, 740
Report on Available Standard Samples and Related Materials for Spectrochemical Analysis 1960. Compiled by R. E. Michaelis. Reviewed by Edwin S. Hodge, 740
Science of Color. Optical Society of America, 1179(N)
Semiconducting III-V Compounds. C. Hilsum and A. C. Rose-Innes. Reviewed by Henry Levinstein, 315
Studies in Optics. A. A. Michelson. Reviewed by George W. Stroke, 480
Symposium on Spectroscopic Excitation. American Society for Testing Materials. Reviewed by James E. Paterson, 316
Tables of Einstein Functions: Vibrational Contributions to Thermodynamic Functions. Joseph Hilsenrath and Guy G. Ziegler. Reviewed by L. Haar, 838
Technical Glasses. M. B. Volf. Reviewed by Given W. Cleek, 584
Temperature Measurement in Engineering. Volume II. *Design, Construction, and Operation of Effective Temperature Measurement Devices.* H. Dean Baker, E. A. Ryder, and N. H. Baker. Reviewed by S. S. Penner, 282
Thermoelectricity: An Introduction to the Principles. D. K. C. MacDonald. Reviewed by Alton Karoli, 316
Vision Research—An International Journal. Edited by T. Shipley, F. Crescitelli, H. J. A. Dartnall, Y. LeGrand, H. Schober, and A. Sorsby. Reviewed by C. J. Bartleson, 310
Wave Mechanics of Crystalline Solids. R. A. Smith. Reviewed by G. H. Dieke, 490

Bubble Chambers
  British National, 1086(N)
  Brookhaven, 1024, 1048(N)
  Illumination
    Of the 80-in. (E/T), 1003
    Of the CERN 2-m-hydrogen (E), 1017
  Optics (review), 981, 1167, (E/T) 999, (E) 1017
  Trigger-circuit (E), 997
  University of Michigan, 998 (N)
  Windows, (E/T) 999, (E) 1037

Calcium Fluoride
  Index of refraction 0.23–9.7 μ (E/T), 1103

Calorimetry
  Graphite resistor source of image furnace research (E), 758 (L)
  Liquid, for high-energy laser (E), 163 (L)

Camera Tubes **(see** *Image Tubes*)

Cameras
  Astronomical, 549 (P)
  New family of flat-field (T), 1081
  Photoelectric exposure control, 548 (P)
  Scintillation for gamma rays, 652 (P)

Carbon Monoxide
  Abundance in ground-level air (E), 176 (L)

Chopper
  Electronic, for spectral lamps (E), 542 (L)
  Precision disk (E), 1333 (L)

Cloud Chambers
  Electronic flash illumination of large Wilson (E/T), 1013
  Optical measurement of aerosols (E), 207

Coal
- Use of infrared spectra of chars, in research (E), 1109

Coblentz, W. W.
- Astrophysics work (E), 1101
- Infrared spectroscopy contributions (E), 1090
- Memorial lecture, 1097 (N)
- Personal sketch, 1089
- Radiometry, influence on, 1098

Collimators
- Penetrative radiation to control field of view, 333 (P)

Color
- Books, 1108, 1179
- Diffusion transfer process, 651 (P)
- Masking by xerography, 547 (P)
- Photography, with electrostatic developing powder, 1316 (P), 1316 (P), 1316 (P)
- Projection system, 548 (P)

Colorimeters
- For color sorting, 1316 (P)
- For mixtures, 1270 (P)

Comparators
- Automatic readout with photoelectric detection (E), 1330 (L)
- Image inverter for spectral projector (E), 763 (L)
- New, 226 (N)
- Optical, to show size and shape of workpieces, 332 (P)

Computers
- Bi-optric elements for storage, 454 (N)
- Lens design by (T), 1233; (T), 1239; (T), 1247; (T), 1257; (T), 1265; (E/T), 1281
  - Automatic (review) (T), 1209, (T) 1227, (T) 1331 (L)
- Optical, 225 (N)
- Photographic emulsions for storage media (T), 421

Condensers
- New, for sun-powered continuous laser (E), 827

Conferences (see *Meetings*)

Constants (see also *Optical Constants*)
- Force, policy on publication, 222 (N)

Coronagraphs
- Reduction of scattered light in (E), 131
- Reflecting (E), 977

Cosmotron
- Brookhaven, 1015 (N)

Counters
- Photon, 226 (N)

Crystals
- Growth kinetics, 1132 (N)
- Growth of large, 1132 (N)
- Method of evaluating laser potentialities (E/T), 291

Crystallography
- Methods of optical, 282 (B)
- Observations of imperfections, 298 (B)
- Organic chemical, 282 (B)

Densitometer
- For scanning angularly oriented spectral lines (E), 1207

Depth Measuring Device, 1270 (P)

Detectors (see also *Radiometry*)
- Bolometric characterization (T/E), 1201 (L)
- Information capacity of radiation (T), 351
- Infrared, liquid nitrogen dewar attachment (E), 760 (L)
- Lead sulfide
  - Recovery from intense radiation, 454 (B)
  - Variation of response with incident angle and orientation (E), 1204 (L)
- Photoionization, for the vacuum ultraviolet (E), 735

Diffraction
- Losses in laser interferometers (T), 544, 545 (L)

Diffusion
- Calculation of coefficients, from Rayleigh interference fringes (T), 66 (L)

Discharges
- Gaseous, enhancement of krypton by mercury and xenon (E/T), 299

Dispersion
- Infrared
  - Gas absorption lines (T/E), 495
  - Of some oxide glasses (E), 741
- Prism, with no deviation, 1168 (P)

Editor
- From the, 30, 218, 228, 420, 463, 616, 714, 853, 946, 1036, 1140, 1256

Einstein Functions
- Tables of, 838 (B)

Electrodynamics
- Classical, 480 (B)

Electroluminescence, 886 (B)

Electro-optics
- Effect
  - Gallium arsenide (E), 647 (L)
  - Hexamethylenetetramine (E), 320 (L)
  - Quartz (E), 868 (L)
- Light modulation
  - Cubic crystals (T/E), 839
  - Stressed plate (E/T), 1175
  - Quartz with UHF (E), 868 (L)

Emission
- Infrared, interferometric measurement of lines (E), 1155
- Sky at 15–26 μ (E), 571

Errata, 725, 810, 1167, 1250

Evaporation
- Heated filament material (T), 1055

Exploding Wires
- As blast shutter (E), 441
- Optical pumping of lasers using (E), 451 (L)

Fabry-Perot (see also *Interferometry and Films*)
- Diffraction patterns of neodymium in glass laser (E), 867
- Etalons used in PEPSIOS scanning spectrometer (E/T), 873

Faraday Rotation
- In FeNi films (E/T), 411

Fiber Optics
- Combination of images for three-color television, 333 (P)
- Light-conducting, 1168 (P)
- Measurement of hot objects, 652 (P)

Fibers
- Glass, for structural purposes, 548 (P)
- Crossed glass, for flying spot film measuring (E), 1025

Filaments
- Evaporation rate from heated (T), 1055

Films
- Apparatus for deposition for electrical conduction and light transmission, 1116 (P)
- Dielectric coatings, selection of multilayer, for Fabry-Perot (E), 727

- Effect of MgF_2 and SiO on reflectance of aluminized mirrors (E), 156 (L)
- Faraday rotation in FeNi (E/T), 411
- Image intensifying photosensitive, 548 (P)
- Magnesium fluoride, unusual property in infrared (E), 91 (L)
- Multilayer reflection coatings on a metal mirror (T), 445
- Silver for multiple-beam interferometry (E), 539, 725 (L)
- Thickness control for vacuum deposited, 330 (P)
- Thin, low index, on infrared transmitting materials, 331 (P)

Filters
- Alkali metal ultraviolet, 330 (P)
- Birefringent for monochromator use (E/T), 193

Flames
- Infrared spectroradiometry of liquid propellant (E), 1133
- Optics of, 886 (B)

Flash Illumination
- Large Wilson cloud chamber (E/T), 1013

Flying Spot
- Film measuring machine with crossed glass fibers (E), 1025

Fourier Transforms
- Correction of phase errors in interferograms (T), 491, 1332 (L), 1332 (L)

Furnaces
- Graphite resistor source for image research (E), 758 (L)
- Solar and arc imaging, kaleidoscope for uniform flux in (T/E), 265

Gallium Arsenide
- Electro-optic effect (E), 647 (L)

Gases
- Circulating loop for infrared system for reacting (E), 1165

Gauges
- Thickness, low-cost noncontact (E), 92 (L)

Germany
- Optics in German Democratic Republic, 1069

Glass
- Advances in technology, 589 (B)
- Alkali silicates with bi- and trivalent silicates, 1180 (P)
- Coating to reduce crazing, 331 (P)
- Fibers, 548 (P), 549 (P)
- High chemical durability, 549 (P)
- Infrared transmitting, 331 (P)
- Lithia-free soft, 652 (P)
- Method of preparing, 1180 (P)
- Optical, new, 454 (N), 454 (N), 454 (N), 547 (P)
- Oxide, infrared dispersion of (E), 741
- Polishing, 590 (B)
- Technical, 584 (B)

Gratings (see also ***Spectrographs*****)**
- Concave for astronomical spectrographs (E/T), 187
- Concave, spectrograph, wavelength measurement (E), 715
- High-resolution, spectrographs, predisperser for (E), 963
- Platinum or gold for surface at grazing incidence (T/E), 450 (L)
- Spectrometer or analyzer, 330 (P)
- Spectrometer, fore-prism drive (E), 175(L)

Helium
- Continuum source for 600–1100Å (E), 617

Heterodyning
- Optical, spurious harmonic generation in (E), 823

History
- Coblentz, W. W., 1089, 1090, 1098, 1101
- Photographic, of Mars, 1060 (B)
- Young, Thomas, 639

Illumination
- Bubble chambers (E/T), 1003, (E) 1017
- Cloud chamber, large Wilson (E/T), 1013
- For optical devices, 1180 (P)
- Slit source of the Hough-Powell digitizer (E/T), 1085 (L)

Image Evaluation (see also ***Transfer Functions*****)**
- By spot diagrams with computer (T), 1247
- Optical, and the transfer function (T/E), 335
  - Computer to minimize spot sizes (E/T), 1281
  - Role of eikonal and matrix methods (T), 1239

Image Formation
- In aerial cameras (T/E), 545 (L)
- Limitation of quality in large telescopes (E/T), 23
- Stellar telescopic analyzer (E/T), 31

Image Intensifiers
- Photosensitive films, 548 (P)

Image Inverters
- Spectral projector comparator (E), 763 (L)

Image Motion
- Experimental transfer characteristics and air conditions in aerial photography (E/T), 379

Image Projection Systems
- Device, 1116 (P)
- Multiple superimposed images, 651 (P)

Image Recording
- Xerography and magnetic means, 547 (P)

Image Rectifier
- Photogrammetry, 651 (P)

Image Stabilizer
- For telescope, 651 (P)

Images
- Spectrographic, brighter by using anamorphic optics (T), 755

Image Tubes
- Image orthicon astronomy at Dearborn Observatory (E/T), 157, 810
- Infrared to visible, 333 (P)
- Isocon scan (E/T), 253

Information
- Capacity of radiation detectors and of light (T), 351
- Optical storage in solids (T), 393
- Retrieval systems, 224 (N)
- Storing and retrieval by optical method (T/E) 387, 764
- Storing in computer with photographic emulsions (T), 421

Infrared
- Absorption, absorptance
  - Atmospheric gas bands at nonuniform pressures (T), 605
  - Chromium ions in ruby in far, at liquid helium temperatures (E), 977 (L)
  - Magnesium hydroxide and calcium hydroxide spectra (E/T), 1147
  - Measurement errors due to water on walls (E), 1196 (L)
  - Near, total, by water vapor (E), 585
  - Water band at $2.7\ \mu$ (T/E), 1117
- Atomic emission spectra (E), 691, 1155
- Attenuating media, literature review, 454 (N)
- Books, 378, 364, 358
- Detectors
  - Hot-box, 333 (P)
  - Liquid-nitrogen dewar attachment (E), 760 (L)
  - Mount, cooled for cell, 1316 (P)
- Dispersion
  - Of some oxide glasses (E), 741
- Emission of sky in 15–26 μ region (E), 571
- Far, bibliography, 1132 (N)
- Glasses for transmission, 331 (P)
- Image converter to visible, 333 (P)

  In-line spectrometer, 331 (P)
  Interferometer for earth temperature distribution, 1100 (N)
  Magnesium fluoride, unusual property in (E), 91 (L)
  Modulated, to measure properties of materials, 651 (P)
  Near, literature on, attenuating media, 454 (N)
  Photometer, astronomical for 8–14 μ (E), 749
  Polarized radiation in magneto-optical studies of semiconductors (E), 527
  Proximity warning for aircraft installation, 333 (P)
  Ranging system, 1270 (P)
  Reflection and transmission
    Materials in 2–50 μ region (E), 591
    Materials, bibliography, 596
  Refracting system, 454 (N)
  Scanner, 332 (P)
  Scanning system, reticle design (T/E), 229
  Solids, absorptance in 2–25 μ region (E), 1169
  Source, continuous carbon furnace (E), 1340 (L)
  Spectra
    Books, 480
    Circulating loop for reacting gases (E), 1165
    Use in chars in coal structure research (E), 1109
  Spectrograph, six-meter Ebert-type (E), 1123, 1127
  Spectrometer, two-wavelength, two-frequency ratio recording (E), 969
  Spectrophotometers, extraneous radiation effect (T/E), 1141
    Optical null double-beam, double-pass (E), 1309
    Photometric calibration (E), 1303
  Spectroscopy
    Dispersion measurement of vibration–rotation lines in gases (T/E), 495
    High-resolution, application to study of simple molecules (E), 909
    Liquid propellant flames (E), 1133
  Transmission
    Atmospheric (T), 561
    Atmospheric to solar radiation (E/T), 887
  Transmitting components, low-index films on, 331 (P)
  Units and terminology, 714 (N)

Instruments
  Optical (E), 227
  Transactions of Instrument Society of America, 290 (B)

Intensity
  Continuously variable controller (E/T), 1203 (L)

Interference
  Fringes, measurement of photographic records of (E), 487
  Rayleigh fringes, calculation of diffusion coefficients from (T), 66 (L)
  Rings in ruby maser beams (E), 811

Interferometers
  Alignment (T), 541 (L)
  Comparators for line standards (E), 471
  Laser
    Diffraction losses in (T), 544, 545 (L)
    Mode selector (E), 448 (L)
  Measurements
    Velocity of light (E), 481
    Vibration amplitudes (E), 1061
  Microscope, dichroic multiple-beam (E), 540 (L)
  Plano, instrument, 822 (N)
  Precision angle measurements (E), 762 (L)
  Quantum limit to wavelength determination (T), 465
  Shearing for measurement of transfer functions of the microscope (E/T), 371
  Spherical mirror oscillating (E), 865 (L)

Interferometry
  Grating light divider, 1322 (P)
  Measurement of infrared atomic emission lines (E), 1155
  Multiple-beam, silver films for (E), 539, 725 (L)
  Phase error correction (T), 491, 1332 (L), 1332 (L)
  Scanning spectrometer, high-resolution (E/T), 873
  Selection of multilayer dielectric coatings for Fabry-Perot (E), 727
  Tilted-plate, with large plate separation (E), 817, 1330 (L)
  Twyman-Green, optical quality and radiation patterns of ruby lasers (E), 855

Integrating Spheres
  Asymmetry of (E), 631

Ionization of Gases
  Ruby laser (E), 546 (L)

Iron
  Group elements, Mn^+, Ni^+, V^+, second spectra, recent work (E), 687
  Oxide (FeO), molecule emission spectra (E), 1335 (L)
  Wavelength of lines, measured by new technique (E), 177 (L)

Irradiance
  New standard of spectral (E/T), 1151

Jeffries–Abragam Effect
  In a four-level system (T), 787

Kaleidoscope
  With flowing liquids, 1269 (P)

KDP (potassium dihydrogen phosphate)
  Refractive index (E), 1334 (L)

Krypton
  Absorption coefficients in 600–886 Å region (E), 947
  Enhancement by mercury and xenon in gaseous discharges (E/T), 299

Lamps (see *Sources*)

Lasers (see *Masers*)

Lead Sulfide
  Variation of response with incident angle and orientation (E), 1204 (L)

Length
  International standard (E), 455

Lenses (see also *Optical Systems*)
  Adapter, 652 (P)
  Adjustable mount, 1322 (P)
  Afocal attachment, 549 (P)
  Aerial photographic, 548 (P)
  Anamorphic system, 333 (P)
  Binocular, Erfle-type, 549 (P)
  Bubble chamber (E/T), 1003
  Catadioptric objective, 548 (P), 549 (P)
  Design by computers (see also *Computers*)
    By localized two paraxial ray paths (T), 1275
    Graphical first-order method (T), 1251
  Design data for calculation of optical transfer function (T), 359, (T) 1239
  Design of superachromats (T), 553
  Dielectric rod, focusing of light (T), 303
  For brighter spectrographic images (T), 755
  Gaussian, wide-angle, 549 (P)
  High-aperture objective, 550 (P)
  High-speed, cinematographic wide-angle, 548 (P)
  High-speed, wide-angle, photographic 548 (P)
  Highly corrected optical objective, 1180 (P)
  Photographic, high-aperture, small field-of-view, 1180 (P)
  Photographic, measurement of distortion (E), 759 (L)
  Photographic objective, 333 (P), 333 (P), 549 (P)

- Symmetrical *f*/5.6, 1322 (P)
- Symposium designed, 272 (N), (T) 1227, 1331 (L)
- Telephoto, 548 (P)
- Telephoto converter, 1322 (P)
- Television, 548 (P)
- Triplet, 550 (P)
- Varifocal systems, 549 (P), 549 (P), 1322 (P)
- Zoom, 548 (P), 1322 (P), 1366 (P)
- Zoom, focusing, 550 (P)
- Zoom, mechanical linkages, 549 (P)

Light
- Information capacity of (T), 351
- Modulation
  - Cubic crystals (T/E), 839
  - Gallium arsenide (E), 647 (L)
  - Quartz at UHF (E), 868 (L)
- Production of charge of image recording, 1168 (P)
- Rays, angular distribution from a gas discharge source (E), 540 (L)
- Velocity, measurement by interferometer (E), 481

Lines
- Profile
  - Polychromator for time-dependent observation (E), 205
  - Pressure-broadened spectra, errors due to slits, (T), 1195 (L)
  - Studies of long, magnetically confined, high-current, steady-state vacuum arcs (E), 699

Magnetic Fields
- Influence on gas discharge lasers (E), 861 (L)

Magneto-Optics
- Studies of semiconductors by polarized infrared radiation (E), 527

Mars
- Atmosphere, 297 (B)
- Photographic history, 1060 (B)

Masers
- Lasers
  - Abstracts (periodical), 979 (N)
  - Beam divergence measurements and interpretation (E/T), 319 (L)
  - Books, 479, 806
  - Communications, new aspects (T), 311
  - Continuous, sun-powered, new condenser for (E), 827
  - Crystals, method of evaluating, for potentialities (E/T), 291
  - Dictionary definition, 838 (N)
  - Developments, new, 225 (N), 226 (N), 453 (N), 1131 (N)
  - Dielectric rod, focusing of light (T), 303
  - Diffraction losses in interferometers (T), 544, 545 (L)
  - Gaseous, power dip at line center (T), 869 (L)
  - Helium–argon
    - Operation at 3.39 μ (E/T), 317
  - Helium–neon
    - Source for light scattering measurements (E), 1205
  - High-index of refraction spherical sheath composite rod (E/T), 431
  - Indium phosphide injection, 872 (N)
  - Intensity distribution of ruby beams (E), 1198 (L)
  - Interference rings in ruby beams (E), 811
  - Interferometer
    - Mode selector (E), 448 (L)
    - Spherical mirror oscillating (E), 865 (L)
  - Hole-burning model of oscillation (E), 807, (T) 1085 (L)
  - Liquid, 872 (N)
  - Liquid calorimeter for high-energy (E), 163 (L)
  - Magnetic fields, influence upon gas discharge (E), 861 (L)
  - Neodymium
    - Far-field Fabry-Perot diffraction patterns (E), 867
    - Operation of, at 9180 Å (E/T), 87 (L)
    - Performance of a CW (E), 833
  - Optical pumping, nondestructive by high explosives (E), 1339 (L)
  - Optical pumping using exploding wires (E), 451 (L)
  - Radiation transfer by elliptical cylinder reflectors (T), 509
  - Raman scattering, stimulated, analysis of giant pulse (T), 847
  - Ruby
    - Better control of, for, 453 (N)
    - Characteristics using microwave phototubes (E/T), 767
    - Ionization of gases (E), 546 (L)
    - Optical quality and radiation patterns (E), 855
    - Output spikes, correlation from different portions (E), 151 (L)
    - Sea water attenuation (E/T), 1202 (L)
  - Sénarmont polariscope in analysis of light (E/T), 801
  - Tilted-plate interferometry with large plate separations (E), 817
  - Transients, analysis, and stability in idealized two-level system (T), 862 (L)
- Optical
  - Applied Optics supplement, 225 (B)
  - Heterodyne, 453 (N)
  - Polytechnic Institute of Brooklyn Symposium, 447 (N)

Measurements
- Analysis of microscopic particles in blood, 652 (P)
- Angles
  - Interferometer for precision (E), 762 (L)
  - Ronchi ruling (E), 77 (L)
- Aspherics, immersion test (T/E), 1336 (L)
- Depth, 1270 (P)
- Distance by improved geodimeter, 330 (P)
- Gauge, low-cost noncontact thickness (E), 92 (L)
- Homogeneity of large-aperture glass plates (T), 1337 (L)
- Material particles by modulated infrared, 651 (P)
- Optical, of aerosols in cloud chamber (E), 207
- Precision, seminars, 1132 (N)
- Radiometers with linearized final output, 332 (P)
- Sinusoidal test object production and use (T/E), 273
- Surveying transit, 652 (P)
- Temperature, by fiber optics, 652 (P)
- Vibration amplitudes (E), 1061

Meetings
- Aerospace and Navigational Electronics, 9th East Coast Conf., Baltimore, Oct. 1963, 410
- American Physical Society, 1962 Winter Mtg., Stanford, California, Dec. 1962, 508
- American Society of Photogrammetry, 29th Ann. Mtg., Washington, D. C., March 1963, 826
- Analytical Chemistry and Applied Spectroscopy, 14th Ann. Pittsburgh Conf., March 1963, 706
- Astrophysics, 11th Internatl. Colloq., Liège, July 1962, 271
- Electromagnetic Waves and Antennas, URSI Internatl. Symp., Copenhagen, June 1962, 236
- Far Infrared Spectroscopy, Internatl. Symp., Cincinnati, Ohio, Aug. 1962, 663
- Glass, 6th Internatl. Cong., Washington, D. C., July 1962, 604
- High-Speed Photography, VI Internatl. Conf., Scheveningen, Netherlands, Sept. 1962, 570
- Hungarian Optical Conf., 2nd, Budapest, May 1963, 962
- Information Theory, 1962 Internatl. Symp., Brussels, Sept. 1962, 444
- Infrared Radiation, 1st Czechoslovak Conf., Brno, Nov. 1962, 603
- Interference and Coherence Conf., Sydney, Australia, Aug. 1964, 629

  Lasers and Applications, Ohio State U. Symp., Columbus, Nov. 1962, 440
  Lasers, Technical and Military Applications, s'Gravenhage, Netherlands, Apr. 1962, 430
  Meter, International Advisory Committee on Definition of, Sèvres, France, Oct. 1962, 501
  Millimeter and Submillimeter Conf., IRE, Orlando, Fla., Jan. 1963, 792
  Molecular Structure and Spectroscopy, 18th Symp., Ohio State U., Columbus, June 1963, 1042
  Molecular Structure and Spectroscopy, Internatl. Symp., Tokyo, Sept. 1962, 663
  Optical Maser Symp., Polytechnic Inst. of Brooklyn, New York, Apr. 1963, 826
  Optical Society of America, Jacksonville, Fla., March 1963, 726
  Optical Society of America, Rochester, N. Y., Oct. 1962, 7
  Optics, Topics in, 8th Ann. AFOSR Summer Scientific Seminar, Cloudcroft, N. M., June 1963, 1232
  Photographic Instrumentation Engineers, Society of, 7th Technical Symp., N. Y., Aug. 1962, 276
  Photography and Spectroscopic Optics, Tokyo and Kyoto, Sept. 1964, 629
  Precision Electromagnetic Measurements, Internatl. Conf., NBS, Boulder, Colo., Aug. 1962, 8
  Quantitative Spectroscopy, 3rd, and Special Problems of Space Sciences Conf., Caltech, Pasadena, March 1963, 726
  Quantum Electronics, Masers and Optical Maser Techniques, 10th Ann. Solid State Circuits Conf., Philadelphia, Feb. 1963, 800
  Quantum Electronics, 3rd Internatl. Symp., Paris, France, Feb. 1963, 800
  Scattering, Electromagnetic, Interdisciplinary Conf., Clarkson Col. of Technology, Potsdam, N. Y., Aug. 1962, 501
  WESCON, 1962, Los Angeles, Aug. 1962, 507
  Western Spectroscopy Association, 10th Ann. Mtg., Asilomar, Calif., Jan. 1963, 664

Meetings Calendar, 221, 329, 464, 560, 674, 786, 980, 996 1102, 1302

Mercury
  Optical excitation for fluorescence (E), 1323

Methane
  Abundance in ground-level air (E), 176

Metric System, 228 (N), 420 (N), 616 (N), 634 (N), 946 (N), 1256 (N)

Microdensitometer (see *Densitometer*)

Microscope
  Apparatus for high temperature use, 332 (P)
  Condenser for increased resolution, 1270 (P)
  Field ion, 222 (N)
  Interferometer, dichroic multiple-beam (E), 540 (L)
  Objective, 333 (P)
  Shearing interferometer to measure transfer functions of objective (E/T), 371

Microspectrophotometry
  Spectral properties of biological materials (E), 899

Mirrors
  Aluminized, reflectance of and protective coatings of MgF_2 and SiO (E), 156 (L)
  Analysis and design by matrix methods (T/E), 1271
  Bent axis focusing (E), 761 (L)
  Lightweight (E), 623 (N)
  Null corrector for paraboloidal (T/E), 153
  Scattering by surfaces (E), 977

Modulation Transfer Function (see *Transfer Function*)

Modulators
  Electro-optical by stressed plate shutter (E/T), 1175
  Optical, push-pull (T), 1197

Molecular Spectra (see *Spectra*)

Monochromators
  Birefringent, for high-order grating spectra (E/T), 193
  Double systems (T/E), 1049, 1250
  Ultraviolet, 1322 (P)

Moon
  Near infrared observations of, 222 (N)
  Optical problems of television recording from approaching spacecraft (E/T), 41

Muscovite
  Alteration of absorption spectrum, by KBr pellet preparation (E), 177 (L)

Navigation
  Optical device, 1270 (P)

Nitrous Oxide
  Abundance in ground-level air (E), 176 (L)

Optical Activities
  Industry, 328, 623, 978, 1088, 1294
  Universities, 16, 323

Optical Beats
  In ruby laser light sources (E), 807

Optical Constants
  Measurement of N and K by photorefractometer (T/E), 1043

Optical Devices
  Absorption method to detect impurities, 330 (P)
  Afocal, protecting against radiation, 651 (P)
  Alignment
    Interferometer (T), 541 (L)
    Lamps and reflectors, 333 (P)
    Optical instrument, 1168 (P)
  Automatic focusing, 332 (P)
  Automatic leveling, 1168 (P)
  Auxiliary, for Kitt Peak telescopes (E/T), 141
  Bent-axis focusing mirrors (E), 761 (L)
  Combined range and viewfinder, 1116 (P)
  Curve comparison, 1116 (P)
  Determination of object position, 1116 (P)
  Diamond band saw, 408 (N)
  Dispersion prism with no deviation, 1168 (P)
  Electronic control of optical radiation, 651 (P)
  High-index, large-diameter, glass beads for reflection markers, 333 (P)
  Illuminating arrangement, 1180 (P)
  Image inverting for copying, 550 (P)
  Inspecting bodies of revolution, 332 (P)
  Justifying system, 549 (P)
  Light-tight optical joint, 333 (P)
  Microprobe analysis, 822 (N)
  Multi-stable optical feedback storage, 331 (P)
  Navigation, 1270 (P)
  Optical graticules for reducing geophysical prospecting data, 331 (P)
  Optical inspection of surfaces by reflection, 331 (P)
  Optical positioning of jig borer, 651 (P)
  Optical straight line of great accuracy, 224 (N)
  Photographic information storage, 330 (P)
  Rodolite, optical straight line, 224 (N)
  Sighting instrument, 547 (P)

Slicing of optical elements, 454 (N)
Stabilization of optical sighting systems, 332 (P)
Synchronizer with scanning beam, 1168 (P)
Telescopic finder for motion picture camera, 333 (P)
Tool positioning, 1269 (P)
Transducer of electroluminescent cells, 332 (P)
Viewfinder
  Block-type Albada, 1180 (P)
  Including instrument pointer, 333 (P)

Optical Systems
Anastigmatic catoptric, 550 (P)
Auxiliary, for Kitt Peak telescopes (E), 141
Catadioptric for flat-field cameras (T), 1081
Catadioptric, Bouwers-type, high-aperture, 550 (P)
Design, automatic (review) (T), 1209
Plane mirror, matrix design (T/E), 1271
Scanning, 1116 (P)

Optical Transfer Function (see *Transfer Function*)

Optics
An action program, 653
German Democratic Republic, 1069
Instruments, 584 (B)
Junior science symposium, 453 (N)
Opticists and, 222, 453, 973, 1100, 1328
"Opticists" word, 1328
Physics research in small liberal arts college, 1075
Pictures of phenomena, 908 (B)
Publications of National Bureau of Standards in radio propagation, 1068
Russia, 1132
Studies, 470 (B)
Terminology, 218 (N)
United States, neglected in, 1088
Universities
  In the, 16, 323
  Michigan, fundamentals of infrared technology course, 739
  Minnesota, infrared spectroscopy course, 350
  Rochester, summer course in modern optics, 400
  Utah, seminars, 224

Overhauser Effect
In four-level system (T), 787

Ozone
Absorption in 4.75-μ solar spectrum (E), 581

Particles
Microscopic, analysis of, 652 (P)
Planetary, interplanetary, and interstellar, wavelength polarization effects (E/T), 67

Patents (see under subject)
National catalog of, 223 (B, N)
University research and policy, 1100 (N)

Photocells
Automatic for film, 548 (P)
Method of forming photoemissive surfaces, 331 (P)
Photovoltaic, simple voltage amplifier for (E), 249

Photoconductors
Lead sulfide, variation of response with incident angle and orientation (E), 1204 (L)
Recovery from intense radiation, 454 (N)

Photodetection
Spurious harmonic generation in optical heterodyning (E), 823

Photoelasticity
Opaque models by reflected light, 331 (P)
Polariscope, 1316 (P)
Scanner for stress pattern, 1269 (P)
Stress-plate shutter for light modulator (E/T), 1175

Photogrammetry
Image rectifier, 651 (P)
Two-stage rectifier, 1270 (P)

Photography (see also *Lenses*)
Aerial, experimental transfer characteristic of image motion and air conditions (E/T), 379
Antihalation and filter layers, 331 (P)
Correction of measured star position to standard coordinates (E/T), 17
Elimination of matting layers, 331 (P)
Emulsions as computer storage media (T), 421
Exposure-charged, produced for image recording, 1168 (P)
High-speed motion picture for transparent drops (E), 1287
Instrumental, 832 (B)
Measurement of interference fringes by (E), 487
Objective for, Gauss-type, 333 (P)
Photometer for, 1270 (P)
Practical aspects of ground targets for aerial cameras (T/E), 545 (L)
Problems in long-focus astrometry (E), 9
Production and use of sinusoidal test objects (T/E), 273
Simple method for photometry (E), 648 (L)
Three-lens system of, and projecting wide-field, 332 (P)
Vocal cords in action, 1100 (N)
Xerographic image reversal, 1168 (P)
Yellow filters of multilayer color elements, 330 (P)

Photoionization
Use as detector for vacuum ultraviolet (E), 735

Photolithography
Projecting device, 549 (P)

Photometry (see also *Polarimetry, Spectrophotometry*)
Amplifier, simple voltage, for photovoltaic cells (E), 249
Astronomical polarization (E/T), 67
Asymmetry of an integrating sphere (E), 631
Extraneous radiation effect on accuracy (T/E), 1141
Flame, 490 (B)
Improved measurement of relative intensity of two beams, 651 (P)
Infrared astronomical, in 8–14 μ region (E), 749
Isocon scanning techniques (E/T), 253
Low level, 1269 (P)
Photoelectric, multicolor for satellites (E), 625
Photographic, device, 1270 (P)
Photographic, simple method for (E), 648 (L)
Photomultiplier, temperature effects in astronomical (E), 51
Visual in solar research (E), 89

Photomixing
Spurious harmonic generation in (E), 823

Photomultipliers
Temperature effects in, and astronomical photometry (E), 51
Tests of, for astronomical pulse-counting applications (E), 181

Photoreceptors
Studied by microspectrophotometry (E), 899

Photorefractometer
Extension of sensitivity and range (T/E), 425
Measurement of N and K (E), 1043

Physics, Applied
Japanese journal, 489

Physics, Dictionary
Six-language, 908 (B)

Planets
Optical problems of television recording from approaching spacecraft (E/T), 41
Telescopes for (review), 111

Planimeter
Large-stage photoelectric (E), 1317

Plasma
Spectral properties (E), 699

Plates
Technique for evaluating half-wave and quarter-wave (E), 864 (L)

Pockels Effect
Crystals of cubic symmetry (T/E), 839
Hexamethylenetetramine (E), 320 (L)
Quartz at UHF (E), 868 (L)

Polarimetry
Photoelectric, 651 (P)
Sénarmont in analysis of laser light (E/T), 801
Technique for evaluating half-wave and quarter-wave plates (E), 864 (L)
Telescopes and, for polarization measurements (E/T), 67

Polarization
Achromatic rotators, 1180 (P)
Apparatus to measure ellipticity of surface reflected, 1180 (P)
Astronomical measurements, effects of telescopes on (T/E), 61
Circular polarizers, 1270 (P)
Film for stereoscopy, 1270 (P)
Light, film for, 330 (P)
Metallized grids for producing, 549 (P)
Semiconductor reflection, 1269 (P)
Thin film on glass, 1116 (P)
Wavelength dependence of particle (E/T), 67

Prisms
Isosceles total internal reflectors as optical elements (T/E), 1191

Projection System
Attachment to increase focal length, 1322 (P)
Color, 548 (P)
Image, 1116 (P)
Improved illumination device, 1270 (P)
Multiple superimposed images, 651 (P)
Photolithography, 549 (P)
Stereo pictures, 651 (P)

Pulse Counting
Photomultipliers for astronomical applications (E), 181

Pumping (see also *Masers*)
Using exploding wires (E), 451 (L)

Pyrometer
Optical, high-temperature, 1270 (P), 1322 (P)

Quantum Limit
To precision of wavelength determination (T), 465

Radiation
Detectivities, of cryogenic bolometers (T), 649 (L)
Detectors, information capacity, (T), 351
Electronic control of optical, 651 (P)
Passive, proximity detector, 332 (P)
Review of reviews of atomic spectroscopy, 657
Spectral variation of blackbody (T), 1113
Thermal, from hemispherical source in contact with infinite Lambert plane (T), 283
Transfer, by elliptical cylinder reflectors (T), 509

Radiometry (see also *Detectors*)
Influence of W. W. Coblentz on (E), 1098
Null-type device, 1316 (P)
Observation of extraphotographic infrared atomic emission spectra (E), 691
Small temperature difference measurement, 1322 (P)

Raman Scattering
Spectra of $Mg(OH)_2$ and $Ca(OH)_2$ (E/T), 1147
Stimulated, by giant laser pulse (T), 847

Rangefinders
Combined, and viewfinder, 1116 (P)
Prediction of systems performance (T), 277
System, 547 (P)

Ranging Systems
Infrared, 1270 (P)
Optical, pulse echo, 1270 (P)

Rare Earths
Atomic spectra (review/E), 665
Spectra of the doubly and triply ionized (E/T), 675

Ratio-Recording
Infrared spectrometer analyzer (E), 969

Referees, 179, 392, 1140, 1194

Reflection
Elliptical cylinder, radiation transfer by (T), 509
Infrared materials, bibliography, 596
Isosceles, total internal, as optical elements (T/E), 1191
Materials in 2–50 μ region (E), 591
Multilayer, coatings on metal mirrors (T), 445
Parabolic system, light weight portable for space, 1316 (P)
Reduction of internal, 651 (P)

Refraction Index
Calcium fluoride 0.23–9.7 μ (E/T), 1103
KDP (potassium dihydrogen phosphate) (E), 1334 (L)

Refractometer
Photo, extension of sensitivity and range (T/E), 425

Reticles
Comparison of AM and FM systems (T/E), 229

Ronchi Ruling
Angular measurements using (E), 77 (L)

Satellite
Photoelectric photometer for (E), 625

Scanning Systems
Condenser for flying spot, 332 (P)
Infrared, 332 (P)
Multislit, 331 (P)
Optical, 1116 (P)
Processing, one- and two-dimensional, in line (T), 401

Scattering
By mirror surfaces (E), 977
Helium–neon laser as source of measurements (E), 1205 (L)
Meter, design for submersible (T), 245
Raman, produced by giant laser pulse (T), 847
Reduction in coronagraph (E), 131
Wavelength dependence of particles on (E/T), 67

Schmidt Camera
Flat-field catadioptric (T), 1081

Scintillation
Camera for gamma rays, 652 (P)
Organic, 740 (B)

Screens
Fluorescent, 651 (P)

Semiconductors
III–V compounds, 315 (B)
Study by polarized infrared in magneto-optical studies (E), 527

Sea Water
Attenuation measurements with ruby laser (E/T), 1202 (L)

Sextant
Space, coaxial dual-field optics (E), 1265

Shadowgraph
Self-luminous objects (E), 78 (L)
Shock Tubes
Spectroscopy of excited powdered solids (E), 919
Shutters
Exploding wire blast (E), 441
Sighting Instrument
Telescope for, 548 (P)
Slits
Errors by, in pressure-broadened line measurements (T), 1195 (L)
Light collection to illuminate, in Hough-Powell digitizer (E/T), 1085 (L)
Replacement of, by screen of alternate transparent and nontransparent zones (T/E), 79
Sodium Salicylate
Preparation of layers for luminescent screens (E), 1334 (L)
Solids
Information, optical storage (T), 393
Wave mechanics of crystalline, 490 (B)
Sources
Atomic spectroscopy (review), 657
Bubble chamber, trigger-circuit for (E), 997
Electrodeless discharge, in atomic spectra analysis (E), 707
Electronic chopper for (E), 542 (L)
Gas discharge, angular distribution of light from (E), 540 (L)
Generation of sinusoidal light intensity (T), 263
Graphite resistor, for image furnace research (E), 758 (L)
Helium continuum for 600–1100 Å region (E), 617
He–Ne laser for light scattering measurements (E), 1205 (L)
Infrared, continuous from carbon arc (E), 1340 (L)
Oxide emission (E), 1335 (L)
Spectral, decay characteristics (E), 542 (L)
Spectrophotometer to measure energy distribution (E), 237
Spectrophotometers for spectroradiometry (E), 1207 (L)
Standard, new, for spectral irradiance (E/T), 1151
Ultraviolet, extreme, Schueler, improved cathode for (E), 864 (L)
Xenon, parameters and characteristics (E), 793
Spectra (see also *Spectrophotometry*)
Absorption alteration of muscovite by KBr pellet preparation (E), 177 (L)
Analysis, especially far ultraviolet, 652 (P)
Atomic, electrodeless discharge lamps in the analysis (E), 707
Atomic emission, observation of extraphotographic infrared (E), 691
Energy distribution of sources by spectrophotometer (E), 237
Excitation of second, by jet-controlled arc (E), 635
High-order grating, isolation by birefringent monochromator (E/T), 193
Infrared
  Absorption of thin films, 652 (P)
  Interferometric measurement of atomic emission (E), 1155
  Of chars in coal structure research (E), 1109
  Precision measurements (E), 1127
  Reacting gases, circulating loop for (E), 1165
Iron, wavelengths by new technique (E), 177 (L)
Iron group, Mn$^+$, Ni$^+$, V$^+$, second spectrum (E), 687
Irradiance, new standard (E/T), 1151
Lattice vibration of Mg(OH)$_2$ and Ca(OH)$_2$ (E/T), 1147
Line profile
  Polychromator for time-dependent observations (E), 205
  Vacuum arcs (E), 699
  Mercury Optical excitation by resonance radiation (E), 1323
Microdensitometer for scanning angularly oriented lines (E), 1207 (L)
Oxide molecule emission (E), 1335 (L)
Rare earths
  Atomic (review/E), 665
  Doubly and triply ionized (E/T), 675
Recording of band intensities (E), 611
Sky in 15–26 μ region (E), 571
Slit introduced errors in measurements (T), 1195 (L)
Standards, international wavelength, 224 (N)
Thermoluminescence, spectrophotometer (E), 243
Wavelength measurement with concave grating spectrograph (E), 715
Spectrograph
Automatic speed-of-scan double-beam infrared, 1168 (P)
Bass-Kessler grating, construction and calibration (E), 451 (L)
Concave gratings for astronomical (E/T), 187
High-resolution, application to study of simple molecules (E), 909
Infrared, six-meter Ebert-type (E), 1123, 1127
Predisperser for high-resolution grating (E), 963
Wavelength measurement with concave grating (E), 715
X-ray, 548 (P)
Spectrometers
Cell structure, cavity-type liquid for, 332 (P)
Concave gratings for astronomical (E/T), 187
Direct recording of band intensities (E), 611
Grating, or analyzer, 330 (P)
Grating, foreprism drive (E), 175 (L)
Grating, improved operation, 1322 (P)
In-line infrared, 331 (P)
Interferometric, high-resolution scanning (E/T), 873
Mass, improved resolution, 330 (P)
Null-type device, 1316 (P)
Quantum limit to wavelength determination (T), 465
Replacement of slits by screen of alternate transparent and nontransparent zones (T/E), 79
Servo correction for errors, 1322 (P)
Two-wavelength, two-frequency ratio recording infrared analyzer (E), 969
Spectrophotometry
Atomic absorption (E), 931
Asymmetry of an integrating sphere (E), 631
Density-recording ultraviolet, vacuum (E), 321
Dual-channel pulse-counting astronomical (E), 165
Flame, temperature compensation for, 331 (P)
Infrared
  Calibration (E), 1303
  Effect of extraneous radiation on (T/E), 1141
  Optical null (E), 1309
Micro (E), 899
Rapid scanning for thermoluminescence spectra (E), 243
Spectral energy distribution of light sources (E), 237
Universal (E), 1295
Used as spectroradiometers (E), 1207 (L)
Wedge for double-beam, 330 (P)
Spectroradiometry
Infrared, of liquid propellant flames (E), 1133
Use of spectrophotometers for (E), 1207 (L)
Spectroscopy
Absorption cell of simple construction, White-type multiple pass (E), 764 (L)
Advances, 740 (B)
Atomic (review), 657
Automatic dispersion controlled, 1180 (P)
Brighter images using anamorphic optics (T), 755
Device, 549 (P)

- Dielectric coatings, selection of, for Fabry-Perot interferometry (E), 727
- Dispersion measurement of vibration–rotation lines in gases (E), 495
- Electron chopper for spectral lamps (E), 542 (L)
- Excitation in spark discharge, 734 (B)
- Excitation symposium, 316 (B)
- Flame, bibliography, 1132 (N)
- Image inverter for projector comparator (E), 763 (L)
- Infrared, Coblentz contributions (E), 1090
- Infrared, far, absorption at liquid helium temperature from chromium ions in ruby (E), 977 (L)
- Interference comparators of line standards (E), 471
- Interferometry, tilted-plate, with large plate for high resolution (E), 817
- Molecular, 740 (B)
- Plasma, 734 (B)
- Shock-excited powdered solids (E), 919
- Solar simulations (E), 105
- Standards, 740 (B)
- Ultraviolet, extreme, Schueler lamp (E), 864 (L)
- X-ray, performance of curved crystals in range 3–12 Å (E), 955

Spin-Coupled Systems
- Electron-nuclear, non-Boltzmann population distribution in four-level system (T), 787

Spot Diagrams (see *Image Evaluation*)

Standards
- Infrared by Fabry-Perot fringe scanning (E), 1155
- Length, international (E), 455
- Line, interference comparators for (E), 471
- Spectral irradiance, new (E/T), 1151
- Wavelength, secondary, 224 (N)

Star Tracker, 1270 (P)

Stereoscopy
- Attachment for viewers, 1180 (P)
- Polarization film for, 1270 (P)
- Projection of pictures, 651 (P)
- Transparent screen to produce, 1116 (P)

Sun
- Absorption by ozone in the 4.75-μ spectrum (E), 581
- Absorptivity calculations, selected ordinates (T/E), 109, 810
- Atomic spectra of the rare earths, presence in, (review/E), 665
- Imaging furnace, kaleidoscope for uniform flux (T/E), 265
- Low, phenomena (E), 199, 1336 (L)
- Observatory on Long Island (E), 93
- Optics
  - In equipment to utilize energy, 454 (B,N)
- Radiation, infrared transmission of atmosphere (E/T), 887
- Reflecting coronagraph (E), 977
- Research, sensitive visual photometer for (E), 89
- Spectra, absorptance of infrared by atmospheric gases (T), 605
- Spectra, simulation with filtered high-pressure xenon lamp (E), 105

Surfaces
- Aluminum, uncolored anodized, appearance (E), 448 (L)
- Fabrication of aspherical (E), 1181

Tachistoscope
- Projection, 1269 (P)

Telescopes
- Alignment device, 548 (P)
- Analyzer for stellar images (E/T), 31
- Auxiliary optical systems for Kitt Peak (E/T), 141
- Binocular, 333 (P)
- Corrector plate, 548 (P)
- Design
  - Baker-type off-axis $f/0.35$ solid Schmidt camera, (T/E), 201
- Dual-image reflecting, 1316 (P)
  - $f/5$ solid telescope (T/E), 201
- Focusing objective of, 550 (P)
- Image quality, limitations of, of large (E/T), 23
- Image stabilizer, 651 (P)
- Planetary (review), 111
- Polarization measurements
  - Effects of, on astronomical (T/E), 61
  - Use in (E/T), 67
- Problems in long-focus photographic astrometry (E), 9
- Schmidt–Cassegrain, short, for sextant (E), 1265
- Sighting instrument use, 548 (P)
- Solar, Kitt Peak, 222 (N)
- U. S. Naval Observatory 60-in. astrometric reflector (E), 1

Television
- Problems of, recording of moon and planets from spacecraft (E/T), 41
- Three-color image using fiber optics, 333 (P)

Temperature
- Measurement, 282 (B)
  - By pyrometer, 1270 (P)
- Optical methods to measure, in plasma, 298 (B)
- Radiometer measurement of small difference, 1322 (P)

Theodolite
- Coordinate, 1269 (P)

Thermoelectricity, 316 (B)

Thermoluminescence
- Spectra, spectrophotometer for (E), 243

Transfer Characteristics
- Contrast, role of eikonal and matrix, in calculations (T), 1239
- Image motion and air condition, in aerial photography (E/T), 379

Transfer Functions
- Image evaluation and (T/E), 335
- Optical
  - Calculation from lens-design data (T), 359
  - Measurement
    - Instrument (E/T), 365
    - Shearing interferometer for microscope (E/T), 371
  - Modulation, use in testing aerial cameras (T/E), 545 (L)
- Test objects, sinusoidal (T/E), 273

Transistor
- Optical, 1173 (N)

Transit
- Surveying, 652 (P)

Transmission
- Infrared
  - Atmosphere (T), 561
  - Atmosphere to solar radiation (E/T), 887
  - Materials, bibliography, 596
- Material in 2–50 μ region (E), 591
- Optimum, in absorption measurements and Beer's law (T/E), 937
- Single path band, factors, from double path measurements (T), 503
- Water band, infrared in 2.7 μ (T/E), 1117

Turbulence
- Effect on transfer characteristics in aerial photography (E), 379

Ultraviolet
- Absorber for, added to organic polymeric structure, 651 (P)
- Alkali metal filter, 330 (P)
- Extreme, Schueler lamp, improved cathode (E), 864 (L)

- Far, spectra analysis, 652 (P)
- Monochromator, 1322 (P)
- Sodium salicylate, layer preparation for screens (E), 1334 (L)
- Units and dimensions, 714 (N)
- Vacuum
  - Density-recording spectrophotometer (E), 321 (L)
  - Photoionization detector (E), 735

Venus
- Atmosphere, 297 (B)

Viewfinder
- Block-type Albada, 1180 (P)

Viewers
- Attachment for stereoscopic, 1180 (P)

Vision
- Research, journal, 310

Water Vapor
- Adsorption on walls, introduces infrared absorption errors (E), 1196 (L)
- Infrared absorption at 2.7-μ band (T/E), 1117
- Infrared, near, total absorptance (E), 585

Wavefront Reconstruction
- Three-dimensional (E), 409

Wavelength
- Determination, quantum limit to (T), 465
- Measurement with concave grating spectrograph (E), 715

Windows
- Bubble-chamber
  - Optical and mechanical properties (E/T), 999, (E) 1037, 1137

Xenon Lamps
- Flash, effect of pre-excitation on quality (E), 1329 (L)
- Flash for large Wilson cloud chamber (E/T), 1013
- Limiting parameters and generalized characteristics (E), 793
- Solar spectrum simulation (E), 105

Xerography
- Magnetic image recording, 547 (P)
- Masking, color, 547 (P)
- Type, process, 1316 (P)

X Rays
- Advances, 806 (B)
- Curved crystal performance in range 3–12 Å (E), 955
- Fifty years of, diffraction, 832 (B)
- Photofluorography, light meter, 1269 (P)
- Reflections from crystals, 885 (B)
- Spectrograph, 548 (P)
- Spectroscopy, bibliography, 885 (B)

Young, Thomas
- Biography, 639

Author Index
to
Volume 2

Aagard, R. L., 509, 540
Aikens, R. S., 157
Alamichel, C., 495
Altman, J. H., 648
Arcas, Ph., 909
Arndt, J., 507
Ashley, E. J., 156
Assous, R., 495

Baird, D. H., 839
Baird, K. M., 177, 455, 471, 591
Baker, J. G., 111
Ballard, S. S., 16, 323
Barchewitz, P., 909
Barker, W. A., 787
Barnes, M. W., 177
Barr, E. S., 639
Bartleson, C. J., 310
Bartz, A. M., 969
Bass, A. M., 1335
Baurer, T., 451
Bell, W. E., 317
Bennett, H. E., 156
Bennett, J. M., 156, 1330
Berkowitz-Mattuck, J. B., 265
Bernstein, J. B., 1169
Billings, B. H., 430
Birks, J. B., 740
Blachman, N. M., 444
Bloembergen, N., 8
Bloom, A. L., 317
Bloom, L. R., 839
Boettner, E. A., 105
Bohlin, D., 131
Bolle, H. J., 571
Bond, W. L., 761
Borkan, H., 253
Bowen, D. E., 833
Bowie, G. E., 1061
Bowman, R. L., 176
Bradbury, R. A., 867
Bradley, D. J., 539, 725
Brixner, B., 1281, 1331
Brouwer, W., 1239
Brown, W. M., 401
Brunelle, Jr., H. E., 1265
Buchanan, R. A., 1147
Buhrer, C. F., 647, 839
Burch, D. E., 585
Burge, D. K., 1202
Burke, T. G., 1165
Buser, R. G., 861

Cagle, Jr., F. W., 282
Calfee, R. F., 1117
Callahan, L. G., 401
Caplan, P. J., 291
Carman, P. D., 1317
Carpenter, R. O'B., 229
Caspers, H. H., 1147
Chabbal, R., 873
Chace, W. G., 441
Chapman, R. M., 297
Chen, M. M., 265
Christensen, R. L., 1049
Church, C. H., 451
Clark, G. L., 806
Cleek, G. W., 584, 590, 741
Clough, S. A., 611
Cohen, A. J., 604
Cohen, H. G., 1231
Collins, D. A., 411
Collins, S. A., 448
Conway, J. G., 707
Cooke, F., 328, 408, 978, 1088, 1294
Cooper, III, W. S., 205
Cope, A. D., 253
Crawford, Jr., B. L. 489
Crosby, J. K., 1339
Crosswhite, H. M., 675
Cummins, H. Z., 823

Dalton, Jr., M. L., 1195
Damon, E. K., 163, 440, 546
Davis, S. P., 727, 963
Davis, W. W., 66
Decius, J. C., 664
Deeg, E. W., 999
DeKinder, Jr., R. E., 827
Deirmendjian, D., 1336
Delano, E., 1251
de Lhery, G., 291
DeMaria, A. J., 807, 1085
Dennis, J. H., 1334
De Vany, A. S., 201
Dhumwad, R. K., 1335
Diago, M. C., 687
Di Domenico, Jr., M., 431
Dieke, G. H., 675
Dreyfus, M. G., 1113
Dufault, R. A., 540
Dyson, J. J., 487

Eden, D. D., 868
Edgerton, H. E., 570, 1013
Eichhorn, H., 17
Eisner, E., 755
Ejiri, A., 321
Elliott, Jr., S. D., 625
Evans, J. W., 193
Evtuhov, V., 319
Ewanizky, T., 291

Feder, D. P., 272, 1209, 1227
Feibelman, W. A., 199
Feldman, C., 734
Ferriso, C. C., 175, 760
Fish, C. V., 441
Fish, R. A., 31
Flynn, J. T., 163
Fox, A. G., 544
Fraley, P. E., 1127, 1340
France, W. L., 585
Fred, M., 715
Friedel, R. A., 1109
Friedman, B., 236
Früngel, F., 1017

Gagosz, R., 807
Gardner, I. C., 832
Garing, J. S., 358
Gates, D. M., 887, 1117
Gehrels, T., 67
Gelles, R., 1081
George, T. V., 1198
Ghosh, A. K., 243
Gibb, Jr., T. R. P., 282
Girard, A., 79
Givens, M. P., 885
Glaser, P. E., 265
Görlich, P., 1069
Green, A. E. S., 561
Griggs, M., 561
Groner, W., 1204
Grosjean, C. C., 501
Grosof, G., 299
Grosso, R. P., 764
Grum, F., 237
Gullón, M. N., 687
Gumlich, H.-E., 886
Gutmacher, R. G., 707
Haar, L., 838
Hadni, A., 977
Haeusler, C., 909
Hall, A. C., 864
Hammond, III, H. K., 1207
Hanes, G. R., 465
Hansen, D. W., 1117
Harrick, N. J., 1203
Harrop, W. J., 887
Haun, Jr., R. D., 451
Hauser, S. M., 1175
Heard, H. G., 1329
Heavens, O. S., 479, 800
Hegarty, J. C., 78
Hellerstein, D., 801
Hellwarth, R. W., 847
Hemmendinger, H., 1108
Hendeberg, L. O., 379
Hennes, J. P., 735
Herriott, D. R., 826, 865
Herzberger, M., 553
Ho, L., 647
Hodge, E. S., 740, 763
Hoffman, A. R., 649, 1201
Holleran, R. T., 1336
Honey, R. C., 1339
Hook, L., 66
Hopkins, R. E., 1227
Horey, Jr., E. C., 763
Howard, J. N., 30, 218, 228, 378, 420, 463, 616, 714, 853, 946, 1036, 1140, 1196, 1256
Howlett, L. E., 455
Huffman, R. E., 617, 947
Hughes, H. K., 937

Humphreys, C. J., 691, 1155
Hyde, W. L., 227, 962, 1232

Iglesias, L., 687
Imbusch, G. F., 817, 1330
Ingelstam, E., 908
Irland, M. J., 540

Jackson, J. K., 1151
Jaffe, J. H., 734
Joffrin, C., 909
Jones, J. L., 955
Jones, R. C., 351
Jones, R. N., 1090
Julich, H., 263

Kahn, H. L., 931
Kainz, J., 861
Kapany, N. S., 425, 1043
Karoli, A., 316
Kaye, W., 1295
Keck, P. H., 827, 833
Kester, J. E., 283
Kingston, R. H., 1334
Kirk, D. D., 1169
Knable, N., 823
Knapp, R. A., 1334
Köhler, H., 1017
Kotin, L., 66
Kreidl, N. J., 589

Laikin, M., 91
Lamberts, R. L., 273
Landon, D. O., 450
Langton, W. G., 364
Larrabee, J. C., 617, 947
Legay, F., 495
Levi, L., 421
Levine, M. A., 78
Levinstein, H., 315
Lewis, B., 886
Li, T., 544
Liller, W., 187
Loewenstein, E. V., 491, 1332
Low, F. J., 649
Ludman, J. E., 862
Lynnworth, L. C., 92

MacAdam, D. L., 7, 648
Mack, J. E., 873
Mackey, R. C., 542
Mahan, A. I., 908
Malitson, I. H., 741, 1103
Marchand, E., 359
Marlowe, D. G., 1175
Marquet, L. C., 963
Marquis, D. C., 726
Marshak, I. S., 793
Martz, D. E., 749
Martz, Jr., E. P., 41
Maurer, R. D., 87
Maust, Jr., E. E., 758
McCaa, D. J., 581
McCarthy, D. E., 591
McClure, N. R., 553
McCrone, W. C., 298
McCubbin, Jr., T. K., 764
McKenna, J., 303
McKiernan, M. A., 503
McLachlan, Jr., D., 832
McMurtry, B. J., 767
McNally, Jr., J. R., 699
McNutt, D. P., 873
McQuaid, R. W., 320
Meggers, W. F., 657
Megla, G. K., 311
Mertz, L., 1332
Meyer, C., 909
Meyer-Arendt, J. R., 77, 409, 508
Miedler, L. J., 105
Miller, R. H., 61
Miller, W. A., 93
Minami, S., 1309
Minardi, J. E., 283
Miner, Jr., E. D., 77
Miyamoto, K., 1247
Mollenauer, L. F., 817, 1330
Moore, C. E., 665
Moore, Jr., F. L., 635
Moore, J. G., 625
Moos, H. W., 817, 1330
Morgan, S. P., 544
Murphy, J., 1147
Murray, B. C., 749
Murty, M.V.R.K., 1337
Mutschlecner, J. P., 1202

Narchal, M. L., 787
Neeland, J. K., 319
Nelson, D. F., 410
Newburgh, R. G., 864
Newkirk, Jr., G., 131, 977
Newman, A. H., 365
Nicholls, R. W., 919
Nicholson, J. B., 955
Nielsen, H. H., 1123
Noyce, R. H., 177

Offner, A., 153
Öhman, Y., 89
Olson, O. H., 109, 631
Onaka, R., 321
O'Neill, E. L., 1239
Osial, T. A., 451
Overend, J., 1042

Paix, D., 249
Palik, E. D., 527
Palmer, R. B., 1025
Parkinson, W. H., 919
Paschen, K. W., 955
Patrick, F. B., 277
Paul, Jr., E., 691
Penner, S. S., 282
Pfeiffer, A., 1287
Phillips, R., 359
Plass, G. N., 515
Plyler, E. K., 480, 1089
Pollack, S. A., 542
Pontarelli, D. A., 425, 631, 1043
Potter, R. J., 1049
Powers, W. T., 157

Ramsay, D. A., 740
Rao, K. N., 1123, 1127, 1340

Reader, J., 963
Ready, J. F., 151
Redmann, J. J., 827, 833
Reeves, E. M., 919
Regelson, E., 1202
Reinhard, H. P., 1017
Reitmayer, F. O., 999
Rempel, R. C., 317
Rodman, J. P., 165, 181
Roesler, F. L., 873
Rohlin, J., 762
Rosenau, Jr., M. D., 545
Rosin, S., 1003, 1085
Rothstein, J., 1191
Rottmann, H. R., 1333
Ruhl, H. D., 969
Ruthberg, S., 177

Sakurai, T., 1181
Sanderson, J. A., 1098
Saunders, J. B., 541
Saur, R. L., 448
Schawlow, A. L., 817, 1330
Schermer, E. B., 540
Schneider, W. E., 1151
Schraeder, A. E., 1323
Schuldt, S. B., 509, 540
Schulte, D. H., 141
Schurin, B., 611
Schwab, W. G., 1165
Scolnik, R., 735
Scott, R. M., 584
Shannon, R. R., 365
Sharp, J. V., 826
Shaw, J. H., 176, 581, 605
Sherman, B., 276
Shishido, K., 1181
Shortley, G., 480
Siegler, E. H., 663
Silverman, S., 726
Sims, W. P., 997
Skidmore, M. R., 699
Slama, L., 1198
Slavin, W., 931
Smith, D. F., 1165
Smith, D. S., 177
Smith, F. D., 335
Smith, H. J., 181
Smith, L. S., 1175
Somers, E. V., 451
Spanbauer, R., 1340
Spencer, G. H., 1257
Speyer, E., 207
Spillman, G. R., 205
Stair, R., 1151
Stammreich, H., 740
Stavroudis, O. N., 741
Sterzer, F., 1197
Stewart, J. E., 1141, 1303
Stickley, C. M., 855, 867
Stierwalt, D. L., 1169
Stober, A. K., 735
Stoicheff, B. P., 811
Stoliar, A. P., 1204
Strand, K. Aa., 1
Strandberg, M. W. P., 792
Stroke, G. W., 470, 481
Strong, J., 1101
Strother, G. K., 899
Sullivan, J., 861
Sutton, L. E., 741, 1275
Svelto, O., 431
Szabo, A., 811

Tanaka, Y., 617, 947
Tang, C. L., 545
Targ, R., 299
Taylor, C. A., 885
Taylor, J. H., 1075
Teska, T. M., 67
Texereau, J., 23
Theissing, H. H., 291
Thiess, G. H., 868
Thygesen, K. H., 635
Tomkins, F. S., 715
Tomlinson, R. G., 546
Tourin, R. H., 298, 1133
Tsuruta, T., 371
Twersky, V., 236
Tyler, J. E., 245

Van de Kamp, P., 9
van Heerden, P. J., 387, 393, 764
van Thanh, N., 909
Vaško, A., 603
Velasco, R., 687

Walther, A., 1239
Warnke, W. E., 758
Weber, J., 806
Welander, W. E., 379
Welford, W. T., 981, 1037
Wessely, H. W., 503
Westphal, J. A., 749
White, C. E., 827, 833
White, G. R., 448
Wieder, H. H., 411
Wiberly, S. E., 706
Wiebe, A. F., 1207
Wilcox, J. M., 205
Willey, Jr., R. R., 1265
Williams, D., 271, 585
Williamson, D. E., 290, 611
Wilson, A. D., 1055
Wilson, M. K., 664
Winsberg, S., 869
Witmer, E. E., 800
Wolfhard, H. G., 490
Wolken, J. J., 899
Woodward, D. H., 1205
Worden, E. F., 707
Wormell, P. M. J. H., 1233
Wynne, C. G., 1233

Yamamoto, S. S., 997
Yeh, Y., 823
Yoder, Jr., P. R., 1175
Yokoyama, M., 1198
Young, A. T., 51, 1060
Young, L., 445

Zimmerman, J., 759
Zirin, H., 977
Zisk, S. H., 31
Zito, Jr., R., 1323

OSA Around-the-World Group Flight 1964

Revised Information # 2

The International Commission for Optics' Symposium on Photographic and Spectrographic Optics will be held in Tokyo 1–8 September 1964, preceded by a Conference on Interference and Coherence, convened under the auspices of ICO and the Australian Academy of Science, in Sydney 23–29 August 1964. The airlines have recently approved an around-the-world group flight fare for 15 persons or more, and OSA now wishes to learn the number of members who are interested in attending these two meetings and participating in this group flight. There will also be an informal universities tour in Israel and in Hong Kong, and time for sightseeing in New Delhi, Bangkok, and Teheran. Our revised schedule now looks like:

Aug.	8	leave New York, Idlewild Airport
	9–12	Israel
	13	Teheran
	14–17	New Delhi
	17–20	Bangkok
	20–22	Hong Kong
	23–31	Sydney, ICO meeting
Sept.	1–10	Tokyo, ICO meeting
	10	return to NYC via San Francisco*

The group fare will be **$1475** economy class round trip. Only OSA members and their immediate dependents may participate. Would members who are interested fill in and return the form below. The interest of those who have already written in is recorded, **and a $100 deposit is now needed.** Please send in your deposits as soon as possible. Deposits, less 10% handling charge, will be returned in the event of cancellation before 1 June 1964.

See also page, A16

Assistant Secretary, OSA
Room 101
1155 16th Street, N.W.
Washington, D.C. 20036

REPLY

I am interested in participating in the OSA 1964 AROUND-THE-WORLD GROUP FLIGHT and I wish to have information as it becomes available.

☐ I shall travel alone ☐ accompanied by my wife ☐ my children (state how many)

☐ I enclose $...... representing deposits for .... tickets.

*☐ I would like to stay the extra three days to enable me to take the post-conference tour in Japan (cost $50–70). Information available from organizers of Japanese meeting.

Name.. OSA Membership #................

Address..

....

....

....

GURLEY

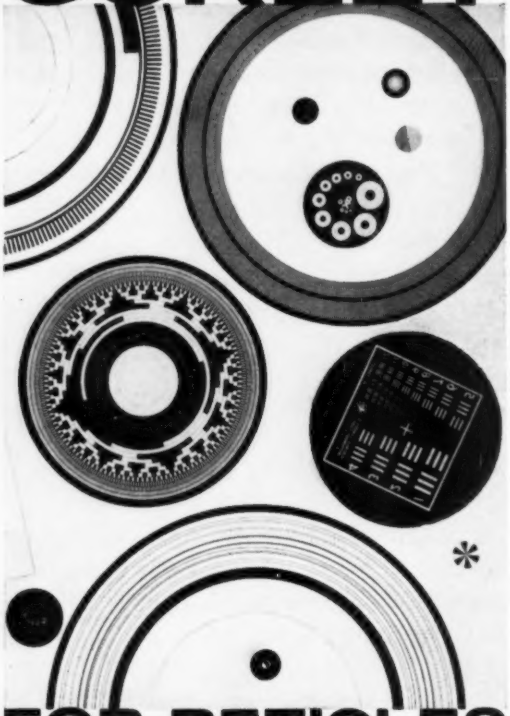

FOR RETICLES

- Glass reticles for all types of telescopes and optical measuring instruments on contract basis .... BOOKLET RD
- Precision code patterns (stock Binary, Sine-Cosine; and others to specification) .... BULLETIN 7000
- Precision resolution targets
  N.B.S., Lyle, Sayce, and others ...... BULLETIN 8000
  U.S.A.F.-type .... BULLETIN 8010
- Precision dividing, circular or linear, by ruling, scribing and photographic projection .... BOOKLET RD
- Precision patterns on glass for photoelectric readout devices
- Electroforming of metals

For additional information, write or call

W. & L. E. GURLEY
548 Fulton Street, Troy, N. Y.
Area Code 518 AShley 2-6300

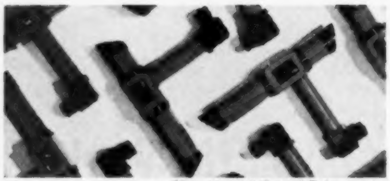

Visual and Infrared Telescopes

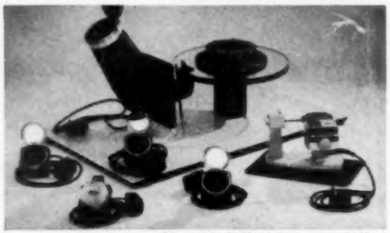

Vernac® Optical Instrumentation

PRECISION OPTICS IN QUANTITY

Designers and manufacturers of scientific optics for industrial and military applications since 1926. New plant (one of the largest and best equipped in the U.S.) offers unique facilities for production of optical components and complete systems at sensible costs.

INFRARED INDUSTRIES, INC.
Optical Systems Division

Formerly Simpson Optical
Santa Barbara, Calif.
(805) 684-4141

"OPTICS AT IRI"
New Book—Ask for it

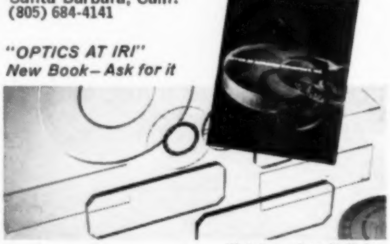

Metal-on-glass Reticles

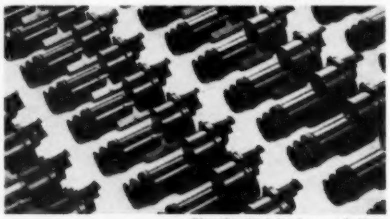

Fire Control Instrumentation

Precision Components

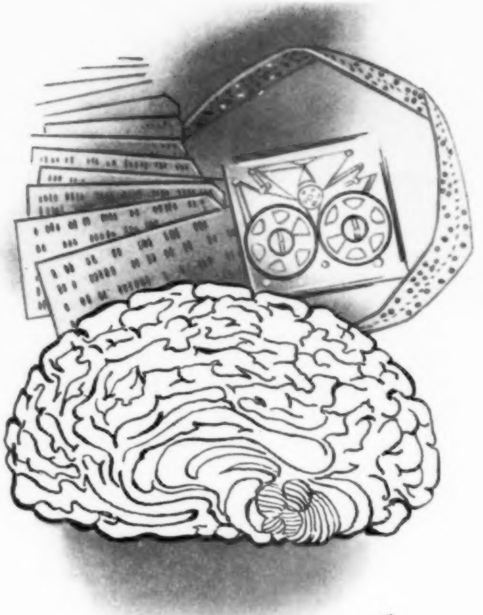

automated

LENS DESIGN?

NOT COMPLETELY . . .

The design of all Diffraction Limited lenses begins and ends with the all-important human and very skillful lens designer. True, the electronic computer speeds up the tedious numerical calculations — but the vital decisions are always made by the human brain.

DL's design staff, equipped with the best of both — brains and computers — is regularly producing designs which are in the forefront of the state-of-the-art.

Why not consult DL on your next design problem?

Send for our new facilities brochure.

TEL: 617 275-8212

Diffraction Limited INC.
OPTICS

MIDDLESEX TURNPIKE • BEDFORD, MASS., 01730

MULTI-LAYER INTERFERENCE FILMS

Made in our
New Rochelle High Vacuum Coating Laboratory

For dichroic and achromatic beam splitters and filters.
High efficiency . . . Relatively wide band

Our coatings were used in the first TELSTAR color TV transmission

For lasers and masers

Over 99% reflectivity

#530–630	reflects 530 mμ to 660 mμ
#N-6343	reflects 610 mμ to 710 mμ
#N-680	reflects 670 mμ to 750 mμ
#N-1064	reflects 980 mμ to 1120 mμ
#N-1150	reflects 1120 mμ to 1220 mμ

Coatings are also available with peak reflectivity at any other desired wavelength.

Unaffected by immersion in liquid nitrogen. Can easily be cleaned with Acetone, Alcohol, or normal detergents.

Thin Glass Substrate Material

Ground and polished: .020–.030″ thick
Machine drawn: .010–.020″ thick

SCHOTT

Narrow Band Interference Filters

Jena Glass

For the spectral region from 300 to 2000 mμ with transmission up to 60% and half-widths down to 5 mμ, depending on filter type.

Available as line and band filters, line and band double filters, broad band filters, spectral band filters, and wedge filters.

ABSORPTION TYPE COLORED OPTICAL FILTER GLASS

Processed in our New Rochelle Optical Shop in about 100 types for the ultra-violet (from 250 mμ), visible, and infrared (to 3000 mμ) spectral regions. Available in flat or as solid bars for the manufacture of tubing for liquid laser excitation.

Also Anti-Laser Eye-Protection Filter Glass BG-18

•

NEODYMIUM DOPED GLASSES
FOR SOLID STATE LASERS

Type	LG-2	LG-4
Basic Glass	Borosilicate glass	Lanthanum-Borosilicate glass
Doping	2 weight % Nd_2O_3	2 weight % Nd_2O_3

Emission wavelength: 1.06 μ

FISH-SCHURMAN CORPORATION
90 Portman Road, New Rochelle, N. Y.

CONFERENCE ON INTERFERENCE AND COHERENCE

Sydney, Australia, 24—25 August 1964

Provisional Subjects to be covered at a short ICO-AAS Conference on Interference and Coherence to be held preceding the conference in Tokyo and Kyoto (1–8 September 1964) include applications of interferometry to length standards and measurements, testing of optical systems, studies of the properties of materials, and to radio astronomy; new techniques in interferometry and new types of interferometers; and coherence and correlations. Both invited lectures and short papers on these topics are planned.

Provisional Timetable: Reunions at private homes on 23 August; conference sessions in Sydney University on 24 and 25 August; visits to National Standards and Radiophysics Laboratories, Sydney University, and University of New South Wales on 26 August; visits to scientific installations outside Sydney 27–29 August either as tours or by private arrangement made at the conference. OSA's Around-the-World Group Flight provides transport to this and the Tokyo meeting.

Scientific Tours could include visits to Narrabri, a country town 565 km north of Sydney, where there is an intensity interferometer for measuring stellar diameters and a radioheliograph for mapping the sun; Parkes, a country town 400 km west of Sydney and the site of a large radio telescope; Canberra, the national capital, 320 km south of Sydney (enroute to Melbourne) and the home of the Australian National University and Mount Stromlo Observatory; and Melbourne, capital of State of Victoria, the location of CSIRO Division of Physical Chemistry, the University of Melbourne, and Monash University.

Accommodations can be arranged at one of the University Colleges either for the conference only or for the full week at £A2.12.6 ($7.00) a day including meals.

Registration fee will be £A4 ($9.00) including the conference dinner. Students may register for the meeting only for £A1 ($2.20). Tours will be extra.

Additional Information can be obtained from the Australian National Committee for Optics, W. H. Steel, Convenor, CSIRO Division of Physics, City Road, Chippendale, N.S.W., Australia.

International Commission for Optics — See page A13

CONFERENCE ON PHOTOGRAPHIC AND SPECTROSCOPIC OPTICS

Tokyo and Kyoto 1–8 September 1964

arranged by

SCIENCE COUNCIL OF JAPAN and JAPANESE SOCIETY OF APPLIED PHYSICS

A Conference on Photographic and Spectroscopic Optics, arranged on an international level by the Science Council of Japan and the Japanese Society of Applied Physics under the auspices of the International Commission for Optics, will be held in Tokyo and Kyoto, Japan, 1–8 September 1964. The Conference will be composed of some 10 sessions, and each session will include one or two invited papers (30–40 min presentation time) and some contributed papers (15 min each). The subjects to be dealt with at the Conference will be:

Design and Evaluation of Photographic and Spectroscopic Optical Systems
Recent Instrumentation in the Far Infrared and the Extreme Ultraviolet
Optical Materials for Use in Photographic and Spectroscopic Optics

Offers of papers should be made no later than 31 January 1964, by sending an abstract to the Organizing Committee. This abstract must be adequate for the Committee to decide on the suitability of the paper: the scope of the paper should be indicated, and principal new results included. The working languages of the Conference will be English, French, and German. However, in view of the fact that English will be the only language comprehensible to the majority of participants, speakers are strongly recommended to read their papers in English.

Visits to research institutes, universities, and optical companies are being planned. More detailed information will be circulated in due course.

All inquiries concerning the Conference should be addressed to: Prof. H. Kubota, Secretary, Organizing Committee, ICO-Tokyo & Kyoto, Science Council of Japan, Ueno Park, Tokyo. For planning purposes the Japanese Committee is very eager to estimate the number of people who will attend; If you are interested in this meeting please write immediately to Prof. Kubota for further information.

IBM®

GROWTH OPPORTUNITIES

OPTICAL ENGINEERING

The IBM facility in Lexington, Kentucky, in the delightful bluegrass area, has an outstanding opportunity and a rewarding career for you involving exploratory development of small-scale optical systems.

You should be familiar with lens specifications, optical instrumentation and evaluation of high-intensity light source radiometry tests. You will work with highly skilled teams in the development of image-processing devices. An advanced degree in physics, or optics, or related experience, is required.

This location is excellent for people who like to combine a fine working environment, good housing, and easy access to outdoor vacation areas. You will find good schools and a fine cultural atmosphere in this university community. An unusually well-planned, company-paid benefits program provides meaningful protection for you and your family. Opportunities for growth and continued education are excellent. IBM is an Equal Opportunity Employer.

If you would like to explore these opportunities, please write (or call collect), outlining your qualifications and interests, to:

George G. Pelfrey, Dept. 619L
IBM Corporation
703 New Circle Road, N.W.
Lexington, Ky. 40507
(606) 252-2252

IBM®

INTERNATIONAL BUSINESS
MACHINES CORPORATION

LIGHT BEAM SPLITTERS

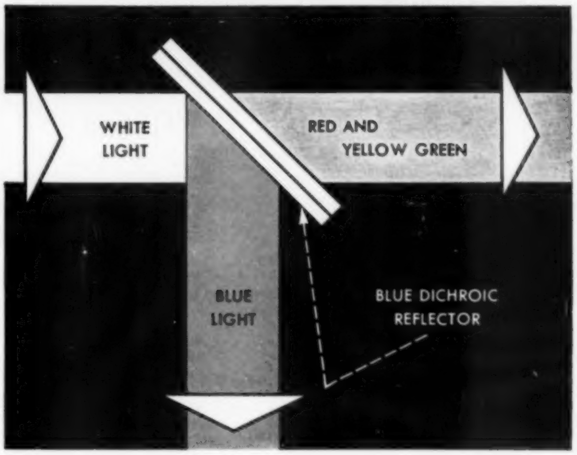

Dichroic reflectors can put light and heat to work as you specify

What do you want to do with a light beam? In millimicrons, what wave lengths do you want reflected? Where do you want spectrophotometric reflection to peak?

Liberty Mirror offers a standard line of dichroic coatings that reflect 90% or more of incident light in wave lengths from as low as 350 millimicrons up to 1,000 millimicrons. If a Hi-Efficiency dichroic coating hasn't already been pinpointed to meet your specifications, Liberty Mirror will develop one that does.

Vacuum-deposited coatings of various metals are used to make front-surface mirrors, neutral filters, transparent mirrors, high-efficiency beam splitters, beam-splitting dichroic mirrors and filters. Metallic and transparent electrically conducting coatings are available for resistance heating. Static-dissipating and high-frequency shielding coatings are also available.

Applied to all types of glass, metal or plastic, the coatings are used in such varied products as scientific and optical instruments, cameras, toys, pin setters, wheel-aligning equipment, aircraft and missiles. Free data sheets are available on all coatings.

Write L·O·F, Liberty Mirror Division, 55123 Libbey·Owens·Ford Building, Toledo 2, Ohio.

LIBERTY
MIRROR DIVISION
LIBBEY·OWENS·FORD

MADE IN U.S.A.
LOF
GLASS

MATRIX METHODS
IN OPTICAL
INSTRUMENT DESIGN

Willem Brouwer

THE FIRST text to introduce matrix methods at the introductory level, this volume applies basic principles of geometrical optics to practical problems of optical instrument design.

CONTENTS

1 Plane Reflecting Surfaces
2 Ray Tracing
3 Paraxial Optics
4 Paraxial Properties of Lens Systems
5 Pupils of Optical Systems
6 Some Remarks about Real Rays
7 Color Aberrations
8 Third-Order Aberrations
9 The Numerical Calculation of the Third-Order Aberration Coefficients
10 Aberrations of Various Systems
11 Some Visual Instruments
12 The Microscope
13 Other Optical Instruments
14 Measurement, Testing, and Linear Filter Theory
References
Appendix I Introduction to Matrix Algebra

$5.95 paperbound — 280 pages — $9.00 clothbound

—×—

save shipping charges
prepay your order

W. A. BENJAMIN, INC.
2465 Broadway New York 25, N. Y.

THE SCIENCE OF COLOR

THIS DEFINITIVE BOOK ON COLOR, prepared by OSA's Colorimetry Committee and setting forth the history, physics, physiology, psychology, and technology of color vision and color measurement, has been reprinted by OSA.

LIMITED EDITION. Twenty-five color plates make this book uniquely beautiful, and, when the original supply of color sheets is exhausted, they cannot be reproduced. Therefore, this edition is limited.

AUTHORITATIVE DATA, mostly unavailable in other books, 39 tables, 102 figures, 340 pages of text, 22 pages of bibliography, and 23 pages of glossary-index have all been critically re-examined and corrected. The new **SCIENCE OF COLOR** is therefore the most up-to-date as well as the most complete source book for color science.

ORDER NOW
SEND CASH WITH ORDER
PRICE $10.00; OSA MEMBERS $8.50

Order Form

Optical Society of America
Room 101, 1155 16th Street N.W.
Washington, D.C. 20036

Please send one .... copy of SCIENCE OF COLOR.

☐ Cash/check herewith
☐ $10.00
☐ $8.50 (OSA Member price)

Name ______________________

OSA Membership # ______________________

Address ______________________

____

____

HIGH QUALITY STANDARDS

. . . in Optical Crystal Blanks

Calcium Fluoride	Sodium Chloride
Barium Fluoride	Potassium Chloride
Lithium Fluoride	Potassium Bromide

- *Prompt Delivery* • *Large Size Availability*
- *Precision Cutting* • *Scattering Free*
- *Impurity Absorption Free* • *Strain Free*

. . . in Optical Maser Crystals

$U^{+3} \cdot CaF_2$	$Dy^{+2} \cdot CaF_2$	$Nd^{+3} \cdot CaF_2$
$U^{+3} \cdot BaF_2$	$Sm^{+2} \cdot CaF_2$	$Nd^{+3} \cdot BaF_2$
$U^{+3} \cdot SrF_2$	$Sm^{+2} \cdot SrF_2$	$Nd^{+3} \cdot SrF_2$
$Tm^{+3} \cdot SrF_2$	$Tm^{+2} \cdot CaF_2$	$Ho^{+3} \cdot CaF_2$

Also, all other trivalent rare earths in CaF_2, BaF_2 and SrF_2.

Indicative of our quality, most of the above were first mased in Optovac grown crystals.

OPTOVAC, INC.

NORTH BROOKFIELD, MASSACHUSETTS

STAFF APPOINTMENT

CARLYLE BARTON LABORATORY
THE JOHNS HOPKINS UNIVERSITY
QUANTUM ELECTRONICS
SOLID STATE PHYSICS
PHYSICISTS M.S.
or
ENGINEER M.S.E.E.

With background in geometrical and Physical optics, spectroscopy, quantum electronics or solid state physics.

An excellent opportunity for a qualified individual to continue graduate studies to the Ph.D. in Physics or Electrical Engineering. Carlyle Barton Laboratory is a new, modern research facility located on the Homewood Campus of The Johns Hopkins University. The research program of the Laboratory is sponsored by several government agencies and is related to areas of academic interest to the Department of Physics and Electrical Engineering.

Appointment to this position is contingent upon acceptance by the Graduate School of the University and the Department considered.

REPLY

Carlyle Barton Laboratory
The Johns Hopkins University
Charles and 34th Streets
Baltimore, Maryland 21218

U. S. Citizenship Required
An Equal Opportunity Employer.

A NEW Catalog

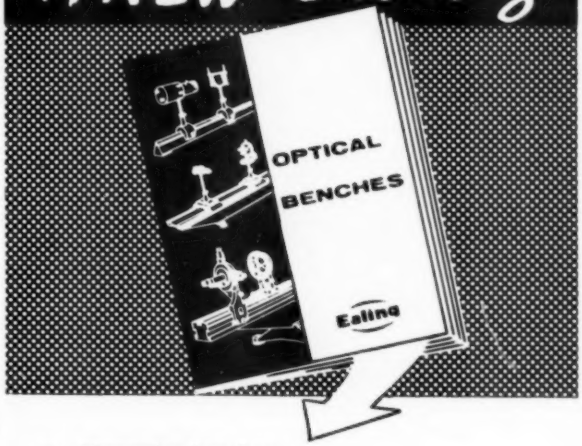

- triangular benches
- lathe bed benches
- massive research benches
- non-magnetic and student-teaching benches

Just write to:

THE **Ealing** CORPORATION

2239 Massachusetts Ave., Cambridge, Mass. 02140

COMPACT ARC LAMPS

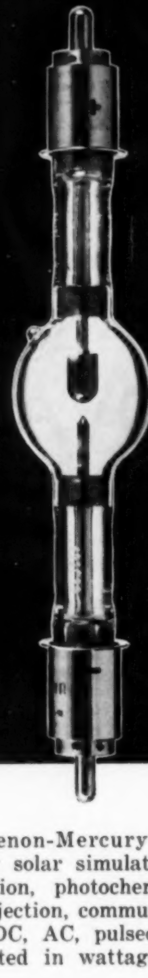

- Xenon, Xenon-Mercury and Mercury Lamps for solar simulation, lasers, instrumentation, photochemistry, searchlights, projection, communications
- Operates DC, AC, pulsed, simmer-flash or modulated in wattages from 80 to 5,000
- Features high intensity, high brightness, full spectrum, long life, complete reliability, rapid start and no maintenance
- One universal starter for all lamps
- Only Hanovia makes the lamp *and* all associated equipment such as electrical controls and power supplies
- Made in the U.S.A.

Write today for complete technical information.

★ ENGELHARD HANOVIA, INC. ★
HANOVIA
LAMP DIVISION
100 CHESTNUT STREET • NEWARK 5, NEW JERSEY

HIGH QUALITY SUPER PRESSURE OSRAM MERCURY LAMPS

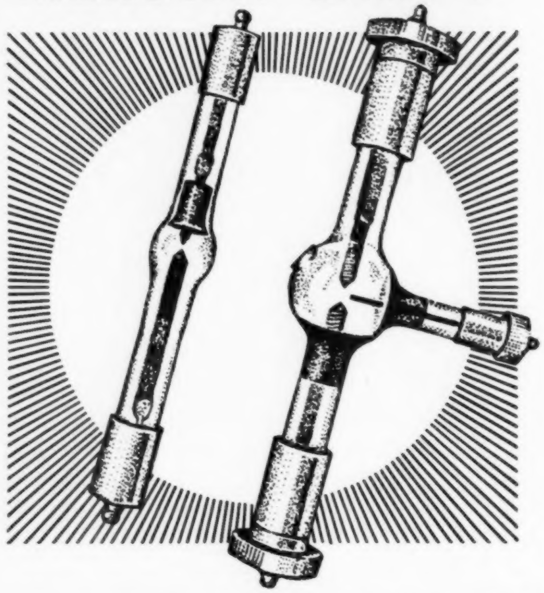

AT REDUCED PRICES!

HBO 75W	**$36.45**
HBO 100W/1 (3 Electrode)	**40.85**
HBO 100W/2 (2 Electrode)	**37.90**
HBO 200W (3 Electrode)	**37.90**
HBO 200W/2 (2 Electrode)	**35.00**
HBO 500W (3 Electrode)	**80.25**

Complete line of auxiliary ballasts, igniters and accessory hardware available.

Osram Xenon short arc lamps (XBO series) are also available from 150 to 6500 watts; long arc (XBF water-cooled) lamps, in 1000, 2500, and 6000 watt sizes; long arc (XQO extended tubular lamps designed to operate in ambient air temperature), in 6000, 10,000 and 20,000 watt sizes.

All lamp prices include Federal Excise Tax. For complete price information, delivery, OEM and end user quantity discounts, please contact Macbeth Sales Corporation at the address shown below.

Literature is available on request. Ask for your copy of "The Exciting World of Xenon Light Energy," a full color brochure which includes company background and product information.

Macbeth

MACBETH SALES CORPORATION
P. O. BOX 950 — DEPT. 4 • NEWBURGH, NEW YORK

from the **HOUSE OF RHODES**

. . . the most complete line of cerium polishing materials for all types of optical work

produced by

LINDSAY™

FOR OVER HALF A CENTURY THE HALLMARK OF DEPENDABILITY

CEROX®
•
BARNESITE®
•
Super-Ce®
•
AND THE NEW
MARK V
PASTE

Rhodes has been serving all facets of the optical industry for more than fifty years.

You can depend on the Rhodes organization, anywhere from coast to coast, for helpful technical service.

Your Rhodesman always has available for service to you the comprehensive facilities of the LINDSAY research laboratory which is staffed by a technical group with many years of practical experience in optical polishing materials and processes.

How can we serve you today?

COLOSSUS
BRAND™
Since 1898

®Registered trademarks of Rare Earth (Lindsay) Division, American Potash & Chemical Corporation

THE HOUSE OF RHODES / JAMES H. RHODES & COMPANY

General Offices: 1028 West Jackson Blvd., Chicago 7, Illinois • Regional Offices: Long Island City, N. Y. and San Marino, Calif.

STATEMENT required by the Act of 24 August 1912, as amended by the Acts of 3 March 1933, 2 July 1946, and 11 June 1960 (74 Stat. 208) showing the ownership, management, and circulation of *Applied Optics*, published monthly and entered as second class mail at Easton, Pa., for 22 December 1961.

1. The names and addresses of the publisher, editor, and business managers are: *Publisher and Business Manager:* Optical Society of America, 1155 16th St. N.W., Washington, D.C. 20036. *Editor:* J. N. Howard, AFCRL, Bedford, Mass., *Managing Editor:* P. R. Wakeling, OSA, 1155 16th St. N.W. Washington, D.C. 20036.

2. The owner is the Optical Society of America, Inc., 1155 16th St., N.W., Washington, D.C. 20036.

3. The bondholders are: None.

4. The average number of copies of each issue of this publication sold or distributed, through the mails or otherwise, to paid subscribers during the 12 months preceding September 1963 was: 4640.

(signed) P. R. Wakeling, Managing Editor

Use **THIN FILM (8μ) BEAM SPLITTERS**

NO GHOSTS!

NO REFRACTIVE ERRORS!

- Flatness to 1/8" wave and parallelism to less than 1 fringe per inch; on special order.
- Sizes: Up to 24" (and still growing).
- Large coating selection, including dichroics.

SEND FOR FREE BOOKLET

"Application and Specification of Pellicles"

Important reading for manufacturers, designers and users of glass beam splitters, mirrors, filters and prisms.

NPC National Photocolor Corp.
53 Water Street, South Norwalk, Conn.
203 - VO 6-1800

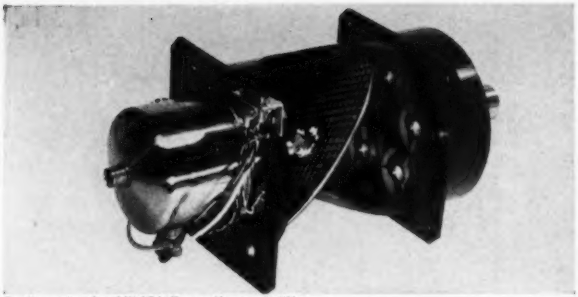
Radiometer for NIMBUS weather satellite

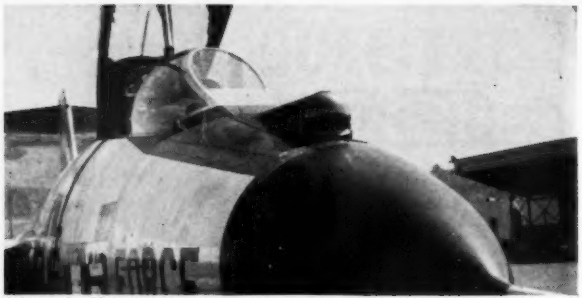
Interceptor IR installation

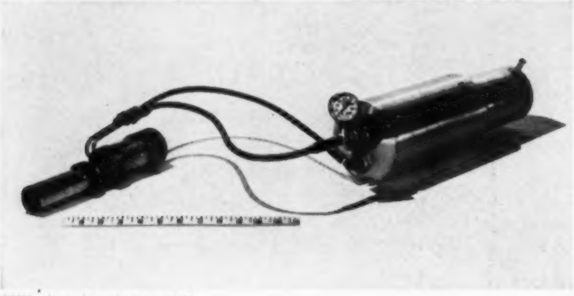
12°K closed-cycle cryostat

90C IR search/track set

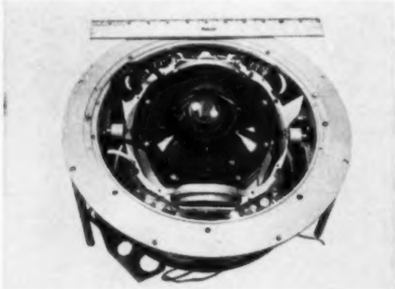
IR multi-channel tracking radiometer

Star tracker for SURVEYOR spacecraft

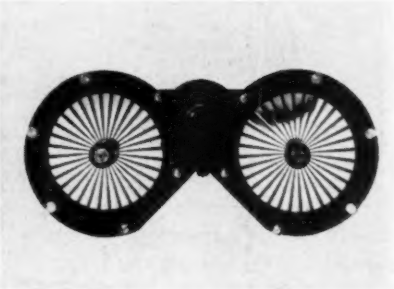
Modulated IR source

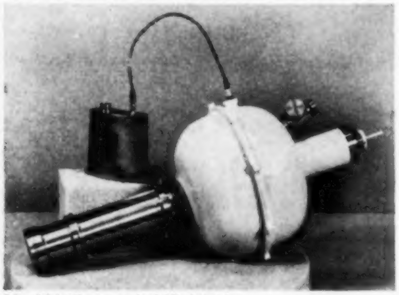
Liquid-helium-cooled IR detector

IR anti-tank missile controller

Expanding Infrared Programs

create new career assignments

Rapid growth of HUGHES Infrared activities in the Aerospace Divisions and the Santa Barbara Research Center has created many responsible positions for qualified engineers and scientists in all phases of IR systems development from conception through production engineering.

Immediately available assignments include openings in such diverse technologies as semiconductor physics, optical design, cryogenics, mechanical engineering, precision electro-mechanisms, electronic circuit design, servo systems...and many other areas.

Current HUGHES IR contracts include advanced systems for space exploration, weather reconnaissance, anti-ballistic missile defense, anti-submarine warfare, interceptor weapon guidance & fire control, bomber defense and tactical weapon control.

Professional experience, an accredited degree and U.S. Citizenship required.

For immediate consideration,
please airmail your resume to:

MR. ROBERT A. MARTIN
Hughes Aerospace Divisions
11940 W. Jefferson Blvd.
Culver City 66, Calif.

HUGHES

HUGHES AIRCRAFT COMPANY
AEROSPACE DIVISIONS
An equal opportunity employer

When
you
think
of

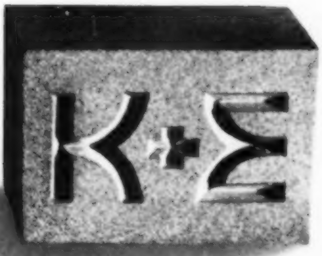

Undoubtedly you think of slide rules . . . transits . . . tracing paper. Correct? But to round out the picture, please enter K&E in your file for these highly advanced space-age instruments . . .

SPACE AND MISSILES SYSTEMS

Solar and Star Simulators • Cine and Special Theodolites • Antenna Contour Checking Instruments • Contour Probing Instruments • Polaris Guidance and Fire Control Instruments • Collimation Test Instruments • Deviators • Borescopes — Electronic and Visual

R&D AND LABORATORY INSTRUMENTS

Auto-Collimators — Electronic and Visual • Electronic Levels • Gravity Reference Instrument • Jig Theodolite • Angle Index Tables and Readout Devices • Gratings • Targets and Special Scales

INSTRUMENTS FOR MANUFACTURING, INSPECTION, QUALITY CONTROL

A complete line of alignment instruments and accessories

Want specific product information? Write K&E today. Our O&M Division can assist you with R&D.

OPTICS AND METROLOGY
DIVISION

KEUFFEL & ESSER CO.
HOBOKEN, NEW JERSEY

3704

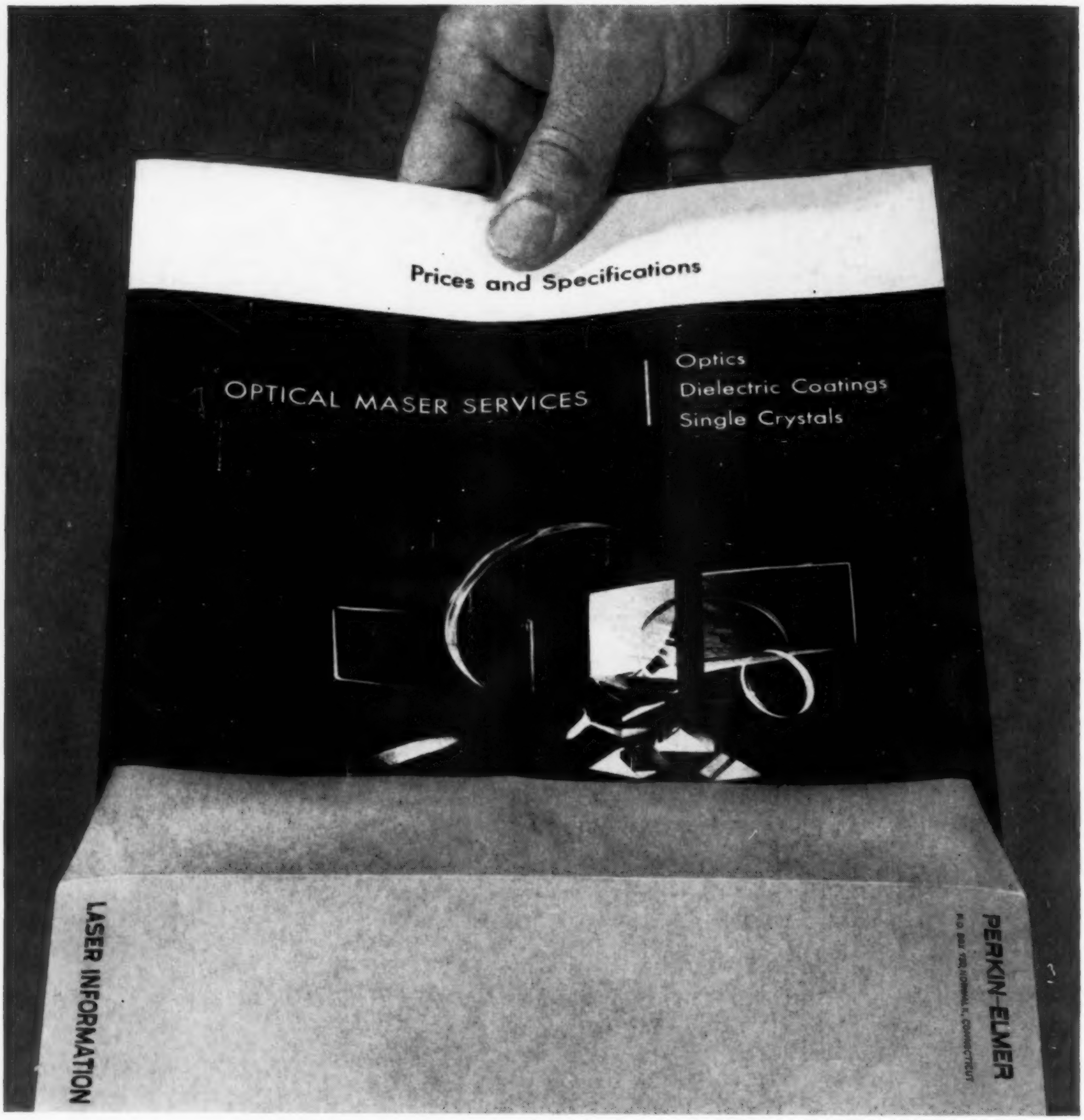

HANDY GUIDE TO
OPTICS FOR LASERS
WRITE OR PHONE FOR YOUR COPY

Here in one compact catalog you will find detailed specifications and prices on Perkin-Elmer's comprehensive optical maser services. Included are such data as coating transmission curves, material transmission characteristics and typical dimensional tolerances.

These and other products are available in quantity for research or production programs:

Interferometer Flats 1.0", 1.5" and 2.0" diameter. Surface: 1/10 to 1/200 wave. BK-7 or Quartz.

Spherical Mirrors 1.0", 1.5" and 2.0" diameter. 1M, 2M, 3M, 4M, 5M, 10M, 25M, 50M radius of curvature. BK-7 or Quartz.

Windows 1.0", 1.5" and 2.0" diameter. Standard or Brewster's angle. BK-7 or Quartz.

Dielectric Coating Durable, minimum loss, specified reflectivities for the full spectrum of laser research and development.

Solid State Laser Materials Tungstate, Molybdate, Sapphire, Garnet, Emerald, Fluoride, Glass.

Special Optics Trihedral and 90° prisms with deviation within 2 seconds.

Gas Laser and Accessories He-Ne laser with D.C. excitation. Compact, lightweight, suitable for laboratory research, military systems or industrial processes. Series V mounts accommodate complete line of adaptive optical accessories. Provides continuous wave, coherent, visible or IR output.

Please direct your request for "Prices and Specifications—Optical Maser Services" to Perkin-Elmer Corporation, Optical Maser Marketing, Norwalk, Connecticut. Phone (203) 847-0411

PERKIN-ELMER